Palaeoenvironmental proxy development and application of leaf wax n-alkanes in Australia

Siân Howard

A thesis submitted in fulfilment of the
requirements for the degree of
Doctor of Philosophy

THE UNIVERSITY of ADELAIDE

FACULTY OF SCIENCES

FEBRUARY 2019

TABLE OF CONTENTS

ABSTRACT

This project explores the signals of plant-derived *n*-alkanes in plants, soils and sediments in Australia, in order to better understand their usefulness as a proxy for the plants and environments in which they were formed. Leaf wax *n*-alkanes are useful compounds for analysis because they are highly recalcitrant and ubiquitous in the sedimentary record. As such, leaf wax *n*-alkanes are an ideal tool for examining past environmental conditions where other macro and micro plant fossils are rare or simply not present. In this thesis, I examine *n*-alkane chain length distribution as well as carbon and hydrogen isotope ratios through a modern field study, a laboratory experiment, and an ancient cave sediment record.

When analysing leaf wax *n*-alkanes in soils and sediments, the temporal and spatial scales of inputs from plants to soils needs to be understood. Therefore modern day calibrations are required to understand what the ancient signals represent. Here we compare leaf wax *n*-alkanes in modern soils and the immediate surrounding plant community along a latitudinal transect across Australia. Results show that while *n*-alkane distributions in surface soils do not correlate with local, current vegetation, they do correlate with proportional grass and tree cover, suggesting they provide a faithful record of large-scale ecosystem structure. Further, the signals observed in sedimentary records are likely to reflect a regional, time-averaged signal that is not heavily susceptible to short-term variability or small-scale spatial heterogeneity in climate.

To determine whether the lack of correlation between surface soils and local, current vegetation observed above is as a result of degradation processes occurring in the soils, the effects of post depositional modification to leaf wax *n*-alkane signals in soils are examined through laboratory experiments. To confirm the reliability of leaf

wax *n*-alkane signals in soils and sediments, it is necessary to understand whether alteration to the signals has occurred. The effects of post depositional modification were isolated by incubating soils mixed with organic composts. Results show that degradation processes significantly decrease leaf wax *n*-alkane concentrations post-depositionally, and this decrease primarily occurs within the first month of incubation. However, despite a significant decrease in concentration, the average chain length distribution of leaf wax *n*-alkanes remains unchanged after incubation, providing confidence in this signal in soils and sediments and for use in palaeoenvironmental research.

Based on the findings from our modern day calibration work, I examine the leaf wax *n*-alkanes signals in Blanche Cave sediments from Naracoorte, in south eastern Australia, spanning an age range of 70,000 to 17,000 years old. Isotopic analysis of leaf wax *n*-alkanes provides information about the vegetation and hydrological conditions before, during and after the mass megafauna extinction event that occurred Australia-wide at around 40ka. Carbon isotope analysis shows that C3 and C4 vegetation abundances vary across this time. Further, hydrogen isotopic analysis provides insight into fluctuating hydrological conditions. The results from this study provide environmental context to the causes and effects of megafauna extinction in Naracoorte.

DECLARATION

I certify that this work contains no material which has been accepted for the award of any other degree or diploma in my name in any university or other tertiary institution and, to the best of my knowledge and belief, contains no material previously published or written by another person, except where due reference has been made in the text. In addition, I certify that no part of this work will, in the future, be used in a submission in my name for any other degree or diploma in any university or other tertiary institution without the prior approval of the University of Adelaide and where applicable, any partner institution responsible for the joint award of this degree.

I acknowledge that copyright of published works contained within this thesis resides with the copyright holder(s) of those works.

I give permission for the digital version of my thesis to be made available on the web, via the University's digital research repository, the Library Search and also through web search engines, unless permission has been granted by the University to restrict access for a period of time.

I acknowledge the support I have received for my research through the provision of an Australian Government Research Training Program Scholarship.

Siân Howard

28 February 2019

ACKNOWLEDGEMENTS

I must firstly acknowledge the endless support of my primary supervisor, Francesca McInerney. I was given a sage piece of advice by my sister-in-law Katie Howard prior to undertaking my Honours year: I should choose my project based primarily on the person supervising rather than prioritising the project topic first. This excellent piece of advice served me very well and I was lucky enough to end up with not only an excellent supervisor, but also an exciting project all in the one package. Over the year that followed, and on throughout my PhD, I could not have asked for a supervisor with more dedication, passion, support, kindness, patience, understanding or humanity and someone I am also greatly honoured to be able to call my friend. Thank you, Cesca, you really are the biggest reason I stuck this out.

My co-supervisors, Gavin Prideaux and Lee Arnold have also been an excellent source of wisdom, kindness and advice. I really think I hit the jackpot in terms of supervisory excellence; a fortune too few PhD candidates can claim!

To all the co-authors who have been involved in each of my chapters, thank you all for sharing with me your wonderfully diverse expertise. You have each helped to shape me as a researcher and provide me with a much more well-rounded understanding of how my work fits into this world.

Several people who have been instrumental in helping to make this project come together, in no particular order: Kristine Nielson, for being lab manager extraordinaire and being a true ally in understanding the struggles of PhD life; Jake Andrae, for having been there with me since Honours and always being able to provide ludicrously fast input and advice on data and figures; Stefan Caddy-Retalic, for your sharp wit, dark humour and for challenging me to dig deeper; Jacinta Greer and Ellyse Bunney for being

dedicated, inspiring and kind fellow lab group members; Emrys Leitch and Alex Holman, for managing to understand my jumbled up questions and always happily helping me to get to the bottom of them; and, Tony Hall for constantly supporting me with my instrument and data woes and being a fellow sympathiser to the absurdity of it all.

Thanks also go to my friends and family who truly have much more faith in my abilities than I do and constantly told me that I could do this when I frequently doubted it myself. I don't know if this is my magnum opus Mum, but I gave it a go. I also include here all the dog family members in my life, because they're the real heroes when it comes to comic and stress relief.

Last, but by no means least, I must acknowledge my long suffering sweetheart, Simon. You have unwaveringly supported me mentally, emotionally, financially and always with encouragement. You've been my stalwart supporter in times of doubt and trouble, as well as success. There are so many reasons I could not have done this without you. The final chapter of this thesis is the rest of our lives!

DEDICATION

I dedicate this thesis to my paternal grandparents, Jean and Fred, who both passed away during my PhD. They were kind and simple folk who showed me that nothing is more important in this world than love and the happy memories we create for ourselves by living a loving life.

CHAPTER 1

INTRODUCTION

1. Importance of palaeoenvironmental reconstruction

Humanity's role in accelerated rates of climate change and the need for action is becoming increasingly hard to ignore. Human impact on climate is largely a function of population size which in 2017 was reported by the UN to be 7.55 billion, with expected increases to 8.55 billion by 2030 and 11.24 billion by 2100 (United Nations 2017). Increased global population size requires greater use of the land for food production and industry as well as increased natural resource consumption, all of which produce significant greenhouse gas emissions, resulting in measurable global warming (IPCC 2014). As global temperatures increase, it is expected that weather extremes will become more intense and frequent, and species and ecosystem vulnerability will be tested, with many species predicted to be unable to adapt to current climate change projections (IPCC 2014).

Understanding the capacity for ecosystems to adapt to human-induced climate change requires a long-term perspective of ecosystem responses to stress. Previously, work has been focussed on maintaining ecosystems to a similar state to their historical configuration, but new conservation methods are now looking to maximise the capacity of ecosystem adaptability (Hellmann and Pfrender 2011, Barnosky et al. 2017). Conservation palaeobiology models past species' ecological and evolutionary responses to environmental change. It compares conditions before and after ecosystem disturbance, examines species and ecosystem response to stress, examines the range of variability an ecosystem can endure and identifies human-induced versus non-human-induced impact on ecosystem change (Dietl et al. 2015). In order to model these

outcomes, extensive palaeoenvironmental reconstruction is necessary. Reconstructing past environments is possible through the analysis of different proxies such as plant and animal fossils, sedimentary structures and chemical signatures preserved in the geological record. This thesis focuses on the isotopic and molecular composition of plant molecular fossils, or biomarkers, as a means of reconstructing palaeoenvironments.

2. Plant molecular biomarkers

Research using molecular biomarkers, is becoming increasingly prevalent in the field of palaeoenvironmental reconstruction. Different organisms produce a variety of molecular compounds that can provide information about their mode of life and the environment and climate in which they lived. In particular, *n*-alkanes are a group of straight chained aliphatic hydrocarbons that are used as biomarkers, with different groups of organisms producing different ranges of *n*-alkane chain lengths (Pu et al. 2011). For example, bacteria produce dominantly short-chained, even-numbered *n*-alkanes whereas algae produce short-chained, odd-numbered *n*-alkanes (Sachse et al. 2004). Leaf wax *n*-alkanes from terrestrial plants are dominantly long-chained, odd-numbered *n*-alkanes, ranging from 25 to 35 carbon atoms in length (Sachse et al. 2004, Eglinton and Eglinton 2008).

Plants synthesize their *n*-alkanes by sequential elongation of a C_2 primer through condensation–elongation, forming acyl chains with a greater predominance of odd over even chain lengths (Shepherd and Wynne Griffiths 2006). Most land plants have an outer protective wax layer composed of lipids that include these long, straight chain *n*-alkanes, as well as alkanols and alkanoic acids. They produce these compounds to provide a protective wax coating to their outer surfaces, such as their leaves, flowers and fruits as a means of reducing moisture loss and herbivorous attack (Eglinton and

Hamilton 1967, Eigenbrode and Espelie 1995, Banthorpe 2006, Jetter and Riederer 2016), with their leaves producing the greatest concentration of these compounds relative to other plant organs (Gamarra and Kahmen 2015).

An emerging paradigm is that the relative abundance of the different *n*-alkane chain lengths, often measured as an average chain length (ACL) may be affected by prevailing environmental conditions. However, the limited research that has been conducted in this area has seen a conflation of environmental conditions with species variation between different biomes, which makes it difficult to differentiate between fixed chemotaxonomic patterns and plant response to the prevalent environmental conditions (Bush and McInerney 2013, Carr et al. 2014, Bush and McInerney 2015). Due to their role in regulating a plant's moisture balance (Eglinton and Hamilton 1967, Dodd and Poveda 2003, Jetter and Riederer 2016), the primary environmental conditions that are thought to show a relationship with *n*-alkane distribution are temperature and precipitation (Bush and McInerney 2015, Andrae et al. 2018). Plants respond to dry conditions by increasing their *n*-alkane production to form a protective wax layer that reduces water loss from the leaf (Hoffmann et al. 2013). Hoffmann (2013), however, goes on to suggest that caution be given when using ACL of *n*-alkanes as a palaeoenvironmental indicator, and recommends only using this proxy in conjunction with other indicators, such as leaf δD values, which indicate leaf water evapotranspiration rate, as different plants species can show different ACL trends in response to climate. It is also important to consider the timing of *n*-alkane production in plants when interpreting ACL, because the ACL signature recorded in the leaf waxes is specific to the prevailing climatic conditions at the time of leaf flush (Tipple et al. 2013). In order to interpret the *n*-alkane signals observed in soils and sediments, it is

necessary to understand the temporal and spatial scale of inputs from plants to soils (Diefendorf and Freimuth 2017).

3. Leaf wax *n*-alkanes in the sedimentary record

Leaf waxes are readily removed from the leaf surface by ablation from wind and water. They form a component of dust particles, as well as being deposited as a part of any immediate plant detritus, and this is how they come to be found in sediments (Rommerskirchen et al. 2006b). Soil organic matter, including any *n*-alkanes present, persists in soils for extended periods despite being thermodynamically unstable, because of the physicochemical and biological influences of the surrounding environment that slow the rate of decomposition (Schmidt et al. 2011).

High molecular weight *n*-alkanes can be preserved for millions of years and have been extracted from sediments from the Cretaceous–Paleogene boundary (Yamamoto et al. 2010), as well as the Eocene (Smith et al. 2007), Miocene (Huang et al. 2001) and Holocene (Schwark et al. 2002). This preservation is likely to be because *n*-alkanes are water insoluble and, for the longer chain lengths, relatively non-volatile and relatively resistant to biodegradation (Eglinton and Eglinton 2008, Diefendorf and Freimuth 2017). Because *n*-alkanes are so well preserved in the sedimentary record, they make ideal proxies for the vegetation they were synthesized by and are useful for studying changes in vegetation patterns (Hughen 2004, Smith et al. 2007, Diefendorf et al. 2011). They are particularly important when larger plant fossil remains are rare or absent in the sedimentary record.

4. Chain length distribution of *n*-alkanes

As a result of their persistence, *n*-alkanes are abundant throughout the sedimentary record and there are a number different ways that these preserved *n*-alkanes can be analysed to obtain different information about past environments and climate. The relative abundance of the different *n*-alkane chain lengths produced by plants, or average chain length, has been observed to be widely variable amongst different plants, but has also been thought to provide information about prevailing climate conditions and plant growth form (Brincat et al. 2000, Dodd and Poveda 2003, Diefendorf et al. 2011, Bush and McInerney 2013). Historically, specific *n*-alkane chain lengths preserved in sediments were regarded as being representative of different plant groups such as woody versus graminoid plant types. One such example includes a study of lake sediments from the late glacial-Holocene in Germany that found that particular chain lengths were diagnostic of different types of vegetation when analysed in conjunction with pollen data (Schwark et al. 2002). Additionally, a study of Lake Baikal sediments showed that the sediments from the last glacial maximum (LGM) were dominant in the *n*-alkane chain length C_{31}, and the Holocene aged sediments were dominant in C_{27}, thought to indicate a change in terrestrial vegetation as a result of climate (Brincat et al. 2000). Additional research has shown that, apart from *Sphagnum* mosses, ACL does not strongly indicate for different plant types when analysed at a global scale (Bush and McInerney 2013). Different plant growth forms can show strong similarities in their cuticle wax composition and leaf wax lipid distributions, and plants of the same growth form can show significant variation, suggesting that *n*-alkane distributions are not adequately diagnostic of plant growth form (Bush and McInerney 2013). However, analysis of plant and soil *n*-alkane distributions in Africa found that plants within different biomes demonstrated different chain-length distributions, which

were also reflected in the soils of the same biomes, suggesting that *n*-alkane signals in soils and sediments may be useful on a regional scale (Carr et al. 2014).

5. Isotopic composition of *n*-alkanes

The isotopic composition of sedimentary leaf wax *n*-alkanes can provide insight into past vegetation and hydrological conditions that plants were exposed to in the past. Isotopes of an element contain the same number of protons and electrons, but differing numbers of neutrons, for example, carbon (C) has two stable isotopes of ^{12}C and ^{13}C, which both consist of an atomic number of 6, but have 6 and 7 neutrons respectively (Michener and Lajtha 2007). The isotopic composition of different materials, such as leaves or seawater for example, is expressed in parts per thousand deviation from an internationally accepted standard by the following equation:

$$\delta(‰) = \left(\frac{R_{sample}}{R_{standard}} - 1\right) \times 1000$$

Where *R* is the ratio of the abundance of the heavy isotope relative to the abundance of the light isotope in either sample or the standard (Michener and Lajtha 2007). For hydrogen, the internationally accepted standard used is Vienna Standard Mean Ocean Water (VSMOW) and for carbon it is Vienna Pee Dee Belemnite (VPBD) (Michener and Lajtha 2007).

The hydrogen and carbon in leaf wax *n*-alkanes have measurable isotopic compositions that can be used to examine environmental and ecological conditions. The hydrogen isotopic composition of leaf wax *n*-alkanes provides information about hydrological conditions a plant was exposed to during the time over which the leaf formed, with the hydrogen that forms a component of the *n*-alkanes having been sourced from soil water and modified through transpiration in the leaf (Sachse et al.

2012, Cernusak et al. 2016). The isotopic composition of leaf wax *n*-alkanes can be used to infer aridity, with higher values of δD often indicating drier conditions and lower values indicating wetter conditions (Smith and Freeman 2006, Douglas et al. 2012, Kahmen et al. 2013, Schwab et al. 2015). Analyses of δD values of leaf wax *n*-alkanes preserved in modern and ancient lake and marine sediments have demonstrated that it is possible to examine past hydrological conditions from ancient sediment deposits (Sachse et al. 2004, Polissar and Freeman 2010, Garcin et al. 2012, Niedermeyer et al. 2016).

The carbon isotope values of leaf wax *n*-alkanes provide insight into vegetation type. Fixation of carbon during photosynthesis results in fractionation of carbon isotopes, with both C3 and C4 photosynthetic pathways fixing carbon with different values of $\delta^{13}C$ (Farquhar et al. 1989). The $\delta^{13}C$ is recorded in the leaf wax *n*-alkanes, and as such, *n*-alkanes are a useful tool for reconstructing past C3 versus C4 vegetation (Garcin et al. 2014). Generally, the $\delta^{13}C$ values of *n*-alkanes in C3 plants are more negative than for C4 plants (Collister et al. 1994, Chikaraishi and Naraoka 2003). The predominance of C3 or C4 vegetation is thought to be driven by climate (Rommerskirchen et al. 2006a). Generally, C4 plants are favoured by high growing season temperatures, high aridity, warm season precipitation and low pCO_2 (Ehleringer et al. 1997, Sage et al. 1999). In Australia, C3 vegetation is dominantly associated with trees, forbs and shrubs, and C4 vegetation is dominantly associated with grasses and chenopods (Supplementary Fig. S1, Appendix 3).

6. Australian ecosystem changes

Globally, grassland expansion occurred over the course of the Cenozoic and became widely dominant across the world, taking the place of many forested regions

(Strömberg 2011). However, in some parts of the world, such as Australia, C4 grassland expansion has been observed to occur later than other parts of the world, at ~3.5 Ma (Andrae et al. 2018). Further, regional vegetation reconstruction for the south east of Australia at around 185 – 157 ka found that mean annual temperatures were much lower than present, and there was a dominance of C3 vegetation, with sparse C4 grasslands (Desmarchelier et al. 2000). More recently in the south east of Australia, an abrupt shift from C4 to C3 dominance was observed to have occurred at 44 – 42 ka (Lopes dos Santos et al. 2013), the timing of which is significant, because it coincides with the timing of megafauna extinction in Australia (Prideaux et al. 2010, Johnson et al. 2016). Further, previous work examining climate in south western Australia at the time of megafauna extinction found that the climate was somewhat wetter than it is today, in addition to a shift from closed-canopy forests from about 100 ka through to more open vegetation at about 30 ka (Prideaux et al. 2010). There is much debate about the cause of megafauna extinction in Australia, focussing primarily on the role of climate versus humans (Bird et al. 2013, Cooper et al. 2015, Saltre et al. 2016, van der Kaars et al. 2017). In order to provide context to the debate, it is necessary to reconstruct environmental conditions at the time megafauna became extinct in Australia.

7. Post depositional modification to *n*-alkanes

Although *n*-alkanes are present in very old sediments, it is important to understand whether they are altered chemically or isotopically during preservation in soil and sediments. Therefore, analysis of the effects of post-depositional modification to *n*-alkanes in soils is necessary, because it is not well understood how their signals may be affected over time. Litterbag studies have examined how leaf wax *n*-alkanes change as a result of microbial and/or herbivorous activity acting on buried leaves. A

four year litterbag study investigating the effects of burial on leaves found that some alteration of long-chain *n*-alkanes occurred during leaf degradation, indicating that some caution may be required when considering them as an unaltered record (Nguyen Tu et al. 2011). The concentrations of *n*-alkanes in litterbag studies have been found to decrease after burial, likely due to microbial degradation which may affect the *n*-alkane signals observed in soils (Li et al. 2017). In addition, concentration of long chain *n*-alkanes (C_{25} – C_{33}) was observed to decrease in sediments that were stored in sealed plastic bags at room temperature for 3 years (Brittingham et al. 2017). Further investigation of *n*-alkane preservation in soils and sediments after the *n*-alkanes have been removed from the leaf surface is required to determine whether the signal observed in soils has been altered by post-depositional microbial activity and processes in the soil.

8. Thesis aims and structure

The aims of this thesis are to examine terrestrial plant *n*-alkane signals in modern day soils and ancient sediments from Australia, in order to determine how well *n*-alkanes are preserved and what environmental signals they record in soils and sediments in Australia. Specifically, the thesis seeks to explore what leaf wax *n*-alkane signals represent after they become integrated into soils by examining the dominant plant species found in the landscape and how their *n*-alkane signals compare to that of the soils they live in. Further, I examine the effects of microbial activity on leaf wax *n*-alkanes in soils in order to determine the reliability of the signals extracted from soils and sediments. Finally, based on the reliability of the signals determined from the modern calibrations and modelling conducted in Chapters 2 and 3, I then examine the *n*-alkanes signals preserved in ancient sediments to explore their potential value in

palaeoenvironmental reconstruction for the time megafauna became extinct in Australia.

8.1 Chapter 2: Leaf wax n-alkane inputs to soils

In Chapter 2, I compare leaf wax *n*-alkanes in modern soils with those of the immediate plant community along a latitudinal transect across Australia. I examine how the *n*-alkane signals preserved in the soils reflect the vegetation in order to provide confidence in their use in palaeoenvironmental reconstruction from ancient sediments. Specifically, I examine the leaf wax *n*-alkane signals of modern plants and soils, to determine the dominant temporal and spatial source inputs of leaf wax *n*-alkanes in soils (Fig. 1).

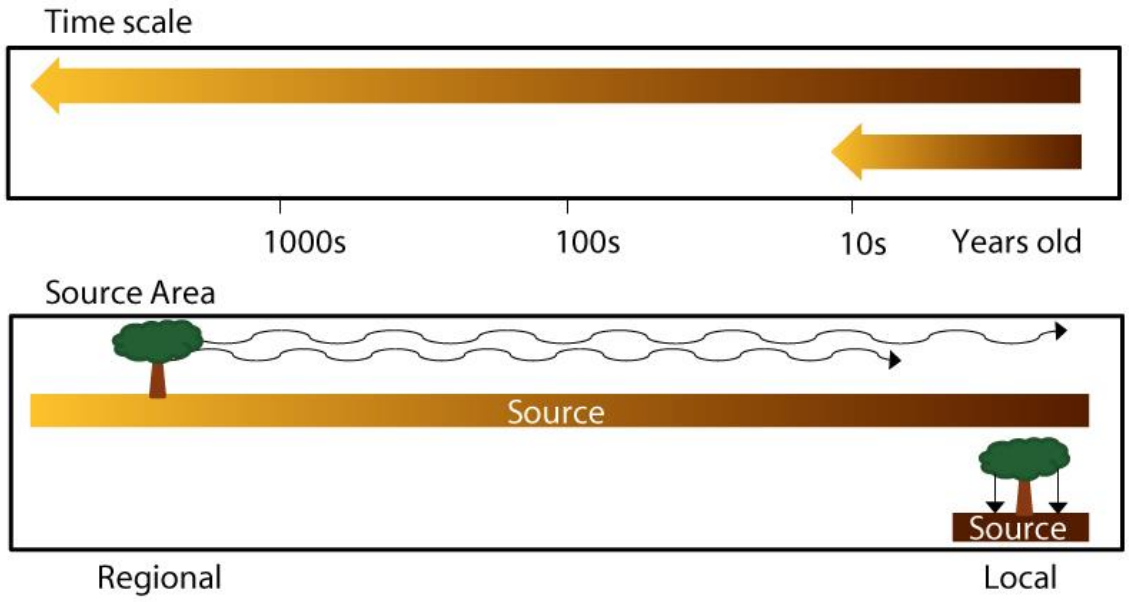

Figure 1. Conceptual model for *n*-alkane inputs to soils. Chapter 2 examines whether the dominant leaf wax *n*-alkane signals observed in soils reflect long-term deposition into soils, or recent inputs (top box), and also whether the dominant signal observed in soils represents a more regional or more local source (bottom box).

8.2 Chapter 3: Experimental modification of n-alkane signals in soils

In Chapter 3, I used controlled experiments to examine the effects of microbial activity on leaf wax *n*-alkane signals in soils (Fig. 2). This experimental analysis allows for the isolation of microbial activity at the time of *n*-alkane deposition by incubating soils mixed with organic composts. By doing this, I eliminate the effects of herbivory on the leaves that the *n*-alkanes are sourced from, and examine *n*-alkanes that are no longer associated with leaf tissue. This work builds on the existing body of work utilising litter bags by examining of the effects of post-depositional modification directly after deposition. This work enables us to determine the reliability of *n*-alkane signals in soils and sediments when using them for palaeoenvironmental research.

Figure 4. An incubation vessel containing chromosol soil and organic amendment (image courtesy of CSIRO).

8.3 Chapter 4: Environmental reconstruction during megafaunal extinction in Australia

To address the issue of megafaunal extinction related to environmental change, in Chapter 4, I reconstruct environmental conditions at the time of the megafauna extinction in Australia at around 40 ka by examining leaf wax *n*-alkane signals preserved in cave sediments containing megafauna fossils. The Blanche Cave infill sedimentary sequence from Naracoorte in south eastern Australia (Fig 3.) spans 70 – 17 ka, during which time megafauna fossils abruptly disappear from the sequence. Analysis of the isotopic composition of leaf wax *n*-alkanes in these sediments allows for a direct comparison of vegetation and hydrological conditions before, during and after megafauna extinction in Naracoorte.

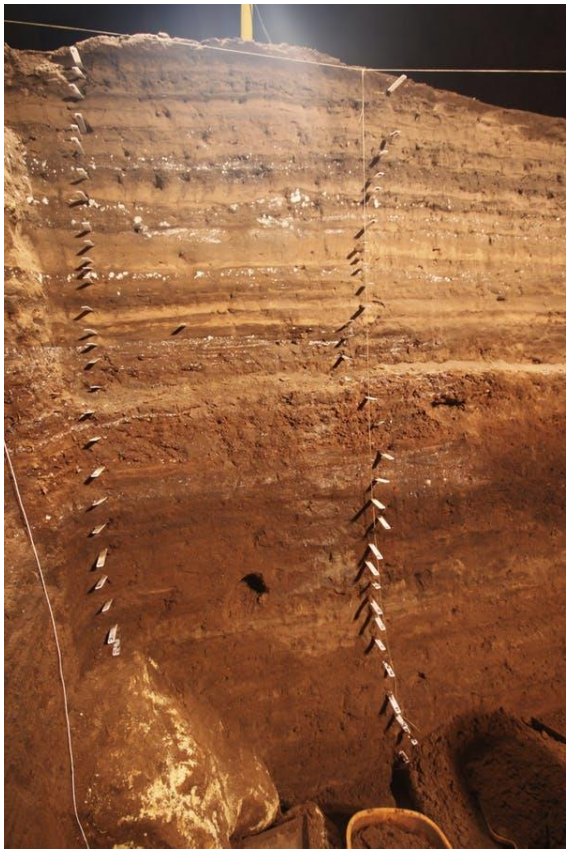

Figure 3. Pit excavation showing the layered sedimentary deposit in Blanche Cave, Naracoorte. The tags indicate the separate layers sampled for analysis (Photo taken by Steven Bourne and provided by Elizabeth Reed).

8.4 Chapter 5: Thesis discussion

Chapter 5 provides a synthesis of how this body of work fits into the broader context of prior research examining the delivery and modification of leaf wax *n*-alkanes in soils and their use in palaeoenvironmental reconstruction. It examines a number of questions that this work has raised, and suggests future opportunities to build on this body of work.

References

ANDRAE J. W., MCINERNEY F. A., POLISSAR P. J., SNIDERMAN J. M. K., HOWARD S., HALL P. A. & PHELPS S. R. 2018. Initial Expansion of C4 Vegetation in Australia During the Late Pliocene, *Geophysical Research Letters*. **45**, 4831-4840.

BANTHORPE D. V. 2006 Natural Occurrence, Biochemistry and Toxicology. Alkanes and Cycloalkanes (1992). pp. 895-926. John Wiley & Sons, Ltd,

BARNOSKY A. D., HADLY E. A., GONZALEZ P., HEAD J., POLLY P. D., LAWING A. M., ERONEN J. T., ACKERLY D. D., ALEX K., BIBER E., BLOIS J., BRASHARES J., CEBALLOS G., DAVIS E., DIETL G. P., DIRZO R., DOREMUS H., FORTELIUS M., GREENE H. W., HELLMANN J., HICKLER T., JACKSON S. T., KEMP M., KOCH P. L., KREMEN C., LINDSEY E. L., LOOY C., MARSHALL C. R., MENDENHALL C., MULCH A., MYCHAJLIW A. M., NOWAK C., RAMAKRISHNAN U., SCHNITZLER J., DAS SHRESTHA K., SOLARI K., STEGNER L., STEGNER M. A., STENSETH N. C., WAKE M. H. & ZHANG Z. 2017. Merging paleobiology with conservation biology to guide the future of terrestrial ecosystems, *Science*. **355**.

BIRD M. I., HUTLEY L. B., LAWES M. J., LLOYD J., LULY J. G., RIDD P. V., ROBERTS R. G., ULM S. & WURSTER C. M. 2013. Humans, megafauna and environmental change in tropical Australia, *Journal of Quaternary Science*. **28**, 439-452.

BRINCAT D., YAMADA K., ISHIWATARI R., UEMURA H. & NARAOKA H. 2000. Molecular-isotopic stratigraphy of long-chain n-alkanes in Lake Baikal Holocene and glacial age sediments, *Organic Geochemistry*. **31**, 287-294.

BRITTINGHAM A., HREN M. T. & HARTMAN G. 2017. Microbial alteration of the hydrogen and carbon isotopic composition of n-alkanes in sediments, *Organic Geochemistry*. **107**, 1-8.

BUSH R. T. & MCINERNEY F. A. 2013. Leaf wax *n*-alkane distributions in and across modern plants: Implications for paleoecology and chemotaxonomy, *Geochimica et Cosmochimica Acta*. **117**, 161-179.

--- 2015. Influence of temperature and C4 abundance on *n*-alkane chain length distributions across the central USA, *Organic Geochemistry*. **79**, 65-73.

CARR A. S., BOOM A., GRIMES H. L., CHASE B. M., MEADOWS M. E. & HARRIS A. 2014. Leaf wax *n*-alkane distributions in arid zone South African flora: Environmental controls, chemotaxonomy and palaeoecological implications, *Organic Geochemistry*. **67**, 72-84.

CERNUSAK L. A., BARBOUR M. M., ARNDT S. K., CHEESMAN A. W., ENGLISH N. B., FEILD T. S., HELLIKER B. R., HOLLOWAY-PHILLIPS M. M., HOLTUM J. A. M., KAHMEN A., MCINERNEY F. A., MUNKSGAARD N. C., SIMONIN K. A., SONG X., STUART-WILLIAMS H., WEST J. B. & FARQUHAR G. D. 2016. Stable isotopes in leaf water of terrestrial plants, *Plant, Cell & Environment*. **39**, 1087-1102.

CHIKARAISHI Y. & NARAOKA H. 2003. Compound-specific δD–δ13C analyses of n-alkanes extracted from terrestrial and aquatic plants, *Phytochemistry*. **63**, 361-371.

COLLISTER J. W., RIELEY G., STERN B., EGLINTON G. & FRY B. 1994. Compound-specific δ 13C analyses of leaf lipids from plants with differing carbon dioxide metabolisms, *Organic Geochemistry*. **21**, 619-627.

COOPER A., TURNEY C., HUGHEN K. A., BROOK B. W., MCDONALD H. G. & BRADSHAW C. J. A. 2015. Abrupt warming events drove Late Pleistocene Holarctic megafaunal turnover, *Science*.

DESMARCHELIER J. M., GOEDE A., AYLIFFE L. K., MCCULLOCH M. T. & MORIARTY K. 2000. Stable isotope record and its palaeoenvironmental interpretation for a late Middle Pleistocene speleothem from Victoria Fossil Cave, Naracoorte, South Australia, *Quaternary Science Reviews*. **19**, 763-774.

DIEFENDORF A. F., FREEMAN K. H., WING S. L. & GRAHAM H. V. 2011. Production of n-alkyl lipids in living plants and implications for the geologic past, *Geochimica et Cosmochimica Acta*. **75**, 7472-7485.

DIEFENDORF A. F. & FREIMUTH E. J. 2017. Extracting the most from terrestrial plant-derived *n*-alkyl lipids and their carbon isotopes from the sedimentary record: A review, *Organic Geochemistry*. **103**, 1-21.

DIETL G. P., KIDWELL S. M., BRENNER M., BURNEY D. A., FLESSA K. W., JACKSON S. T. & KOCH P. L. 2015. Conservation Paleobiology: Leveraging Knowledge of the Past to Inform Conservation and Restoration, *Annual Review of Earth and Planetary Sciences*. **43**, 79-103.
DODD R. S. & POVEDA M. M. 2003. Environmental gradients and population divergence contribute to variation in cuticular wax composition in Juniperus communis, *Biochemical Systematics and Ecology*. **31**, 1257-1270.
DOUGLAS P. M. J., PAGANI M., BRENNER M., HODELL D. A. & CURTIS J. H. 2012. Aridity and vegetation composition are important determinants of leaf-wax δD values in southeastern Mexico and Central America, *Geochimica et Cosmochimica Acta*. **97**, 24-45.
EGLINTON G. & HAMILTON R. J. 1967. Leaf Epicuticular Waxes, *Science*. **156**, 1322-1335.
EGLINTON T. I. & EGLINTON G. 2008. Molecular proxies for paleoclimatology, *Earth and Planetary Science Letters*. **275**, 1-16.
EHLERINGER J. R., CERLING T. E. & HELLIKER B. R. 1997. C4 photosynthesis, atmospheric CO2, and climate, *Oecologia*. **112**, 285-299.
EIGENBRODE S. D. & ESPELIE K. E. 1995. Effects of Plant Epicuticular Lipids on Insect Herbivores, *Annual Review of Entomology*. **40**, 171-194.
FARQUHAR G. D., EHLERINGER J. R. & HUBICK K. T. 1989. Carbon Isotope Discrimination and Photosynthesis, *Annual Review of Plant Physiology and Plant Molecular Biology*. **40**, 503-537.
GAMARRA B. & KAHMEN A. 2015. Concentrations and δ2H values of cuticular n-alkanes vary significantly among plant organs, species and habitats in grasses from an alpine and a temperate European grassland, *Oecologia*. **178**, 981-998.
GARCIN Y., SCHWAB V. F., GLEIXNER G., KAHMEN A., TODOU G., SÉNÉ O., ONANA J.-M., ACHOUNDONG G. & SACHSE D. 2012. Hydrogen isotope ratios of lacustrine sedimentary n-alkanes as proxies of tropical African hydrology: Insights from a calibration transect across Cameroon, *Geochimica et Cosmochimica Acta*. **79**, 106-126.
GARCIN Y., SCHEFUß E., SCHWAB V. F., GARRETA V., GLEIXNER G., VINCENS A., TODOU G., SÉNÉ O., ONANA J.-M., ACHOUNDONG G. & SACHSE D. 2014. Reconstructing C3 and C4 vegetation cover using n-alkane carbon isotope ratios in recent lake sediments from Cameroon, Western Central Africa, *Geochimica et Cosmochimica Acta*. **142**, 482-500.
HELLMANN J. J. & PFRENDER M. E. 2011. Future Human Intervention in Ecosystems and the Critical Role for Evolutionary Biology, *Conservation Biology*. **25**, 1143-1147.
HOFFMANN B., KAHMEN A., CERNUSAK L. A., ARNDT S. K. & SACHSE D. 2013. Abundance and distribution of leaf wax *n*-alkanes in leaves of Acacia and Eucalyptus trees along a strong humidity gradient in northern Australia, *Organic Geochemistry*. **62**, 62-67.
HUANG Y., STREET-PERROTT F. A., METCALFE S. E., BRENNER M., MORELAND M. & FREEMAN K. H. 2001. Climate change as the dominant control on glacial-interglacial variations in C3 and C4 plant abundance, *Science*. **293**, 1647-1651.
HUGHEN K. A. E. T. I. X. L. M. 2004. Abrupt Tropical Vegetation Response to Rapid ClimateChanges, *Science*. **304**, 1955-1959.
IPCC 2014 Climate Change 2014: Synthesis Report. Contribution of Working Groups I, II and III to the Fifth Assessment Report of the Intergovernmental Panel on Climate Change. pp. 151. [Core Writing Team, R.K. Pachauri and L.A. Meyer (eds.)], IPCC, Geneva, Switzerland.
JETTER R. & RIEDERER M. 2016. Localization of the Transpiration Barrier in the Epi- and Intracuticular Waxes of Eight Plant Species: Water Transport Resistances Are Associated with Fatty Acyl Rather Than Alicyclic Components, *Plant Physiology*. **170**, 921-934.
JOHNSON C. N., ALROY J., BEETON N. J., BIRD M. I., BROOK B. W., COOPER A., GILLESPIE R., HERRANDO-PÉREZ S., JACOBS Z., MILLER G. H., PRIDEAUX G. J., ROBERTS R. G., RODRÍGUEZ-REY M., SALTRÉ F., TURNEY C. S. M. & BRADSHAW C. J. A. 2016. What caused extinction of the pleistocene megafauna of sahul?, *Proceedings of the Royal Society B: Biological Sciences*. **283**, 1-8.
KAHMEN A., HOFFMANN B., SCHEFUß E., ARNDT S. K., CERNUSAK L. A., WEST J. B. & SACHSE D. 2013. Leaf water deuterium enrichment shapes leaf wax n-alkane δD values of angiosperm plants

II: Observational evidence and global implications, *Geochimica et Cosmochimica Acta*. **111**, 50-63.

LI R., FAN J., XUE J. & MEYERS P. A. 2017. Effects of early diagenesis on molecular distributions and carbon isotopic compositions of leaf wax long chain biomarker n-alkanes: Comparison of two one-year-long burial experiments, *Organic Geochemistry*. **104**, 8-18.

LOPES DOS SANTOS R. A., DE DECKKER P., HOPMANS E. C., MAGEE J. W., METS A., SINNINGHE DAMSTE J. S. & SCHOUTEN S. 2013. Abrupt vegetation change after the Late Quaternary megafaunal extinction in southeastern Australia, *Nature Geosci*. **6**, 627-631.

MICHENER R. H. & LAJTHA K. 2007 Stable isotopes in ecology and environmental science. (2nd ed. edition). Blackwell Publishing, USA.

NGUYEN TU T. T., EGASSE C., ZELLER B., BARDOUX G., BIRON P., PONGE J. F., DAVID B. & DERENNE S. 2011. Early degradation of plant alkanes in soils: A litterbag experiment using 13C-labelled leaves, *Soil Biology and Biochemistry*. **43**, 2222-2228.

NIEDERMEYER E. M., FORREST M., BECKMANN B., SESSIONS A. L., MULCH A. & SCHEFUß E. 2016. The stable hydrogen isotopic composition of sedimentary plant waxes as quantitative proxy for rainfall in the West African Sahel, *Geochimica et Cosmochimica Acta*. **184**, 55-70.

POLISSAR P. J. & FREEMAN K. H. 2010. Effects of aridity and vegetation on plant-wax δD in modern lake sediments, *Geochimica et Cosmochimica Acta*. **74**, 5785-5797.

PRIDEAUX G. J., GULLY G. A., COUZENS A. M. C., AYLIFFE L. K., JANKOWSKI N. R., JACOBS Z., ROBERTS R. G., HELLSTROM J. C., GAGAN M. K. & HATCHER L. M. 2010. Timing and dynamics of Late Pleistocene mammal extinctions in southwestern Australia, *Proceedings of the National Academy of Sciences*. **107**, 22157-22162.

PU Y., ZHANG H., WANG Y., LEI G., NACE T. & ZHANG S. 2011. Climatic and environmental implications from *n*-alkanes in glacially eroded lake sediments in Tibetan Plateau: An example from Ximen Co, *Chinese Science Bulletin*. **56**, 1503-1510.

ROMMERSKIRCHEN F., EGLINTON G., DUPONT L. & RULLKÖTTER J. 2006a. Glacial/interglacial changes in southern Africa: Compound-specific $\delta^{13}C$ land plant biomarker and pollen records from southeast Atlantic continental margin sediments, *Geochemistry, Geophysics, Geosystems*. **7**, p.DOI: 10.1029/2005GC001223.

ROMMERSKIRCHEN F., PLADER A., EGLINTON G., CHIKARAISHI Y. & RULLKÖTTER J. 2006b. Chemotaxonomic significance of distribution and stable carbon isotopic composition of long-chain alkanes and alkan-1-ols in C4 grass waxes, *Organic Geochemistry*. **37**, 1303-1332.

SACHSE D., RADKE J. & GLEIXNER G. 2004. Hydrogen isotope ratios of recent lacustrine sedimentary *n*-alkanes record modern climate variability, *Geochimica et Cosmochimica Acta*. **68**, 4877-4889.

SACHSE D., BILLAULT I., BOWEN G. J., CHIKARAISHI Y., DAWSON T. E., FEAKINS S. J., FREEMAN K. H., MAGILL C. R., MCINERNEY F. A., VAN DER MEER M. T. J., POLISSAR P., ROBINS R. J., SACHS J. P., SCHMIDT H.-L., SESSIONS A. L., WHITE J. W. C., WEST J. B. & KAHMEN A. 2012. Molecular Paleohydrology: Interpreting the Hydrogen-Isotopic Composition of Lipid Biomarkers from Photosynthesizing Organisms, *Annual Review of Earth and Planetary Sciences*. **40**, 221-249.

SAGE R. F., WEDIN D. A. & MEIRONG L. 1999 The biogeography of C4 photosynthesis: Patterns and controlling factors. *In* SAGE R. F. & MONSON R. K. eds. C4 Plant Biology. pp. 313-373. Academic Press,

SALTRE F., RODRIGUEZ-REY M., BROOK B. W., JOHNSON C. N., TURNEY C. S. M., ALROY J., COOPER A., BEETON N., BIRD M. I., FORDHAM D. A., GILLESPIE R., HERRANDO-PEREZ S., JACOBS Z., MILLER G. H., NOGUES-BRAVO D., PRIDEAUX G. J., ROBERTS R. G. & BRADSHAW C. J. A. 2016. Climate change not to blame for late Quaternary megafauna extinctions in Australia, *Nat Commun*. **7**.

SCHMIDT M. W. I., TORN M. S., ABIVEN S., DITTMAR T., GUGGENBERGER G., JANSSENS I. A., KLEBER M., KOGEL-KNABNER I., LEHMANN J., MANNING D. A. C., NANNIPIERI P., RASSE D. P., WEINER S. & TRUMBORE S. E. 2011. Persistence of soil organic matter as an ecosystem property, *Nature*. **478**, 49-56.

SCHWAB V. F., GARCIN Y., SACHSE D., TODOU G., SÉNÉ O., ONANA J.-M., ACHOUNDONG G. & GLEIXNER G. 2015. Effect of aridity on δ13C and δD values of C3 plant- and C4 graminoid-derived leaf wax lipids from soils along an environmental gradient in Cameroon (Western Central Africa), *Organic Geochemistry*. **78**, 99-109.

SCHWARK L., ZINK K. & LECHTERBECK J. 2002. Reconstruction of postglacial to early Holocene vegetation history in terrestrial Central Europe via cuticular lipid biomarkers and pollen records from lake sediments, *Geology*. **30**, 463-466.

SHEPHERD T. & WYNNE GRIFFITHS D. 2006. The effects of stress on plant cuticular waxes, *New Phytologist*. **171**, 469-499.

SMITH F. A. & FREEMAN K. H. 2006. Influence of physiology and climate on δD of leaf wax n-alkanes from C3 and C4 grasses, *Geochimica et Cosmochimica Acta*. **70**, 1172-1187.

SMITH F. A., WING S. L. & FREEMAN K. H. 2007. Magnitude of the carbon isotope excursion at the Paleocene–Eocene thermal maximum: The role of plant community change, *Earth and Planetary Science Letters*. **262**, 50-65.

STRÖMBERG C. A. E. 2011. Evolution of Grasses and Grassland Ecosystems, *Annual Review of Earth and Planetary Sciences*. **39**, 517-544.

TIPPLE B. J., BERKE M. A., DOMAN C. E., KHACHATURYAN S. & EHLERINGER J. R. 2013. Leaf-wax n-alkanes record the plant–water environment at leaf flush, *Proceedings of the National Academy of Sciences of the United States of America*. **110**, 2659-2664.

UNITED NATIONS 2017 World Population Prospects: The 2017 Revision, Volume II: Demographic Profiles (ST/ESA/SER.A/400). Department of Economic and Social Affairs, Population Division.

VAN DER KAARS S., MILLER G. H., TURNEY C. S. M., COOK E. J., NÜRNBERG D., SCHÖNFELD J., KERSHAW A. P. & LEHMAN S. J. 2017. Humans rather than climate the primary cause of Pleistocene megafaunal extinction in Australia, *Nature Communications*. **8**, p.14142.

YAMAMOTO S., HASEGAWA T., TADA R., GOTO K., ROJAS-CONSUEGRA R., DÍAZ-OTERO C., GARCÍA-DELGADO D. E., YAMAMOTO S., SAKUMA H. & MATSUI T. 2010. Environmental and vegetational changes recorded in sedimentary leaf wax *n*-alkanes across the Cretaceous–Paleogene boundary at Loma Capiro, Central Cuba, *Palaeogeography, Palaeoclimatology, Palaeoecology*. **295**, 31-41.

CHAPTER 2

Modelling leaf wax *n*-alkane inputs to soils along a latitudinal transect across Australia

Howard, S.[a], McInerney, F.A.[a], Caddy-Retalic, S.[b,c], Hall, P.A.[a], Andrae, J.W.[a]

[a]*University of Adelaide, Sprigg Geobiology Centre and School of Physical Sciences*

[b]*University of Adelaide, School of Biological Sciences*

[c]*University of Sydney, School of Life and Environmental Sciences*

Statement of Authorship

Title of Paper	Modelling leaf wax *n*-alkane inputs to soils along a latitudinal transect across Australia
Publication Status	☑ Published ☐ Accepted for Publication ☐ Submitted for Publication ☐ Unpublished and Unsubmitted work written in manuscript style
Publication Details	Howard, S., McInerney, F.A., Caddy-Retalic, S., Hall, P.A., Andrae, J.W., 2018. Modelling leaf wax *n*-alkane inputs to soils along a latitudinal transect across Australia. Organic Geochemistry 121, 126-137.

Principal Author

Name of Principal Author (Candidate)	Siân Howard		
Contribution to the Paper	Designed the study. Conducted sample processing and analysis. Conducted data analysis and interpretation. Wrote manuscript.		
Overall percentage (%)	75		
Certification:	This paper reports on original research I conducted during the period of my Higher Degree by Research candidature and is not subject to any obligations or contractual agreements with a third party that would constrain its inclusion in this thesis. I am the primary author of this paper.		
Signature		Date	13/12/2018

Co-Author Contributions

By signing the Statement of Authorship, each author certifies that:

i. the candidate's stated contribution to the publication is accurate (as detailed above);

ii. permission is granted for the candidate in include the publication in the thesis; and

iii. the sum of all co-author contributions is equal to 100% less the candidate's stated contribution.

Name of Co-Author	Dr Francesca A. McInerney		
Contribution to the Paper	Supervised SH. Designed the study. Provided input into data analysis, interpretation and manuscript. Reviewed and edited final manuscript.		
Signature		Date	13/12/2018

Name of Co-Author	Dr Stefan Caddy-Retalic		
Contribution to the Paper	Provided advice on sample context. Reviewed and edited final manuscript.		
Signature		Date	14/12/2018

Name of Co-Author	Dr Philip A. Hall		
Contribution to the Paper	Provided GC-MS quantification of samples. Reviewed and edited final manuscript.		
Signature		Date	13/12/2018

Name of Co-Author	Jake Andrae		
Contribution to the Paper	Provided assistance with data analysis. Reviewed and edited final manuscript.		
Signature		Date	14/12/2018

Abstract

Leaf wax *n*-alkanes provide a valuable palaeoecological proxy, but their interpretation requires an understanding of the scale of temporal and spatial integration in soils. Leaf wax *n*-alkanes are continually deposited into soils directly from local plants as well as from more distant plants via wind or water transport. In addition, *n*-alkanes can persist in soils for thousands of years, and tend to decrease in age at shallower depth. To explore whether the uppermost soils reflect recent leaf fall inputs we compare surface soils and modern vegetation from 20 sites along a transect across Australia. At each site, the three most dominant plant species and a soil sample from the top 3 cm were analysed for *n*-alkane concentration, average chain length (ACL), proportional abundance of C_{33} and C_{29} (Norm33) and carbon preference index (CPI). Chain length distributions differ between trees and grasses, with a higher proportion of C_{29} in trees and C_{33} in grasses. Norm33 in soils correlates with proportional grass to tree cover across the transect. To model *n*-alkane inputs for each site, we calculated a predicted ACL, Norm33 and CPI using the dominant plants at that site, weighted by proportional species cover and *n*-alkane concentration. Predicted ACL, Norm33 and CPI inputs are generally higher than the soils, demonstrating that recent and local inputs do not dominate soil *n*-alkanes at our study sites. Thus, *n*-alkane distributions in surface soils do not correlate with local, current vegetation, but do correlate with proportional grass and tree cover, suggesting they provide a faithful record of large scale ecosystems structure.

Keywords

Leaf wax, *n*-alkanes, Average Chain Length, Carbon Preference Index, soils, palaeoecology, vegetation reconstruction.

1. Introduction

Plant waxes provide critical protection for leaves by limiting non-stomatal water loss from the leaf surface (Eglinton and Hamilton 1967, Dodd and Poveda 2003, Jetter and Riederer 2016), protecting against damage from UV radiation (Shepherd and Wynne Griffiths 2006, Koch et al. 2009), and resisting fungal infection and herbivory (Eigenbrode and Espelie 1995, Banthorpe 2006). Plant waxes contain a range of compounds, including long chain *n*-alkanes, which are non-polar, unbranched, straight chained hydrocarbons (Eglinton and Hamilton 1967, Banthorpe 2006). Long chained, odd-numbered *n*-alkanes (C_{25} – C_{35}) are produced nearly exclusively as part of the waxes of terrestrial plants (Eglinton and Hamilton 1967). Plants generally produce greater quantities of odd than even chain lengths due to synthesis by sequential elongation or condensation of a C_2 primer, where even-numbered fatty acid chains become decarboxylated to produce odd chain length alkanes (Khan and Kolattukudy 1974, Shepherd and Wynne Griffiths 2006). Higher plants produce different distributions of chain lengths that range between C_{25} to C_{35} (Sachse et al. 2004, Pu et al. 2011, Bush and McInerney 2013). The majority of plant wax *n*-alkanes in soils and sediments should derive from leaves due to the high proportional biomass of leaves, and the high concentrations of *n*-alkanes in leaves relative to other plant organs (Gamarra and Kahmen 2015). Roots can contribute *n*-alkanes to the soil directly, but their concentration is one or two orders of magnitude less than leaves and thus they are unlikely to be the dominant source of *n*-alkane signals in surface soils (Gamarra and Kahmen 2015, Angst et al. 2016, Jansen and Wiesenberg 2017).There is some evidence that insects also produce long chain *n*-alkanes with an odd-over-even predominance, however their biomass is orders of magnitude less than that of terrestrial plants and

their annual *n*-alkane production rate is unquantified, so their contribution to soils and sediments is considered negligible in comparison to plants (Chikaraishi et al. 2012).

Plant lipid biomarkers, such as leaf wax *n*-alkanes, are very common in the sedimentary record, compared to macrofossils which are comparatively rare. Leaf wax *n*-alkanes are valuable recorders of past vegetation (Eglinton and Eglinton 2008, Diefendorf and Freimuth 2017) and can be distinguished from petroleum sources by their odd-over-even predominance (Eglinton and Hamilton 1967, Yamamoto and Kawamura 2010). However, to interpret the signatures preserved in sediments, we must understand how sedimentary leaf wax *n*-alkanes reflect the vegetation both temporally and spatially (Diefendorf and Freimuth 2017).

Direct ^{14}C dating suggests that leaf wax *n*-alkanes can be pre-aged in soils for hundreds to thousands of years prior to remobilisation and transport to lacustrine and marginal marine sediments (Smittenberg et al. 2006, Drenzek et al. 2007, Douglas et al. 2014, Gierga et al. 2016), resulting in potentially highly time averaged *n*-alkane accumulations. Once buried in sediments, *n*-alkanes can persist for millions of years and have been extracted from Cretaceous-Paleogene boundary (Yamamoto et al. 2010), Paleocene–Eocene (Smith et al. 2007), Miocene (Huang et al. 2001) and Holocene sediments (Schwark et al. 2002).

Although *n*-alkanes can persist for thousands of years in deeper subsoils and millions of years in buried sediments, analyses of modern soils demonstrates that more recent *n*-alkane inputs dominate near the soil surface (Angst et al. 2016). Direct ^{14}C dating of *n*-alkanes and soil organic carbon in soils and lake sediments shows increasing age with depth (Huang et al. 1996, Angst et al. 2016, Gierga et al. 2016). Makou *et al.* (2018) found ^{14}C dating of long, odd chain length *n*-alkanes in a surface soil indicated a pool of pre-aged *n*-alkanes attributed to erosional inputs from adjacent slopes, however

the dominant chain length present in the soil, C_{27}, was modern in age and attributed to inputs of fresh leaf waxes from nearby beech trees. Therefore, surface soils appear to be the least time-averaged, and predominantly represent the most recent *n*-alkane inputs.

Leaf fall and breakdown of leaf litter represents direct *n*-alkane deposition to soils (Cranwell 1981, Lichtfouse et al. 1998), resulting in soil *n*-alkane signatures representative of local sources. Previous work examining the relationship between chain length and biome type showed that the chain length distributions associated with the plants were similar to those in the soils of those respective biomes (Carr et al. 2014). However, leaf wax *n*-alkanes are also readily ablated and wind-dispersed, which would lead soil deposits to represent a regional catchment area (van Gardingen et al. 1991, Gao et al. 2012). Wind-blown *n*-alkanes can travel as far as between continents (Bendle et al. 2007, Yamamoto and Kawamura 2010, Nelson et al. 2017) and are primarily deposited with particulates scrubbed from the atmosphere by precipitation (Meyers and Hites 1982, Diefendorf and Freimuth 2017). Similarly, water can transport leaf wax *n*-alkanes long distances via streams, rivers and runoff, either by moving fallen leaves or deposited particulate matter (Rouillard et al. 2016, Diefendorf and Freimuth 2017). The relative importance of these processes in delivering *n*-alkanes to soils will determine whether soil records represent a regional or more localized vegetation sample (Jansen and Wiesenberg 2017).

Here, we test the hypothesis that *n*-alkane distributions in surface soils correlate with *n*-alkane distributions of current local vegetation. We sampled a latitudinal transect across Australia to capture a climatically and ecologically diverse set of sites (Fig. 1). The continent-wide transect spans from monsoonal tropics in the north to arid desert in the centre, to the winter-wet Mediterranean climate zone in the south. The biomes sampled include tropical and subtropical grasslands, savannas and shrublands

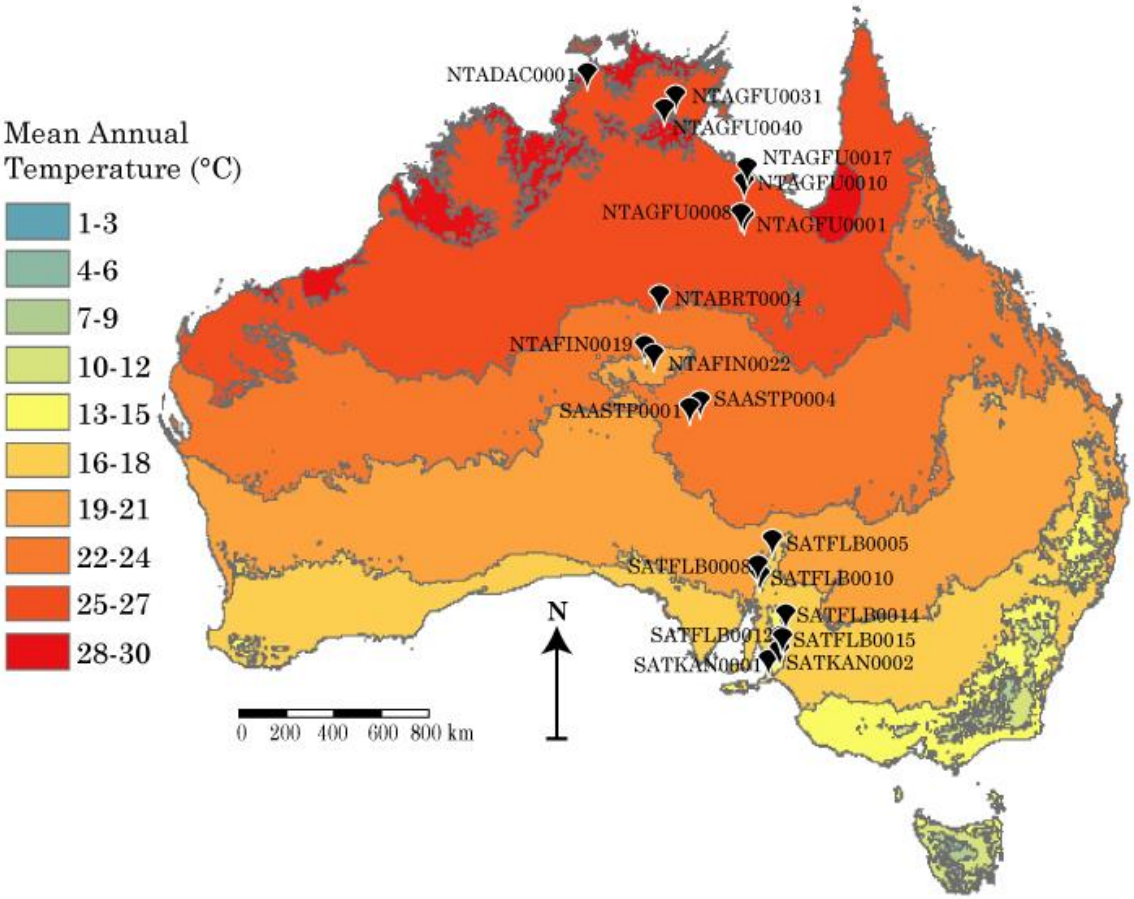

Figure 1. Location map of selected AusPlots sites (black pins) across Australia with mean annual temperature shown as context. Climate data based on a standard 30-year climatology (1961-1990) and reproduced with permission from Bureau of Meteorology (© Commonwealth of Australia).

in the north; desert and xeric shrublands in the centre; and Mediterranean shrublands and woodlands in the south (Supplementary Table S1, Appendix 1). At each site, we characterise the *n*-alkane abundance and distribution from the three most dominant plant species. At the vast majority of sites, the three dominant species represent the majority of the plant cover (Table 1). While it does not equate directly to biomass, dominant coverage provides us with a reasonable estimate of the dominant *n*-alkane contributors to the surface soils and improves on previous studies that sample plants without respect to their coverage in the landscape. Using the concentration and distribution of *n*-alkanes of the dominant vegetation to account for differences in production, we model their inputs to surface soils and compare them to the distributions measured from the soils (top 3 cm). The degree to which local and recent vegetation contributes to soil *n*-alkane signatures will determine how well our modelled inputs match our measured soil *n*-alkane distributions. This comparison provides a direct test of the hypothesis that the leaf wax *n*-alkane signals in surface soils are dominated by local and recent inputs rather than regional and/or long-term inputs. We also examine whether soil *n*-alkane distributions broadly reflect plant cover growth form (e.g. grasses versus trees) at each site. The results constrain the nature of delivery and turnover of *n*-alkane soils across a large and diverse transect, and provide bounds on the range of possible paradigms for the development of *n*-alkane records in soils.

2. Methods

2.1 Sample collection

Soil and plant samples were collected from 20 sites on a north-south transect across Australia (Fig. 1), using the AusPlots Rangelands survey methodology (White et al. 2012). These samples were collected by and made available for this research by

Australia's Terrestrial Ecosystem Research Network (TERN). The sites monitored by TERN are permanent plots where baseline surveys of soils and vegetation are conducted as a source of ongoing and long term ecosystem data for research (White et al. 2012). Sites analysed here were distributed through seven Australian bioregions (See Supplementary Table S1, Appendix 1 for descriptions). A single surface soil sample from the middle of each site, taken from a maximum of 3 cm depth (total n = 20), was selected for analysis after having been air dried and stored in calico. Soils were sieved with 1000 and 250 micron sieves to remove large plant material, such as leaves, bark and roots. Particle size percentages were determined using mid-infrared particle size analysis.

Proportional plant species cover and growth form cover was determined from point intercept data obtained from the online Soils2Satellites portal (www.soils2satellites.org.au). At each one hectare site, 1010 points were assessed and all vegetation occurrences were recorded (White et al. 2012). The total number of occurrences for each species and growth form was divided by the total number of vegetation occurrences per site to determine the proportional species cover and growth form (trees, grasses, forbs and shrubs, inclusive of chenopods) cover at each site.

$$\text{Proportional species cover} = \frac{\text{number of species occurrences}}{\text{total vegetation occurrences}} \quad (1)$$

$$\text{Proportional growth form cover} = \frac{\text{number of growth form occurrences}}{\text{total vegetation occurrences}} \quad (2)$$

Leaves from the three most dominant plant species, in terms of proportional species cover, were selected for analysis from each site, except for one site from which the two most dominant were available (total n = 59). The leaves were placed in gauze bags and dried on silica gel. The total proportional species cover that the three most dominant plant species represent ranges from 42 – 99% (Table 1).

2.2 Lipid extraction from plants

Dried plant samples were ground to a fine powder with a mortar and pestle in liquid nitrogen. Lipids were extracted from the ground plant samples in a 9:1 volume optima grade dichloromethane:methanol (DCM:MeOH) solvent mixture in a Soniclean 250TD sonicator. Sample weights ranged from 5.8 – 52.3 mg; with 51 of the 59 plant samples ≥ 50 mg. Excess solvent was evaporated from the total lipid extract (TLE) under nitrogen gas using a FlexiVap nitrogen blow down station.

2.3 Lipid extraction from soils

Lipid extraction of the < 250 μm soil fraction was conducted using a Thermo Scientific Dionex Accelerate Solvent Extractor (ASE) 350 using a 9:1 DCM:MeOH. Samples weights ranged from 4.5 – 26.6 g, with 15 of the 20 soils samples ≥ 10 mg. The ASE sequence was set to 100 °C with a 12 minute preheat, three static cycles of five minutes, and a rinse volume of 60%. Excess solvent was evaporated from the TLE under nitrogen gas.

2.4 n-Alkane purification

The polar and non-polar fractions of both the plant and the soil TLEs were separated through a silica gel glass short column by eluting them with 4 ml of hexane to

collect the non-polar, aliphatic hydrocarbon fraction, followed by 4 ml 1:1 DCM:MeOH eluent to collect the polar fraction, (modified from Bastow et al. 2007). The aliphatic hydrocarbon fraction was dried under nitrogen gas.

2.5 GC-MS Lipid Quantification

Quantification of *n*-alkanes was conducted using gas chromatography mass spectrometry (GC-MS) analysis of the non-polar lipid fraction. Analysis was performed on a Perkin Elmer Clarus 500 GC-MS with the following specifications: The capillary was an SGE CPSil-5MS, 30 m (length) x 0.25 mm (internal diameter) x 0.25 udf (phase thickness). The carrier gas was helium with a 1 ml/min constant flow. The injection temperature was 300 °C, with a temperature program of 50 °C (hold 1 minute), ramped at 8 °C/min to 340 °C (hold for 7.75 minutes). Injection was set to 1 µl in either split mode, with a 50:1 split for higher concentration samples, or pulsed splitless for low sample concentrations. Perkin Elmer Turbomass software was used for data interpretation and quantification of *n*-alkane homologues (C_{25} to C_{35}). 1-1'binaphthyl internal standard was added to each sample at a concentration of 1 µg/mL for quantification. Concentrations of *n*-alkanes were calculated from the response factor of each homologue against the internal standard plotted against a seven point calibration curve prepared and analysed in triplicate using known concentrations of a homologous suite of *n*-alkanes (C_7 to C_{40}) with the same 1 µg/mL 1-1' binaphthyl internal standard concentration ($r^2 > 0.96$).

2.6 Calculations

Relative abundances of *n*-alkane chain lengths were characterised by calculating average chain length (ACL):

$$\text{ACL} = \frac{(25C_{25}+27C_{27}+29C_{29}+31C_{31}+33C_{33}+35C_{35})}{(C_{25}+C_{27}+C_{29}+C_{31}+C_{33}+C_{35})} \quad (3)$$

Where C_x is the total concentration of each *n*-alkane with x carbon atoms.

Carbon preference index (CPI) for each sample was calculated using the equation:

$$\text{CPI} = \frac{[\sum_{\text{odd}}(C_{25-33})+\sum_{\text{odd}}(C_{27-35})]}{2(\sum_{\text{even}} C_{26-34})} \quad \text{Modified from Marzi et al. (1993)} \quad (4)$$

Where $\Sigma_{\text{odd}}C_{x\text{-}y}$ indicates the sum of all peak areas for *n*-alkanes with an odd carbon chain length from x-y inclusive and $\Sigma_{\text{even}}C_{a\text{-}b}$ is the sum of the peak area for *n*-alkanes with an even number of carbon chain lengths from a-b inclusive. Values where CPI > 1.5 were considered to represent an *n*-alkane source of primarily plant origin (Bush and McInerney 2013).

Predicted soil ACL was calculated as an average of the three dominant plant species' ACL, weighted by both proportional species cover (%cover) and concentration (conc):

$$\text{Predicted ACL} = \frac{(\%\text{cover}_1\times\text{conc}_1\times\text{ACL}_1)+(\%\text{cover}_2\times\text{conc}_2\times\text{ACL}_2)+(\%\text{cover}_3\times\text{conc}_3\times\text{ACL}_3)}{(\%\text{cover}_1\times\text{conc}_1)+(\%\text{cover}_2\times\text{conc}_2)+(\%\text{cover}_3\times\text{conc}_3)} \quad (5)$$

Predicted soil CPI was calculated as an average of the three dominant plant species' CPI, weighted by both species proportion (%cover) and concentration (conc):

$$\text{Predicted CPI} = \frac{(\%\text{cover}_1\times\text{conc}_1\times\text{CPI}_1)+(\%\text{cover}_2\times\text{conc}_2\times\text{CPI}_2)+(\%\text{cover}_3\times\text{conc}_3\times\text{CPI}_3)}{(\%\text{cover}_1\times\text{conc}_1)+(\%\text{cover}_2\times\text{conc}_2)+(\%\text{cover}_3\times\text{conc}_3)} \quad (6)$$

The proportional abundance of the C_{33} and C_{29} *n*-alkanes, termed Norm33, was calculated modified from Carr et al. (2014).

$$\text{Norm33} = \frac{CC_{33}}{(C_{29}+C_{33})} \quad (7)$$

where C_x is the total concentration of each *n*-alkane with x carbon atoms.

2.7 Statistical Analysis

Welch's t-tests were conducted using KaleidaGraph to examine the differences between the average ACL and Norm33 of the different plant growth forms and the soil. Least squares regression analysis was used to determine the strength of the relationships between the measured *n*-alkanes signals and plant growth form coverage, climate and particle size. Two-sided Kolmogorov-Smirnov tests were conducted using the ks.test function in base R (R Core Team 2018) and used to compare the relative proportions of different chain lengths in association with different plant growth forms.

2.8 Climate Data

Long-term site values for mean annual temperature (MAT), mean annual precipitation (MAP) and annual moisture index (MI), lowest quarter mean MI, highest period radiation and maximum temperature of the hottest month were extracted from ANUCLIM 6.1 layers of a 1960-2014 long term average (Xu and Hutchinson 2013) through the Atlas of Living Australia (www.ala.org.au).

3. Results

In the plants, C_{31} had the highest concentration in the majority of samples (Fig. 2a, Supplementary Table S2, Appendix 1). The ACL for plant samples ranged from 26.7 – 32.4, with a mean value of 30.4 ± 1.4 standard deviation (SD; Table 1). Concentrations of total *n*-alkanes in plants were generally less than 10 μg/mg dry weight, with the exception of three shrubs that ranged up to 50.88 μg/g dry weight (Supplementary Fig. S1, Appendix 1).

In the soils, C_{29} had the highest concentration in the majority of samples (Fig. 2b, Supplementary Table S3, Appendix 1). The measured ACL in the soils ranged from 27.4 – 30.9, with a mean value of 28.8 ± 0.9 SD (Table 2).

Table 1. Plant species sampled from each site, proportional species cover at each site, *n*-alkane concentration, ACL.

SITE	Latitude	Dominant Plant Species 1	Growth Form	% Cover	Total µg/mg (C25 to C35)	ACL	Dominant Plant Species 2	Growth Form	% Cover	Total µg/mg (C25 to C35)	ACL	Dominant Plant Species 3	Growth Form	% Cover	Total µg/mg (C25 to C35)	ACL	Total Site Plant Cover (%)
NTABRT 0004	-22.3	*Acacia aptaneura*	Shrub	55	11.84	32.1	*Aristida holathera*	Grass	24	1.33	32.4	*Triodia schinzii*	Grass	7.2	0.38	30.4	85.7
NTADAC 0001	-13.2	*Sorghum plumosum*	Grass	57	0.09	31.8	*Eucalyptus tetrodonta*	Tree	19	0.49	30.3	*Eucalyptus miniata*	Tree	7.8	0.38	29.9	84.3
NTAFIN 0019	-24.4	*Cenchrus ciliaris*	Grass	67	1.98	31.9	*Acacia estrophiolata*	Tree	19	5.63	30.4	*Enchylaena tomentosa*	Grass	2.3	1.37	29.3	88.4
NTAFIN 0022	-24.6	*Eremophila freelingii*	Shrub	50	50.88	30.2	*Enneapogon polyphyllus*	Grass	15	1.58	32.1	*Aristida contorta*	Grass	7.6	1.18	31.7	72
NTAGFU 0001	-18.9	*Aristida pruinosa*	Grass	17	0.58	30.8	*Enneapogon polyphyllus*	Grass	13	0.08	32.1	*Eucalyptus pruinosa*	Tree	13	0.04	27.6	42.22
NTAGFU 0008	-18.8	*Triodia pungens*	Grass	45	1.43	30.8	*Aristida contorta*	Grass	19	7.08	28.5	*Fimbristylis dichotoma*	Grass	14	0.5	32.1	78.2
NTAGFU 0010	-17.9	*Triodia pungens*	Grass	63	1.37	31.1	*Eucalyptus leucophloia*	Tree	36	0.33	30.7	N/A	N/A	N/A	N/A	N/A	99
NTAGFU 0017	-17.4	*Melaleuca viridiflora*	Shrub	31	0.08	28.2	*Chrysopogon fallax*	Grass	9.4	1	30.5	*Schizachyrium fragile*	Grass	7	0.09	31.5	47.6
NTAGFU 0031	-14.1	*Melaleuca viridiflora*	Shrub	30	0.71	31.1	*Schizachyrium pachyarthron*	Grass	28	0.13	31.1	*Petalostigma banksii*	Shrub	9.1	0.05	29.8	66.7
NTAGFU 0040	-14.7	*Acacia dimidiata*	Shrub	27	0.74	31.3	*Heteropogon contortus*	Grass	16	0.27	31.3	*Eucalyptus tectifica*	Tree	9.7	0.06	28.1	52.2
SAASTP 0001	-26.3	*Maireana aphylla*	Shrub	31	0.66	28.6	*Eragrostis setifolia*	Grass	12	0.25	31.1	*Acacia aneura var. tenuis*	Shrub	7.7	3.67	31.7	50.6
SAASTP 0004	-26.1	*Malvastrum americanum var. americanum*	Forb	26	1.72	29.6	*Rutidosis helichrysoides subsp.*	Forb	19	10.13	31.7	*Sida fubulifera*	Forb	12	5.06	32.2	55.8
SATFLB 0005	-31.3	*Dodonaea viscosa subsp. angustissima*	Shrub	22	20.02	28.9	*Eucalyptus flindersii*	Tree	19	0.48	26.7	*Chrysocephalum semipapposum*	Forb	13	5.08	30.5	53.6

Table 1 (cont.). Plant species sampled from each site, proportional species cover at each site, *n*-alkane concentration, ACL.

SITE	Latitude	Dominant Plant Species 1	Growth Form	% Cover	Total µg/mg (C25 to C35)	ACL	Dominant Plant Species 2	Growth Form	% Cover	Total µg/mg (C25 to C35)	ACL	Dominant Plant Species 3	Growth Form	% Cover	Total µg/mg (C25 to C35)	ACL	Total Site Plant Cover (%)
SATFLB 0008	-32.3	*Triodia scariosa*	Grass	45	0.13	30.2	*Cassinia laevis*	Shrub	23	1.3	30.3	*Casuarina pauper*	Shrub	12	2.51	31.3	79.6
SATFLB 0010	-32.8	*Eucalyptus odorata*	Tree	65	0.21	26.8	*Rhagodia paradoxa*	Shrub	9.9	0.33	30.2	*Enchylaena tomentosa var. tomentosa*	Shrub	6	0.3	30.5	81
SATFLB 0012	-34.9	*Allocasuarina muelleriana subsp.*	Shrub	42	6.16	31.1	*Hibbertia crinita*	Shrub	16	0.14	30	*Eucalyptus fasciculosa*	Tree	13	0.04	28.3	70.2
SATFLB 0014	-34	*Eucalyptus odorata*	Tree	33	0.32	29.8	*Xanthorrhoea quadrangulata*	Shrub	18	0.22	30.3	*Allocasuarina verticillata*	Shrub	14	4.96	31	64.5
SATFLB 0015	-34.9	*Eucalyptus obliqua*	Tree	60	1.1	28.2	*Lepidosperma semiteres*	Grass	8.3	0.49	31.1	*Hibbertia crinita*	Shrub	6.5	0.6	28.3	74.8
SATKAN 0001	-35.6	*Eucalyptus baxteri*	Tree	43	1.41	29.9	*Lepidosperma semiteres*	Grass	11	0.09	31.5	*Pultenaea involucrata*	Shrub	10	0.37	31.8	63.9
SATKAN 0002	-35.3	*Eucalyptus obliqua*	Tree	55	0.07	29.1	*Lepidosperma semiteres*	Grass	9.1	0.2	31.9	*Hakea rostrata*	Shrub	8.2	0.48	30.4	72

Table 2. Soil samples from each site. Predicted CPI and ACL modelled from the plants.

SITE	Total µg/mg (C_{25}-C_{35})	Measured CPI	Predicted CPI	Measured ACL	Predicted ACL
NTABRT 0004	0.017	6.0	14.6	30.9	32.1
NTADAC 0001	0.341	1.3	3.3	27.8	30.7
NTAFIN 0019	0.0004	5.8	23.9	29.6	31.2
NTAFIN 0022	0.224	1.1	1.9	27.9	30.2
NTAGFU 0001	0.006	3.6	3.1	30.0	30.8
NTAGFU 0008	0.003	3.6	14.3	29.8	29.4
NTAGFU 0010	0.028	6.1	42.8	29.9	31.1
NTAGFU 0017	0.044	3.4	4.7	28.1	30.1
NTAGFU 0031	0.002	2.2	2.1	29.3	31.1
NTAGFU 0040	0.022	4.5	4.7	29.4	31.3
SAASTP 0001	0.125	1.4	13.2	27.4	30.4
SAASTP 0004	0.002	1.2	8.2	28.2	31.5
SATFLB 0005	0.16	2.1	3.3	28.2	29.0
SATFLB 0008	0.113	1.9	4.6	28.5	30.8
SATFLB 0010	0.141	1.9	2.2	28.2	27.7
SATFLB 0012	0.001	1.8	31.6	28.2	31.1
SATFLB 0014	0.005	2.5	48.7	29.0	30.8
SATFLB 0015	0.005	4.9	4.8	27.8	28.4
SATKAN 0001	0.339	6.4	5.6	28.6	30.0
SATKAN 0002	0.007	3.3	36.3	28.1	30.1

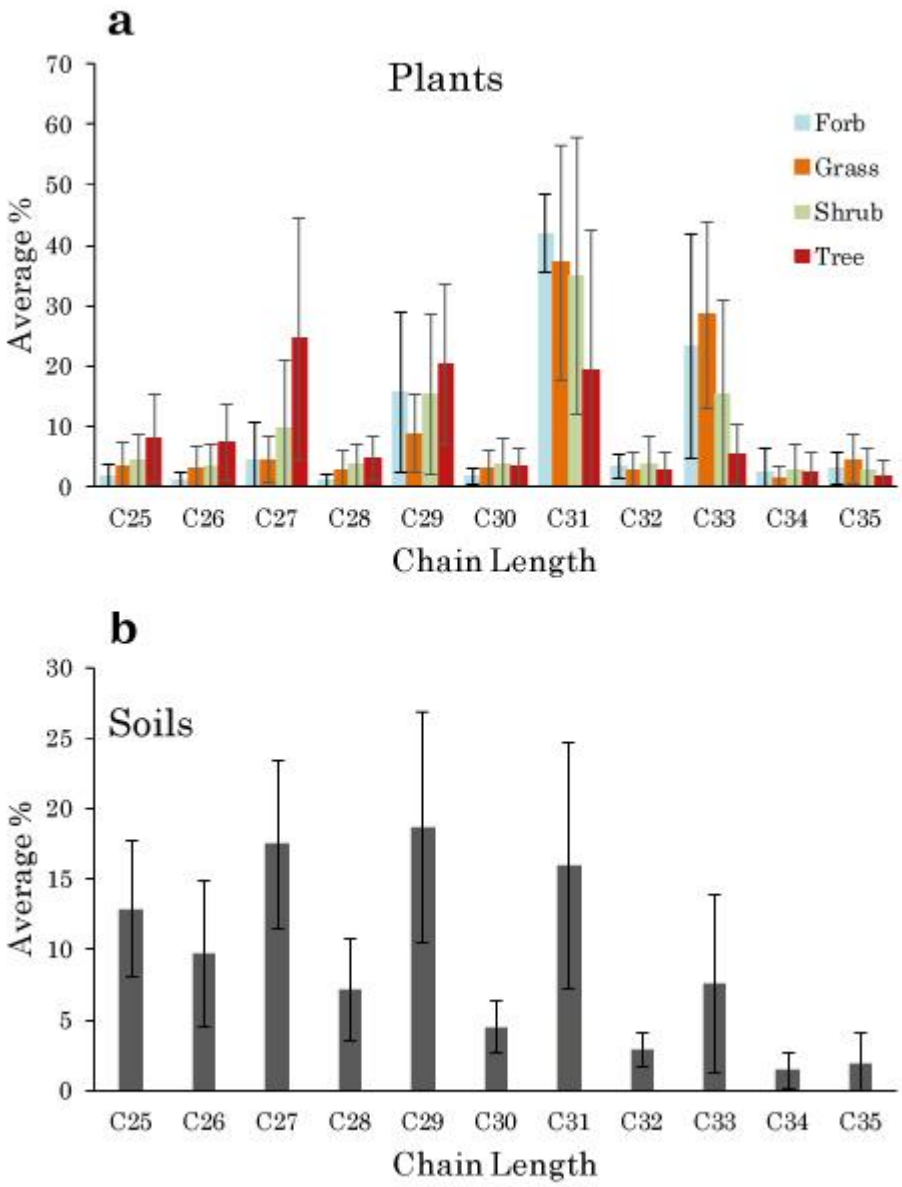

Figure 2. Relative abundance of *n*-alkanes from (a) plants, separated into their different growth forms and (b) soils displayed as average percentage for each chain length relative to total *n*-alkanes (C_{25}-C_{35}). Error bars represent one standard deviation.

The average ACL of trees was 28.9 ± 1.4 SD (n = 13) and was lower and significantly different to that of forbs (31.0 ± 1.2 SD, n = 4, p = 0.02), grasses (31.2 ± 0.9 SD, n = 22, p < 0.0001), and shrubs (30.3 ± 1.2 SD, n = 20, p = 0.005 inclusive of

chenopods) (Fig. 3a). No other pair-wise comparisons between plant growth form and between plants and soils were statistically distinguishable ($p > .0.5$) (Fig. 3a).

From north to south, tree cover increased and grass cover decreased (Fig. 4). The measured soil ACL showed a weak but statistically significant positive correlation with grass cover ($R^2 = 0.265$, $p = 0.02$) and no relationship with tree cover ($R^2 = 0.04$, $p = 0.4$) (Fig. 5a and b).

The average Norm33 of trees was 0.209 ± 0.177 SD (n = 13) and was lower and significantly different to that of grasses (0.712 ± 0.244 SD, n = 22, $p < 0.0001$), and shrubs (0.465 ± 0.465 SD, n = 20, $p = 0.007$), but not distinguishable from that of forbs (0.599 ± 0.277 SD, n = 4, $p = 0.2$) (Fig. 3b). The Norm33 of grasses was statistically different from shrubs ($p = 0.01$). No other pairwise comparisons showed statistical difference ($p > 0.05$) (Fig. 3b).

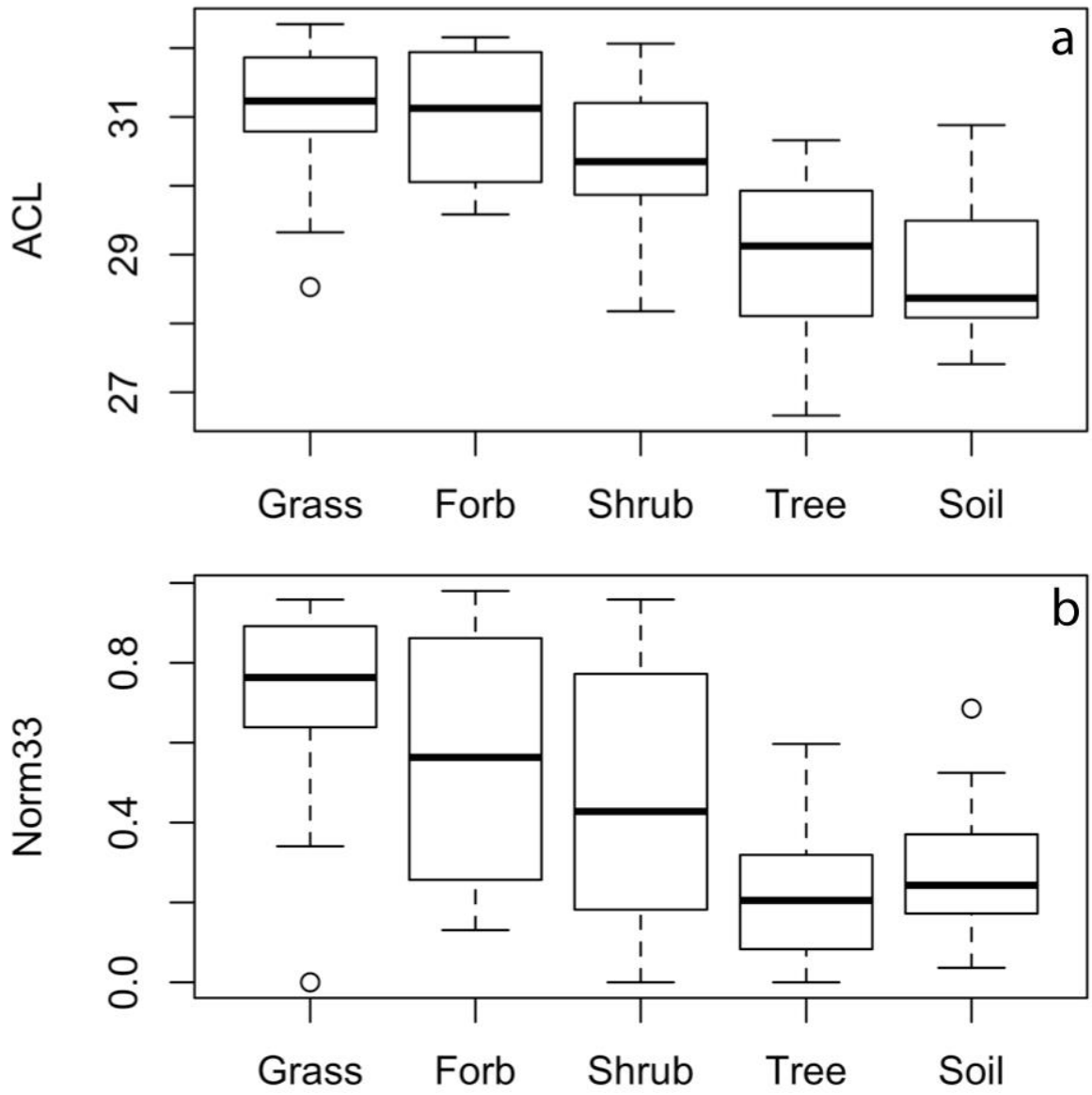

Figure 3. a) Boxplots of ACL values for plants, grouped by plant growth form, and soils. b) Boxplots of Norm33 values for plants, grouped by plant growth form, and soils. Boxes represent 50% of the data, with the median shown by the line. Whiskers indicate lower and upper quartiles.

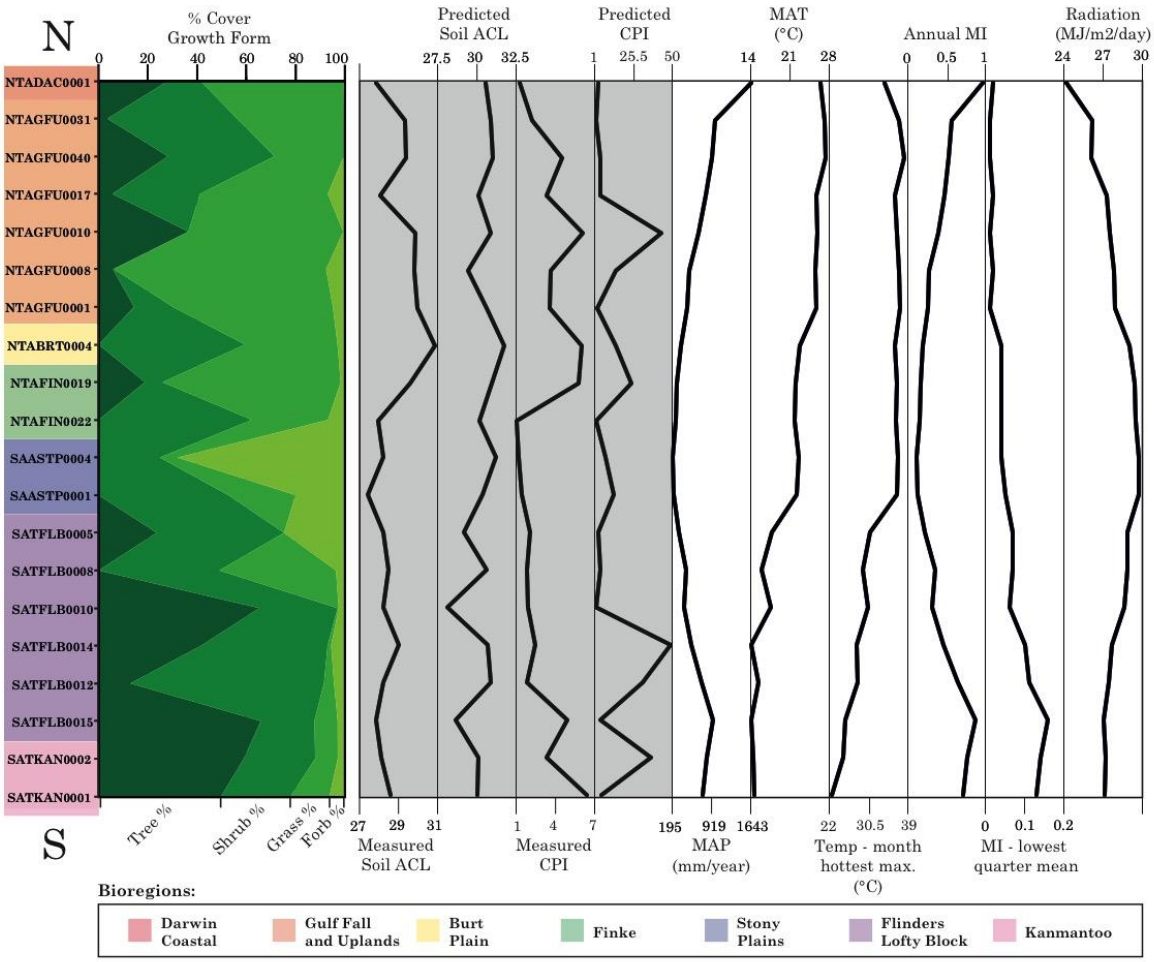

Figure 4. Proportional coverage of the plant growth forms at each site compared to the measured and predicted soil ACL (unitless), the measured and predicted soil CPI (unitless), MAP, MAT, maximum temperature of the hottest month, annual and lowest quarter mean MI (unitless) and highest period of radiation for each site. Site bioregions (see Supplementary Table S1, Appendix 1 for descriptions) indicated by colour bar.

The measured soil Norm33 showed a weak but statistically significant positive relationship with grass cover ($R^2 = 0.212$, $p = 0.04$) and a weak but statistically negative relationship with tree cover ($R^2 = 0.229$, $p = 0.03$) (Fig. 5c and d).

Kolmogorov-Smirnov tests of leaf wax *n*-alkane distributions indicated that grasses (n=20) contain significantly higher proportions of C_{33} than trees (n=13) and

shrubs (n=21); trees contain a significantly higher proportion of C_{29} than grasses; and shrubs are indistinguishable from grasses or trees in terms of the proportion of C_{29} (Fig 2. and Supplementary Fig. S2, Appendix 1).

Plant CPI values ranged from 0.6 – 106.6, with all but one plant showing an odd-over-even carbon number preference (CPI > 1). The one sample that did not have an odd-over-even predominance was *Rhagodia paradoxa*, a chenopod, with a CPI of 0.6. The CPI for the soils ranged from 2.2 – 12.5. This strong odd-over-even predominance, indicates that the source of the *n*-alkanes in the soils was from a terrestrial higher plant origin.

In most cases, the predicted soil ACL and Norm33, was longer than the measured soil ACL and Norm33 (Fig. 6a and b). The degree of offset (measured soil– predicted) did not correlate with any climate variables ($p > 0.05$) (Fig. 4 and Supplementary Fig. S3, Appendix 1) suggesting that model performance does not vary as a function of climate. Similarly, predicted soil CPI was longer than the measured soil CPI for the majority of sites (Fig. 6c.). Particle size analysis revealed no relationship between *n*-alkane concentration, ACL or Norm33 and percentage clay, silt or sand of the soils (Supplementary Fig. S4, Appendix 1).

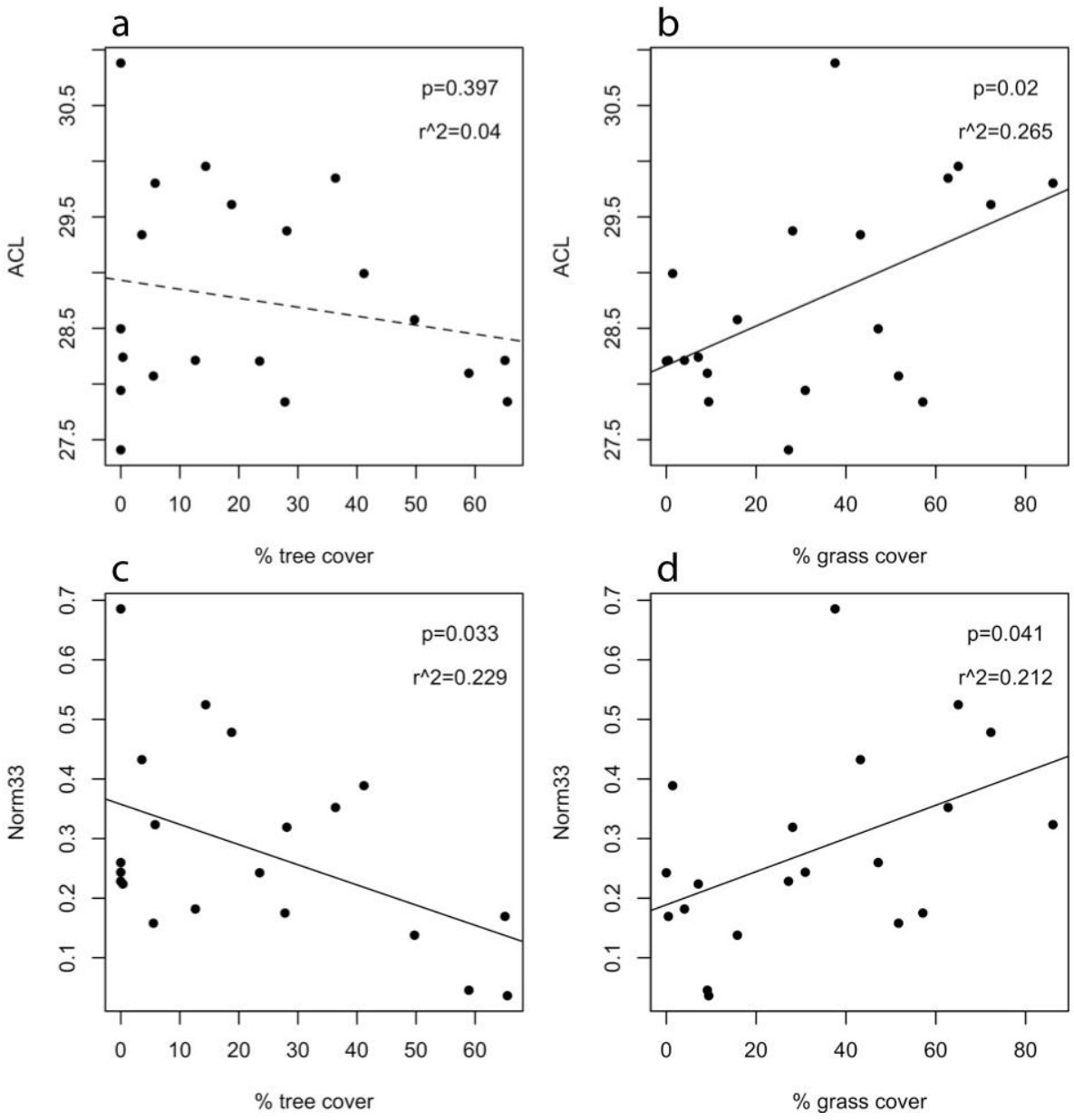

Figure 5. Plots showing the relationship between ACL measured in the soils versus a) the percentage of tree cover and, b) the percentage of grass cover; plots showing the relationship between Norm33 measured in the soils versus c) the percentage of tree cover and, d) the percentage of grass cover. Black solid trend lines indicate a significant relationship ($p < 0.05$), a dashed trendline indicates a non-significant relationship ($p > 0.05$).

4. Discussion

Long-chain *n*-alkanes extracted from sedimentary archives derived from ancient soils are routinely used as biomarkers for plants, therefore it is vital to understand what these archives represent. Cave sediments, such as Naracoorte Caves in SE Australia, represent a major archive derived largely from terrestrial soils (Macken et al. 2013). Similarly, tectonically active settings, such as the Bighorn Basin and the Siwalik Group preserve paleosols across key intervals of geologic history, such as the Paleocene–Eocene Thermal Maximum and Miocene, respectively (Zaleha 1997, Smith et al. 2007, Ghosh et al. 2017). To better characterise the nature of these records, we compared *n*-alkanes in plants and soils along a transect across Australia to examine whether *n*-alkanes in surface soils are dominated by inputs from the current, local vegetation. We use point intercept data to approximate the proportional species cover of each of the three most dominant species present at a site. We then measure the concentration and distribution of long-chain *n*-alkanes from each of these species and from the surface soils at each site. *n*-Alkane inputs from vegetation are modelled as the cover- and concentration-weighted average of the three most dominant taxa at each site. If local and recent vegetation were the dominant component of surface soil *n*-alkanes, we would expect the modelled *n*-alkane distributions to match those measured in soils. However, the modelled values of both ACL and Norm33 are offset from observed *n*-alkane characteristics, with measured values generally lower than the modelled ones (Figs. 6a and 6b). The offset between our modelled and observed distributions could be the result of integration of records over larger spatial scales/longer temporal scales than represented by the surveys; could reflect unaccounted fluxes of leaf waxes to soils; or could reflect post-depositional modification. These possibilities are evaluated below.

4.1 Regional vegetation inputs to soils

The modern vegetation survey used here encompasses one hectare plots (0.01 km^2), however, soils may accumulate *n*-alkanes from further afield. Aerosol samples collected from a mid-latitude forest in Germany have shown that their distribution of leaf wax *n*-alkane δD values differs significantly from that of local plants, suggesting that wind dispersal can transport *n*-alkanes across long-distances ranging from hundreds to thousands of kilometres (Nelson et al. 2017). Furthermore, Conte et al. (2003) demonstrated that the isotopic composition of ablated waxes in aerosols collected above a prairie canopy in southern Alberta, Canada, represented a regional scale catchment. Air mass trajectories have shown that wind-blown *n*-alkanes can travel as far as between continents, as well as having a regional or local source (Bendle et al. 2007, Yamamoto and Kawamura 2010, Nelson et al. 2017). While *n*-alkanes in the atmosphere necessarily represent wind-blown aerosols, it is unclear whether in soils the aerosol deposition represents a significant contribution in comparison to local direct leaf fall. The offset observed here between measured and modelled *n*-alkane distributions may indicate that the signals recorded in the surface soils are integrating across a larger area than the one hectare survey plot.

We observe a systematically shorter chain length distribution in the surface soils than that of the local plant community, which could result if regional aerosol or water borne inputs have shorter chain length distributions. Our results show that of all the growth forms, trees have the shortest average chain length (Fig. 3a). Therefore if trees from outside of the hectare plots are contributing significantly to soils, this would explain the systematic offset between the local plant community and the surface soils. We hypothesize that trees may be overrepresented in the surface soils relative to other plant types due to their height in the landscape making them more susceptible to

ablation by wind as compared to plants lower in stature, such as small shrubs and grasses.

4.2 Time averaging of n-alkanes in soils

The model uses the plants surveyed at the time of soil collection as the basis for the vegetation inputs to examine whether leaf waxes in surface soils are dominated by recent vegetation. However, *n*-alkanes can accumulate in soils over hundreds or thousands of years and then be re-mobilised and deposited with younger lacustrine and marine sediments (Smittenberg et al. 2006, Drenzek et al. 2007, Douglas et al. 2014, Gierga et al. 2016). If the *n*-alkanes in the surface soils accumulated over thousands of years, the standing plant community would be a poor predictor of soil *n*-alkane distributions because the dominant vegetation and climate across Australia have changed radically over this time (Hope 2017). Over the course of the Late Pleistocene into the Holocene, variable but increasing aridity has resulted in a shift from forested to herbaceous vegetation in the Western Plains of Victoria (Edney et al. 1990) and an increase in the dominance of eucalypt dominated grassy woodlands in the last 5000 years in mainland SE Australia (Kershaw et al. 1991). More recently, vegetation has changed since European settlement. Australia's vegetation prior to European settlement had greater plant cover than today, with forests and woodlands in greater abundance (COAG Standing Council on Environment and Water 2012). Past ecosystems with a different *n*-alkane contributors would have produced different *n*-alkane distributions in soils. Environmental changes over the lifetime of the soil would cause a difference between the modern plant community and the temporally integrated soils. This would prevent soils from providing annual or decadal records, but not impact on using soils as recorders of long-term vegetation over centuries to millennia.

4.3 Unconstrained fluxes from plants to soils

Despite accounting for the relative abundances of the plants and differences in *n*-alkane concentration among the plants, we are unable to quantify the actual flux of *n*-alkanes from the plants to the surface soils. The flux can vary with the rate of litter fall, which is a function of leaf lifespan (Wright and Cannon 2001), or with wax turnover rates within leaves due to physical removal (e.g. by wind ablation and herbivore removal and subsequent deposition) and regeneration of waxes (Koch et al. 2004). Leaf lifespan represents the duration of photosynthetic return to the plant and is balanced against the cost of producing greater leaf mass area (Wright et al. 2004). A global study of leaf economics has shown that in general plants that grow in arid conditions with higher mean annual temperature tend to have longer leaf lifespans (Wright et al. 2004). Our transect represents a broad range of climatic conditions, ranging from monsoonal tropics in the north, to arid central deserts, to winter rainfall in the south. These climatic differences are likely to contribute to variations in both leaf lifespan and the flux of litter to surface soils across the transect. Furthermore, the seasonal dominance of some annual species (e.g. *Sorghum* spp.) would lead to intra-annual variability in both local and regional *n*-alkane inputs.

Similarly, differences in the rate of wax production and replacement within a leaf, particularly in rarer species, would result in inputs to surface soils that are not proportional to the standing vegetation composition and concentration. Our inability to constrain fluxes from plants to surface soils would contribute to the spread in the offset between modelled and measured values. However, it is unlikely to explain the systematic overestimates in modelled ACL and CPI.

4.4 Post-depositional modification

Our model tests the local, modern day inputs of *n*-alkanes, but does not measure the fate of these compounds once they have been deposited in the soils. In theory, post-depositional modification to the *n*-alkanes could alter the chain length distributions in soils. In Australian soils, carbon content of soils is positively correlated with precipitation and negatively correlated with temperature; high pH and high clay content also facilitate preservation (Oades 1988, Carvalhais et al. 2014). Soil particle size is considered to play an important role in turnover of carbon, with decreasing carbon content and increasing carbon turnover rates in soils of increasing particle size (Cayet and Lichtfouse 2001, Quenea et al. 2004, Quénéa et al. 2006). However, our study finds no correlation between particle size and *n*-alkane concentration or distribution (Supplementary Fig. S4, Appendix 1).

At a global scale, organic matter turnover times vary across different biomes with shorter turnover times in tropical forests, savannahs and grasslands and longer turnover times in temperate forests, grasslands and shrublands (Carvalhais et al. 2014). We expect that variation in edaphic conditions could result in differential preservation potential of lipids. Bull et al. (2000) found an increase in *n*-alkane concentrations in soils with a higher pH and Pisani et al. (2015) found that soil warming resulted in a decrease in aliphatic lipid concentrations in the soil mineral horizon. Wang et al. (2017a) similarly find a decrease in concentration of *n*-alkanes with experimental heating at diagenetic temperatures ranging from 60-300 °C, as well as a decrease in ACL over time. However, due to our use of surface soils at a depth of only 3 cm, we expect temperatures to be significantly lower than in this experiment, and thus diagenetic effects to be minimised. Validated modelling of soil temperatures across Australia at 5

cm depths, a depth at which air temperature is the primary driver of the subsequent soil temperature, showed that even at extreme maximum temperatures of the year and day, soil temperature did not exceed 40 °C (Horton 2012). In addition, if variations in climate controlled the degree of post-depositional modification, we would expect the offset between modelled and measured values to vary with climate. However, we find the degree of offset between our modelled and measured ACL does not correlate with temperature or precipitation (Supplementary Fig. S3, Appendix 1). Thus, there is no evidence for climate-driven differences in post-depositional processing in our dataset.

Litterbag studies have explored the effects of microbial degradation on leaf waxes, but the effects varied among studies. Zech et al. (2011) find a decrease in concentration of odd, long-chain *n*-alkanes, as well a decrease in their odd-over-even predominance in a leaf litter bag experiment over 27 months which they interpret as a degradation signal. Similarly, our results show that overall the soils have a lower CPI than do the modelled plant inputs (Fig. 6c), which may indicate that degradation processes impact *n*-alkane signals in the soil. In contrast, Nguyen et al. (2017) noted that degradation processes resulted in a decrease in concentration of *n*-alkanes in a two-year litterbag study of beech leaves submerged in a pond, but did not result in a change to CPI, nor ACL. Additionally, Celerier et al. (2009) found that the longer chain lengths were not preferentially removed with depth in a soil profile of a long-term field experiment in France and show high resistance to microbial degradation. There is some evidence that differences in soil conditions may have an effect, where Li et al. (2017) find a small change to ACL of buried leaves at one of their study sites, but not at another with a different soil type. This evidence suggests that the ACL is not drastically altered by degradation processes in the soils, but that instead the odd-over-even predominance may vary in soils significantly as a result of degradation. As such, post-depositional

modification is not a likely explanation for the ACL offset between the plants and surface soils.

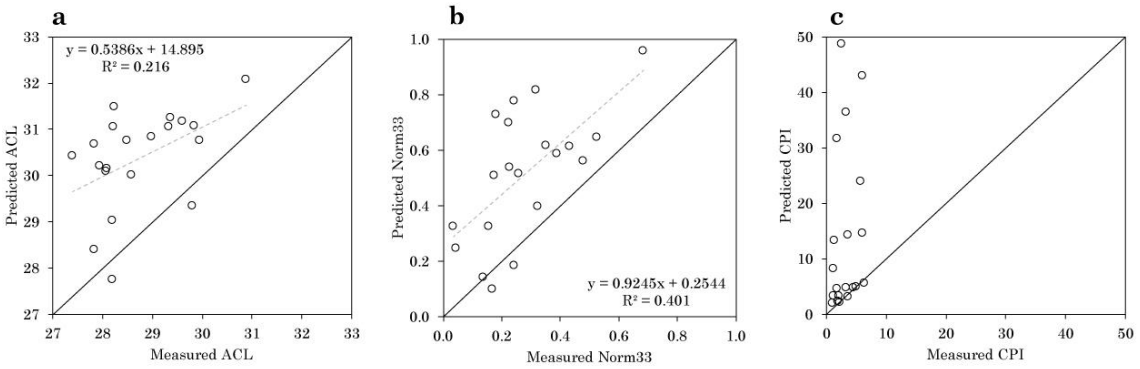

Figure 6. Predicted versus measured soil ACL (a), Norm33 (b) and CPI (c). Prediction represents a concentration- and cover-weighted average of three most dominant plants at each site. The grey dashed line represents the trend. Black 1:1 line for comparison.

4.5 Vegetation type and climatic effects on n-alkane distribution

A meta-analysis of plants from around the globe showed that in general grasses do not have longer ACL than woody vegetation (Bush and McInerney 2013). However, within Africa, C4 monocots (grasses and sedges) produce more C_{33} than C3 plants, and C3 plants tend to produce more C_{29} than C4 monocots (Garcin et al. 2014). Similarly, in Australia, the grasses, which were predominantly C4, produced proportionally more C_{33} and had significantly longer ACL than trees (Fig. 3); trees produced statistically more C_{29}, and had a shorter ACL than grasses (Fig. 3). Shrubs and forbs produced a widely varying range of chain lengths (Fig. 3). Plant coverage effects are also evident in the soils. We find statistically significant ($p<0.05$) correlations between % grass cover with both Norm33 and ACL and between % tree cover and Norm33 (Fig. 5). Similarly variations between biomes are seen in sediments from the southwest African

continental margin, with longer chain lengths associated with savannahs, compared to shorter chain lengths in rainforests (Rommerskirchen et al. 2006). Carr (2014) found that although there was considerable individual plant variability in the succulent karoo and fynbos biomes of South Africa, the succulent karoo was associated with longer maximum chain lengths than the fynbos, and these longer chain lengths were mirrored in the soils.

An alternative hypothesis for the cause of plant type differences observed here is that chain length distributions could be directly influenced by climate (Bush and McInerney 2013, Bush and McInerney 2015). Evidence of correlations between ACL and climate (e.g. temperature, relative humidity) have been found in North America (Tipple and Pagani 2013, Bush and McInerney 2015), Italy (Leider et al. 2013), on the Tibetan Plateau (Qiuhuan et al. 2016) and in Australia (Hoffmann et al. 2013). We found no relationship between any climate variables and the ACL of plants or soils, testing both climatic extremes and annual means of both temperature and precipitation (Fig. 4, Supplementary Figs. S5 & S6, Appendix 1). This is similar to the findings of Wang et al. (2017b), who did not find a strong relationship with temperature and ACL in soils across a > 1000 km transect in SW China. Plant type appears to be a greater determinant of ACL than climate in this study. Carr et al. (2014), found that climate was only very weakly correlated with ACL, while there were clear differences between growth forms. Phylogenetic constraints on leaf wax concentration and distribution was shown among conifers (Diefendorf et al. 2015) and may play a role in constraining responses to climate in other groups as well.

4.6 Evaluation of factors influencing soil n-alkane signatures

Our results suggest that soil *n*-alkanes are not dominantly from local and recent vegetation at the sites examined in this study. Moreover, a greater influence of trees from more distant, or previous plant communities could cause shorter ACL in the soils than that observed in modern, local vegetation. Our inability to account for the flux of waxes from the local plants into the soils is noteworthy, but unlikely to result in systematic overestimates by the models. Post-depositional microbial modification may contribute to the reduction in CPI in soils compared to plants, but is unlikely to affect ACL. The offsets between the modelled and measured ACL and Norm33 most likely reflect that soils integrate over larger spatial and/or temporal scales than those sampled by our plant survey. The correspondence between plant cover type (% grass or % trees) and *n*-alkane distributions (Norm33, ACL) in soils suggests that soil *n*-alkanes faithfully record larger scale ecosystem features, rather than localised plant communities.

4.7 Implications for palaeoecology

Our results show that we can be confident that the *n*-alkanes found in the surface soils are of a terrestrial plant origin due to their odd-over-even predominance. We suggest that the leaf waxes in the soils represent a spatially and/or temporally integrated signal. A distinct benefit for palaeoecology is that *n*-alkanes in soils should not be susceptible to microclimates, spatial heterogeneity of vegetation, or short term changes in vegetation due to interannual variability. The correspondence of *n*-alkane distributions in soils with plant cover type (grass or tree) suggests that information on vegetation structure is preserved in soils. Although we detect degradation processes occurring in the soils, with a decrease in soil CPI relative to the vegetation, we do not

expect that the ACL of the soils is affected by degradation based on the results of previous studies, however further work to investigate this at greater depth is necessary.

5. Conclusions

Characterising the temporal and spatial scale of inputs of *n*-alkanes from plants to surface soils allows us to better understand the environmental or climatic signal that we are measuring when analysing these compounds. Our results show an offset between the modelled signals based on current and local vegetation, and the measured signals in the soils. This offset allows us to reject the hypothesis of recent and local source, and indicates spatial and/or temporal averaging of inputs into the soils. We further suggest that trees, including those further afield than the one hectare field site are the likely source of the shorter ACL observed in the soils. This is due to their elevation in the landscape, making them potentially more susceptible to wind ablation than lower-statured species, and due to their greater presence in Australia's pre-European settlement as compared to today. Vegetation cover type (% grass or % tree) correlates with surface soil *n*-alkane distributions (Norm33), suggesting that large-scale features of vegetation structure are preserved in soil *n*-alkanes. The signals we observe in sedimentary records are likely to reflect a regional, time-averaged signal that is not heavily susceptible to short-term variability or small-scale spatial heterogeneity in climate.

Acknowledgements

The authors thank the Terrestrial Ecosystem Research Network, for providing the samples and vegetation cover data used in this study. Thanks also to Kristine Nielson for assistance in the lab, Emrys Leitch for help with vegetation data and David

McInerney for statistical advice. We also wish to thank three anonymous reviewers for their helpful comments. Funding was provided by the Australian Research Council to FAM (FT110100793). This research is also supported by Australian Government Research Training Program (RTP) Scholarships to SH, SC-R and JWA.

References

ANGST G., JOHN S., MUELLER C. W., KÖGEL-KNABNER I. & RETHEMEYER J. 2016. Tracing the sources and spatial distribution of organic carbon in subsoils using a multi-biomarker approach, *Scientific Reports*. **6**, p.DOI: 10.1038/srep29478.

BANTHORPE D. V. 2006 Natural Occurrence, Biochemistry and Toxicology. Alkanes and Cycloalkanes (1992). pp. 895-926. John Wiley & Sons, Ltd,

BASTOW T. P., VAN AARSSEN B. G. K. & LANG D. 2007. Rapid small-scale separation of saturate, aromatic and polar components in petroleum, *Organic Geochemistry*. **38**, 1235-1250.

BENDLE J., KAWAMURA K., YAMAZAKI K. & NIWAI T. 2007. Latitudinal distribution of terrestrial lipid biomarkers and *n*-alkane compound-specific stable carbon isotope ratios in the atmosphere over the western Pacific and Southern Ocean, *Geochimica et Cosmochimica Acta*. **71**, 5934-5955.

BULL I. D., BERGEN P. F. V., NOTT C. J., POULTON P. R. & EVERSHED R. P. 2000. Organic geochemical studies of soils from the Rothamsted classical experiments—V. The fate of lipids in different long-term experiments, *Organic Geochemistry*. **31**, 389-408.

BUSH R. T. & MCINERNEY F. A. 2013. Leaf wax *n*-alkane distributions in and across modern plants: Implications for paleoecology and chemotaxonomy, *Geochimica et Cosmochimica Acta*. **117**, 161-179.

--- 2015. Influence of temperature and C4 abundance on *n*-alkane chain length distributions across the central USA, *Organic Geochemistry*. **79**, 65-73.

CARR A. S., BOOM A., GRIMES H. L., CHASE B. M., MEADOWS M. E. & HARRIS A. 2014. Leaf wax *n*-alkane distributions in arid zone South African flora: Environmental controls, chemotaxonomy and palaeoecological implications, *Organic Geochemistry*. **67**, 72-84.

CARVALHAIS N., FORKEL M., KHOMIK M., BELLARBY J., JUNG M., MIGLIAVACCA M., MU M., SAATCHI S., SANTORO M., THURNER M., WEBER U., AHRENS B., BEER C., CESCATTI A., RANDERSON J. T. & REICHSTEIN M. 2014. Global covariation of carbon turnover times with climate in terrestrial ecosystems, *Nature*. **514**, 213-217.

CAYET C. & LICHTFOUSE E. 2001. δ13C of plant-derived n-alkanes in soil particle-size fractions, *Organic Geochemistry*. **32**, 253-258.

CELERIER J., RODIER C., FAVETTA P., LEMEE L. & AMBLES A. 2009. Depth-related variations in organic matter at the molecular level in a loamy soil: reference data for a long-term experiment devoted to the carbon sequestration research field, *European Journal of Soil Science*. **60**, 33-43.

CHIKARAISHI Y., KANEKO M. & OHKOUCHI N. 2012. Stable hydrogen and carbon isotopic compositions of long-chain (C21–C33) n-alkanes and n-alkenes in insects, *Geochimica et Cosmochimica Acta*. **95**, 53-62.

COAG STANDING COUNCIL ON ENVIRONMENT AND WATER 2012 Australia's Native Vegetation Framework. Canberra: Australian Government, Department of Sustainability, Environment, Water, Population and Communities.

CONTE M. H., WEBER J. C., CARLSON P. J. & FLANAGAN L. B. 2003. Molecular and carbon isotopic composition of leaf wax in vegetation and aerosols in a northern prairie ecosystem, *Oecologia*. **135**, 67-77.

CRANWELL P. A. 1981. Diagenesis of free and bound lipids in terrestrial detritus deposited in a lacustrine sediment, *Organic Geochemistry*. **3**, 79-89.

DIEFENDORF A. F., LESLIE A. B. & WING S. L. 2015. Leaf wax composition and carbon isotopes vary among major conifer groups, *Geochimica et Cosmochimica Acta*. **170**, 145-156.

DIEFENDORF A. F. & FREIMUTH E. J. 2017. Extracting the most from terrestrial plant-derived *n*-alkyl lipids and their carbon isotopes from the sedimentary record: A review, *Organic Geochemistry*. **103**, 1-21.

DODD R. S. & POVEDA M. M. 2003. Environmental gradients and population divergence contribute to variation in cuticular wax composition in Juniperus communis, *Biochemical Systematics and Ecology*. **31**, 1257-1270.

DOUGLAS P. M. J., PAGANI M., EGLINTON T. I., BRENNER M., HODELL D. A., CURTIS J. H., MA K. F. & BRECKENRIDGE A. 2014. Pre-aged plant waxes in tropical lake sediments and their influence on the chronology of molecular paleoclimate proxy records, *Geochimica et Cosmochimica Acta*. **141**, 346-364.

DRENZEK N. J., MONTLUÇON D. B., YUNKER M. B., MACDONALD R. W. & EGLINTON T. I. 2007. Constraints on the origin of sedimentary organic carbon in the Beaufort Sea from coupled molecular ^{13}C and ^{14}C measurements, *Marine Chemistry*. **103**, 146-162.

EDNEY P. A., KERSHAW A. P. & DE DECKKER P. 1990. A late Pleistocene and Holocene vegetation and environmental record from Lake Wangoom, Western Plains of Victoria, Australia, *Palaeogeography, Palaeoclimatology, Palaeoecology*. **80**, 325-343.

EGLINTON G. & HAMILTON R. J. 1967. Leaf Epicuticular Waxes, *Science*. **156**, 1322-1335.

EGLINTON T. I. & EGLINTON G. 2008. Molecular proxies for paleoclimatology, *Earth and Planetary Science Letters*. **275**, 1-16.

EIGENBRODE S. D. & ESPELIE K. E. 1995. Effects of Plant Epicuticular Lipids on Insect Herbivores, *Annual Review of Entomology*. **40**, 171-194.

GAMARRA B. & KAHMEN A. 2015. Concentrations and δ2H values of cuticular n-alkanes vary significantly among plant organs, species and habitats in grasses from an alpine and a temperate European grassland, *Oecologia*. **178**, 981-998.

GAO L., BURNIER A. & HUANG Y. 2012. Quantifying instantaneous regeneration rates of plant leaf waxes using stable hydrogen isotope labeling, *Rapid Communications in Mass Spectrometry*. **26**, 115-122.

GARCIN Y., SCHEFUß E., SCHWAB V. F., GARRETA V., GLEIXNER G., VINCENS A., TODOU G., SÉNÉ O., ONANA J.-M., ACHOUNDONG G. & SACHSE D. 2014. Reconstructing C3 and C4 vegetation cover using n-alkane carbon isotope ratios in recent lake sediments from Cameroon, Western Central Africa, *Geochimica et Cosmochimica Acta*. **142**, 482-500.

GHOSH S., SANYAL P. & KUMAR R. 2017. Evolution of C4 plants and controlling factors: Insight from n-alkane isotopic values of NW Indian Siwalik paleosols, *Organic Geochemistry*. **110**, 110-121.

GIERGA M., HAJDAS I., VAN RADEN U. J., GILLI A., WACKER L., STURM M., BERNASCONI S. M. & SMITTENBERG R. H. 2016. Long-stored soil carbon released by prehistoric land use: Evidence from compound-specific radiocarbon analysis on Soppensee lake sediments, *Quaternary Science Reviews*. **144**, 123-131.

HOFFMANN B., KAHMEN A., CERNUSAK L. A., ARNDT S. K. & SACHSE D. 2013. Abundance and distribution of leaf wax *n*-alkanes in leaves of Acacia and Eucalyptus trees along a strong humidity gradient in northern Australia, *Organic Geochemistry*. **62**, 62-67.

HOPE G. S. 2017 Quaternary Vegetation. *In* HILL R. S. ed. History of the Australian Vegetation: Cretaceous to Recent. pp. 368-389. University of Adelaide Press,

HORTON B. 2012. Models for estimation of hourly soil temperature at 5 cm depth and for degree-day accumulation from minimum and maximum soil temperature, *Soil Research*. **50**, 447-454.

HUANG Y., BOL R., HARKNESS D. D., INESON P. & EGLINTON G. 1996. Post-glacial variations in distributions, 13C and 14C contents of aliphatic hydrocarbons and bulk organic matter in three types of British acid upland soils, *Organic Geochemistry*. **24**, 273-287.

HUANG Y., STREET-PERROTT F. A., METCALFE S. E., BRENNER M., MORELAND M. & FREEMAN K. H. 2001. Climate change as the dominant control on glacial-interglacial variations in C3 and C4 plant abundance, *Science*. **293**, 1647-1651.

JANSEN B. & WIESENBERG G. L. B. 2017. Opportunities and limitations related to the application of plant-derived lipid molecular proxies in soil science, *SOIL*. **3**, 211-234.

JETTER R. & RIEDERER M. 2016. Localization of the Transpiration Barrier in the Epi- and Intracuticular Waxes of Eight Plant Species: Water Transport Resistances Are Associated with Fatty Acyl Rather Than Alicyclic Components, *Plant Physiology*. **170**, 921-934.

KERSHAW A. P., D'COSTA D. M., MCEWEN MASON J. R. C. & WAGSTAFF B. E. 1991. Palynological evidence for Quaternary vegetation and environments of mainland southeastern Australia, *Quaternary Science Reviews*. **10**, 391-404.

KHAN A. A. & KOLATTUKUDY P. E. 1974. Decarboxylation of long chain fatty acids to alkanes by cell free preparations of pea leaves (Pisum sativum), *Biochemical and Biophysical Research Communications*. **61**, 1379-1386.
KOCH K., NEINHUIS C., ENSIKAT H. J. & BARTHLOTT W. 2004. Self assembly of epicuticular waxes on living plant surfaces imaged by atomic force microscopy (AFM), *Journal of Experimental Botany*. **55**, 711-718.
KOCH K., DOMMISSE A., NIEMIETZ A., BARTHLOTT W. & WANDELT K. 2009. Nanostructure of epicuticular plant waxes: Self-assembly of wax tubules, *Surface Science*. **603**, 1961-1968.
LEIDER A., HINRICHS K.-U., SCHEFUß E. & VERSTEEGH G. J. M. 2013. Distribution and stable isotopes of plant wax derived *n*-alkanes in lacustrine, fluvial and marine surface sediments along an Eastern Italian transect and their potential to reconstruct the hydrological cycle, *Geochimica et Cosmochimica Acta*. **117**, 16-32.
LI R., FAN J., XUE J. & MEYERS P. A. 2017. Effects of early diagenesis on molecular distributions and carbon isotopic compositions of leaf wax long chain biomarker n-alkanes: Comparison of two one-year-long burial experiments, *Organic Geochemistry*. **104**, 8-18.
LICHTFOUSE É., CHENU C., BAUDIN F., LEBLOND C., DA SILVA M., BEHAR F., DERENNE S., LARGEAU C., WEHRUNG P. & ALBRECHT P. 1998. A novel pathway of soil organic matter formation by selective preservation of resistant straight-chain biopolymers: chemical and isotope evidence, *Organic Geochemistry*. **28**, 411-415.
MACKEN A. C., MCDOWELL M. C., BARTHOLOMEUSZ D. N. & REED E. H. 2013. Chronology and stratigraphy of the Wet Cave vertebrate fossil deposit, Naracoorte, and relationship to paleoclimatic conditions of the Last Glacial Cycle in south-eastern Australia, *Australian Journal of Earth Sciences*. **60**, 271-281.
MAKOU M., EGLINTON T., MCINTYRE C., MONTLUÇON D., ANTHEAUME I. & GROSSI V. 2018. Plant Wax n-Alkane and n-Alkanoic Acid Signatures Overprinted by Microbial Contributions and Old Carbon in Meromictic Lake Sediments, *Geophysical Research Letters*. **45**, 1049-1057.
MARZI R., TORKELSON B. E. & OLSON R. K. 1993. A revised carbon preference index, *Organic Geochemistry*. **20**, 1303-1306.
MEYERS P. A. & HITES R. A. 1982. Extractable organic compounds in midwest rain and snow, *Atmospheric Environment (1967)*. **16**, 2169-2175.
NELSON D. B., KNOHL A., SACHSE D., SCHEFUß E. & KAHMEN A. 2017. Sources and abundances of leaf waxes in aerosols in central Europe, *Geochimica et Cosmochimica Acta*. **198**, 299-314.
NGUYEN TU T. T., EGASSE C., ANQUETIL C., ZANETTI F., ZELLER B., HUON S. & DERENNE S. 2017. Leaf lipid degradation in soils and surface sediments: A litterbag experiment, *Organic Geochemistry*. **104**, 35-41.
OADES J. M. 1988. The retention of organic matter in soils, *Biogeochemistry*. **5**, 35-70.
PISANI O., FREY S. D., SIMPSON A. J. & SIMPSON M. J. 2015. Soil warming and nitrogen deposition alter soil organic matter composition at the molecular-level, *Biogeochemistry*. **123**, 391-409.
PU Y., ZHANG H., WANG Y., LEI G., NACE T. & ZHANG S. 2011. Climatic and environmental implications from *n*-alkanes in glacially eroded lake sediments in Tibetan Plateau: An example from Ximen Co, *Chinese Science Bulletin*. **56**, 1503-1510.
QIUHUAN J. I. A., QING S. U. N., MAMNAN X. I. E., YABING S., YUAN L., QINGZENG Z. H. U. & MINGZHONG T. 2016. Normal Alkane Distributions in Soil Samples along a Lhasa-Bharatpur Transect, *Acta Geologica Sinica - English Edition*. **90**, 738-748.
QUENEA K., DERENNE S., LARGEAU C., RUMPEL C. & MARIOTTI A. 2004. Variation in lipid relative abundance and composition among different particle size fractions of a forest soil, *Organic Geochemistry*. **35**, 1355-1370.
QUÉNÉA K., LARGEAU C., DERENNE S., SPACCINI R., BARDOUX G. & MARIOTTI A. 2006. Molecular and isotopic study of lipids in particle size fractions of a sandy cultivated soil (Cestas cultivation sequence, southwest France): Sources, degradation, and comparison with Cestas forest soil, *Organic Geochemistry*. **37**, 20-44.
R CORE TEAM 2018. R: A language and environment for statistical computing. <https://www.R-project.org/>. (retrieved.

ROMMERSKIRCHEN F., EGLINTON G., DUPONT L. & RULLKÖTTER J. 2006. Glacial/interglacial changes in southern Africa: Compound-specific $\delta^{13}C$ land plant biomarker and pollen records from southeast Atlantic continental margin sediments, *Geochemistry, Geophysics, Geosystems*. **7**, p.DOI: 10.1029/2005GC001223.

ROUILLARD A., GREENWOOD P. F., GRICE K., SKRZYPEK G., DOGRAMACI S., TURNEY C. & GRIERSON P. F. 2016. Interpreting vegetation change in tropical arid ecosystems from sediment molecular fossils and their stable isotope compositions: A baseline study from the Pilbara region of northwest Australia, *Palaeogeography, Palaeoclimatology, Palaeoecology*. **459**, 495-507.

SACHSE D., RADKE J. & GLEIXNER G. 2004. Hydrogen isotope ratios of recent lacustrine sedimentary *n*-alkanes record modern climate variability, *Geochimica et Cosmochimica Acta*. **68**, 4877-4889.

SCHWARK L., ZINK K. & LECHTERBECK J. 2002. Reconstruction of postglacial to early Holocene vegetation history in terrestrial Central Europe via cuticular lipid biomarkers and pollen records from lake sediments, *Geology*. **30**, 463-466.

SHEPHERD T. & WYNNE GRIFFITHS D. 2006. The effects of stress on plant cuticular waxes, *New Phytologist*. **171**, 469-499.

SMITH F. A., WING S. L. & FREEMAN K. H. 2007. Magnitude of the carbon isotope excursion at the Paleocene–Eocene thermal maximum: The role of plant community change, *Earth and Planetary Science Letters*. **262**, 50-65.

SMITTENBERG R. H., EGLINTON T. I., SCHOUTEN S. & DAMSTÉ J. S. S. 2006. Ongoing Buildup of Refractory Organic Carbon in Boreal Soils During the Holocene, *Science*. **314**, 1283-1286.

TIPPLE B. J. & PAGANI M. 2013. Environmental control on eastern broadleaf forest species' leaf wax distributions and D/H ratios, *Geochimica et Cosmochimica Acta*. **111**, 64-77.

VAN GARDINGEN P. R., GRACE J. & JEFFREE C. E. 1991. Abrasive damage by wind to the needle surfaces of Picea sitchensis (Bong.) Carr. and Pinus sylvestris L, *Plant, Cell & Environment*. **14**, 185-193.

WANG C., ELEY Y., OAKES A. & HREN M. 2017a. Hydrogen isotope and molecular alteration of n-alkanes during heating in open and closed systems, *Organic Geochemistry*. **112**, 47-58.

WANG C., HREN M. T., HOKE G. D., LIU-ZENG J. & GARZIONE C. N. 2017b. Soil *n*-alkane δD and glycerol dialkyl glycerol tetraether (GDGT) distributions along an altitudinal transect from southwest China: Evaluating organic molecular proxies for paleoclimate and paleoelevation, *Organic Geochemistry*. **107**, 21-32.

WHITE A., SPARROW B., LEITCH E., FOULKES J., FLITTON R., LOWE A. & CADDY-RETALIC S. 2012 AusPlots Rangelands Survey Protocols Manual. Terrestrial Ecosystem Research Network. pp. 84. University of Adelaide: University of Adelaide Press.

WRIGHT I. J. & CANNON K. 2001. Relationships between leaf lifespan and structural defences in a low-nutrient, sclerophyll flora, *Functional Ecology*. **15**, 351-359.

WRIGHT I. J., REICH P. B., WESTOBY M., ACKERLY D. D., BARUCH Z., BONGERS F., CAVENDER-BARES J., CHAPIN T., CORNELISSEN J. H. C., DIEMER M., FLEXAS J., GARNIER E., GROOM P. K., GULIAS J., HIKOSAKA K., LAMONT B. B., LEE T., LEE W., LUSK C., MIDGLEY J. J., NAVAS M.-L., NIINEMETS U., OLEKSYN J., OSADA N., POORTER H., POOT P., PRIOR L., PYANKOV V. I., ROUMET C., THOMAS S. C., TJOELKER M. G., VENEKLAAS E. J. & VILLAR R. 2004. The worldwide leaf economics spectrum, *Nature*. **428**, 821-827.

XU T. & HUTCHINSON M. F. 2013. New developments and applications in the ANUCLIM spatial climatic and bioclimatic modelling package, *Environmental Modelling & Software*. **40**, 267-279.

YAMAMOTO S., HASEGAWA T., TADA R., GOTO K., ROJAS-CONSUEGRA R., DÍAZ-OTERO C., GARCÍA-DELGADO D. E., YAMAMOTO S., SAKUMA H. & MATSUI T. 2010. Environmental and vegetational changes recorded in sedimentary leaf wax *n*-alkanes across the Cretaceous–Paleogene boundary at Loma Capiro, Central Cuba, *Palaeogeography, Palaeoclimatology, Palaeoecology*. **295**, 31-41.

YAMAMOTO S. & KAWAMURA K. 2010. Compound-specific stable carbon and hydrogen isotopic compositions of *n*-alkanes in urban atmospheric aerosols from Tokyo, *Geochemical Journal*. **44**, 419-430.

ZALEHA M. J. 1997. Siwalik Paleosols (Miocene, northern Pakistan); genesis and controls on their formation, *Journal of Sedimentary Research*. **67**, 821-839.

ZECH M., PEDENTCHOUK N., BUGGLE B., LEIBER K., KALBITZ K., MARKOVIĆ S. B. & GLASER B. 2011. Effect of leaf litter degradation and seasonality on D/H isotope ratios of *n*-alkane biomarkers, *Geochimica et Cosmochimica Acta*. **75**, 4917-4928.

CHAPTER 3

Post-depositional modification of *n*-alkane signals in incubated soils

Howard, S.[a], McInerney, F.A.[a], Farrell, M.[b] & Hall, P.A.[a]

[a]*School of Physical Sciences, Department of Earth Science, Sprigg Geobiology Centre, University of Adelaide, Australia*

[b]*CSIRO Agriculture & Food, Locked Bag 2, Glen Osmond, SA 5064, Australia*

Statement of Authorship

Title of Paper	Post-depositional modification of *n*-alkane signals in incubated soils
Publication Status	☐ Published ☐ Accepted for Publication ☐ Submitted for Publication ☑ Unpublished and Unsubmitted work written in manuscript style
Publication Details	

Principal Author

Name of Principal Author (Candidate)	Siân Howard		
Contribution to the Paper	Designed the study. Conducted sample processing and analysis. Conducted data analysis and interpretation. Wrote manuscript.		
Overall percentage (%)	75		
Certification:	This paper reports on original research I conducted during the period of my Higher Degree by Research candidature and is not subject to any obligations or contractual agreements with a third party that would constrain its inclusion in this thesis. I am the primary author of this paper.		
Signature		Date	13/12/2018

Co-Author Contributions

By signing the Statement of Authorship, each author certifies that:

i. the candidate's stated contribution to the publication is accurate (as detailed above);

ii. permission is granted for the candidate in include the publication in the thesis; and

iii. the sum of all co-author contributions is equal to 100% less the candidate's stated contribution.

Name of Co-Author	Dr Francesca A. McInerney		
Contribution to the Paper	Supervised SH. Designed the study. Provided input into data analysis, interpretation and manuscript. Reviewed and edited final manuscript.		
Signature		Date	13/12/2018

Name of Co-Author	Dr Mark Farrell		
Contribution to the Paper	Provided samples from incubation experiments and advice on sample context. Provided assistance with data interpretation. Reviewed and edited final manuscript.		
Signature		Date	22/02/2019

Name of Co-Author	Dr Philip A. Hall		
Contribution to the Paper	Provided GC-MS quantification of samples. Reviewed and edited final manuscript.		
Signature		Date	22/2/2019

Abstract

In order to interpret leaf wax *n*-alkane characteristics observed in soils and sediments in terms of past vegetation and environment, we need to understand whether post-depositional modification has altered the original plant-derived signatures. To determine whether degradation processes alter *n*-alkane signals in soils, we conducted 18 month incubation experiments of soils combined with different organic composts to examine the effects of post depositional modification in isolation from herbivory. After 18 months of incubation, *n*-alkane concentration decreased by up to 85%, with the greatest decrease occurring within the first month. Carbon preference index (CPI) also decreased across all samples, suggesting that CPI may be a good indicator of the degree of degradation. Despite large decreases in *n*-alkanes concentration, average chain length (ACL) of long chain *n*-alkanes remained stable throughout the experiment. The alkyl/o-alkyl ratio shows that there is greater *n*-alkane loss in those samples where there is a greater relative abundance of lipid-related carbon added via the composts. This suggests that *n*-alkanes are unstable at the time of deposition and are susceptible to soil processes before stabilisation and preservation. The results presented here indicate that CPI may be a useful indicator of *n*-alkane degradation. These findings provide confidence in the use of *n*-alkane ACL signals preserved in soils for palaeoenvironmental research, despite the effects of post depositional modification.

Keywords

n-alkanes, soils, incubation experiment, ACL, CPI, A/OA

1. Introduction

The compounds contained in leaf waxes are useful for palaeoecological research because they play a critical role in protecting the plant from its environment and can therefore record information about past ecosystems. Leaf waxes provide protection against non-stomatal water loss from the leaf surface of plants, as well as provide protection against herbivory, fungal infection and UV radiation (Eglinton and Hamilton 1967, Eigenbrode and Espelie 1995, Shepherd and Wynne Griffiths 2006). They are made up of multiple compound types, including *n*-alkanes (Eglinton and Hamilton 1967, Banthorpe 2006). In the leaf waxes of terrestrial higher plants, the *n*-alkanes are long chained (C_{25}-C_{35}), with an odd-over-even chain length predominance and these specific characteristics make them useful as proxies or biomarkers that record past vegetation (Eglinton and Hamilton 1967). The strong odd-over-even predominance of chain lengths forms as a result of the decarboxylation of even-numbered fatty acid chains (Khan and Kolattukudy 1974, Shepherd and Wynne Griffiths 2006). The relative abundance of the different *n*-alkane chain lengths produced in leaf waxes is quantified as an average chain length (ACL), and the predominance of odd over even chain lengths observed in terrestrial higher plants is quantified as a carbon preference index (CPI).

Implicit in the interpretation in palaeoecological studies is that the *n*-alkane signals found in the sediments are representative of the plant community that deposited them (Pearson and Eglinton 2000, Eglinton and Eglinton 2008). Our recent work showed that surface soil samples did not reflect the *n*-alkane signals of the local (<1 hectare) standing plant community, but instead appeared to represent either a spatially and temporally integrated signal of the contributing plants, or an altered signal influenced by post-depositional modification (Howard et al. 2018).

Temporal and spatial averaging is regarded as an important consideration when interpreting the signals from leaf wax *n*-alkanes observed in soils and sediments (Diefendorf and Freimuth 2017). These compounds become deposited into soils as a result of wind ablation and leaf fall (Cranwell 1981, Lichtfouse et al. 1998). There they accumulate and can remain preserved in palaeosols for millions of years (Smith et al. 2007, Yamamoto et al. 2010). Studies exploring the pre-aging of leaf wax *n*-alkanes in soils and sediments have found that they can have residence times of decades, or up to hundreds to thousands of years before becoming remobilised and redeposited (Pearson and Eglinton 2000, Smittenberg et al. 2006, Douglas et al. 2014, Gierga et al. 2016).

In addition to temporal and spatial averaging, post-depositional modification that occurs in the soils may result in plant and soil *n*-alkane signals differing from one another (Howard et al. 2018). Understanding the potential impact of edaphic modification of *n*-alkane signals is critical to their interpretation in palaeoecological research. Litterbag studies have increased our understanding of the role that microbes and herbivorous fauna play in altering *n*-alkane signals observed on abscised leaves in litter and soil. Specifically, litterbag studies have shown that *n*-alkanes do breakdown while still in association with leaves and have found that lipid content decreased by up to 99 percent over the course of an experiment (Nguyen Tu et al. 2011, Li et al. 2017). However, carbon preference index (CPI) changes were variable between experiments, with some showing a decrease in CPI (Li et al. 2017) and others observing a stable CPI over the course of the experiments (Wang et al. 2014). Further, when examining ACL, litterbag studies have revealed that ACL remained stable or only slightly changed over the course of the experiments (Wang et al. 2014, Li et al. 2017). These litterbag studies replicate various post-abscission effects on *n*-alkanes while still in direct association with leaves, but have shown variable results potentially due to differences among

studies. This may be due to the variation between plant species as observed by Li et al. (2017), or due to differences in experimental set up, with some experiments being buried (Wang et al. 2014, Li et al. 2017) and others being left exposed on the soil surface (Nguyen Tu et al. 2011). Further, litterbag studies do not provide insight into the fate of leaf wax *n*-alkanes that have been disseminated in soils and are no longer in association with the leaf cuticle. In addition to *n*-alkanes associated with leaf litter, there is also a separate pool of isolated leaf wax *n*-alkanes accumulated in soils, which may be subject to further post-depositional modification and organo-mineral interactions, which litterbag studies are unable to examine. Our study builds on the litterbag work by examining the change in *n*-alkane composition after the leaves have decomposed and been mixed into soils through a controlled experiment.

In order to measure post depositional effects on *n*-alkane signals in soils, controlled incubation experiments were conducted of soils mixed with different types of compost (organic amendments) as an analogue for the processes of herbivory and breakdown of whole leaf matter. By comparing the signatures of the *n*-alkanes in the amended soils prior to and after incubation for 18 months, we can infer the effects of microbial degradation on the *n*-alkane signals. This controlled experiment eliminates the natural variations in plant sources and time-averaging in different soils found in the natural world (Howard et al. 2018) and allows for examination of different organic materials with a broad range of chemistries. Additionally, differences within and between plant species as a result of climate and phylogeny introduces significant variability *n*-alkane chain length distributions (Bush and McInerney 2013, Bush and McInerney 2015, Diefendorf et al. 2015). This study helps to overcome the challenges associated with variation between individual plants and between environments by examining the input of *n*-alkanes into soil from homogenised organic matter from

different sources. By examining *n*-alkane degradation in soil in this manner, we seek to replicate conditions of an integrated signal observed in the natural environment.

2. Methods

2.1 Soil incubation

Australian agricultural chromosol (Isbell and National Committee on Soil Terrain 2016) had different organic composted amendments added (Table 1). Prior to their addition to the soil, nuclear magnetic resonance (NMR) analysis was conducted on the composts in order to examine their alkyl/o-alkyl (A/OA) ratio (Table 1, Baldock et al. 1997, Farrell et al. 2015) following NMR conditions of Baldock et al. (2013). Amended soils were incubated in the dark in 250 mL sealed jars at a stable temperature of 22 °C with a small vessel containing water to maintain humidity for 18 months. Headspace was refreshed regularly throughout this incubation period to prevent anoxia. To observe changes over time, replicate samples were destructively harvested at 0, 1, 3, 6, 12 and 18 months by halting incubation and subsequent microbial activity by drying at 40°C to a constant mass (Farrell et al. 2015).

Table 1. Details of the different organic amendments added to and homogenised with the soils and their respective A/OA ratios (Baldock et al. 2013, Farrell et al. 2015).

Sample	A/OA	Details of Organic Amendment
C001	0.28	Mixture of pig manure and straw
C004	0.31	Composted chicken manure
C005	1.19	Fresh biosolids
C008	0.40	Composted green organics (green waste and food waste)
C009	0.11	Fresh green waste (garden clippings etc)
C046	1.06	Composted cotton trash
C047	0.40	Composted green waste and biosolids
C049	0.54	Municipal green waste composted
C053	0.12	Green waste and timber

C054	0.78	Composted cow manure, straw, hay, clay and rock dust (latter two as stabilisers)
C063	0.19	Composted green waste and biosolids
Chromosol	0.57	No amendment

2.2 Sample selection

Eleven samples of amended soil were selected from the larger experiment to examine the stability of *n*-alkanes. These samples were selected based upon the wide spread of chemistries of the composts used, and thus were expected to be a robust test of how *n*-alkanes from disparate sources responded to microbial decomposition. Soils were incubated for 0 or 18 months prior to subsampling. Additionally, an unamended, unincubated chromosol control sample was examined. Finally, in order to examine changes at a finer temporal resolution, samples at 1, 3, 6 and 12 months incubation were subsampled from two of the samples, C009 and C047. Total organic carbon (TOC) of all samples was determined through elemental analysis using a LECO Corporation Trumac CN (Farrell et al. 2015).

2.3 Lipid extraction

Lipid extraction of the samples was conducted using a Thermo Scientific Dionex Accelerated Solvent Extractor (ASE) 350 using a 9:1 DCM:MeOH. The ASE extraction occurred at 100 °C and a pressure of ~11,000 kPa with a 12 minute preheat, three static cycles of five minutes, and a rinse volume of 60%. Excess solvent was evaporated from the TLE under nitrogen gas using a FlexiVap nitrogen blow down station.

2.4 n-Alkane purification

The polar and non-polar fractions of the TLEs were separated by solid phase extraction using ~0.5g of activated silica gel in short glass columns eluting them with 4

ml of hexane to collect the non-polar, aliphatic hydrocarbon fraction, followed by 4 ml 1:1 DCM:MeOH eluent to collect the polar fraction (Bastow et al. 2007). The aliphatic hydrocarbon fraction was dried under nitrogen gas.

2.5 GC-MS Lipid Quantification

Quantification of *n*-alkanes was conducted using gas chromatography mass spectrometry (GC-MS) analysis of the non-polar lipid fraction. Analysis was performed on a Perkin Elmer Clarus 500 GC-MS with the following specifications: The capillary was an SGE CPSil-5MS, 30 m (length) x 0.25 mm (internal diameter) x 0.25 μm phase thickness. The carrier gas was helium with a 1 ml/ min constant flow. The injection temperature was 300 °C, with a temperature program of 50 °C (hold 1 minute), ramped at 8 °C/ min to 340 °C (hold for 7.75 minutes). Injection was set to 1 μl in either split mode, with a 50:1 split for higher concentration samples, or pulsed splitless for low sample concentrations. Perkin Elmer Turbomass software was used for data interpretation and quantification of *n*-alkane homologues (C_{25} to C_{35}). 1-1'binaphthyl internal standard was added to each sample at a concentration of 1 μg/mL. Concentrations of *n*-alkanes were calculated from the response factor of each homologue against the internal standard plotted against a seven point calibration curve prepared and analysed in triplicate using known concentrations of a homologous suite of *n*-alkanes (C_7 to C_{40} Saturated Alkanes Standard, Supelco 49452-U) with the same 1 μg/mL 1-1' binaphthyl internal standard concentration ($r^2 > 0.96$, with a precision of ±10% based on 10 replicate standard injections).

2.6 Calculations

The distribution of *n*-alkane chain lengths were characterised by calculating average chain length (ACL),

$$ACL = \frac{(25C_{25}+27C_{27}+29C_{29}+31C_{31}+33C_{33}+35C_{35})}{(C_{25}+C_{27}+C_{29}+C_{31}+C_{33}+C_{35})} \quad (1)$$

where C_x is the concentration of each *n*-alkane with x carbon atoms.

Carbon preference index (CPI) for each sample was calculated using the below equation, modified from Marzi et al. (1993):

$$CPI = \frac{[\sum_{odd}(C_{25-33})+\sum_{odd}(C_{27-35})]}{2(\sum_{even} C_{26-34})} \quad (2)$$

Where Σ_{odd} refers to the sum of the concentrations of odd carbon numbered *n*-alkanes, and Σ_{even} refers to the sum of concentrations of even carbon numbered for the inclusive range of chain lengths indicated for each.

Loss of *n*-alkanes was calculated as a percentage change in concentration (μg *n*-alkane/mg soil) after 18 months. We also calculated the concentration of *n*-alkanes with respect to total organic carbon (μg *n*-alkane/mg TOC) in order to examine the proportion of *n*-alkane loss that occurred over the 18 month incubation period.

2.7 Statistical methods

Paired sample t-tests were conducted to determine whether there was significant change to the ACL, CPI and concentration of the samples after 18 months of incubation.

3. Results

In all amended samples, total organic carbon (TOC, mg C/g soil) decreased after 18 months of incubation, with samples having a starting TOC of 30.1 – 34.5 mg TOC/g soil and decreasing to 15.8 – 27.6 mg TOC/g soil (Table 2, Fig. 1a).

Total *n*-alkane concentration (C_{15}-C_{35}, µg *n*-alkane/mg soil) also decreased after 18 months of incubation, with samples having starting concentrations ranging from 11.1 - 29.23 µg *n*-alkane/mg soil at 0 months incubation, and 3.67 – 12.05 µg *n*-alkane/mg soil at 18 months incubation (Table 2, Fig. 1b). However, *n*-alkane concentration does not decrease in proportion to TOC (Table 2, Fig. 2).

After the 18 month incubation period, ACL shows no significant change ($t = -0.87$, $p = 0.4$). Although sample C063 had an increase in ACL, all other samples had an ACL that remained almost unchanged after 18 months of incubation (Fig. 1c). Sample C063 had the greatest percent decrease of TOC and total *n*-alkane concentration of all amended samples (Fig. 1c). In all samples, CPI significantly decreased ($t = 3.49$, $p = 0.006$) after 18 months of incubation (Fig. 1 d).

Table 2. Characterisation of amended soils at 0 and 18 months of incubation: Total Organic Carbon (TOC) (mg C/g soil), total *n*-alkane concentration for C_{15}-C_{35} (µg *n*-alkane/mg soil), ACL, CPI sorted in order of decreasing values of the ratio of alkyl to o-alkyl carbon in each sample (A/OA) (Farrell et al. 2015).

		A/OA	TOC			Total *n*-alkane concentration (C_{15} - C_{35})			ACL (C_{25}-C_{35})		CPI (C_{25}-C_{35})	
	Months incubated	N/A	0	18	% Loss	0	18	% Loss	0	18	0	18
Samples	C005	1.19	33.97	25.90	23.7	29.23	4.41	84.9	30.4	30.2	14.1	7.9
	C046	1.06	33.96	21.80	35.8	18.46	3.67	80.1	30.1	30.1	17.6	9.0
	C054	0.78	30.85	25.15	18.5	11.10	5.89	46.9	30.2	30.2	16.9	8.6
	C049	0.54	32.88	16.50	49.8	12.01	6.96	42.1	30.2	30.2	16.7	13.4
	C008	0.40	33.02	25.02	24.2	15.65	5.78	63.1	30.3	30.2	15.0	12.6
	C047	0.40	34.50	16.35	52.6	12.54	8.20	34.6	30.2	30.3	16.4	10.9
	C004	0.31	31.92	25.78	19.2	12.56	8.40	33.1	30.2	30.3	15.2	17.7
	C001	0.28	32.01	22.04	31.2	18.80	6.74	64.1	30.3	30.4	18.7	15.0
	C063	0.19	33.00	27.58	16.4	13.70	12.05	12.1	29.7	30.2	3.3	5.3
	C053	0.12	33.52	15.79	52.9	19.57	9.31	52.4	30.2	30.2	18.0	14.5
	C009	0.11	33.65	24.14	28.2	16.43	8.20	50.1	30.0	30.1	10.1	5.8

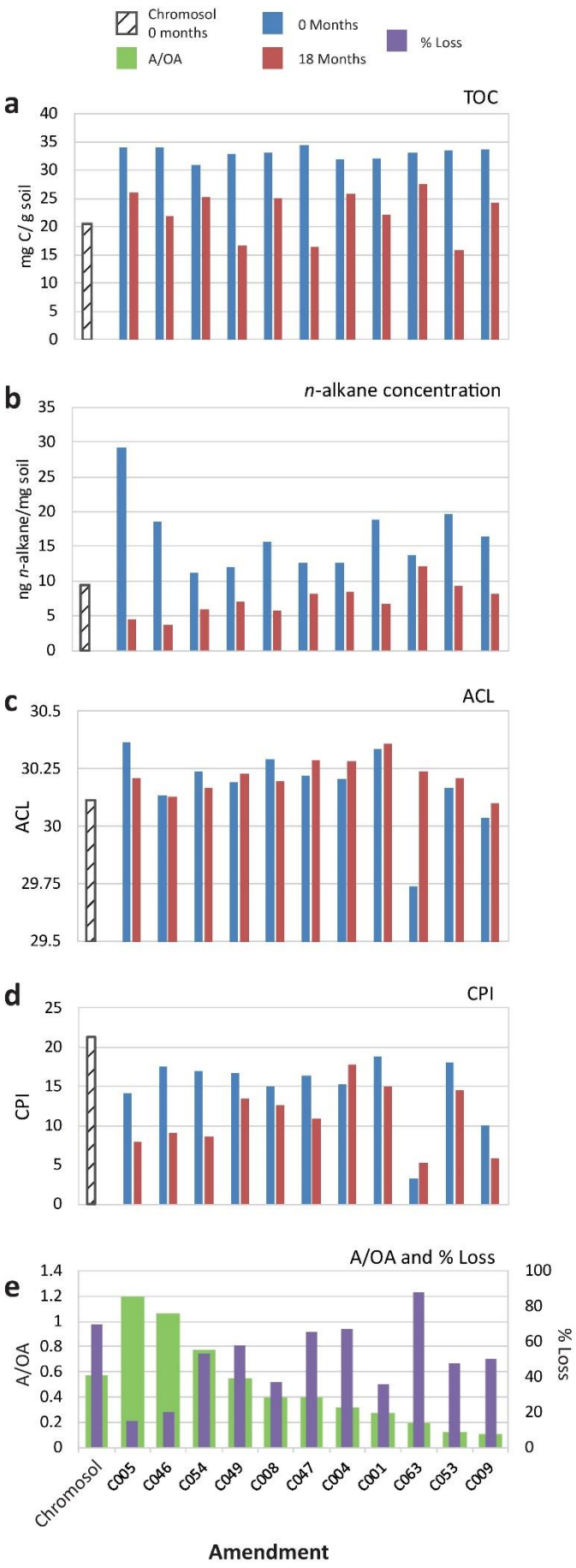
Chromosol 0 months
A/OA
0 Months
18 Months
% Loss
a
TOC
mg C/ g soil
b
n-alkane concentration
ng n-alkane/mg soil
c
ACL
d
CPI
e
A/OA and % Loss
A/OA
% Loss
Chromosol
C005
C046
C054
C049
C008
C047
C004
C001
C063
C053
C009
Amendment

Figure 1. TOC, *n*-alkane concentration (C_{15}-C_{35}), ACL and CPI at 0 and 18 months of incubation, and % Loss over 18 months, presented in order of decreasing alkyl to o-alkyl carbon in each sample (A/OA) (Farrell et al. 2015). Composition of unamended chromosol shown for comparison.

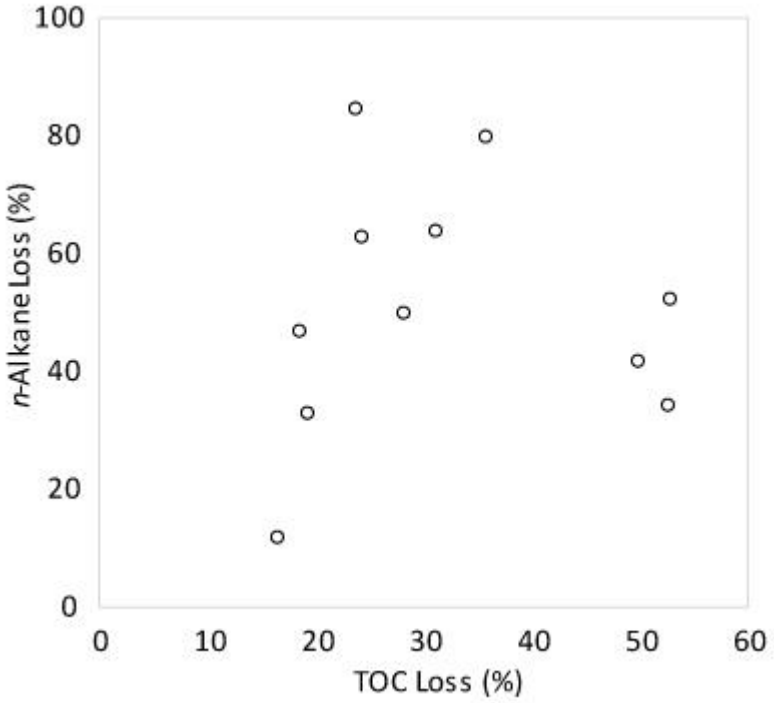

Figure 2. Comparison of loss in total organic carbon and loss in *n*-alkane concentration over 18 months of incubation.

Two samples, C009 (fresh green waste) and C047 (composted green waste and biosolids), were also analysed at 0, 1, 3, 6, 12 and 18 months incubation. In these time series, percent TOC decreased both after 1 month and between 12-18 months of incubation, whereas percent *n*-alkane concentration decreased after 1 month incubation and then remained relatively constant (Fig. 3a and 3b). In all amended samples, we find that all the low molecular weight (C_{15}-C_{24}, LMW) chain lengths

decrease in concentration after incubation, and in all but two amended samples, the high molecular weight (C_{25}-C_{35}, HMW) chain lengths also decrease after incubation (Fig. 4).

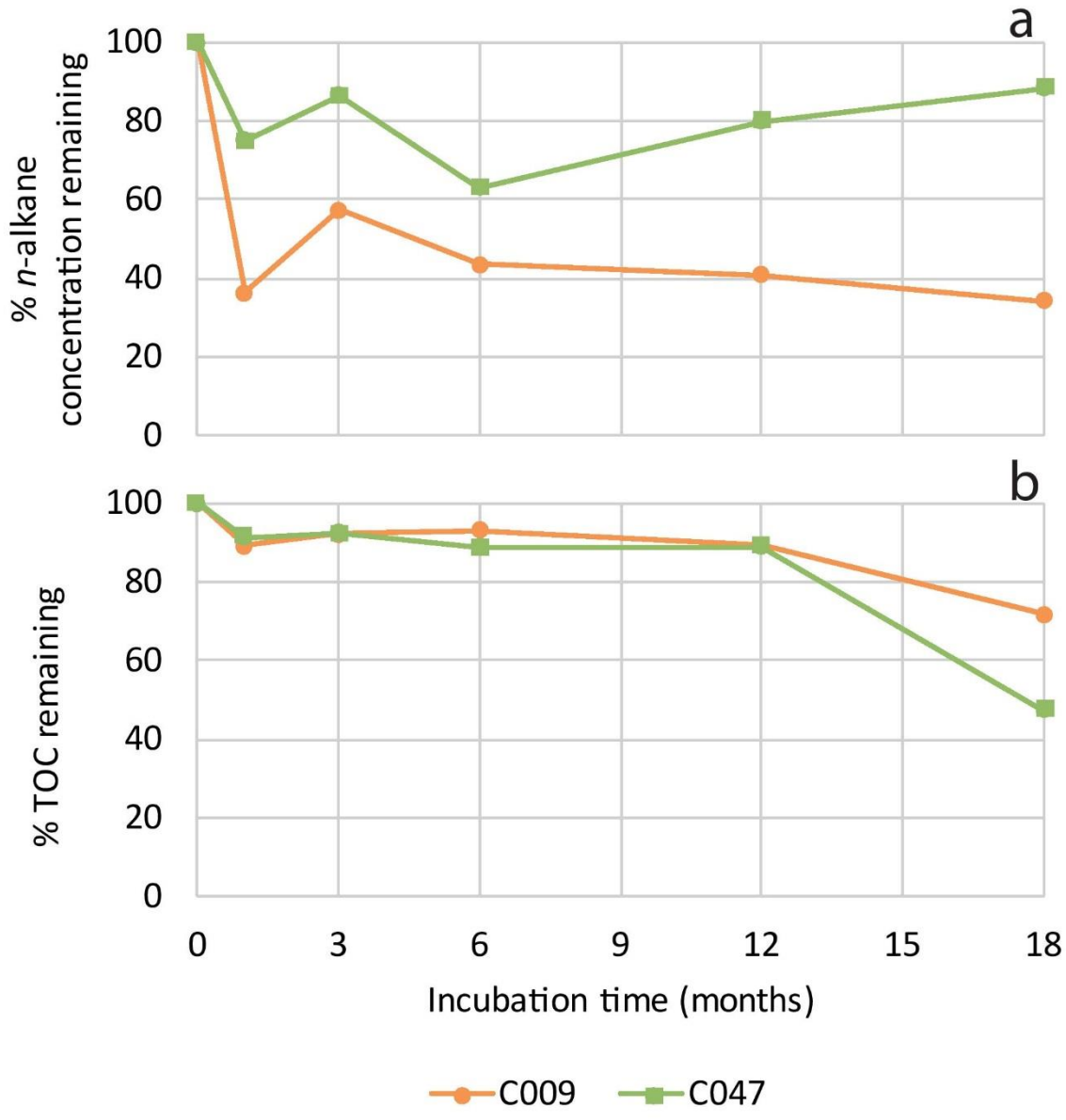

Figure 3. Percent total *n*-alkane concentration remaining (a) and percent TOC remaining (b) at 0, 1, 3, 6, 12 and 18 months of incubation for samples C009 and C047.

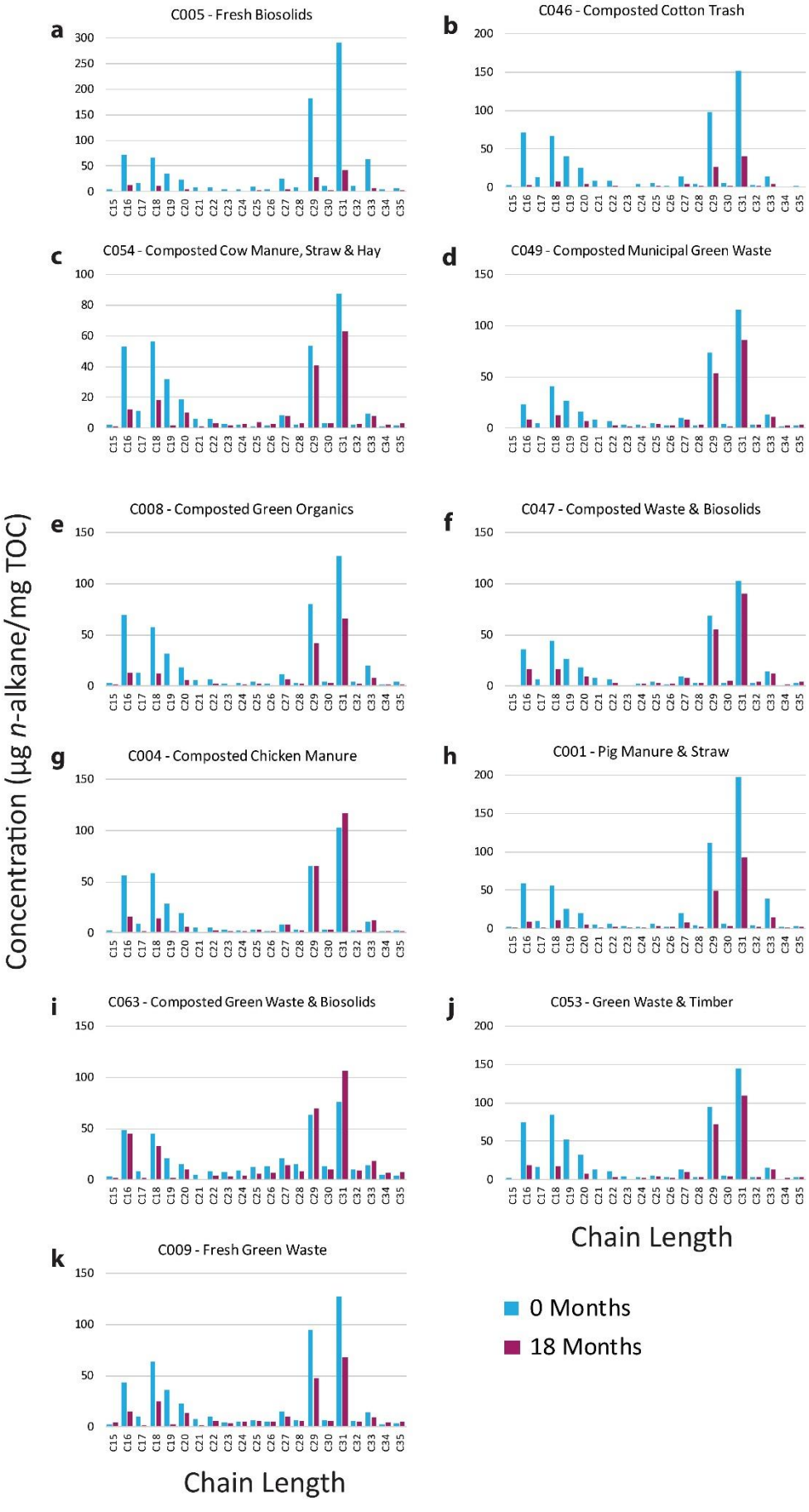
a
C005 - Fresh Biosolids
b
C046 - Composted Cotton Trash
c
C054 - Composted Cow Manure, Straw & Hay
d
C049 - Composted Municipal Green Waste
e
C008 - Composted Green Organics
f
C047 - Composted Waste & Biosolids
g
C004 - Composted Chicken Manure
h
C001 - Pig Manure & Straw
i
C063 - Composted Green Waste & Biosolids
j
C053 - Green Waste & Timber
k
C009 - Fresh Green Waste
Concentration (µg n-alkane/mg TOC)
Chain Length
0 Months
18 Months

Figure 4. Concentration of individual *n*-alkanes at 0 and 18 months of incubation presented in order of decreasing A/OA, as in Figure 1.

The ratio of lipid-related (alkyl) carbon to carbohydrate-related (o-alkyl) carbon of each of the samples was compared with the loss of concentration of *n*-alkanes after 18 months of incubation relative to the control sample from 0 months. Results show that the greatest amount of loss occurred with higher A/OA (Fig. 1e), with a positive correlation ($R^2 = 0.36$, $p = 0.04$) between the loss of *n*-alkane concentration and the starting alkyl/o-alkyl ratio (Fig. 5a). In other words, the greater the relative abundance of lipid-related carbon added via the composts, the greater the percentage of *n*-alkane loss after 18 months of incubation. Further, the change in CPI after 18 months shows a negative correlation with A/OA ($R^2 = 0.41$, $p = 0.03$, Fig. 5b) and percent *n*-alkane loss ($R^2 = 0.44$, $p = 0.03$, Fig. 5c).

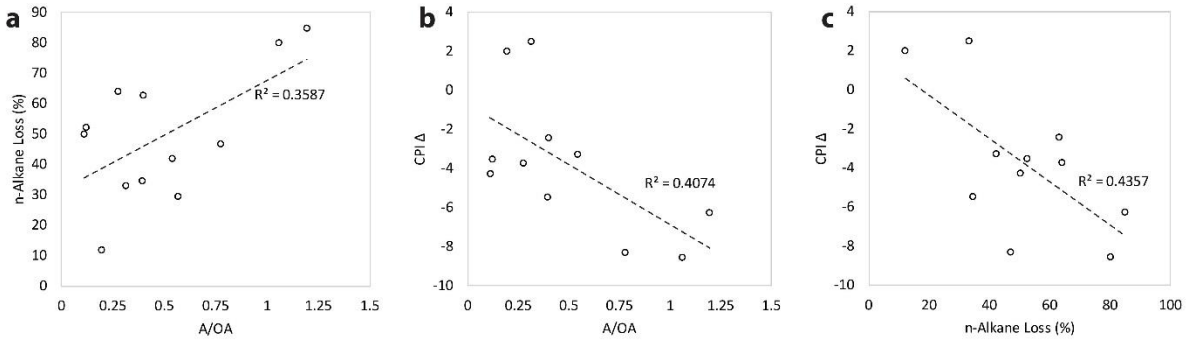

Figure 5. Cross plots of a) the alkyl/o-alkyl ratio (A/OA) of amendment versus percent *n*-alkane loss after 18 months of incubation, b) the A/OA of amendment versus the difference in CPI after 18 months of incubation, and c) the percent *n*-alkane loss after 18 months of incubation versus the difference in CPI after 18 months of incubation.

4. Discussion

This work examines the effects of post depostional modification on *n*-alkanes that have been disseminated into soils after the leaves they are sourced from have undergone breakdown processes, such as digestion or litter decomposition. By incubating different composted organic matter, the controlled experiments conducted here replicate conditions after intial leaf breakdown and hence examines the next steps in *n*-alkane degradation to those tested in existing litterbag studies. Results here show that after 18 months up to 85% of *n*-alkanes were removed from the soils (Table 1, Fig. 1b). Similarly, litterbag studies have observed large decreases in *n*-alkane concentrations over the course of the experiments, with Zech et al. (2011) finding an average of 85% reduction and Nguyen Tu et al. (2011) observing a 99% decrease in total leaf lipids. Our work demonstrates the potential for further degradation of the pool of *n*-alkanes that remain after intital leaf litter degradation after dissociation from leaf tissue and having been mixed into a soil.

As well as seeing a large decrease in concentration, there is also a wide range of variability in loss, ranging from 12 – 85% in *n*-alkane concentration and 16 – 53% in TOC loss (Table 2, Fig. 1). However, the losses in *n*-alkane concentration and percent TOC are not correlated to one another (Fig. 2). Given that the soil and the incubation conditions remained identical between samples, it is likely that this wide range of variability is due to the differences between the composts and their microbial communities. Composts were chosen based on their broad range of compostions and chemistries. Furthermore, the microbes in each incubation would have been heavily influenced by the community derived primarily from the compost, despite being air-dried and finely ground before addition to the soil. Each compost would have had its own individual community of microbes, specific to the composting materials and their specific chemistries (Pérez-Piqueres et al. 2006). The efficacy of these microbial

communites is evident from the two samples that were monitored at a higher temporal resolution which both show that majority of loss occurred after only one month of incubation (Fig. 3).

The different compositions of the composts corresponded with the degree of *n*-alkane loss. Microbes preferentially metabolise o-alkyl compounds (e.g. carbohydrates) because of their greater bioavailability than alkyl (e.g. lipid) compounds, and thus a high alkyl/o-alkyl (A/OA) ratio is regarded as an indicator of greater degradation or decomposition (Baldock and Preston 1995). The amendments varied significantly in A/OA ratios (0.28 to 1.19, Table 1). The A/OA ratio of the composts was significantly correlated with the loss of of *n*-alkanes, with the greater losses in samples with higher A/OA ratios (Fig. 5a). This result seems counter-intuitive because the composts with the highest A/OA ratios (most decomposed prior to addition to the soils) also have the highest loss of *n*-alkanes during the experiment. However, the high alkyl/o-alkyl ratio may force microbes to resort to metabolising the alkyl compounds present when soil conditions (temperature and humidity) are favourable, but only limited o-alkyl compounds are available. In addition, alkyl compounds are kinetically unstable which makes them susceptible to degradation, but their hydrophobicity leads them to become bound to clay particles in soils which can protect them from microbial degradation (Schmidt et al. 2011, Lehmann and Kleber 2015). In this experiment, we examine soils with freshly added composts rich in alkyl compounds that have not yet been stabilised in the soils, and see high losses that correlate with high A/AO ratios. This further supports that *n*-alkanes are unstable at the time of deposition and their long-term preservation in soils and sediments is dependent upon their interaction with clay minerals.

Although A/OA correlated with *n*-alkane loss, it did not correlate with TOC loss and TOC and *n*-alkane concentration do not decrease proportionally to one another (Figs. 1 and 2). This non-proportional decrease in TOC and *n*-alkane concentration is likely as a result of the various organic amendments containing different proportions of organic compounds that may be more susceptible to post-depositional modification than *n*-alkanes. The diverse composition and degree of decomposition of composts contribute to the observed variation in loss of TOC, but the changes in TOC are not an indication of the degree of *n*-alkane breakdown.

The odd-over-even predominance of the long-chain *n*-alkanes (C_{25}-C_{35}), measured as CPI, significantly decreased after 18 months of incubation. This is due to a greater proportion of loss in the odd than the even chain lengths. On average, odd chain length *n*-alkanes (C_{25}–C_{35}) experienced a loss of 23%, whereas even chain lengths decreased by only 12%. Previous litterbag studies have found contrasting results with one showing a decrease in odd over even predominance of chain lengths (Zech et al. 2011) and another finding no changes in either CPI nor ACL (Wang et al. 2014). These contrasting results may be due to differences in experimental set up, or perhaps differing environmental conditions controlling degradation rates. Comparisons of CPI in soils with that of local plant populations found a lower average CPI in the soils as compared to the plants, potentially indicative of degradation of organic matter in soils (Bliedtner et al. 2018, Howard et al. 2018). Further, analysis of changes to CPI with depth have revealed, in one case, decreasing values of CPI and decreasing *n*-alkane concentration with depth, attributed to progressive degradation (Andersson and Meyers 2012). In another case oscillations in *n*-alkane CPI values occurred with depth, attributed to temperature variations causing alternating periods of high and low degradation (Ortiz et al. 2010). In this study, where environment and time were held

constant, we found CPI generally decreased as a result of degradation, with variation observed amongsth composts. Evidence of degradation processes occuring in the soils is further supprted by the greater decrease in CPI occuring where there is a higher A/OA. The greatest break down of *n*-alkanes with a high A/OA leads to a greater change in CPI (Figs. 5b and 5c).

Despite evidence of degradation and a significant decrease in *n*-alkane concentration in the soils over the period of incubation, the ACL in the soils remains unchanged after 18 months of incubation. ACL is widely used in palaeoenvironmental studies as a proxy for vegetation and climate (Diefendorf and Freimuth 2017) and this study provides additional confidence in the durability of ACL signal observed in soils despite microbial degradation. Litterbag studies have been conducted examining the effects of microbial activity on *n*-alkane signals of whole leaves and have found similar results. A litterbag experiment found leaves of one plant species showed no notable change in ACL and only a small increase in ACL in a different plant species after burial for 1 year (Li et al. 2017). Further, a recent 2 year litterbag study in France found no change in *n*-alkane ACL in beech leaves, and suggested that the original plant lipid signatures were able to retain their characteristics despite degradation (Nguyen Tu et al. 2017). Our work expands on the results of litterbag degradation studies by examining the fate of *n*-alkanes after they have been disseminated in soils.

Although the observed decrease in CPI indicates a preferential loss of odd chain lengths over even ones, the stability of ACL demonstrates that microbial metabolism does not preferentially remove shorter or longer odd chain lengths. They are instead metabolised in proportion to one another. Our results show that overall mid chain length *n*-alkanes (C_{21} to C_{24}) concentrations decrease (Fig. 4, Supplementary Table 1) which indicates that microbes are not simply converting longer chain lengths into

shorter chain lengths. Microbial metabolism of *n*-alkanes has been widely studied as an important bioremediation tool for oil spills in soil and water (Pérez-de-Mora et al. 2011, Ji et al. 2013, Mapelli et al. 2017, Varjani 2017). Microbes are able to convert recalcitrant *n*-alkanes into less inert compounds by oxidation of a methyl group to form a primary or secondary alcohol, and then through a series of degradation pathways to form fatty acids, which other microorganisms are able to access and utilise more readily than the *n*-alkanes they are formed from (Pérez-de-Mora et al. 2011, Ji et al. 2013, Varjani 2017). However, it is widely regarded that *n*-alkanes are generally highly resistant to degradation, and the longer the chain length, the lower their degradability (Leahy and Colwell 1990, Hasinger et al. 2012, Ji et al. 2013). Studies examining reservoir oils have previously observed the sequential biodegradation of *n*-alkanes, with the intitial degradation of shorter chain lengths followed by the longer chain lengths as the rate of bacterial attack increases (Wenger et al. 2002). However, subsequent work has found that degradation of all *n*-alkane chain lengths occurs simultaneously, and instead longer chain lengths experience lower rates of degradation which gives the impression of sequential degradation (Head et al. 2006). Results of this study show that in soils, microbial degradation of all chain lengths has occurred, and whilst the longer chain lengths are also susceptible to degradation the difference in the rate of removal of higher molecular weight hydrocarbon homologues is not significant enough to alter the ACL. Work examining the effects of composting as a means of bioremediating soils contaminated with hydrocarbons has found that there is significant enhancement of hydrocarbon degradation as a result of organic amendments being added to soils (Namkoong et al. 2002, Chen et al. 2015).

The use of leaf wax *n*-alkanes for palaeoenvironmental research relies on the signals being interpreted in terms of source plants and post depositional processes. Our

previous work examining the relationship between the *n*-alkane signalsobserved in plants and soils found a mismatch in ACL between the standing plant community and the soils and a lower CPI in the soils than the plants (Howard et al. 2018). The lower CPI in the soils was interpreted as a measure of degradation, which is further supported by the results of the incubation experiment presented here. The ACL mismatch was hypothesized to result from either temporal and spatial averaging of *n*-alkane inputs to soils or from post-depositional modification in the soil. The results presented here provide evidence against post-depositional degradation of *n*-alkanes in soils as the cause for the mismatch in ACL observed between soils and the local plant community, and instead supports that soils reflect a spatial and temporal average of plant communities rather than the local (<1 hectare) plant community. Furthermore, this provides confidence in the stability of ACL, despite post-depositional modification, when examining ACL in soils and sediments for palaeoenvironmental research.

5. Conclusions

Leaf wax *n*-alkanes are widely used as a proxy for the plants that produced them and are particularly useful for palaeoecological research due to their abundance in the sedimentary record (Diefendorf and Freimuth 2017). It is therefore fundamental that we have an understanding of their preservation and whether the signals observed in soils and, subsequently, sediments, are significantly altered. This study experimentally tested the effects of post-depositional modification to *n*-alkane signals in soils using incubation experiments. Our study differs from previous litterbag studies by isolating the effects of microbial degradation in soils from the effects of herbivory and additionally expands on these studies by examining the changes that occur to *n*-alkanes that have been disseminated into soils. The same soil was used across all samples with

variation only in the organic composts and their associated microbial communities. Results from this study find large decreases of up to 85% in *n*-alkane concentration after incubation, with the greatest decrease occurring in the first month. Further, we find that the concentration loss is not correlated to TOC, but it is correlated with the A/OA ratio, with increasing concentration loss at higher A/OA ratio. We hypothesize that this is due to the kinetic instability of *n*-alkanes, making them more readily susceptible to degradation, before they become stabilised in the soil. Additionally, results show that CPI decreases during incubation, providing support for CPI as an indicator of degradation. Despite evidence of significant degradation occurring after *n*-alkanes are added to soils, ACL remains stable. This provides confidence in the use of ACL as a signal for paleaoenvironmental research.

Acknowledgements

The authors thank CSIRO, for providing the samples and used in this study. Thanks also to Kristine Nielson for assistance in the lab. Funding was provided by the Australian Research Council to FAM (FT110100793). This research is also supported by an Australian Government Research Training Program (RTP) Scholarship to SH.

References

ANDERSSON R. A. & MEYERS P. A. 2012. Effect of climate change on delivery and degradation of lipid biomarkers in a Holocene peat sequence in the Eastern European Russian Arctic, *Organic Geochemistry*. **53**, 63-72.

BALDOCK J. A. & PRESTON C. M. 1995 Chemistry of Carbon Decomposition Processes in Forests as Revealed by Solid-State Carbon-13 Nuclear Magnetic Resonance. *In* MCFEE W. W. & KELLY J. M. eds. Carbon Forms and Functions in Forest Soils. pp. 89-117. Soil Science Society of America,

BALDOCK J. A., OADES J. M., NELSON P. N., SKENE T. M., GOLCHIN A. & CLARKE P. 1997. Assessing the extent of decomposition of natural organic materials using solid-state 13C NMR spectroscopy, *Soil Research*. **35**, 1061-1084.

BALDOCK J. A., SANDERMAN J., MACDONALD L. M., PUCCINI A., HAWKE B., SZARVAS S. & MCGOWAN J. 2013. Quantifying the allocation of soil organic carbon to biologically significant fractions, *Soil Research*. **51**, 561-576.

BANTHORPE D. V. 2006 Natural Occurrence, Biochemistry and Toxicology. Alkanes and Cycloalkanes (1992). pp. 895-926. John Wiley & Sons, Ltd,

BASTOW T. P., VAN AARSSEN B. G. K. & LANG D. 2007. Rapid small-scale separation of saturate, aromatic and polar components in petroleum, *Organic Geochemistry*. **38**, 1235-1250.

BLIEDTNER M., SCHÄFER I. K., ZECH R. & VON SUCHODOLETZ H. 2018. Leaf wax n-alkanes in modern plants and topsoils from eastern Georgia (Caucasus) – implications for reconstructing regional paleovegetation, *Biogeosciences*. **15**, 3927-3936.

BUSH R. T. & MCINERNEY F. A. 2013. Leaf wax *n*-alkane distributions in and across modern plants: Implications for paleoecology and chemotaxonomy, *Geochimica et Cosmochimica Acta*. **117**, 161-179.

--- 2015. Influence of temperature and C4 abundance on *n*-alkane chain length distributions across the central USA, *Organic Geochemistry*. **79**, 65-73.

CHEN M., XU P., ZENG G., YANG C., HUANG D. & ZHANG J. 2015. Bioremediation of soils contaminated with polycyclic aromatic hydrocarbons, petroleum, pesticides, chlorophenols and heavy metals by composting: Applications, microbes and future research needs, *Biotechnology Advances*. **33**, 745-755.

CRANWELL P. A. 1981. Diagenesis of free and bound lipids in terrestrial detritus deposited in a lacustrine sediment, *Organic Geochemistry*. **3**, 79-89.

DIEFENDORF A. F., LESLIE A. B. & WING S. L. 2015. Leaf wax composition and carbon isotopes vary among major conifer groups, *Geochimica et Cosmochimica Acta*. **170**, 145-156.

DIEFENDORF A. F. & FREIMUTH E. J. 2017. Extracting the most from terrestrial plant-derived *n*-alkyl lipids and their carbon isotopes from the sedimentary record: A review, *Organic Geochemistry*. **103**, 1-21.

DOUGLAS P. M. J., PAGANI M., EGLINTON T. I., BRENNER M., HODELL D. A., CURTIS J. H., MA K. F. & BRECKENRIDGE A. 2014. Pre-aged plant waxes in tropical lake sediments and their influence on the chronology of molecular paleoclimate proxy records, *Geochimica et Cosmochimica Acta*. **141**, 346-364.

EGLINTON G. & HAMILTON R. J. 1967. Leaf Epicuticular Waxes, *Science*. **156**, 1322-1335.

EGLINTON T. I. & EGLINTON G. 2008. Molecular proxies for paleoclimatology, *Earth and Planetary Science Letters*. **275**, 1-16.

EIGENBRODE S. D. & ESPELIE K. E. 1995. Effects of Plant Epicuticular Lipids on Insect Herbivores, *Annual Review of Entomology*. **40**, 171-194.

FARRELL M., BALDOCK J., CARTER T., CREAMER C., HAWKE B., KOOKANA R., MARTIN S., MCGOWAN J. & SZARVAS S. 2015 An assessment of the carbon sequestration potential of organic soil amendments. pp. 13-53. Department of Agriculture: CSIRO.

GIERGA M., HAJDAS I., VAN RADEN U. J., GILLI A., WACKER L., STURM M., BERNASCONI S. M. & SMITTENBERG R. H. 2016. Long-stored soil carbon released by prehistoric land use: Evidence from

compound-specific radiocarbon analysis on Soppensee lake sediments, *Quaternary Science Reviews*. **144**, 123-131.
HASINGER M., SCHERR K. E., LUNDAA T., BRÄUER L., ZACH C. & LOIBNER A. P. 2012. Changes in iso- and n-alkane distribution during biodegradation of crude oil under nitrate and sulphate reducing conditions, *Journal of Biotechnology*. **157**, 490-498.
HEAD I. M., JONES D. M. & RÖLING W. F. M. 2006. Marine microorganisms make a meal of oil, *Nature Reviews Microbiology*. **4**, p.173.
HOWARD S., MCINERNEY F. A., CADDY-RETALIC S., HALL P. A. & ANDRAE J. W. 2018. Modelling leaf wax n-alkane inputs to soils along a latitudinal transect across Australia, *Organic Geochemistry*. **121**, 126-137.
ISBELL R. & NATIONAL COMMITTEE ON SOIL TERRAIN 2016 The Australian Soil Classification. CSIRO Publishing, Victoria, Australia.
JI Y., MAO G., WANG Y. & BARTLAM M. 2013. Structural insights into diversity and n-alkane biodegradation mechanisms of alkane hydroxylases, *Frontiers in Microbiology*. **4**.
KHAN A. A. & KOLATTUKUDY P. E. 1974. Decarboxylation of long chain fatty acids to alkanes by cell free preparations of pea leaves (Pisum sativum), *Biochemical and Biophysical Research Communications*. **61**, 1379-1386.
LEAHY J. G. & COLWELL R. R. 1990. Microbial degradation of hydrocarbons in the environment, *Microbiological Reviews*. **54**, 305-315.
LEHMANN J. & KLEBER M. 2015. The contentious nature of soil organic matter, *Nature*. **528**, p.60.
LI R., FAN J., XUE J. & MEYERS P. A. 2017. Effects of early diagenesis on molecular distributions and carbon isotopic compositions of leaf wax long chain biomarker n-alkanes: Comparison of two one-year-long burial experiments, *Organic Geochemistry*. **104**, 8-18.
LICHTFOUSE É., CHENU C., BAUDIN F., LEBLOND C., DA SILVA M., BEHAR F., DERENNE S., LARGEAU C., WEHRUNG P. & ALBRECHT P. 1998. A novel pathway of soil organic matter formation by selective preservation of resistant straight-chain biopolymers: chemical and isotope evidence, *Organic Geochemistry*. **28**, 411-415.
MAPELLI F., SCOMA A., MICHOUD G., AULENTA F., BOON N., BORIN S., KALOGERAKIS N. & DAFFONCHIO D. 2017. Biotechnologies for Marine Oil Spill Cleanup: Indissoluble Ties with Microorganisms, *Trends in Biotechnology*. **35**, 860-870.
MARZI R., TORKELSON B. E. & OLSON R. K. 1993. A revised carbon preference index, *Organic Geochemistry*. **20**, 1303-1306.
NAMKOONG W., HWANG E.-Y., PARK J.-S. & CHOI J.-Y. 2002. Bioremediation of diesel-contaminated soil with composting, *Environmental Pollution*. **119**, 23-31.
NGUYEN TU T. T., EGASSE C., ZELLER B., BARDOUX G., BIRON P., PONGE J. F., DAVID B. & DERENNE S. 2011. Early degradation of plant alkanes in soils: A litterbag experiment using 13C-labelled leaves, *Soil Biology and Biochemistry*. **43**, 2222-2228.
NGUYEN TU T. T., EGASSE C., ANQUETIL C., ZANETTI F., ZELLER B., HUON S. & DERENNE S. 2017. Leaf lipid degradation in soils and surface sediments: A litterbag experiment, *Organic Geochemistry*. **104**, 35-41.
ORTIZ J. E., GALLEGO J. L. R., TORRES T., DÍAZ-BAUTISTA A. & SIERRA C. 2010. Palaeoenvironmental reconstruction of Northern Spain during the last 8000calyr BP based on the biomarker content of the Roñanzas peat bog (Asturias), *Organic Geochemistry*. **41**, 454-466.
PEARSON A. & EGLINTON T. I. 2000. The origin of n-alkanes in Santa Monica Basin surface sediment: a model based on compound-specific Δ14C and δ13C data, *Organic Geochemistry*. **31**, 1103-1116.
PÉREZ-DE-MORA A., ENGEL M. & SCHLOTER M. 2011. Abundance and Diversity of n-Alkane-Degrading Bacteria in a Forest Soil Co-Contaminated with Hydrocarbons and Metals: A Molecular Study on alkB Homologous Genes, *Microbial Ecology*. **62**, 959-972.
PÉREZ-PIQUERES A., EDEL-HERMANN V., ALABOUVETTE C. & STEINBERG C. 2006. Response of soil microbial communities to compost amendments, *Soil Biology and Biochemistry*. **38**, 460-470.
SCHMIDT M. W. I., TORN M. S., ABIVEN S., DITTMAR T., GUGGENBERGER G., JANSSENS I. A., KLEBER M., KOGEL-KNABNER I., LEHMANN J., MANNING D. A. C., NANNIPIERI P., RASSE D. P., WEINER S. &

TRUMBORE S. E. 2011. Persistence of soil organic matter as an ecosystem property, *Nature*. **478**, 49-56.
SHEPHERD T. & WYNNE GRIFFITHS D. 2006. The effects of stress on plant cuticular waxes, *New Phytologist*. **171**, 469-499.
SMITH F. A., WING S. L. & FREEMAN K. H. 2007. Magnitude of the carbon isotope excursion at the Paleocene–Eocene thermal maximum: The role of plant community change, *Earth and Planetary Science Letters*. **262**, 50-65.
SMITTENBERG R. H., EGLINTON T. I., SCHOUTEN S. & DAMSTÉ J. S. S. 2006. Ongoing Buildup of Refractory Organic Carbon in Boreal Soils During the Holocene, *Science*. **314**, 1283-1286.
VARJANI S. J. 2017. Microbial degradation of petroleum hydrocarbons, *Bioresource Technology*. **223**, 277-286.
WANG G., ZHANG L., ZHANG X., WANG Y. & XU Y. 2014. Chemical and carbon isotopic dynamics of grass organic matter during litter decompositions: A litterbag experiment, *Organic Geochemistry*. **69**, 106-113.
WENGER L., DAVIS C. & ISAKSEN G. 2002. Multiple Controls on Petroleum Biodegradation and Impact on Oil Quality, *SPE Reservoir Evaluation & Engineering*. **5**, 375-383.
YAMAMOTO S., HASEGAWA T., TADA R., GOTO K., ROJAS-CONSUEGRA R., DÍAZ-OTERO C., GARCÍA-DELGADO D. E., YAMAMOTO S., SAKUMA H. & MATSUI T. 2010. Environmental and vegetational changes recorded in sedimentary leaf wax *n*-alkanes across the Cretaceous–Paleogene boundary at Loma Capiro, Central Cuba, *Palaeogeography, Palaeoclimatology, Palaeoecology*. **295**, 31-41.
ZECH M., PEDENTCHOUK N., BUGGLE B., LEIBER K., KALBITZ K., MARKOVIĆ S. B. & GLASER B. 2011. Effect of leaf litter degradation and seasonality on D/H isotope ratios of *n*-alkane biomarkers, *Geochimica et Cosmochimica Acta*. **75**, 4917-4928.

CHAPTER 4

Vegetation and climate change 70,000 to 17,000 years ago from leaf wax *n*-alkanes preserved in Blanche Cave sediments, Naracoorte, South Australia

Howard, S.[a], McInerney, F.A.[a,] Arnold, L.J.[a], Grice, K.[b], Holman, A.I.[b], Hall, P.A.[a] & Reed, E.H.[a].

[a]*School of Physical Sciences, Department of Earth Science, Sprigg Geobiology Centre, University of Adelaide, Australia*

[b]*Western Australian Organic and Isotope Geochemistry Centre, The Institute for Geoscience Research, School of Earth and Planetary Sciences, Curtin University, Australia*

Statement of Authorship

Title of Paper	Vegetation and climate change 70,000 to 17,000 years ago from leaf wax *n*-alkanes preserved in Blanche Cave sediments, Naracoorte, South Australia
Publication Status	☐ Published ☐ Accepted for Publication ☐ Submitted for Publication ☑ Unpublished and Unsubmitted work written in manuscript style
Publication Details	

Principal Author

Name of Principal Author (Candidate)	Siân Howard		
Contribution to the Paper	Designed the study. Conducted sample processing and analysis. Conducted data analysis and interpretation. Wrote manuscript.		
Overall percentage (%)	75		
Certification:	This paper reports on original research I conducted during the period of my Higher Degree by Research candidature and is not subject to any obligations or contractual agreements with a third party that would constrain its inclusion in this thesis. I am the primary author of this paper.		
Signature		Date	13/12/2018

Co-Author Contributions

By signing the Statement of Authorship, each author certifies that:

i. the candidate's stated contribution to the publication is accurate (as detailed above);

ii. permission is granted for the candidate in include the publication in the thesis; and

iii. the sum of all co-author contributions is equal to 100% less the candidate's stated contribution.

Name of Co-Author	Dr Francesca A. McInerney		
Contribution to the Paper	Supervised SH. Designed the study. Provided input into data analysis, interpretation and manuscript. Reviewed and edited final manuscript.		
Signature		Date	13/12/2018

Name of Co-Author	Dr Elizabeth H. Reed		
Contribution to the Paper	Provided samples and sample context. Reviewed and edited final manuscript.		
Signature		Date	11/2/2019

Name of Co-Author	Dr Lee J. Arnold		
Contribution to the Paper	Provided OSL dating of samples. Reviewed and edited final manuscript.		
Signature		Date	6/2/2019

Name of Co-Author	Prof. Kliti Grice		
Contribution to the Paper	Provided compound specific carbon and hydrogen isotope analysis of samples. Reviewed and edited final manuscript.		
Signature		Date	22/2/2019

Name of Co-Author	Dr Philip A. Hall		
Contribution to the Paper	Provided GC-MS quantification of samples. Reviewed and edited final manuscript.		
Signature		Date	6/2/2019

Name of Co-Author	Dr Alex I. Holman		
Contribution to the Paper	Provided compound specific carbon and hydrogen isotope analysis of samples. Reviewed and edited final manuscript.		
Signature		Date	25/2/2019

Abstract

Vegetation and climate records for Australia before, during and after the time of the megafauna extinction that occurred at around 50 – 40 thousand years ago (ka) are important for examining the environmental factors that may have played a role in the decline of these species. Naracoorte Caves in south eastern Australia is an ideal study locality for reconstructing Australia's late Quaternary vegetation record through examination of sediments found in association with vertebrate fossils preserved in the caves. In particular, Blanche Cave sediments provide an archive of sedimentary *n*-alkanes that record the regional vegetation and climate across the megafauna extinction boundary. We extracted the *n*-alkanes from 23 layers of Blanche Cave sediments, dating from 70 – 17 ka, and examined their $\delta^{13}C$ and δD values in order to reconstruct vegetation and hydroclimate for the region during this time period. The Blanche Cave sedimentary *n*-alkanes reveal evidence for both C3 and C4 vegetation during Marine Isotope Stage (MIS) 4 with C4 vegetation decreasing prior to the disappearance of megafauna fossils. C4 vegetation disappears entirely after the time megafauna fossils disappear, but then rebounds and begins to return to the record with mixed C3 and C4 vegetation by the start of MIS 2. The disappearance of megafauna fossils corresponds with the wettest period in the record, however C4 vegetation does not completely disappear until after this time, as conditions begin to dry. We propose that the initial decrease of C4 vegetation was as a result of an increasingly wet climate and that this vegetation change may have adversely impacted some megafauna species. Further, the subsequent complete disappearance of C4 vegetation after megafauna fossils disappear may be itself a direct result of the loss of large herbivorous species, which would have allowed C3 woody vegetation to proliferate in its place. C4 vegetation then begins to return to the record, which corresponds with dry conditions at this time and may also

be affected by human-induced changes in fire regime. These findings provide an important environmental context for examining the debate surrounding the causes of megafauna extinction in Australia.

Keywords

Naracoorte Caves, *n*-alkanes, leaf wax, sediments, hydrogen isotopes, stable carbon isotopes, megafauna extinction

1. Introduction

1.1 Australia's extinct megafauna

Megafauna are a suite of large animal species that became extinct in Australia at about 45,000 year ago (Prideaux et al. 2010, Roberts and Brook 2010). Australia's late Quaternary vegetation and climate records provide a critical context for understanding the environment before, during and after the megafauna extinction, with much of the debate about the cause of their extinction centring around climate change versus human impacts (Prideaux et al. 2010, Bird et al. 2013, Cooper et al. 2015, Johnson et al. 2016, Saltre et al. 2016). Many megafauna species were herbivorous and major changes to vegetation, either through changes in fire regime, habitat alteration or climate change, may have played a significant role in their extinction (Miller et al. 1999, Prideaux et al. 2010, Rule et al. 2012).

1.2 The isotopic composition of molecular leaf wax n-alkanes

The molecular fossil record provides insight into vegetation changes, particularly where other floral remains can be scarce (Pancost and Boot 2004, Diefendorf and Freimuth 2017). In particular, long chain *n*-alkanes are highly recalcitrant compounds

that are ubiquitous throughout the sedimentary record and have diagnostic characteristics that readily identify them as being sourced from terrestrial plants (Eglinton and Hamilton 1967, Cranwell 1981, Diefendorf et al. 2011). Analysis of the isotopic signatures of leaf wax *n*-alkanes from ancient sediments can provide insight into past vegetation and climate (Eglinton and Eglinton 2008).

Carbon isotope ratios ($\delta^{13}C$) of *n*-alkanes reflect the carbon fixation pathway of the plant that produced them (Collister et al. 1994, Chikaraishi and Naraoka 2003, Grice et al. 2008). Plants preferentially take up ^{12}C over ^{13}C during photosynthesis and the extent to which they discriminate against ^{13}C is dependent on the plant's photosynthetic pathway (Farquhar et al. 1989). As a result, the leaf wax *n*-alkanes from C3 plants exhibit lower $\delta^{13}C$ values than C4 plants. (Collister et al. 1994, Chikaraishi and Naraoka 2003). C3 and C4 plants grow in different climatic conditions, with C4 plants being favoured by high temperatures, high aridity, warm season precipitation and low atmospheric pCO_2 (Ehleringer et al. 1997, Sage et al. 1999). In Australia, trees, forbs and shrubs form the majority of C3 vegetation, with grasses and chenopods comprising the majority of C4 vegetation and C4 grass species being much more prevalent than C3 grass species (Supplementary Fig. S1, Appendix 3).

The δD values of leaf wax *n*-alkanes provides insight into the hydrologic conditions the plant experienced during its life. The factors influencing the isotopic composition of leaf wax *n*-alkanes include the isotopic composition of the rainwater sourced by the plant as well as various environmental, physiological and biosynthetic processes (Sachse et al. 2012). The δD values of rainfall is determined by humidity source and environmental conditions specific to a site or region (Dansgaard 1964, Rozanski et al. 1993). In particular, the environmental conditions that play a role in the isotopic composition of rainfall include: the temperature effect, where decreasing

temperature results in greater rainout and a greater depletion of deuterium (D) (Dansgaard 1964); the continental effect, where deuterium is depleted further inland and with increasing altitude (Rozanski et al. 1993, Araguás-Araguás et al. 2000); and the amount effect, where large rain events become increasingly depleted in deuterium compared to small rain events (Dansgaard 1964). Analysis of modern rainfall in Adelaide, South Australia, shows weak seasonal variation in its isotopic composition with only small fluctuations in temperature and precipitation, with winter minimum and spring-summer maxima, primarily driven by latitude, elevation and distance from the coast (Liu et al. 2010, Hollins et al. 2018). The rain permeates soil and δD values can become further fractionated as a result of evaporation from the soil (Sachse et al. 2012). Plants take up source water from the soil through their roots, which is transported via their xylem to their leaves. While no isotopic fractionation of hydrogen occurs during uptake or transport in xylem water, once the water reaches the leaf, its hydrogen isotopic composition becomes enriched in deuterium as a result of transpiration. This occurs due to faster evaporation of the lighter hydrogen isotope than the heavier deuterium isotope through leaf stomata. The degree of D enrichment varies with relative humidity through its effect on vapour pressure deficit, and can be described by the Craig-Gordon model (Craig et al. 1965, Sachse et al. 2012, Cernusak et al. 2016). The resulting isotopic composition of leaf water exhibits a greater deuterium enrichment with increasingly arid conditions (Kahmen et al. 2013). Leaf water provides the hydrogen required for leaf lipid synthesis, with *n*-alkanes being produced by the acetogenic pathway (Sachse et al. 2012). Variation in biosynthetic fractionation of hydrogen from leaf water to lipid occurs during synthesis of *n*-alkanes as a result of a range of biochemical, and physiological factors (Sachse et al. 2012), and can vary between species (Gamarra and Kahmen 2015). The net effect of both transpiration and

biosynthetic fractionation is referred to as "apparent fractionation" (Sachse et al. 2006, Smith and Freeman 2006, Polissar and Freeman 2010), with some variation in apparent fractionation between different growth forms (Sachse et al. 2012). Further, the strong covalent bond between hydrogen and carbon in *n*-alkanes means that their δD values produced at the time of leaf wax synthesis is well preserved in sediments over geological timescales, as long as they are not exposed to high temperature or pressure (Schimmelmann et al. 1999, Sessions et al. 2004, Zhou et al. 2010, Sessions 2016). Analysis of marine and lake sediments reveal that it is feasible to infer hydrological conditions from the δD values of leaf wax *n*-alkanes preserved in the sedimentary record (Sachse et al. 2004, Polissar and Freeman 2010, Garcin et al. 2012, Niedermeyer et al. 2016).

1.3 Geological setting of Naracoorte Caves

Caves are useful repositories for palaeoenvironmental analysis due to the sedimentary accumulations, fossil remains, speleothems and other physical and geochemical properties that they preserve (Osborne 1984). The Naracoorte Caves National Park in South Australia provides an ideal study area for examining the palaeoenvironmental conditions across the Australian megafauna extinction due to the rich Pleistocene vertebrate fossil assemblages preserved spanning the past 500,000 years (Wells et al. 1984, Moriarty et al. 2000, Reed and Bourne 2000, Prideaux et al. 2007, Reed and Bourne 2009). The fossils have been preserved in sediments that were deposited in the caves via pitfall entrances. These sediments are a valuable resource for examining the palaeoenvironmental conditions at the time Australia's megafauna became extinct due to their direct association with the megafauna fossils (Macken et al. 2013a).

The World Heritage listed Naracoorte Caves National Park is situated in the South East of South Australia, approximately 10 km from the township of Naracoorte (Fig. 1). Blanche Cave is one of the larger caves in the Naracoorte system, formed around 1.1 million years ago in the Naracoorte Member of the late Eocene to Miocene Gambier Limestone (White and Webb 2015). The study site is within the third chamber of Blanche Cave which has a roof collapse window entrance that allowed accumulation and deposition of deep sediment deposits sourced from surficial dune-derived sediments. Sediment deposits in the chamber consist of coarse silts sourced from the Murray-Darling Basin, fine sands sourced from the region's sand units, as well as local organic material, and limestone and fossil fragments (Forbes and Bestland 2007, Darrénougué et al. 2009). The deposit is rich in vertebrate fossils and a palaeontological excavation has been conducted by one the authors (EHR). This revealed a two-metre-deep, finely stratified section consisting of consists of a total of 43 layers that date back 70,000 years (Macken et al. 2013b). Fossil analysis of these cave sediments reveals diverse vertebrate assemblages (Reed and Bourne 2009, Macken and Reed 2013, Macken and Reed 2014), with the last appearance of megafauna species after Layer 27.

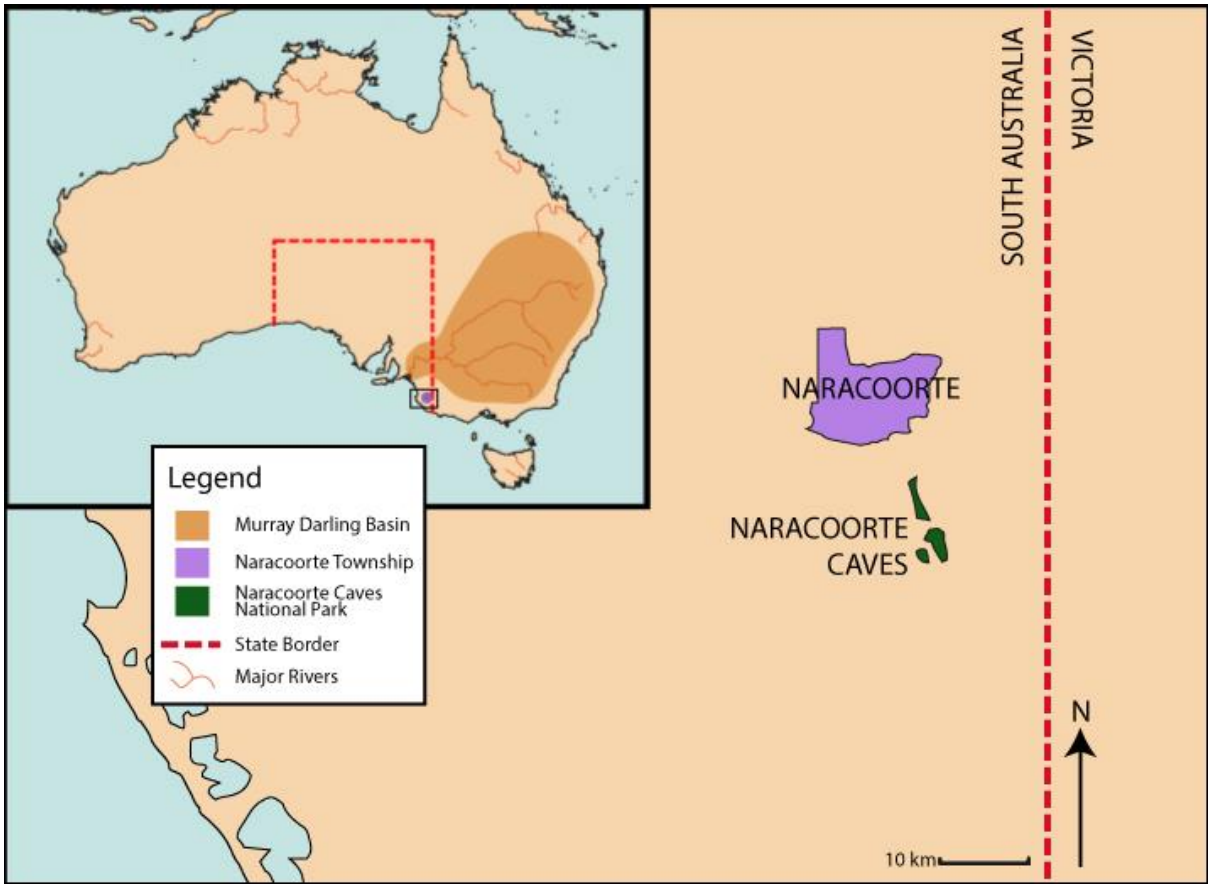

Figure 1. Location map of the Naracoorte Caves National Park, located SE of Adelaide in South Australia, with inset map showing location of Naracoorte in South Australia, made using data provided by naturalearth.com.

1.4 Dating of sedimentary layers

The chronological framework for the Blanche Cave excavation sequence has been established using a combination of radiocarbon (^{14}C) dating of charcoal and single-grain optically stimulated luminescence (OSL) dating of quartz and is summarised in Fig. 2. Macken et al. (2013b) presented 40 ^{14}C ages for Layers 1 to 27 of the sequence, and integrated these results in a stratigraphically constrained Bayesian age-depth model to derive combined age range estimates for each individual layer. We have adopted the 95.4% Bayesian modelled age ranges of Macken et al. (Macken et al. 2013b) for the relevant layers under examination in the present study (Layers 18 to 27). The

chronologies for layers 28 and below are based on five unpublished single-grain OSL dating samples. These single-grain OSL ages were obtained using the experimental procedures and equipment outlined in Arnold et al. (2016), and are reported here with their 2σ uncertainty ranges to enable direct comparisons with the modelled ^{14}C age ranges. The intervening layers in the lower part of the profile that have not been directly dated (i.e., Layers 29, 31-34, 36-37) have been inferred to fall within the age ranges constrained by bracketing OSL samples, in accordance with the principle of superposition.

The sequence is sub-divided into three separate units, broken down according to correspondence with Marine Isotope Stages (Fig. 2, Table 1), in order to ensure our climatic interpretations are not unduly biased by minor stratigraphic inversions in the OSL age ranges and to accommodate the discontinuous nature of the chronological record between Layers 28 and 37.

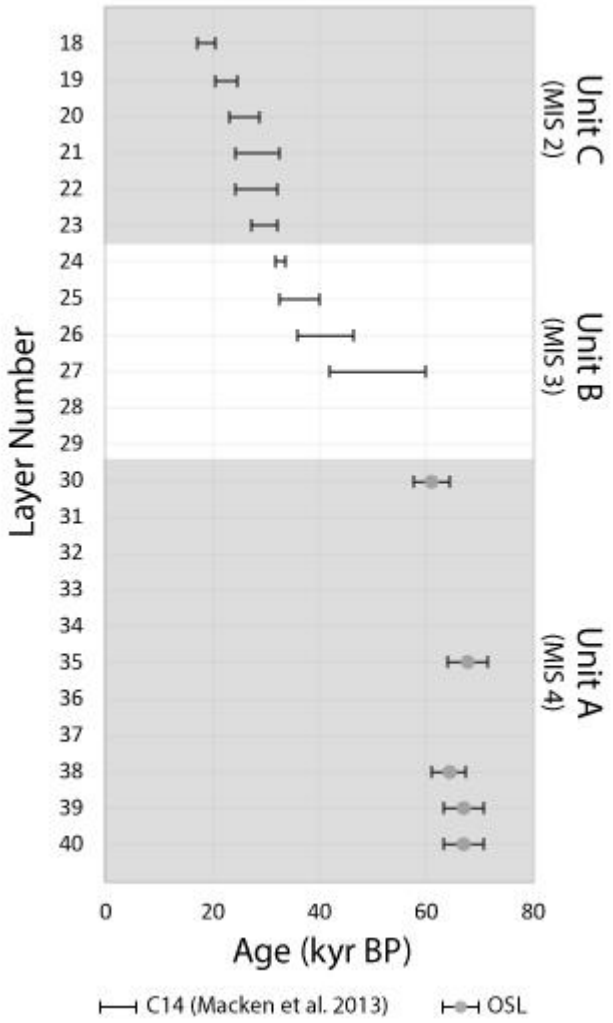

Figure 2. Numerical dating framework for the studied layers of Blanche Cave, with 95.4% Bayesian modelled and calibrated ^{14}C age ranges (Macken et al. 2013b) shown as black bars, and single-grain OSL ages (Arnold et al., pers. comms.) shown as grey circles with their associated 2σ standard error ranges.

Table 1. Details of each of the three units, including the Marine Isotope Stages (MIS) that each unit corresponds to, the layers included in each unit, the average temporal resolution of each layer (kyr), the dating method used and the source of the dates.

Unit	Corresponding interval	Layers	Average resolution (kyr)	Dating Method	Source
A	MIS 4	18-23	1.3	OSL	Unpublished
B	MIS 3	24-29	4.7	^{14}C	Macken et al. (2013b)
C	MIS 2	30-40	2.5	^{14}C	Macken et al. (2013b)

1.5 Naracoorte palaeoclimate

The Blanche Cave sediment layers (18 – 40) analysed in this study were deposited during Marine Isotope Stages (MIS) 4, 3 and 2. MIS 4 (~75 – 59 ka) was a glacial period characterised by colder and drier conditions in southern Australia (De Deckker et al. 2019), whereas MIS 3 (~59 – 30 ka) represents a period of successive stadial and interstadial conditions (Lisiecki and Raymo 2005). MIS 2 (~30 – 12 ka) is glacial period typified by the Last Glacial Maximum (LGM) (Emiliani 1955, Martinson et al. 1987, Dansgaard et al. 1993, Van Meerbeeck et al. 2009). Existing palaeoclimate records at Naracoorte Caves indicate that the climate from 45 to 25 ka, during MIS 3, experienced fluctuating moisture availability, with evidence of increased speleothem growth at this time (Macken et al. 2013a). Further, evidence of significant aeolian sediment deposition containing low percent total organic carbon (TOC), indicate very dry, cold and windy conditions leading up to and including the LGM (Forbes et al. 2007). In addition, the sedimentation at the end of MIS 3 and early stages of MIS 2 into the LGM demonstrate arid conditions (Macken et al. 2013a). Following the LGM, silty laminations indicate cyclic water transport into the caves with increasing climatic fluctuations during deglaciation, as indicated by alternating sand and clay laminations (Macken et al. 2013a). While this extensive work provides valuable insight into the climate conditions across the general time of the megafauna extinction in the Naracoorte region, detailed

work exploring vegetation and climatic shifts is required to help better understand the potential causes and effects of the extinction event.

By examining the isotopic signatures of leaf wax *n*-alkanes preserved in the sediments in Blanche cave, this study aims to explore the palaeoenvironmental conditions at the time of megafauna extinction. We use leaf wax *n*-alkane carbon and hydrogen isotope data to examine evidence for major changes and variability in vegetation and climate of the Naracoorte region from 70 to 17 ka. Using the carbon isotopic composition of the *n*-alkanes preserved in Blanche Cave sediments, we examine shifts in the relative proportions of C3 and C4 vegetation leading up to and across the megafauna extinction period. We additionally examine the hydrogen isotopic composition of the *n*-alkanes to determine regional hydrological conditions across the megafauna extinction event and how those changes related to major global climate dynamics.

2. Methods

2.1 Lipid extraction from sediments

Lipid extraction of sediments was conducted using a Thermo Scientific Dionex Accelerated Solvent Extractor (ASE) 350 using 9:1 DCM:MeOH. The ASE sequence was set to 100 °C with a 12 minute preheat, three static cycles of five minutes, and a rinse volume of 60%. Excess solvent was evaporated from the total lipid extract (TLE) under nitrogen gas.

2.2 n-Alkane purification

The polar and non-polar fractions of TLEs were separated through a silica gel glass short column by eluting them with 4 ml of hexane to collect the non-polar,

aliphatic hydrocarbon fraction, followed by 4 ml 1:1 DCM:MeOH eluent to collect the polar fraction (modified from Bastow et al. 2007). The aliphatic hydrocarbon fraction was dried under nitrogen gas.

2.3 GC-MS Lipid Quantification

Quantification of *n*-alkanes was conducted using gas chromatography mass spectrometry (GC-MS) analysis of the non-polar aliphatic hydrocarbon fraction using a Perkin Elmer Clarus 500 GC-MS with the following specifications: The capillary column was an SGE CPSil-5MS, of 30 m length x 0.25 mm internal diameter x 0.25 μm phase thickness. Helium was the carrier gas used, with a 1 ml/min constant flow. Injection temperature was set to 300 °C, with an oven temperature program of 50 °C (hold 1 minute), ramped at 8 °C/min to 340 °C (hold for 7.75 minutes). Injection was set to 1 μL in either split mode, with a 50:1 split for higher concentration samples, or pulsed splitless for low sample concentrations. Interpretation and quantification of *n*-alkane homologues (C_{25} to C_{35}) was conducted using Perkin Elmer Turbomass software. For quantification, a 1-1'-binaphthyl internal standard was added to each sample at a concentration of 1 μg/mL. *n*-Alkane concentrations were calculated from the response factor of each homologue against the internal standard plotted against a seven point calibration curve from a certified reference material (C_7-C_{40} Saturated Alkanes Standard, Supelco 49452-U) prepared and analysed in triplicate using known concentrations of a homologous suite of *n*-alkanes (C_7 to C_{40}) with the same 1 μg/mL 1-1' binaphthyl internal standard concentration ($r^2 > 0.96$, with a precision of ±10% based on 10 replicate standard injections).

2.4 GC-IRMS Isotopic Analysis

Isotopic analysis of *n*-alkanes was conducted using a Thermo Trace Gas Chromatograph (GC) Ultra with a GC Isolink, Conflo IV interface and a Delta V Advantage isotope ratio mass spectrometer (irMS). The GC column was an Agilent DB-1MS ultra-inert, 60m long, 0.25 mm i.d., 0.25 μm film thickness. The GC oven temperature started at 40 °C, ramped at 10 °C / min to 325 °C, and held for 10 minutes. 1 μL of sample was injected into a split/splitless inlet operating in splitless mode, with an inlet temperature of 280 °C, and helium carrier gas at a constant flow of 1.5 mL/min. Flow from the GC column flowed into the GC Isolink reactors. For $\delta^{13}C$, the combustion reactor contained copper oxide and nickel oxide, held at 1000 °C to combust compounds to CO_2. For δD, the high temperature conversion (HTC) reactor was a graphite-lined ceramic tube, held at 1420 °C, to pyrolyse compounds to H_2. The analyte gas then flowed through the Conflo IV interface to the irMS which measured m/z 44, 45 and 46 (for $\delta^{13}C$) or m/z 2 and 3 (for δD). Samples were measured in triplicate, with standard deviations of replicate measurements less than 0.6‰ for $\delta^{13}C$ and 4.8‰ for δD values of *n*-alkane chain lengths C_{29} and C_{31}. $\delta^{13}C$ and δD was calculated from these ratios by Thermo Isodat software, and calibrated to the international reference scales (Vienna Pee Dee Belemnite (VPDB) for $\delta^{13}C$, Vienna Standard Mean Ocean Water (VSMOW) for δD) by comparison with a mixture of alkane standards of known isotopic composition.

2.5 Accounting for changes in $\delta^{13}C$ values of atmospheric CO_2

Carbon isotope data were adjusted for pre-industrial atmospheric $\delta^{13}C$ by applying the offset between the average $\delta^{13}C$ of atmospheric CO_2 of ice core bubbles spanning 155 kyr to present, measured by Eggleston et al. (2016) and the measured $\delta^{13}C$ of our samples.

2.6 Calculations

We use the same carbon isotope end member values determined by Garcin et al. (2014) and adopted by Uno et al. (2016) and Andrae et al. (2018) to examine the relative proportions of C3 and C4 vegetation in our samples corrected to pre-industrial atmospheric pCO_2 (δ^{13}Catm). For C_{31}, the end member ranges are -33.8 ± 3.9‰ for C3 plants and -20.1 ± 2.5‰ for C4 plants (Garcin et al. 2014). Percent of C4 vegetation was calculated using a mixing model, based on these end member values.

Relative abundances of *n*-alkane chain lengths were characterised by calculating average chain length (ACL):

$$\mathrm{ACL} = \frac{(25C_{25}+27C_{27}+29C_{29}+31C_{31}+33C_{33}+35C_{35})}{(C_{25}+C_{27}+C_{29}+C_{31}+C_{33}+C_{35})}$$

where C_x is the total concentration of each *n*-alkane with x carbon atoms.

3. Results

The δ^{13}C values of C_{29} and C_{31} in Unit A are offset from one another, with C_{29} values ranging from -32.1 ± 0.1‰ to -31.2 ± 0.1‰ and C_{31} values ranging from -30.7 ± 0.2‰ to -28.4 ± 0.1‰ (Table 1, Fig. 3a). Approximate percent C4 for Unit A ranges from 24 to 40%. In Unit B, the δ^{13}C values of C_{29} range from -34.8 ± 0.6‰ to -31.9 ± 0.6‰ and range from -34.2 ± 0.4‰ to -30.4 ± 0.1‰ for C_{31} (Table 1, Fig. 3a). Further, δ^{13}C values of C_{29} and C_{31} converge at Layer 27 and remain very similar through to Layer 24. Estimated percent C4 for Unit B falls from 26% (Layer 29) to 0% (Layer 26) and then rises to 10% (Layers 25 and 24) . The δ^{13}C values of C_{29} and C_{31} in Unit C are offset from one another, with C_{29} values ranging from -32.5 ± 0.2‰ to -31.8 ± 0.04‰ and C_{31} values ranging from -31.3 ± 0.04‰ to -28.8 ± 0.2‰ (Table 1, Fig. 3a). Percent C4 for Unit C ranges from 19 to 37%. We calculate the isotopic divergence of δ^{13}C between C_{31}

and C_{29} ($\Delta\delta^{13}C(C_{31}\text{-}C_{29})$), and find highly diverging values in Unit A, ranging from 1.1 to 3‰ that then converged and fell to -0.2‰ in Layer 27, to high isotopic divergence in Unit C, ranging from 1.2 to 2.9‰ (Table 1, Fig. 3b).

Throughout Unit A, δD values of C_{31} fluctuate, with values ranging from -159‰ to -134‰ (Table 1, Fig. 3c). During Unit B, δD values show a progressive decrease to a minimum of -165‰ in the middle of the Unit at Layer 27 and then increase to -130‰ (Table 1, Fig. 3c). Throughout Unit C the δD values of C_{31} remain relatively stable and high compared to the lower Units, with values ranging from -136‰ to -129‰ (Table 1, Fig. 3c).

Table 2. *n*-Alkane analysis of Blanche Cave sediments, including ACL, carbon and hydrogen isotopic analysis, showing standard deviation (SD) and number of replicate runs (n) and percent C4 for each layer.

		$\delta^{13}C$							δD		
Layer Number	**ACL**	**C_{29} (‰)**	**SD C_{29} (‰)**	**C_{31} (‰)**	**SD C_{31} (‰)**	**n**	**Isotopic Divergence $\Delta\delta^{13}C(C_{31}\text{-}C_{29})$ (‰)**	**% C4**	**C_{31} (‰)**	**SD (‰)**	**n**
18	30.6	-32.0	0.4	-29.8	0.4	3	2.2	30	-136	2.2	3
19	30.5	-32.1	0.1	-29.4	0.0	3	2.7	33	-133	1.9	4
20	30.4	-31.8	0.0	-28.8	0.2	3	2.9	37	-129	1.0	2
21	30.4	-32.0	0.1	-29.3	0.4	3	2.6	33	-135	1.5	3
22	30.7	-31.9	0.1	-29.8	0.3	3	2.1	30	-131	0.7	4
23	31.1	-32.5	0.2	-31.3	0.0	3	1.2	19	-134	0.6	3
24	31.0	-32.8	0.2	-32.7	0.2	6	0.1	9	-130	0.4	4
25	30.9	-32.8	0.1	-32.6	0.1	3	0.2	10	-137	0.7	4
26	30.9	-34.8	0.6	-34.2	0.4	7	0.6	0	-146	0.3	3
27	30.4	-32.0	0.3	-32.2	0.1	3	-0.2	13	-165	0.8	2
28	30.6	-32.5	0.2	-31.2	0.1	3	1.3	20	-143	3.2	3
29	30.4	-31.9	0.6	-30.4	0.1	3	1.5	26	-134	1.6	2
30	30.4	-31.6	0.2	-30.4	0.2	3	1.2	26	-140	1.7	2
31	30.3			-29.2	0.4	3		34	-159	0.9	2
32	30.5	-31.5	0.1	-29.2	0.2	3	2.3	34	-133	1.2	2
33	30.8	-31.7	0.5	-29.2	0.1	3	2.4	34	-150	2.1	1
34	30.8	-31.8	0.4	-30.1	0.1	3	1.7	28	-150	1.3	2
35	30.6	-31.8	0.0	-30.6	0.2	3	1.1	24	-144	1.0	4
36	30.5	-31.8	0.2	-30.3	0.2	3	1.4	26	-136	0.2	3
37	30.5	-32.1	0.0	-30.4	0.2	3	1.7	26	-139	2.2	3
38	30.3								-154	3.1	1
39	30.4	-31.4	0.1	-28.5	0.2	3	3.0	40	-145	1.0	2
40	30.5	-31.2	0.1	-28.4	0.1	3	2.9	40	-134	0.8	4

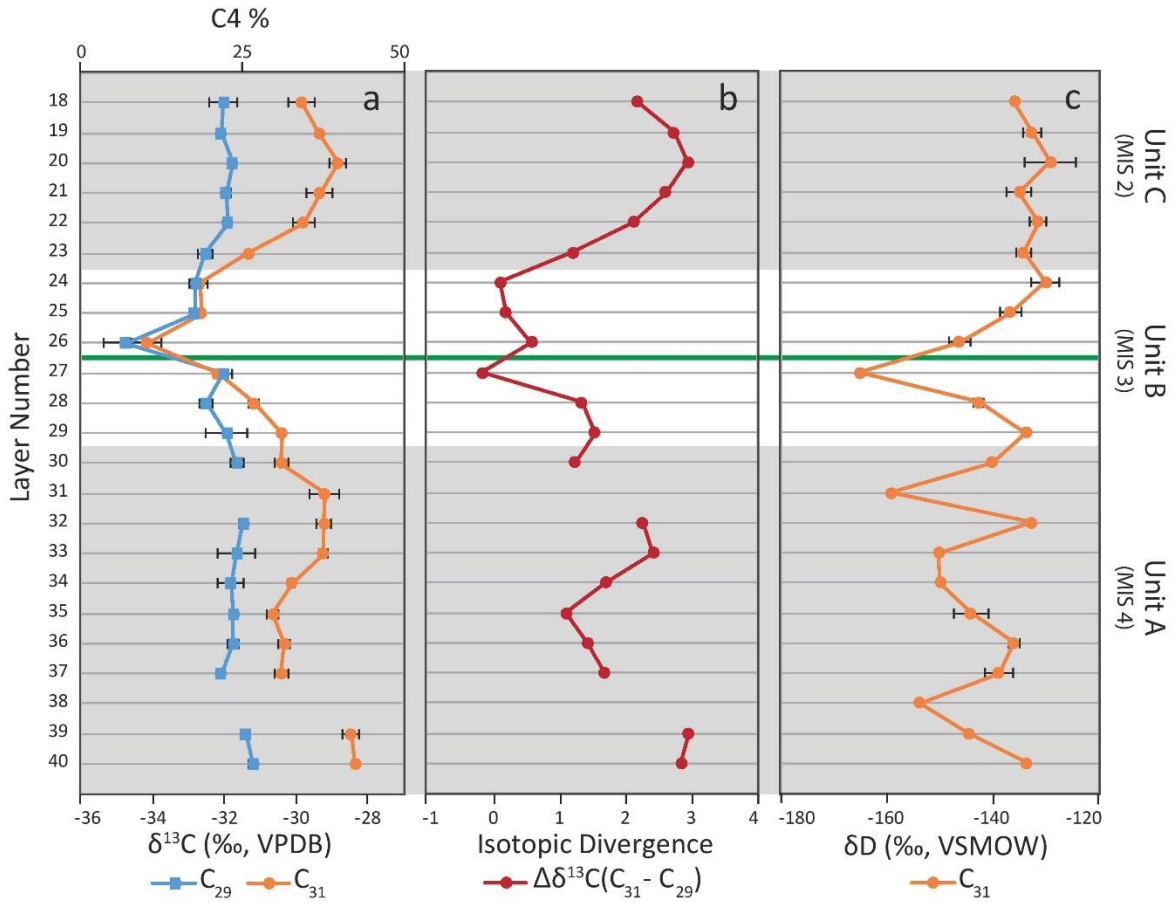

Figure 3. Leaf wax *n*-alkane data showing a) the *n*-alkane $\delta^{13}C$ values of C_{29} and C_{31} (error bars represent one standard deviation of replicate measurements) along with percent C4 vegetation, b) the $\delta^{13}C$ isotopic divergence between C_{31} and C_{29}, and C) the δD values of C_{31} throughout our record (error bars represent one standard deviation of replicate measurements). The green line divides the section between megafauna fossil presence (below the green line) and megafauna fossil absence (above the green line).

Throughout the record, average chain length (ACL) remains quite stable, with a range from 30.3 to 31.1 over the entire record (Table 1). Chain length quantification values can be found in the Supplementary Table S1, Appendix 3.

4. Discussion

4.1 Vegetation: $\delta^{13}C$ values of leaf wax n-*alkanes*

Examination of the $\delta^{13}C$ values of the C_{29} and C_{31} *n*-alkanes provides insight into the relative abundance of C3 and C4 vegetation in the landscape before, during and after the last appearance of megafauna fossils observed in Blanche Cave, Naracoorte. Data on chain length of different plants in Australia indicates that on average, trees produce greater proportions of C_{27} and C_{29} than grasses, while grasses produce greater proportions of C_{31} and C_{33} (Howard et al. 2018). Therefore, the carbon isotope ratio of the C_{31} chain length should be more responsive to changes in the proportion of C4 versus C3 vegetation than C_{29} in Australia. Similarly, in a global compilation of arid-adapted taxa, Rouillard et al. (2016) found that C_3 plants have greater abundances of C_{27} and C_{29} than C4 plants, and C4 plants have greater abundances of C_{31} and C_{33} indicating that C_{29} is biased towards C3 vegetation and C_{31} is more sensitive to C4 grasses in the landscape. Uno et al. (2016) recommend the use of C_{31} for vegetation reconstruction because it reflects vegetation distribution across the landscape.

Throughout the record we observe shifts in $\delta^{13}C$ of the C29 and C31 chain lengths, which indicate changes in the abundance of C4 vegetation across the time that megafauna lived and became extinct in Naracoorte. C_{29} follows a similar trend to C_{31} although the shifts are not as large as they are for C_{31}, which supports that C_{29} is less responsive to shifts in C4 vegetation than C_{31}. We see the presence of C4 vegetation in Unit A (MIS 4), as indicated by the high and stable $\delta^{13}C$ values of C_{31}. The percentage of C4 vegetation then begins to decrease in the lead up to the disappearance of megafauna fossils, and follows with a further decline after megafauna fossils disappear from the record. This is then followed by the return of a C4 vegetation signal to the section in Unit C. Using the end member values of C_{31} determined by Garcin et al (2014), we apply a mixing model to estimate that the percentage of C4 vegetation during MIS 4 (Unit A),

when megafauna were extant, ranged from 24% to 40%. In MIS 3 (Unit B) the percentage of C4 vegetation decreased to 12% at in the layer in which megafauna fossils are last observed (Layer 27) and decreases further to 0% in Layer 26, at the same time that megafauna fossils disappear. Percent C4 vegetation then increases again to 10% above the fossil disappearance boundary (Layers 25 and 24). Furthermore, $\delta^{13}C$ values for C_{29} and C_{31} converge at the base of Unit B (Layer 27) and remain similar throughout this Unit further indicating a shift from mixed C3 and C4, to dominantly C3 vegetation. In Unit C, C4 vegetation returns, and $\delta^{13}C$ values for C_{29} and C_{31} diverge, with estimates ranging from 19% to 37% C4 vegetation throughout the Unit.

Loss of C4 vegetation would have had an adverse effect on megafauna species that were dependent on the presence of C4 vegetation. For example, $\delta^{13}C$ analysis of tooth enamel and dental micro wear has revealed that the giant kangaroo, *Procoptodon goliah*, relied heavily upon a C4 chenopod diet (Prideaux et al. 2009). Carbon isotope analysis of tooth enamel from two fossil deposits in Cuddie Springs in New South Wales also identified a shift from a predominantly C4 diet in the fauna of the middle Pleistocene to a more C3 dominated diet in the late Pleistocene fauna, 40 – 30 ka (DeSantis et al. 2017). The $\delta^{13}C$ of *n*-alkanes from an offshore core recorded a decrease in C4 vegetation across the southeast of Australia during this same time period (Lopes dos Santos et al. 2013). Further, isotopic analysis of eggshells from the extant *Dromaius* (emu) in Australia's arid zone find that its diet contained mixed C3 and C4 prior to 50 ka, but that C4 vegetation disappeared from its diet at around 50 ±5 ka (Johnson et al. 1999, Miller et al. 2005, Miller et al. 2016). The browsing giant megafaunal bird *Genyornis* consumed a diet containing a dominantly C4 vegetation prior to 50 ka and became extinct at 50 ±5 ka (Miller et al. 2016). This extinction is hypothesized to be due to an inability to adapt to an abrupt shift in ecosystem structure (Miller et al. 2016). They suggest that, as a

browser, *Genyornis* was dependent on the chenopod *Atriplex*, a C4 genus common in the arid zone (Miller et al. 2016). While they observe no correlative change in climate at this time, human-induced change to arid zone fire regimes may have resulted he loss of *Atriplex* and other C4 species, subsequently causing the extinction of *Genyornis* and the abrupt change in the diet of *Dromaius* (Miller et al. 2016).

Carbon isotopic records from tooth enamel and eggshell reflect animal diet, and therefore, are subject to dietary selectiveness. In contrast, analysis of the sedimentary leaf wax *n*-alkanes provides a direct record of shifts in vegetation and thereby eliminates the potential effects of selective feeding. Further, the immediate association between the sediments and the megafauna fossils in our record allows for a direct temporal and spatial comparison of the vegetation before, during and after the last occurrence of megafauna fossils at Naracoorte. The results presented here demonstrate a decrease in the abundance of C4 grasses and/or C4 chenopods leading up to the disappearance of megafauna fossils at Naracoorte caves. Following megafauna disappearance C4 vegetation declines further (Fig. 3a).

Unlike Miller et al. (2016) and Johnson et al. (1999), our record shows a return of C4 vegetation to the record after the disappearance of megafauna. We propose that the observed return of C4 vegetation in the Blanche Cave record may be due to the direct measurement of leaf wax *n*-alkanes, which eliminate the potential bias that may occur due to selective feeding by fauna. Further, it may be that the differences in vegetation observed in the Blanche Cave record may also be due to differences in vegetation type growing in the Naracoorte region as compared to that growing in the more northern arid regions analysed by Miller et al. (2016) and Johnson et al. (1999).

The shift from mixed C3 and C4, to exclusively C3 vegetation, and back to mixed C3 and C4 vegetation observed in our record may be the result of human impact and/or

climatic change and or/feedbacks from megafaunal extinction in the Naracoorte region. Previous work has found that between 50 – 45 ka Australia's arid zone lost much of its C4 vegetation, but that this loss did not coincide with significant climate change and instead has been attributed to human impacts on fire regime (Miller et al. 2016). In order to explore the role that climate may play in the shifts observed in C3 and C4 vegetation of the Naracoorte region, we examine the hydrological conditions using *n*-alkane hydrogen isotope ratios preserved in the Blanche Cave sediments.

4.2 Hydroclimate: δD values of leaf wax n-*alkanes*

The δD values of *n*-alkanes in our sediments provides a record of the hydrological conditions present before, during and after the disappearance of megafauna fossils in Blanche Cave. Throughout our record we see large shifts in the δD values of C_{31}, with lower values generally interpreted as indicating wetter conditions and higher values indicating drier conditions (Smith and Freeman 2006, Douglas et al. 2012, Kahmen et al. 2013). Unit A records variable, but overall relatively high δD values (average = -144 ± 8.6‰). This greater degree of variability in Unit A may be an artefact of the higher temporal resolution in this Unit capturing short term variations in climate (Table 1). Following Unit A, there is a sharp decrease in δD values in Unit B, with a minimum in Layer 27 immediately preceding the loss of megafauna fossils in the section. This represents the wettest signal observed throughout the section. This low δD value corresponds to a period of speleothem deposition in Naracoorte Caves from 50 – 40 ka, when it is suggested that precipitation levels outstripped evaporation rates (Ayliffe et al. 1998). Following this period of increased available moisture, the δD values steadily increase for the rest of Unit B, suggesting progressive drying. δD values are stable in

Unit C, with an average of -133 ± 3‰, indicating drier conditions than the Units below it.

4.3 Ecosystem change

Variations in hydroclimate and atmospheric CO_2 concentration play a role in the types of vegetation that dominate in an ecosystem. In general, wetter conditions and higher pCO_2 favour C3 vegetation and drier conditions, summer precipitation and lower pCO_2 favour C4 vegetation (Ehleringer et al. 1997, Sage et al. 1999). In Australia, C4 grasses have been found to be more diverse and in greater abundance where the summer period is wet and less abundant in cooler temperatures and/or lower summer rainfall (Hattersley 1983, Murphy and Bowman 2007). In this study, some but not all of the shifts observed can be explained by the above factors. Throughout Unit A of our record the presence of C4 vegetation remains stable, while moisture is quite variable, although relatively low. Similarly, Unit C records the presence of C4 vegetation, with quite stable dry climate conditions. During MIS 4 and 2, represented by Units A and C respectively, pCO_2 levels were low and glacial conditions prevailed (Bereiter et al. 2015). Thus, in addition to the relatively dry conditions, it is possible that low pCO_2 was also a driver in maintaining the C4 vegetation observed in these Units (Ehleringer et al. 1997).

In Unit B, large changes are reconstructed in both vegetation and climate, but these shifts are not entirely concurrent. Conditions become increasingly wet toward the middle of the Unit and then become dry again in the upper section of the Unit. Around the time of megafauna extinction, the climate conditions in Unit B are consistent with findings elsewhere in Australia, with $\delta^{18}O$ analysis of speleothems from caves in Kosciuszko National Park in New South Wales, revealing wetter conditions throughout

MIS 3 (Webb et al. 2014). In addition, meta analysis of climate records across Australia find that mid-MIS 3, about 49 – 40 ka, was a period of peak wet conditions (Kemp et al. 2019). In Unit B at Layer 27, when megafauna fossils last appear in the record, there is a large decrease in δD values, indicating an increase in available moisture at this time. Wet conditions during deposition of Layer 27 may explain the increasing abundance of C3 vegetation at the expense of C4 vegetation. The decrease in available C4 vegetation may have in turn been the driver for the extinction of megafauna species that were dependent on C4 vegetation in their diet (Johnson et al. 1999, Prideaux et al. 2009, Miller et al. 2016). Johnson et al. (1999) observe the loss of C4 vegetation at the time that megafauna disappear in arid central Australia, which they attribute to a weakening of the Australian summer monsoon resulting in reduced warm-season precipitation. It is unlikely that the Australian summer monsoon was a significant contributor to climate conditions in Naracoorte, however, due to its southerly and coastal location making it much more temperate and susceptible to dominantly winter precipitation (Johnson et al. 1999, Hollins et al. 2018). Nonetheless, the Blanche Cave record indicate increasing wet conditions prior to megafauna extinction, which is a likely cause for decreasing C4 vegetation.

However, the proportion of C4 vegetation continues to decline after the megafaunal extinction and this cannot be explained by changes in the hydrological conditions observed in the record. The wettest conditions are observed in Layer 27, but the lowest proportion of C4 vegetation occurs after this time, in Layer 26, when conditions are becoming relatively drier. Thus, climate does not appear to be the primary driver of C4 vegetation loss at this time. Miller et al. (2016) show climate drivers did not correlate with vegetation change and speculate that the loss of C4 was related to the human-induced removal of herbivores and/or change to fire regime. In contrast, Cohen et al.

(2015) observe significant climatic shifts in arid Australia at the time *Genyornis* went extinct, with drying of the lakes and rivers of the Lake Eyre Basin occurring at 48 ± 2 ka. Given the results of this study do not demonstrate a correlative shift in hydrological conditions with the timing of C4 vegetation loss following the megafaunal extinction, we hypothesize that other factors played a role. It has been hypothesized that anthropogenic changes to fire regime resulted in vegetation shifts tropical Australia (Bird et al. 2013). However, it is expected that increased fire frequency would decrease woody forest vegetation and favour open, grassy C4 vegetation (Bond 2008), and thus cannot explain the loss of C4.

The complete loss of C4 vegetation that followed the megafaunal extinction could be the direct result of the removal of large herbivores. In modern studies, much work has been conducted examining the role of herbivores on African savanna vegetation, with elephant activity found to reduce woody vegetation and increase open grassland vegetation (Guldemond and Aarde 2008, Asner et al. 2009). Furthermore, analysis of global palaeo-data has shown that reduced megafaunal diversity and biomass in the Pleistocene was instrumental in woody vegetation abundance into the Holocene, with a decrease in large fauna resulting in an increase of woody taxa (Bakker et al. 2016). The shift from more open, grassy C4 vegetation to exclusively C3 vegetation, may be explained by the loss of megafauna in Naracoorte.

Following the brief period of complete loss of C4 immediately after megafaunal extinction, C4 vegetation returns to the landscape in the upper section of Unit B. This may be due to the return to more arid climate conditions recorded in the δD values, which would favour the presence of C4 vegetation, or due to an anthropogenic increase in fire frequency, resulting in more open grasslands (Sage et al. 1999, Bond 2008).

Units A and C represent periods of time in which the relative abundance of C3 and C4 vegetation in the landscape correlate with the hydrological conditions present, with drier conditions correlating with the presence of C4 vegetation. It is also possible that a change to fire regimes also contributed to the presence of C4 vegetation in Unit C. However, in Unit B, the layer experiencing the wettest conditions and representing the last presence of megafauna fossils, does not correspond to the lowest percentage of C4 presence, which occurs after the last megafaunal fossils. As such, we infer that the loss of C4 vegetation at this time is unlikely to have been driven by climate change, and may have instead been driven by the removal of megafauna herbivores in the region.

5. Conclusions

The isotopic signatures of leaf wax *n*-alkanes preserved in Blanche Cave sediments indicate that climate and vegetation varied before, during and after megafauna were present in the region. Combined with pCO_2 conditions across the record, changes in hydrological conditions may have been a factor for some of the observed shifts in vegetation. In the lead up to the disappearance of megafauna, C4 vegetation abundance begins to decline. At the same time as C4 vegetation is beginning to decline, climate conditions become increasingly wet, which may have driven the vegetation shift because C4 vegetation is favoured by more arid conditions. Further, given that other workers find that there is evidence to indicate that some megafauna species are dependent on C4 vegetation in their diet, it is possible that this decrease in C4 vegetation may have been a driver for the extinction of megafauna in Naracoorte. However, following the disappearance of megafauna fossils, C4 continues to decrease and vegetation becomes entirely C3 as climate starts to dry. Therefore, the vegetation shift that occurs after megafauna fossil disappearance cannot be explained by climate.

Instead, the disappearance of C4 vegetation may have been due to the removal of large herbivores, which may have otherwise cleared woody vegetation and allowed for a proliferation of C4 grasses. Following this, C4 vegetation then returns to the landscape. This return of C4 vegetation corresponds with a shift to more a more arid climate, which favours C4 over C3 plants. In addition it is plausible that human-induced changes to fire regime may have been a driver for increased opening of the landscape, allowing for an increase of C4 grass abundance. These vegetation and climate records that are in direct association with megafaunal fossils at Blanche Cave provide unparalleled insights into both the causes and consequences of megafaunal extinction in Naracoorte region of Australia.

Acknowledgements

Thanks to Kristine Nielson for assistance in the lab, and Jake Andrae for assistance with data and figures. Funding was provided by the Australian Research Council (ARC) grants to FAM (FT110100793) and the University of Adelaide Environment Institute to EHR, LJA, and FAM. Further thanks to the ARC for ARC LIEFP (LE110100119) to KG for provision of CSIA analyses at Curtin University. This research is also supported by an Australian Government Research Training Program (RTP) Scholarship to SH.

References

ANDRAE J. W., MCINERNEY F. A., POLISSAR P. J., SNIDERMAN J. M. K., HOWARD S., HALL P. A. & PHELPS S. R. 2018. Initial Expansion of C4 Vegetation in Australia During the Late Pliocene, *Geophysical Research Letters*. **45**, 4831-4840.

ARAGUÁS-ARAGUÁS L., FROEHLICH K. & ROZANSKI K. 2000. Deuterium and oxygen-18 isotope composition of precipitation and atmospheric moisture, *Hydrological Processes*. **14**, 1341-1355.

ARNOLD L. J., DUVAL M., DEMURO M., SPOONER N. A., SANTONJA M. & PÉREZ-GONZÁLEZ A. 2016. OSL dating of individual quartz 'supergrains' from the Ancient Middle Palaeolithic site of Cuesta de la Bajada, Spain, *Quaternary Geochronology*. **36**, 78-101.

ASNER G. P., LEVICK S. R., KENNEDY-BOWDOIN T., KNAPP D. E., EMERSON R., JACOBSON J., COLGAN M. S. & MARTIN R. E. 2009. Large-scale impacts of herbivores on the structural diversity of African savannas, *Proceedings of the National Academy of Sciences*. **106**, p.4947.

AYLIFFE L. K., MARIANELLI P. C., MORIARTY K. C., WELLS R. T., MCCULLOCH M. T., MORTIMER G. E. & HELLSTROM J. C. 1998. 500 ka precipitation record from southeastern Australia: Evidence for interglacial relative aridity, *Geology*. **26**, 147-150.

BAKKER E. S., GILL J. L., JOHNSON C. N., VERA F. W. M., SANDOM C. J., ASNER G. P. & SVENNING J.-C. 2016. Combining paleo-data and modern exclosure experiments to assess the impact of megafauna extinctions on woody vegetation, *Proceedings of the National Academy of Sciences*. **113**, 847-855.

BASTOW T. P., VAN AARSSEN B. G. K. & LANG D. 2007. Rapid small-scale separation of saturate, aromatic and polar components in petroleum, *Organic Geochemistry*. **38**, 1235-1250.

BEREITER B., EGGLESTON S., SCHMITT J., NEHRBASS-AHLES C., STOCKER T. F., FISCHER H., KIPFSTUHL S. & CHAPPELLAZ J. 2015. Revision of the EPICA Dome C CO2 record from 800 to 600 kyr before present, *Geophysical Research Letters*. **42**, 542-549.

BIRD M. I., HUTLEY L. B., LAWES M. J., LLOYD J., LULY J. G., RIDD P. V., ROBERTS R. G., ULM S. & WURSTER C. M. 2013. Humans, megafauna and environmental change in tropical Australia, *Journal of Quaternary Science*. **28**, 439-452.

BOND W. J. 2008. What Limits Trees in C4 Grasslands and Savannas, *What Limits Trees in C4 Grasslands and Savannas*. **39**, 641-659.

CERNUSAK L. A., BARBOUR M. M., ARNDT S. K., CHEESMAN A. W., ENGLISH N. B., FEILD T. S., HELLIKER B. R., HOLLOWAY-PHILLIPS M. M., HOLTUM J. A. M., KAHMEN A., MCINERNEY F. A., MUNKSGAARD N. C., SIMONIN K. A., SONG X., STUART-WILLIAMS H., WEST J. B. & FARQUHAR G. D. 2016. Stable isotopes in leaf water of terrestrial plants, *Plant, Cell & Environment*. **39**, 1087-1102.

CHIKARAISHI Y. & NARAOKA H. 2003. Compound-specific δD–δ13C analyses of n-alkanes extracted from terrestrial and aquatic plants, *Phytochemistry*. **63**, 361-371.

COHEN T., JANSEN J., GLIGANIC L., LARSEN J., NANSON G., MAY J.-H., JONES B. & PRICE D. 2015. Hydrological transformation coincided with megafaunal extinction in central Australia, *Geology*. **43**, p.195.

COLLISTER J. W., RIELEY G., STERN B., EGLINTON G. & FRY B. 1994. Compound-specific δ 13C analyses of leaf lipids from plants with differing carbon dioxide metabolisms, *Organic Geochemistry*. **21**, 619-627.

COOPER A., TURNEY C., HUGHEN K. A., BROOK B. W., MCDONALD H. G. & BRADSHAW C. J. A. 2015. Abrupt warming events drove Late Pleistocene Holarctic megafaunal turnover, *Science*.

CRAIG H., GORDON L. I., CONFERENCE ON STABLE ISOTOPES IN OCEANOGRAPHIC S. & PALEOTEMPERATURES 1965 Deuterium and oxygen 18 variations in the ocean and the marine atmosphere. Consiglio nazionale delle richerche, Laboratorio de geologia nucleare, Pisa.

CRANWELL P. A. 1981. Diagenesis of free and bound lipids in terrestrial detritus deposited in a lacustrine sediment, *Organic Geochemistry*. **3**, 79-89.

DANSGAARD W. 1964. Stable isotopes in precipitation, *Tellus*. **16**, 436-468.

DANSGAARD W., JOHNSEN S. J., CLAUSEN H. B., DAHL-JENSEN D., GUNDESTRUP N. S., HAMMER C. U., HVIDBERG C. S., STEFFENSEN J. P., SVEINBJÖRNSDOTTIR A. E., JOUZEL J. & BOND G. 1993. Evidence for general instability of past climate from a 250-kyr ice-core record, *Nature*. **364**, p.218.

DARRÉNOUGUÉ N., DE DECKKER P., FITZSIMMONS K. E., NORMAN M. D., REED L., VAN DER KAARS S. & FALLON S. 2009. A late Pleistocene record of aeolian sedimentation in Blanche Cave, Naracoorte, South Australia, *Quaternary Science Reviews*. **28**, 2600-2615.

DE DECKKER P., ARNOLD L. J., VAN DER KAARS S., BAYON G., STUUT J.-B. W., PERNER K., LOPES DOS SANTOS R., UEMURA R. & DEMURO M. 2019. Marine Isotope Stage 4 in Australasia: A full glacial culminating 65,000 years ago – Global connections and implications for human dispersal, *Quaternary Science Reviews*. **204**, 187-207.

DESANTIS L. R. G., FIELD J. H., WROE S. & DODSON J. R. 2017. Dietary responses of Sahul (Pleistocene Australia-New Guinea) megafauna to climate and environmental change, *Paleobiology*. **43**, 181-195.

DIEFENDORF A. F., FREEMAN K. H., WING S. L. & GRAHAM H. V. 2011. Production of n-alkyl lipids in living plants and implications for the geologic past, *Geochimica et Cosmochimica Acta*. **75**, 7472-7485.

DIEFENDORF A. F. & FREIMUTH E. J. 2017. Extracting the most from terrestrial plant-derived *n*-alkyl lipids and their carbon isotopes from the sedimentary record: A review, *Organic Geochemistry*. **103**, 1-21.

DOUGLAS P. M. J., PAGANI M., BRENNER M., HODELL D. A. & CURTIS J. H. 2012. Aridity and vegetation composition are important determinants of leaf-wax δD values in southeastern Mexico and Central America, *Geochimica et Cosmochimica Acta*. **97**, 24-45.

EGGLESTON S., SCHMITT J., BEREITER B., SCHNEIDER R. & FISCHER H. 2016. Evolution of the stable carbon isotope composition of atmospheric CO2 over the last glacial cycle, *Paleoceanography*. **31**, 434-452.

EGLINTON G. & HAMILTON R. J. 1967. Leaf Epicuticular Waxes, *Science*. **156**, 1322-1335.

EGLINTON T. I. & EGLINTON G. 2008. Molecular proxies for paleoclimatology, *Earth and Planetary Science Letters*. **275**, 1-16.

EHLERINGER J. R., CERLING T. E. & HELLIKER B. R. 1997. C4 photosynthesis, atmospheric CO2, and climate, *Oecologia*. **112**, 285-299.

EMILIANI C. 1955. Pleistocene Temperatures, *The Journal of Geology*. **63**, 538-578.

FARQUHAR G. D., EHLERINGER J. R. & HUBICK K. T. 1989. Carbon Isotope Discrimination and Photosynthesis, *Annual Review of Plant Physiology and Plant Molecular Biology*. **40**, 503-537.

FORBES M. S. & BESTLAND E. A. 2007. Origin of the sedimentary deposits of the Naracoorte Caves, South Australia, *Geomorphology*. **86**, 369-392.

FORBES M. S., BESTLAND E. A., WELLS R. T. & KRULL E. S. 2007. Palaeoenvironmental reconstruction of the Late Pleistocene to Early Holocene Robertson Cave sedimentary deposit, Naracoorte, South Australia, *Australian Journal of Earth Sciences*. **54**, 541-559.

GAMARRA B. & KAHMEN A. 2015. Concentrations and δ2H values of cuticular n-alkanes vary significantly among plant organs, species and habitats in grasses from an alpine and a temperate European grassland, *Oecologia*. **178**, 981-998.

GARCIN Y., SCHWAB V. F., GLEIXNER G., KAHMEN A., TODOU G., SÉNÉ O., ONANA J.-M., ACHOUNDONG G. & SACHSE D. 2012. Hydrogen isotope ratios of lacustrine sedimentary n-alkanes as proxies of tropical African hydrology: Insights from a calibration transect across Cameroon, *Geochimica et Cosmochimica Acta*. **79**, 106-126.

GARCIN Y., SCHEFUß E., SCHWAB V. F., GARRETA V., GLEIXNER G., VINCENS A., TODOU G., SÉNÉ O., ONANA J.-M., ACHOUNDONG G. & SACHSE D. 2014. Reconstructing C3 and C4 vegetation cover using n-alkane carbon isotope ratios in recent lake sediments from Cameroon, Western Central Africa, *Geochimica et Cosmochimica Acta*. **142**, 482-500.

GRICE K., LU H., ZHOU Y., STUART-WILLIAMS H. & FARQUHAR G. D. 2008. Biosynthetic and environmental effects on the stable carbon isotopic compositions of anteiso- (3-methyl) and iso- (2-methyl) alkanes in tobacco leaves, *Phytochemistry*. **69**, 2807-2814.

GULDEMOND R. & AARDE R. 2008. A Meta-Analysis of the Impact of African Elephants on Savanna Vegetation, *Journal of Wildlife Management*. **72**, 892-899.
HATTERSLEY P. W. 1983. The distribution of C3 and C4 grasses in Australia in relation to climate, *Oecologia*. **57**, 113-128.
HOLLINS S. E., HUGHES C. E., CRAWFORD J., CENDÓN D. I. & MEREDITH K. T. 2018. Rainfall isotope variations over the Australian continent – Implications for hydrology and isoscape applications, *Science of The Total Environment*. **645**, 630-645.
HOWARD S., MCINERNEY F. A., CADDY-RETALIC S., HALL P. A. & ANDRAE J. W. 2018. Modelling leaf wax n-alkane inputs to soils along a latitudinal transect across Australia, *Organic Geochemistry*. **121**, 126-137.
JOHNSON B. J., MILLER G. H., FOGEL M. L., MAGEE J. W., GAGAN M. K. & CHIVAS A. R. 1999. 65,000 Years of Vegetation Change in Central Australia and the Australian Summer Monsoon, *Science*. **284**, 1150-1152.
JOHNSON C. N., ALROY J., BEETON N. J., BIRD M. I., BROOK B. W., COOPER A., GILLESPIE R., HERRANDO-PÉREZ S., JACOBS Z., MILLER G. H., PRIDEAUX G. J., ROBERTS R. G., RODRÍGUEZ-REY M., SALTRÉ F., TURNEY C. S. M. & BRADSHAW C. J. A. 2016. What caused extinction of the pleistocene megafauna of sahul?, *Proceedings of the Royal Society B: Biological Sciences*. **283**, 1-8.
KAHMEN A., HOFFMANN B., SCHEFUß E., ARNDT S. K., CERNUSAK L. A., WEST J. B. & SACHSE D. 2013. Leaf water deuterium enrichment shapes leaf wax n-alkane δD values of angiosperm plants II: Observational evidence and global implications, *Geochimica et Cosmochimica Acta*. **111**, 50-63.
KEMP C. W., TIBBY J., ARNOLD L. J. & BARR C. 2019. Australian hydroclimate during Marine Isotope Stage 3: A synthesis and review, *Quaternary Science Reviews*. **204**, 94-104.
LISIECKI L. E. & RAYMO M. E. 2005. A Pliocene-Pleistocene stack of 57 globally distributed benthic δ18O records, *Paleoceanography*. **20**.
LIU J., FU G., SONG X., CHARLES S. P., ZHANG Y., HAN D. & WANG S. 2010. Stable isotopic compositions in Australian precipitation, *Journal of Geophysical Research: Atmospheres*. **115**, n/a-n/a.
LOPES DOS SANTOS R. A., DE DECKKER P., HOPMANS E. C., MAGEE J. W., METS A., SINNINGHE DAMSTE J. S. & SCHOUTEN S. 2013. Abrupt vegetation change after the Late Quaternary megafaunal extinction in southeastern Australia, *Nature Geosci*. **6**, 627-631.
MACKEN A. C., MCDOWELL M. C., BARTHOLOMEUSZ D. N. & REED E. H. 2013a. Chronology and stratigraphy of the Wet Cave vertebrate fossil deposit, Naracoorte, and relationship to paleoclimatic conditions of the Last Glacial Cycle in south-eastern Australia, *Australian Journal of Earth Sciences*. **60**, 271-281.
MACKEN A. C. & REED E. H. 2013. Late Quaternary Small Mammal Faunas of the Naracoorte Caves World Heritage Area, *Transactions of the Royal Society of South Australia*. **137**, 53-67.
MACKEN A. C., STAFF R. A. & REED E. H. 2013b. Bayesian age-depth modelling of Late Quaternary deposits from Wet and Blanche Caves, Naracoorte, South Australia: A framework for comparative faunal analyses, *Quaternary Geochronology*. **17**, 26-43.
MACKEN A. C. & REED E. H. 2014. Postglacial reorganization of a small-mammal paleocommunity in southern Australia reveals thresholds of change, *Ecological Monographs*. **84**, 563-577.
MARTINSON D. G., PISIAS N. G., HAYS J. D., IMBRIE J., MOORE T. C. & SHACKLETON N. J. 1987. Age dating and the orbital theory of the ice ages: Development of a high-resolution 0 to 300,000-year chronostratigraphy, *Quaternary Research*. **27**, 1-29.
MILLER G. H., MAGEE J. W., JOHNSON B. J., FOGEL M. L., SPOONER N. A., MCCULLOCH M. T. & AYLIFFE L. K. 1999. Pleistocene Extinction of *Genyornis newtoni*: Human Impact on Australian Megafauna, *Science*. **283**, 205-208.
MILLER G. H., FOGEL M. L., MAGEE J. W., GAGAN M. K. & ET AL. 2005. Ecosystem Collapse in Pleistocene Australia and a Human Role in Megafaunal Extinction, *Science*. **309**, 287-90.
MILLER G. H., FOGEL M. L., MAGEE J. W. & GAGAN M. K. 2016. Disentangling the impacts of climate and human colonization on the flora and fauna of the Australian arid zone over the past 100 ka using stable isotopes in avian eggshell, *Quaternary Science Reviews*. **151**, 27-57.
MORIARTY K. C., MCCULLOCH M. T., WELLS R. T. & MCDOWELL M. C. 2000. Mid-Pleistocene cave fills, megafaunal remains and climate change at Naracoorte, South Australia: towards a

predictive model using U-Th dating of speleothems, *Palaeogeography, Palaeoclimatology, Palaeoecology*. **159**, 113-143.
MURPHY B. P. & BOWMAN D. M. J. S. 2007. Seasonal water availability predicts the relative abundance of C3 and C4 grasses in Australia, *Global Ecology and Biogeography*. **16**, 160-169.
NIEDERMEYER E. M., FORREST M., BECKMANN B., SESSIONS A. L., MULCH A. & SCHEFUß E. 2016. The stable hydrogen isotopic composition of sedimentary plant waxes as quantitative proxy for rainfall in the West African Sahel, *Geochimica et Cosmochimica Acta*. **184**, 55-70.
OSBORNE R. 1984. Lateral facies changes,unconformities and stratigraphic reversals:Their significance for cave sediment stratigraphy, *Cave Science*. **11**, 175-184.
PANCOST R. D. & BOOT C. S. 2004. The palaeoclimatic utility of terrestrial biomarkers in marine sediments, *Marine Chemistry*. **92**, 239-261.
POLISSAR P. J. & FREEMAN K. H. 2010. Effects of aridity and vegetation on plant-wax δD in modern lake sediments, *Geochimica et Cosmochimica Acta*. **74**, 5785-5797.
PRIDEAUX G. J., LONG J. A., AYLIFFE L. K., HELLSTROM J. C., PILLANS B., BOLES W. E., HUTCHINSON M. N., ROBERTS R. G., CUPPER M. L., ARNOLD L. J., DEVINE P. D. & WARBURTON N. M. 2007. An arid-adapted middle Pleistocene vertebrate fauna from south-central Australia, *Nature*. **445**, 422-425.
PRIDEAUX G. J., AYLIFFE L. K., DESANTIS L. R. G., SCHUBERT B. W., MURRAY P. F., GAGAN M. K. & CERLING T. E. 2009. Extinction implications of a chenopod browse diet for a giant Pleistocene kangaroo, *Proceedings of the National Academy of Sciences*. **106**, 11646-11650.
PRIDEAUX G. J., GULLY G. A., COUZENS A. M. C., AYLIFFE L. K., JANKOWSKI N. R., JACOBS Z., ROBERTS R. G., HELLSTROM J. C., GAGAN M. K. & HATCHER L. M. 2010. Timing and dynamics of Late Pleistocene mammal extinctions in southwestern Australia, *Proceedings of the National Academy of Sciences*. **107**, 22157-22162.
REED E. H. & BOURNE S. J. 2000. Pleistocene fossil vertebrate sites of the South East Region of South Australia, *Transactions of the Royal Society of South Australia*. **124**, 61-90.
--- 2009. Pleistocene Fossil vertebrate Sites of the South East Region of South Australia II, *Transactions of the Royal Society of South Australia*. **133**, 30-40.
ROBERTS R. G. & BROOK B. W. 2010. And Then There Were None?, *Science*. **327**, 420-422.
ROUILLARD A., GREENWOOD P. F., GRICE K., SKRZYPEK G., DOGRAMACI S., TURNEY C. & GRIERSON P. F. 2016. Interpreting vegetation change in tropical arid ecosystems from sediment molecular fossils and their stable isotope compositions: A baseline study from the Pilbara region of northwest Australia, *Palaeogeography, Palaeoclimatology, Palaeoecology*. **459**, 495-507.
ROZANSKI K., ARAGUÁS-ARAGUÁS L. & GONFIANTINI R. 1993 Isotopic Patterns in Modern Global Precipitation. Climate Change in Continental Isotopic Records. American Geophysical Union,
RULE S., BROOK B. W., HABERLE S. G., TURNEY C. S. M., KERSHAW A. P. & JOHNSON C. N. 2012. The Aftermath of Megafaunal Extinction: Ecosystem Transformation in Pleistocene Australia, *Science*. **335**, 1483-1486.
SACHSE D., RADKE J. & GLEIXNER G. 2004. Hydrogen isotope ratios of recent lacustrine sedimentary *n*-alkanes record modern climate variability, *Geochimica et Cosmochimica Acta*. **68**, 4877-4889.
SACHSE D., RADKE J. & GLEIXNER G. 2006. δD values of individual n-alkanes from terrestrial plants along a climatic gradient – Implications for the sedimentary biomarker record, *Organic Geochemistry*. **37**, 469-483.
SACHSE D., BILLAULT I., BOWEN G. J., CHIKARAISHI Y., DAWSON T. E., FEAKINS S. J., FREEMAN K. H., MAGILL C. R., MCINERNEY F. A., VAN DER MEER M. T. J., POLISSAR P., ROBINS R. J., SACHS J. P., SCHMIDT H.-L., SESSIONS A. L., WHITE J. W. C., WEST J. B. & KAHMEN A. 2012. Molecular Paleohydrology: Interpreting the Hydrogen-Isotopic Composition of Lipid Biomarkers from Photosynthesizing Organisms, *Annual Review of Earth and Planetary Sciences*. **40**, 221-249.

SAGE R. F., WEDIN D. A. & MEIRONG L. 1999 The biogeography of C4 photosynthesis: Patterns and controlling factors. *In* SAGE R. F. & MONSON R. K. eds. C4 Plant Biology. pp. 313-373. Academic Press,

SALTRE F., RODRIGUEZ-REY M., BROOK B. W., JOHNSON C. N., TURNEY C. S. M., ALROY J., COOPER A., BEETON N., BIRD M. I., FORDHAM D. A., GILLESPIE R., HERRANDO-PEREZ S., JACOBS Z., MILLER G. H., NOGUES-BRAVO D., PRIDEAUX G. J., ROBERTS R. G. & BRADSHAW C. J. A. 2016. Climate change not to blame for late Quaternary megafauna extinctions in Australia, *Nat Commun*. **7**.

SCHIMMELMANN A., LEWAN M. D. & WINTSCH R. P. 1999. D/H isotope ratios of kerogen, bitumen, oil, and water in hydrous pyrolysis of source rocks containing kerogen types I, II, IIS, and III, *Geochimica et Cosmochimica Acta*. **63**, 3751-3766.

SESSIONS A. L., SYLVA S. P., SUMMONS R. E. & HAYES J. M. 2004. Isotopic exchange of carbon-bound hydrogen over geologic timescales, *Geochimica et Cosmochimica Acta*. **68**, 1545-1559.

SESSIONS A. L. 2016. Factors controlling the deuterium contents of sedimentary hydrocarbons, *Organic Geochemistry*. **96**, 43-64.

SMITH F. A. & FREEMAN K. H. 2006. Influence of physiology and climate on δD of leaf wax n-alkanes from C3 and C4 grasses, *Geochimica et Cosmochimica Acta*. **70**, 1172-1187.

UNO K. T., POLISSAR P. J., JACKSON K. E. & DEMENOCAL P. B. 2016. Neogene biomarker record of vegetation change in eastern Africa, *Proceedings of the National Academy of Sciences*. **113**, 6355-6363.

VAN MEERBEECK C., RENSSEN H. & ROCHE D. 2009 How did Marine Isotope Stage 3 and Last Glacial Maximum climates differ? – Perspectives from equilibrium simulations.

WEBB M., DREDGE J., BARKER P. A., MÜLLER W., JEX C., DESMARCHELIER J., HELLSTROM J. & WYNN P. M. 2014. Quaternary climatic instability in south-east Australia from a multi-proxy speleothem record, *Journal of Quaternary Science*. **29**, 589-596.

WELLS R., MORIARTY K. & WILLIAMS D. L. G. 1984 The fossil vertebrate deposits of Victoria Fossil Cave, Naracoorte: an introduction to the geology and fauna.

WHITE S. & WEBB J. A. 2015. The influence of tectonics on flank margin cave formation on a passive continental margin: Naracoorte, Southeastern Australia, *Geomorphology*. **229**, 58-72.

ZHOU Y., GRICE K., STUART-WILLIAMS H., FARQUHAR G. D., HOCART C. H., LU H. & LIU W. 2010. Biosynthetic origin of the saw-toothed profile in δ13C and δ2H of n-alkanes and systematic isotopic differences between n-, iso- and anteiso-alkanes in leaf waxes of land plants, *Phytochemistry*. **71**, 388-403.

CHAPTER 5

CONCLUSIONS, IMPLICATIONS & FURTHER WORK

In a series of manuscripts, either published or in preparation for submission, this thesis set out to contribute to the wider understanding of the utility and robustness of leaf wax *n*-alkanes in palaeoecological research, particularly in the Australian context.

1. Motivation

At a time when significant global climate change is occurring, understanding ecosystem responses to climatic conditions is essential for future environmental management (IPCC 2014). In order to predict the effects of climate change on different species in the future it is useful to make observations of, and comparisons to, what has occurred to ecosystems in the past. Conservation palaeobiology is an emerging field of research dedicated to better understanding future climate impacts on ecosystems based on past conditions (Dietl et al. 2015, Barnosky et al. 2017). Extensive work has been conducted reconstructing past climate through the use of ice cores, sedimentary deposits, plant and animal macro- and micro-fossils, and molecular fossils. Leaf wax *n*-alkanes make an ideal molecular fossil for environmental analysis due to their pervasiveness in the sedimentary record when other fossil remains are rare or absent (Eglinton and Eglinton 2008, Diefendorf and Freimuth 2017). They are used widely for examining the vegetation that produces them by and are well utilised in palaeoecological research as a means of understanding past environments (Diefendorf and Freimuth 2017). This is of particular interest in the Australian context due to the unique climate conditions and ecosystems that it represents and the relative paucity of records for this continent. However, to interpret the records of the past, it is essential to

make calibrations to modern environments and to also understand the taphonomic and post-depositional processes that may affect the preserved signals. To achieve this, I analysed leaf wax *n*-alkanes in modern plants and soils, soil incubation experiments and ancient cave sediments.

2. Sources of leaf wax *n*-alkanes in soils

In Chapter 2, I examined modern day *n*-alkanes in plants and compared them to the *n*-alkanes in soils to determine what the signals in the soils represent. Results showed a mismatch between the measured *n*-alkane signals in the soils when compared with the modelled *n*-alkane signals from the surveyed plant community. Specifically, the results indicated that, across Australia, the measured leaf wax *n*-alkane average chain length (ACL) of soils is generally shorter than the modelled *n*-alkane ACL, based on the immediate plant community. I hypothesized that the source inputs from plants to soils are not dominantly recent and local, and instead reflect spatial and/or temporal averaged inputs with the potential for post depositional modification to have also played a role. When compared to the average *n*-alkane chain lengths of the different dominant growth forms such as tree, shrub or grass, the *n*-alkane signals in soils most closely resembled those of trees, with trees generally having a shorter average chain length than grasses in particular. I hypothesized that the similarity between the soils and the trees is due to trees experiencing greater susceptibility to wind ablation, as compared to other growth forms that do not stand as tall in the landscape.

The benefit of this work is that it enables greater insight into the temporal and spatial scales of input that the *n*-alkane signals preserved in soils represent. The signals observed in sedimentary archives are likely to reflect a regional, time-averaged signal

that is not heavily sensitive to short-term variability or small-scale spatial heterogeneity in ecosystem structures. These findings provide context for understanding what the leaf wax *n*-alkane signals preserved in ancient sediments represent. The results found here have already contributed to a greater ability to interpret the Australia's past C4 record. Specifically, the different isotopic composition of different chain lengths was interpreted as deriving from different plant types, based on the findings here that, on average, grasses produce more longer chain lengths than trees do (Appendix 4 "Initial expansion of C4 vegetation in Australian during the late Pliocene").

2.1 Future work: Wind blown transport of n-alkanes across continents

Previous work examining wind-blown particles has been conducted in order to determine input sources of *n*-alkanes in aerosols (Gagosian and Peltzer 1986), although this work has been largely limited to marine or urban settings. In China, where the effects of high levels of air pollution are of great concern, extensive work has been conducted examining petroleum-derived *n*-alkanes in aerosols, in order to differentiate between emission sources (Guo et al. 2003, Bai et al. 2017). Work examining leaf wax derived *n*-alkanes of aerosols showed that *n*-alkanes can be sourced from the vegetation in the vicinity of the aerosol sampling location, as well as from further afield (Gagosian et al. 1987, Simoneit et al. 1990). Wind-blown *n*-alkanes can travel thousands of kilometres, with analysis showing that that *n*-alkanes sourced from the African continent can be recognised and quantified across the entire equatorial Atlantic Ocean and with minimal degradation (Schreuder et al. 2018). In terms of the types of vegetation source, carbon isotope analysis of leaf wax *n*-alkanes in aerosol particles has

further revealed that it is possible to discern the relative regional inputs of C3, C4 and CAM vegetation (Simoneit 1997, Schefuß et al. 2003).

The unanswered questions that remain are how wind transports leaf wax *n*-alkanes across a continent, whether the dominant source of transported *n*-alkanes are local or from further afield, whether *n*-alkanes produced by trees are more susceptible to wind-blown transport than lower lying plant species, and whether vegetation density plays a role. These factors could be tested by examining aerosols downwind of known combined C3 tree and C4 grass populations and measuring the carbon isotope ratios of their leaf wax *n*-alkanes to determine relative C3/C4 abundance contained in the aerosols. This would help to determine whether trees are the dominant input source of wind-blown *n*-alkanes into soils and would further constrain what the *n*-alkane signals in soils represent. Aerosol sampling across different types of ecosystems would provide insight into the different vegetation densities that dominate the signal.

3. Post depositional modification of leaf wax *n*-alkanes in soils

To further elucidate what leaf wax *n*-alkane signals observed in soils represent I examined the effects of post-depositional modification occurring in soils. In Chapter 3, I isolated the effects of post depositional modification by incubating soils mixed with organic composts and measured the *n*-alkane concentration and distribution pre- and post-incubation to identify alteration to the *n*-alkane signals during burial. Results showed that *n*-alkane concentrations in the soils decreased significantly during incubation, with the greatest amount of decrease occurring after the first month. I proposed that the significant decrease in the *n*-alkane concentrations of the amended soils in the first month of incubation is due to the *n*-alkanes being freely available for microbial metabolism, as compared to the unamended soil, which contains *n*-alkanes

that are bound up in the clay minerals. I hypothesize that the decreasing rate of concentration loss over time is due to *n*-alkanes stabilising in the soils and sorbing to the clay minerals, and therefore becoming less accessible to microbes. In addition, decreasing CPI over the course of incubation is suggestive of degradation processes occurring to the *n*-alkanes, which is an important consideration when interpreting *n*-alkane signals in soils.

These findings have useful implications for work in palaeoenvironmental research, due to the need to understand whether modification to *n*-alkane signals occurs after burial. Results here showed that degradation processes occurred in the soils and in addition to concentration loss, the alkyl to o-alkyl ratio and CPI signals all indicate evidence of degradation. However, despite this strong evidence of degradation occurring in the soils, ACL remains steady after incubation, which provides confidence in the use of this signal in palaeoenvironmental reconstruction work.

3.1 Future work: The role of clays for n-*alkane preservation*

Work examining soil particle size fraction relationships with organic molecules has found that alkyl carbon is in greatest abundance in the finest particle, or clay, fraction size (Baldock et al. 1992, Höfle et al. 2013). Although alkyl compounds are kinetically unstable and should be readily susceptible to degradation in soils, due to their hydrophobicity they become bound to clay particles which makes them inaccessible for microbial degradation (Schmidt et al. 2011, Lehmann and Kleber 2015). Stabilisation of alkyl carbon in clays is thought to be primarily through interaction with Fe oxides and Al silicates (Kögel-Knabner et al. 2008).

Further work examining the role of clay content on *n*-alkane preservation in soils is required. The original CSIRO incubation experiment, from which the samples for the work discussed in Chapter 3 were obtained, measured the carbon sequestration potential of organic soil amendments using 6 different soil types, each with different clay content proportions (Farrell et al. 2015). A comparison of the *n*-alkane concentration loss and CPI change of the different soils each incubated with the same organic amendment would provide insight into the role of clay content proportion on *n*-alkane preservation in soils.

In addition, work quantifying the amount of time averaging, or degradation of *n*-alkanes occurring in soils could be conducted using C^{14} dating methods, particularly in an Australian context where factors such as aridity and the ancient landscape may affect degradation rates in soils.

4. Vegetation and climate reconstruction across Australia's megafauna extinction boundary

Based on the findings from Chapters 3 and 4, in which I established the robustness of leaf wax *n*-alkane signals for use in palaeoecological reconstruction, I examined the leaf wax *n*-alkanes signals preserved in sediments from Blanche Cave at Naracoorte in south eastern Australia. These leaf wax *n*-alkane signals allowed us to reconstruct environmental conditions across the late Pleistocene megafaunal extinction interval at Naracoorte, due to the direct association between the sediments and the presence and subsequent absence of megafauna fossils within the Blanche Cave deposit. Here, I examined the range of ecological variability across this time period through the comparison of leaf wax *n*-alkane chain length distributions and isotopic ratios. The *n*-alkane $\delta^{13}C$ values showed that mixed C3 and C4 vegetation was present in the region

prior to the disappearance of megafauna fossils, but C4 vegetation abundance was progressively declining. C4 vegetation then disappeared from the record after the megafauna fossils disappeared, but later rebounded and returned. Further, the *n*-alkane δD values indicated wetter conditions in the layer preceding the disappearance of megafauna fossils compared to earlier and later in the record. I proposed that climate played a role in the initial decrease of C4 vegetation, but that the disappearance of C4 vegetation may have been attributed to the loss of large herbivores causing a reduction of an open C4 landscape. I further proposed that the subsequent return of C4 vegetation may have been due to human-induced changes to fire regime, in combination with drier climate conditions, resulting in opening up the landscape and allowing C4 vegetation to again proliferate. These findings provide an important environmental context for examining the climate versus human induced debate surrounding the causes of megafauna extinction in Australia.

4.1 Future work: Determine whether shifts in C4 vegetation in Naracoorte at the time of megafauna extinction indicate a change in the presence of chenopods

In Chapter 4, I find that the carbon isotopic analysis of leaf wax *n*-alkanes show that the relative proportion of C4 vegetation begins to decrease prior to the disappearance of megafauna fossils in Blanche Cave. C4 vegetation then fully disappears from the record at the same time megafauna fossils also disappear at ~42 – 60 ka, and it then reappears in the record following megafauna extinction.

Presently, Australia has a high predominance of C4 grasses, however there have been shifts in the dominance of C4 vegetation recorded in the past (Desmarchelier et al. 2000, Andrae et al. 2018). During the time of the megafauna extinction in the late

Pleistocene, in addition to our work here, records show that C4 vegetation decreased around the time of megafauna extinction (Lopes dos Santos et al. 2013, Miller et al. 2016, DeSantis et al. 2017). However, the type of C4 vegetation present during these periods is not well characterised. In Australia today, the dominant C4 plant growth forms are grasses, followed by chenopods (Supplementary Fig. S1, Appendix 3). Work by Prideaux et al. (2009) reveals that the that the giant kangaroo, *Procoptodon goliah*, relied heavily upon a C4 chenopod diet, suggesting that some megafauna species may have been adversely affected if chenopod predominance changed. Analysis of an offshore core from off the coast of Western Australia reveals that Chenopodiaceae pollen abundance increased at about 46 to 40 ka (van der Kaars and De Deckker 2002). Palynological analysis of the Blanche Cave sediments examined here in this thesis would further elucidate the types of vegetation present before, during and after megafauna extinction in Naracoorte and would provide further context to the environmental conditions that Australia's megafauna were subject to at this time.

5. Final conclusions

Increasing evidence suggests that the leaf wax *n*-alkane signals produced by plants vary regionally, with different species, ecosystems and climates contributing to this variation. The environments represented in Australia are widely diverse and the flora is unique and this makes Australia an ideal study area to gain greater insight into leaf wax *n*-alkane signal variation. However, there has previously only been limited work examining leaf wax *n*-alkanes in the Australian context and there are fewer palaeoclimate records in Australia than compared to the rest of the world. The work presented here in this thesis significantly expands upon this, by providing insights into

the leaf wax *n*-alkane composition of Australian plants and soils, how well they preserve in Australian soil, and what information they can provide about the environment at the time of the Australian megafauna extinction. As such, this work significantly furthers the utility and robustness of leaf wax *n*-alkanes for use in palaeoecological research.

References

ANDRAE J. W., MCINERNEY F. A., POLISSAR P. J., SNIDERMAN J. M. K., HOWARD S., HALL P. A. & PHELPS S. R. 2018. Initial Expansion of C4 Vegetation in Australia During the Late Pliocene, *Geophysical Research Letters*. **45**, 4831-4840.

BAI H., LI Y., PENG L., LIU X., LIU X., SONG C. & MU L. 2017. Stable hydrogen isotope composition of n-alkanes in urban atmospheric aerosols in Taiyuan, China, *Atmospheric Environment*. **153**, 206-216.

BALDOCK J. A., OADES J. M., WATERS A. G., PENG X., VASSALLO A. M. & WILSON M. A. 1992. Aspects of the Chemical Structure of Soil Organic Materials as Revealed by Solid-State ^{13}C NMR Spectroscopy, *Biogeochemistry*. **16**, 1-42.

BARNOSKY A. D., HADLY E. A., GONZALEZ P., HEAD J., POLLY P. D., LAWING A. M., ERONEN J. T., ACKERLY D. D., ALEX K., BIBER E., BLOIS J., BRASHARES J., CEBALLOS G., DAVIS E., DIETL G. P., DIRZO R., DOREMUS H., FORTELIUS M., GREENE H. W., HELLMANN J., HICKLER T., JACKSON S. T., KEMP M., KOCH P. L., KREMEN C., LINDSEY E. L., LOOY C., MARSHALL C. R., MENDENHALL C., MULCH A., MYCHAJLIW A. M., NOWAK C., RAMAKRISHNAN U., SCHNITZLER J., DAS SHRESTHA K., SOLARI K., STEGNER L., STEGNER M. A., STENSETH N. C., WAKE M. H. & ZHANG Z. 2017. Merging paleobiology with conservation biology to guide the future of terrestrial ecosystems, *Science*. **355**.

DESANTIS L. R. G., FIELD J. H., WROE S. & DODSON J. R. 2017. Dietary responses of Sahul (Pleistocene Australia-New Guinea) megafauna to climate and environmental change, *Paleobiology*. **43**, 181-195.

DESMARCHELIER J. M., GOEDE A., AYLIFFE L. K., MCCULLOCH M. T. & MORIARTY K. 2000. Stable isotope record and its palaeoenvironmental interpretation for a late Middle Pleistocene speleothem from Victoria Fossil Cave, Naracoorte, South Australia, *Quaternary Science Reviews*. **19**, 763-774.

DIEFENDORF A. F. & FREIMUTH E. J. 2017. Extracting the most from terrestrial plant-derived *n*-alkyl lipids and their carbon isotopes from the sedimentary record: A review, *Organic Geochemistry*. **103**, 1-21.

DIETL G. P., KIDWELL S. M., BRENNER M., BURNEY D. A., FLESSA K. W., JACKSON S. T. & KOCH P. L. 2015. Conservation Paleobiology: Leveraging Knowledge of the Past to Inform Conservation and Restoration, *Annual Review of Earth and Planetary Sciences*. **43**, 79-103.

EGLINTON T. I. & EGLINTON G. 2008. Molecular proxies for paleoclimatology, *Earth and Planetary Science Letters*. **275**, 1-16.

FARRELL M., BALDOCK J., CARTER T., CREAMER C., HAWKE B., KOOKANA R., MARTIN S., MCGOWAN J. & SZARVAS S. 2015 An assessment of the carbon sequestration potential of organic soil amendments. pp. 13-53. Department of Agriculture: CSIRO.

GAGOSIAN R. B. & PELTZER E. T. 1986. The importance of atmospheric input of terrestrial organic material to deep sea sediments, *Organic Geochemistry*. **10**, 661-669.

GAGOSIAN R. B., PELTZER E. T. & MERRILL J. T. 1987. Long-range transport of terrestrially derived lipids in aerosols from the south Pacific, *Nature*. **325**, p.800.

GUO Z. G., SHENG L. F., FENG J. L. & FANG M. 2003. Seasonal variation of solvent extractable organic compounds in the aerosols in Qingdao, China, *Atmospheric Environment*. **37**, 1825-1834.

HÖFLE S., RETHEMEYER J., MUELLER C. W. & JOHN S. 2013. Organic matter composition and stabilization in a polygonal tundra soil of the Lena Delta, *Biogeosciences*. **10**, 3145-3158.

IPCC 2014 Climate Change 2014: Synthesis Report. Contribution of Working Groups I, II and III to the Fifth Assessment Report of the Intergovernmental Panel on Climate Change. pp. 151. [Core Writing Team, R.K. Pachauri and L.A. Meyer (eds.)], IPCC, Geneva, Switzerland.

KÖGEL-KNABNER I., GUGGENBERGER G., KLEBER M., KANDELER E., KALBITZ K., SCHEU S., EUSTERHUES K. & LEINWEBER P. 2008. Organo-mineral associations in temperate soils: Integrating biology, mineralogy, and organic matter chemistry, *Journal of Plant Nutrition and Soil Science*. **171**, 61-82.

LEHMANN J. & KLEBER M. 2015. The contentious nature of soil organic matter, *Nature*. **528**, p.60.
LOPES DOS SANTOS R. A., DE DECKKER P., HOPMANS E. C., MAGEE J. W., METS A., SINNINGHE DAMSTE J. S. & SCHOUTEN S. 2013. Abrupt vegetation change after the Late Quaternary megafaunal extinction in southeastern Australia, *Nature Geosci*. **6**, 627-631.
MILLER G. H., FOGEL M. L., MAGEE J. W. & GAGAN M. K. 2016. Disentangling the impacts of climate and human colonization on the flora and fauna of the Australian arid zone over the past 100 ka using stable isotopes in avian eggshell, *Quaternary Science Reviews*. **151**, 27-57.
PRIDEAUX G. J., AYLIFFE L. K., DESANTIS L. R. G., SCHUBERT B. W., MURRAY P. F., GAGAN M. K. & CERLING T. E. 2009. Extinction implications of a chenopod browse diet for a giant Pleistocene kangaroo, *Proceedings of the National Academy of Sciences*. **106**, 11646-11650.
SCHEFUß E., RATMEYER V., STUUT J.-B. W., JANSEN J. H. F. & SINNINGHE DAMSTÉ J. S. 2003. Carbon isotope analyses of n-alkanes in dust from the lower atmosphere over the central eastern Atlantic, *Geochimica et Cosmochimica Acta*. **67**, 1757-1767.
SCHMIDT M. W. I., TORN M. S., ABIVEN S., DITTMAR T., GUGGENBERGER G., JANSSENS I. A., KLEBER M., KOGEL-KNABNER I., LEHMANN J., MANNING D. A. C., NANNIPIERI P., RASSE D. P., WEINER S. & TRUMBORE S. E. 2011. Persistence of soil organic matter as an ecosystem property, *Nature*. **478**, 49-56.
SCHREUDER L. T., STUUT J.-B. W., KORTE L. F., SINNINGHE DAMSTÉ J. S. & SCHOUTEN S. 2018. Aeolian transport and deposition of plant wax n-alkanes across the tropical North Atlantic Ocean, *Organic Geochemistry*. **115**, 113-123.
SIMONEIT B. R. T., CARDOSO J. N. & ROBINSON N. 1990. An assessment of the origin and composition of higher molecular weight organic matter in aerosols over Amazonia, *Chemosphere*. **21**, 1285-1301.
SIMONEIT B. R. T. 1997. Compound-specific carbon isotope analyses of individual long-chain alkanes and alkanoic acids in Harmattan aerosols, *Atmospheric Environment*. **31**, 2225-2233.
VAN DER KAARS S. & DE DECKKER P. 2002. A Late Quaternary pollen record from deep-sea core Fr10/95, GC17 offshore Cape Range Peninsula, northwestern Western Australia, *Review of Palaeobotany and Palynology*. **120**, 17-39.

APPENDIX 1

Modelling leaf wax *n*-alkane inputs to soils along a latitudinal transect across Australia

Howard, S.[a], McInerney, F.A.[a], Caddy-Retalic, S.[b,c], Hall, P.A.[a], Andrae, J.W.[a]

[a]*University of Adelaide, Sprigg Geobiology Centre and School of Physical Sciences*

[b]*University of Adelaide, School of Biological Sciences*

[c]*University of Sydney, School of Life and Environmental Sciences*

Supplementary Tables and Figures

Supplementary Table S1. Details of the bioregions sampled.

Bioregion	Location	Area	Description	Climate	Source
Darwin Coastal	Western coastline of the Northern Territory	27,800 km^2	Generally flat, low-lying country, drained by several large rivers. Vegetation communities include eucalypt forest and woodlands with tussock and hummock grass understory. Land use is mixed, with urban development around Darwin, Aboriginal land, pastoral leases and conservation reserves.	Tropical monsoonal climate with a distinct wet and dry season.	Australian Government - Department of the Environment and Energy
Gulf Fall and Uplands	Northern half of Northern Territory, extending into Queensland	118,480 km^2	Landscape includes spectacular gorges, water holes and dissected sandstone plateaus. Vegetation is predominantly eucalypt woodlands over spinifex grasslands. Cattle grazing and mining are the main industries. Other land uses include Aboriginal land and conservation reserves.	Monsoonal climate with much higher rainfall in the north.	Australian Government - Department of the Environment and Energy
Burt Plain	Southern Northern Territory	73,800 km^2	Characterised by plains and low rocky ranges. Vegetation is predominantly mulga and other acacia woodlands with short grasses and forbs, and spinifex grasslands. The predominant land use is cattle grazing, with some Aboriginal land.	Arid with predominantly summer rainfall.	Australian Government - Department of the Environment and Energy
Finke	Crosses the border of the Northern Territory and South Australia	72,700 km^2	Arid sand plains with dissected uplands and valleys, including some major rivers (Finke, Hugh and Palmer rivers). Dominated by mulga with various *Senna* , *Eremophila* and other *Acacia* species present over short grasses and forbs. Major land uses are cattle grazing and Aboriginal land management.	Arid and hot, with very low rainfall and high evaporation.	Australian Government - Department of the Environment and Energy
Stony Plains	Northern South Australia with the northern tip extending into the Northern Territory	134,200 km^2	Includes tablelands and low gibber plains within some of the most arid areas in Australia. Vegetation includes chenopod shrublands, gidgee and mulga woodlands. Land use is mostly pastoral, with cattle in the north and both sheep and cattle grazing in the south. Opal mining occurs too.	Very arid climate with extreme temperatures.	Australian Government - Department of the Environment and Energy
Flinders Lofty Block	Southeast South Australia	57,930 km^2	General pattern of mountain ranges, ridges and wide, flat plains. Vegetation types are related to landforms, with eucalypts on hills and ranges that receive higher rainfall, mulga in drier areas, and sparse low shrubs or spinifex on stony areas. The area is mainly used for sheep and cattle grazing. Conservation reserves and associated tourism are also important. Coal is mined at Leigh Creek and there is limited dryland agriculture in the south and east.	Semiarid to arid climate with unreliable and erratic, winter-dominant rainfall.	Australian Government - Department of the Environment and Energy
Kanmantoo	Includes Kangaroo Island and the Fleurieu Peninsula and part of the Mount Lofty Ranges in South Australia	8,120 km^2	Diverse landscape with rugged and inaccessible terrain as well as significant lowland areas. A large amount of the vegetation has been cleared, however dominant vegetation includes mallee shrublands and woodlands, heath, eucalypt woodlands and eucalypt open forests. The land is mainly used for grazing, nature conservation and cereal cropping.	Temperate climate with warm summers and winter-dominant rainfall.	Government of South Australia - Natural Resources Adelaide & Mt Lofty Ranges

Supplementary Table S2. Sample, site, species, coverage and *n*-alkane data of the plants analysed.

Voucher No	Site	Bioregion	Species Name	Growth Form	PFT	% Cover	ng/mg C25	ng/mg C26	ng/mg C27	ng/mg C28	ng/mg C29	ng/mg C30	ng/mg C31	ng/mg C32	ng/mg C33	ng/mg C34	ng/mg C35	%C25	%C26	%C27	%C28	%C29	%C30	%C31	%C32	%C33	%C34	%C35	ACL	CPI
NTA 001317	NTABRT0004	Burt Plain	Triodia schinzii	Hummock Grass	Graminoid	7.2	0.033	0.038	0.045	0.024	0.041	0.007	0.060	0.005	0.116	0.005	0.010	8.59	9.88	11.65	6.12	10.77	1.93	15.65	1.38	30.02	1.38	2.62	30.38	3.56
NTA 001318	NTABRT0004	Burt Plain	Aristida holathera	Tussock Grass	Graminoid	23.6	0.003	0.000	0.005	0.000	0.033	0.004	0.412	0.021	0.758	0.010	0.083	0.24	0.00	0.38	0.00	2.48	0.27	31.01	1.55	57.09	0.72	6.26	32.35	37.09
NTA 001301	NTABRT0004	Burt Plain	Acacia aptaneura (or aneura)	Shrub	Shrub	54.9	0.029	0.037	0.123	0.051	0.270	0.096	4.262	0.474	6.233	0.148	0.122	0.25	0.32	1.04	0.43	2.28	0.81	35.98	4.00	52.62	1.25	1.03	32.06	13.61
NTA 005954	NTADAC0001	Darwin Coastal	Sorghum plumosum	Tussock Grass	Graminoid	57.1	0.003	0.003	0.004	0.002	0.004	0.003	0.023	0.003	0.033	0.000	0.010	3.43	3.43	4.12	2.52	4.58	3.43	25.86	3.89	37.76	0.00	10.98	31.84	5.99
NTA 006020	NTADAC0001	Darwin Coastal	Eucalyptus tetrodonta	Tree/Palm	Tree	19.4	0.021	0.023	0.033	0.029	0.132	0.029	0.060	0.028	0.073	0.028	0.031	4.28	4.63	6.79	6.04	27.16	6.00	12.32	5.73	15.07	5.65	6.32	30.28	2.37
NTA 006042	NTADAC0001	Darwin Coastal	Eucalyptus miniata	Tree/Palm	Tree	7.8	0.027	0.025	0.037	0.033	0.064	0.030	0.051	0.028	0.033	0.027	0.029	7.08	6.52	9.68	8.61	16.56	7.90	13.19	7.18	8.71	7.13	7.44	29.93	1.48
NTA 000754	NTAFIN0019	Finke	Cenchrus ciliaris	Tussock Grass	Graminoid	67.3	0.003	0.003	0.011	0.006	0.081	0.019	0.932	0.036	0.835	0.000	0.051	0.15	0.17	0.54	0.31	4.11	0.97	47.12	1.83	42.21	0.00	2.60	31.86	29.05
NTA 000784	NTAFIN0019	Finke	Acacia estrophiolata	Tree/Palm	Tree	18.8	0.011	0.011	0.451	0.043	0.909	0.117	3.836	0.123	0.127	0.000	0.000	0.20	0.19	8.01	0.77	16.15	2.09	68.14	2.19	2.26	0.00	0.00	30.36	18.08
NTA 000761	NTAFIN0019	Finke	Enchylaena tomentosa	Tussock Grass	Graminoid	2.3	0.126	0.131	0.141	0.144	0.154	0.156	0.170	0.170	0.174	0.000	0.000	9.24	9.61	10.34	10.52	11.25	11.44	12.44	12.44	12.72	0.00	0.00	29.32	1.17
NTA 000962	NTAFIN0022	Finke	Enneapogon polyphyllus	Tussock Grass	Graminoid	14.8	0.023	0.021	0.029	0.023	0.051	0.030	0.481	0.045	0.728	0.037	0.110	1.48	1.30	1.87	1.48	3.25	1.91	30.46	2.86	46.07	2.32	6.99	32.08	8.69
NTA 000960	NTAFIN0022	Finke	Aristida contorta	Tussock Grass	Graminoid	7.6	0.023	0.024	0.034	0.029	0.059	0.038	0.421	0.047	0.404	0.034	0.068	1.97	2.01	2.88	2.46	5.00	3.21	35.63	4.01	34.16	2.91	5.77	31.68	5.59
NTA 000964	NTAFIN0022	Finke	Eremophila freelingii	Shrub	Shrub	49.6	4.780	6.195	6.686	4.999	3.866	2.456	3.250	1.750	13.379	1.382	2.141	9.39	12.18	13.14	9.82	7.60	4.83	6.39	3.44	26.29	2.72	4.21	30.18	1.83
NTA 001525	NTAGFU0001	Gulf Fall and Uplands	Enneapogon polyphyllus	Tussock Grass	Graminoid	12.8	0.003	0.002	0.003	0.001	0.002	0.002	0.015	0.003	0.043	0.000	0.005	3.54	2.27	3.28	1.77	2.53	2.27	19.44	3.79	54.80	0.00	6.31	32.06	8.41
NTA 001524	NTAGFU0001	Gulf Fall and Uplands	Aristida pruinosa	Tussock Grass	Graminoid	16.72	0.023	0.025	0.034	0.031	0.041	0.036	0.216	0.035	0.073	0.030	0.033	4.03	4.29	5.81	5.37	7.18	6.25	37.45	6.03	12.69	5.22	5.66	30.81	2.50
NTA 001531	NTAGFU0001	Gulf Fall and Uplands	Eucalyptus pruinosa	Tree Mallee	Tree	12.7	0.004	0.007	0.022	0.002	0.006	0.000	0.002	0.000	0.002	0.000	0.000	9.05	15.84	48.87	4.98	14.03	0.00	3.62	0.00	3.62	0.00	0.00	27.58	3.59
NTA 002012	NTAGFU0008	Gulf Fall and Uplands	Triodia pungens	Hummock grass	Graminoid	44.8	0.005	0.000	0.048	0.009	0.394	0.016	0.597	0.007	0.344	0.000	0.006	0.32	0.00	3.37	0.66	27.61	1.15	41.89	0.47	24.13	0.00	0.41	30.79	42.72
NTA 002018	NTAGFU0008	Gulf Fall and Uplands	Fimbristylis dichotoma	Sedge	Graminoid	14.2	0.018	0.019	0.021	0.022	0.026	0.025	0.063	0.029	0.166	0.030	0.076	3.63	3.90	4.26	4.45	5.32	5.01	12.69	5.87	33.43	6.07	15.37	32.06	2.58
NTA 002011	NTAGFU0008	Gulf Fall and Uplands	Aristida contorta	Tussock Grass	Graminoid	19.2	1.133	0.990	1.043	0.727	0.965	0.413	0.780	0.241	0.499	0.136	0.152	16.01	13.98	14.73	10.27	13.64	5.84	11.01	3.40	7.04	1.92	2.14	28.53	1.57
NTA 002136	NTAGFU0010	Gulf Fall and Uplands	Triodia pungens	Hummock grass	Graminoid	62.6	0.003	0.003	0.038	0.004	0.169	0.010	0.796	0.012	0.333	0.000	0.006	0.25	0.22	2.73	0.29	12.32	0.74	57.91	0.88	24.24	0.00	0.41	31.13	45.55
NTA 002140	NTAGFU0010	Gulf Fall and Uplands	Eucalyptus leucophloia	Tree Mallee	Tree	36.4	0.003	0.000	0.004	0.000	0.062	0.006	0.227	0.007	0.025	0.000	0.000	1.01	0.00	1.12	0.00	18.47	1.84	67.91	2.19	7.46	0.00	0.00	30.66	23.71
NTA 002610	NTAGFU0017	Gulf Fall and Uplands	Chrysopogon fallax	Tussock Grass	Graminoid	9.4	0.027	0.031	0.055	0.059	0.206	0.079	0.311	0.038	0.120	0.029	0.041	2.70	3.11	5.53	5.93	20.62	7.95	31.25	3.85	12.07	2.93	4.06	30.49	3.06
NTA 002681	NTAGFU0017	Gulf Fall and Uplands	Schizachyrium fragile	Tussock Grass	Graminoid	7	0.001	0.001	0.002	0.000	0.005	0.002	0.044	0.002	0.035	0.000	0.000	1.08	1.08	2.38	0.00	5.18	2.16	48.16	2.16	37.80	0.00	0.00	31.52	17.42
NTA 002634	NTAGFU0017	Gulf Fall and Uplands	Melaleuca viridiflora	Shrub	Shrub	31.2	0.003	0.003	0.036	0.004	0.017	0.002	0.013	0.000	0.000	0.000	0.000	3.33	4.10	46.15	5.13	22.56	2.31	16.41	0.00	0.00	0.00	0.00	28.18	7.52
NTA 003588	NTAGFU0031	Gulf Fall and Uplands	Schizachyrium pachyarthron	Tussock Grass	Graminoid	27.7	0.008	0.006	0.011	0.003	0.017	0.003	0.026	0.000	0.038	0.000	0.016	6.25	4.61	8.88	2.63	13.49	2.63	20.07	0.00	29.28	0.00	12.17	31.08	8.20
NTA 003622	NTAGFU0031	Gulf Fall and Uplands	Melaleuca viridiflora	Shrub	Shrub	29.9	0.032	0.037	0.048	0.040	0.055	0.063	0.080	0.088	0.086	0.091	0.088	4.48	5.29	6.75	5.71	7.78	8.85	11.26	12.49	12.10	12.91	12.38	31.08	1.02
NTA 003613	NTAGFU0031	Gulf Fall and Uplands	Petalostigma banksii	Shrub	Shrub	9.1	0.002	0.002	0.004	0.002	0.011	0.005	0.018	0.000	0.003	0.000	0.000	5.02	5.02	9.21	5.02	22.18	9.62	38.08	0.00	5.86	0.00	0.00	29.76	3.96
NTA 003995	NTAGFU0040	Gulf Fall and Uplands	Heteropogon contortus	Tussock Grass	Graminoid	15.8	0.004	0.004	0.008	0.004	0.018	0.009	0.146	0.006	0.066	0.000	0.010	1.28	1.44	3.04	1.44	6.39	3.35	53.19	2.24	23.96	0.00	3.67	31.33	10.52
NTA 004200	NTAGFU0040	Gulf Fall and Uplands	Acacia dimidiata	Shrub	Shrub	26.7	0.027	0.023	0.035	0.025	0.041	0.028	0.217	0.054	0.227	0.030	0.029	3.64	3.10	4.70	3.40	5.56	3.78	29.53	7.31	30.90	4.10	3.97	31.33	3.43
NTA 003965	NTAGFU0040	Gulf Fall and Uplands	Eucalyptus tectifica	Tree/Palm	Tree	9.7	0.000	0.000	0.027	0.000	0.034	0.000	0.000	0.000	0.000	0.000	0.000	0.00	0.00	44.63	0.00	55.37	0.00	0.00	0.00	0.00	0.00	0.00	28.11	
SAA 000294	SAASTP0001	Stony Plains	Eragrostis setifolia	Tussock Grass	Graminoid	11.9	0.002	0.000	0.003	0.000	0.010	0.002	0.206	0.000	0.028	0.000	0.000	0.94	0.00	1.02	0.00	4.01	0.94	81.84	0.00	11.24	0.00	0.00	31.05	104.50
SAA 000250	SAASTP0001	Stony Plains	Maireana aphylla	Chenopod	Shrub	31	0.122	0.021	0.111	0.023	0.144	0.020	0.210	0.006	0.006	0.000	0.000	18.42	3.17	16.66	3.53	21.71	2.96	31.70	0.93	0.93	0.00	0.00	28.55	7.58
SAA 000338	SAASTP0001	Stony Plains	Acacia aneura var. tenuis	Shrub	Shrub	7.7	0.026	0.035	0.124	0.044	0.206	0.069	1.298	0.172	1.504	0.100	0.089	0.72	0.94	3.37	1.19	5.62	1.89	35.40	4.69	41.03	2.72	2.43	31.71	7.61
SAA 000019	SAASTP0004	Stony Plains	Malvastrum americanum var. americanum	Forb	Forb	25.6	0.069	0.025	0.236	0.036	0.548	0.051	0.639	0.023	0.082	0.000	0.011	4.02	1.43	13.70	2.12	31.84	2.99	37.16	1.33	4.79	0.00	0.63	29.58	11.41
SAA 000016	SAASTP0004	Stony Plains	Rutidosis helichrysoides subsp. Helichrysoides	Forb	Forb	18.5	0.017	0.000	0.048	0.016	1.071	0.081	3.907	0.383	3.109	0.845	0.652	0.17	0.00	0.48	0.15	10.57	0.80	38.58	3.78	30.69	8.34	6.44	31.73	6.40
SAA 000022	SAASTP0004	Stony Plains	Sida fibulifera	Forb	Forb	11.7	0.000	0.000	0.008	0.000	0.048	0.030	2.057	0.308	2.326	0.064	0.215	0.00	0.00	0.16	0.00	0.94	0.58	40.69	6.09	46.00	1.27	4.26	32.16	11.32
SAT 000287	SATFLB0005	Flinders Lofty Block	Chrysocephalum semipapposum	Forb	Forb	13.1	0.140	0.151	0.194	0.097	0.978	0.144	2.610	0.113	0.607	0.000	0.046	2.75	2.98	3.81	1.91	19.26	2.84	51.38	2.22	11.94	0.00	0.91	30.53	8.87
SAT 000316	SATFLB0005	Flinders Lofty Block	Dodonaea viscosa subsp. angustissima	Shrub	Shrub	21.8	2.076	1.964	2.939	1.868	4.504	1.081	4.025	0.459	0.826	0.168	0.113	10.37	9.81	14.68	9.33	22.50	5.40	20.10	2.29	4.13	0.84	0.57	28.85	2.42
SAT 000286	SATFLB0005	Flinders Lofty Block	Eucalyptus flindersii	Tree Mallee	Tree	18.7	0.115	0.051	0.261	0.013	0.038	0.000	0.003	0.000	0.000	0.000	0.000	23.90	10.57	54.11	2.79	7.94	0.00	0.68	0.00	0.00	0.00	0.00	26.66	5.59
SAT 000424	SATFLB0008	Flinders Lofty Block	Triodia scariosa	Hummock grass	Graminoid	45.1	0.007	0.000	0.007	0.000	0.019	0.000	0.094	0.000	0.000	0.000	0.000	5.47	0.00	5.16	0.00	15.31	0.00	74.06	0.00	0.00	0.00	0.00	30.16	
SAT 000419	SATFLB0008	Flinders Lofty Block	Cassinia laevis	Shrub	Shrub	22.5	0.051	0.044	0.131	0.042	0.216	0.069	0.351	0.094	0.117	0.092	0.088	3.91	3.43	10.11	3.26	16.67	5.29	27.13	7.23	9.03	7.14	6.80	30.29	2.59
SAT 000401	SATFLB0008	Flinders Lofty Block	Casuarina pauper	Shrub	Shrub	12	0.026	0.032	0.046	0.038	0.151	0.065	1.371	0.098	0.504	0.093	0.088	1.03	1.29	1.82	1.51	6.03	2.57	54.58	3.90	20.06	3.72	3.49	31.33	6.52
SAT 000552	SATFLB0010	Flinders Lofty Block	Rhagodia paradoxa	Chenopod	Shrub	9.9	0.012	0.029	0.019	0.032	0.035	0.050	0.026	0.054	0.015	0.037	0.021	3.73	8.75	5.91	9.64	10.47	15.14	7.75	16.32	4.67	11.35	6.27	30.16	0.55
SAT 000550	SATFLB0010	Flinders Lofty Block	Enchylaena tomentosa var. tomentosa	Chenopod	Shrub	6	0.018	0.025	0.020	0.027	0.035	0.027	0.037	0.027	0.028	0.028	0.029	5.96	8.25	6.81	9.10	11.52	8.90	12.17	8.97	9.23	9.42	9.69	30.48	1.07
SAT 000535	SATFLB0010	Flinders Lofty Block	Eucalyptus odorata	Tree/Palm	Tree	65.1	0.034	0.039	0.107	0.009	0.012	0.002	0.002	0.000	0.000	0.000	0.000	16.49	19.16	52.05	4.39	5.91	0.95	1.05	0.00	0.00	0.00	0.00	26.78	2.75
SAT 000649	SATFLB0012	Flinders Lofty Block	Allocasuarina muelleriana subsp. Muelleriana	Shrub	Shrub	42	0.042	0.029	0.053	0.015	0.256	0.043	4.928	0.101	0.696	0.000	0.000	0.68	0.47	0.86	0.25	4.15	0.69	79.98	1.64	11.29	0.00	0.00	31.07	31.76
SAT 000657	SATFLB0012	Flinders Lofty Block	Hibbertia crinita	Shrub	Shrub	15.5	0.012	0.002	0.007	0.002	0.029	0.002	0.078	0.002	0.010	0.000	0.000	8.54	1.22	5.01	1.49	19.92	1.08	54.34	1.36	7.05	0.00	0.00	29.98	17.59
SAT 000630	SATFLB0012	Flinders Lofty Block	Eucalyptus fasciculosa	Tree Mallee	Tree	12.7	0.006	0.003	0.011	0.002	0.006	0.001	0.005	0.001	0.003	0.001	0.001	14.78	7.88	27.59	4.43	15.76	2.96	12.81	2.46	6.40	3.45	1.48	28.31	3.34
SAT 000791	SATFLB0014	Flinders Lofty Block	Xanthorrhoea quadrangulata	Shrub	Shrub	18.2	0.008	0.004	0.019	0.003	0.038	0.000	0.125	0.000	0.026	0.000	0.000	3.63	1.90	8.47	1.56	16.85	0.00	55.83	0.00	11.75	0.00	0.00	30.32	27.40
SAT 000775	SATFLB0014	Flinders Lofty Block	Allocasuarina verticillata	Shrub	Shrub	13.8	0.010	0.012	0.078	0.015	0.513	0.030	3.525	0.029	0.748	0.000	0.000	0.21	0.24	1.57	0.30	10.34	0.60	71.08	0.58	15.08	0.00	0.00	31.02	57.04
SAT 000746	SATFLB0014	Flinders Lofty Block	Eucalyptus odorata	Tree Mallee	Tree	32.5	0.025	0.021	0.027	0.024	0.031	0.026	0.061	0.029	0.045	0.029	0.000	7.81	6.57	8.43	7.44	9.67	8.12	19.28	9.05	14.32	9.30	0.00	29.80	1.37
SAT 000860	SATFLB0015	Flinders Lofty Block	Lepidosperma semiteres	Sedge	Graminoid	8.3	0.020	0.021	0.026	0.024	0.043	0.027	0.136	0.029	0.097	0.027	0.039	4.05	4.33	5.40	4.88	8.77	5.60	27.78	5.91	19.76	5.60	7.94	31.11	2.57
SAT 000866	SATFLB0015	Flinders Lofty Block	Hibbertia crinita	Shrub	Shrub	6.5	0.016	0.004	0.189	0.010	0.367	0.000	0.014	0.000	0.000	0.000	0.000	2.59	0.71	31.57	1.62	61.23	0.00	2.27	0.00	0.00	0.00	0.00	28.29	41.29
SAT 000816	SATFLB0015	Flinders Lofty Block	Eucalyptus obliqua	Tree/Palm	Tree	60	0.135	0.081	0.367	0.072	0.164	0.041	0.053	0.037	0.077	0.034	0.037	12.31	7.34	33.45	6.57	14.90	3.77	4.82	3.38	6.98	3.07	3.40	28.23	2.82
SAT 000167	SATKAN0001	Kanmantoo	Lepidosperma semiteres	Sedge	Graminoid	11.2	0.001	0.001	0.001	0.000	0.006	0.000	0.048	0.000	0.029	0.000	0.003	1.33	1.55	1.55	0.00	6.19	0.00	53.76	0.00	32.30	0.00	3.32	31.52	62.07
SAT 000124	SATKAN0001	Kanmantoo	Pultenaea involucrata	Shrub	Shrub	10.2	0.004	0.003	0.005	0.003	0.019	0.000	0.159	0.000	0.160	0.000	0.016	1.12	0.80	1.38	0.85	5.22	0.00	43.13	0.00	43.24	0.00	4.26	31.82	57.95
SAT 000122	SATKAN0001	Kanmantoo	Eucalyptus baxteri	Tree/Palm	Tree	42.5	0.022	0.218	0.026	0.178	0.488	0.111	0.193	0.035	0.044	0.046	0.048	1.59	15.50	1.82	12.63	34.66	7.84	13.69	2.49	3.14	3.24	3.39	29.86	1.34
SAT 000218	SATKAN0002	Kanmantoo	Lepidosperma semiteres	Sedge	Graminoid	9.1	0.000	0.000	0.001	0.000	0.008	0.000	0.093	0.002	0.086	0.000	0.006	0.00	0.00	0.71	0.00	4.17	0.00	47.26	0.91	43.70	0.00	3.25	31.90	106.56
SAT 000207	SATKAN0002	Kanmantoo	Hakea rostrata	Shrub	Shrub	8.2	0.003	0.000	0.009	0.000	0.123	0.011	0.317	0.004	0.009	0.000	0.000	0.66	0.00	1.97	0.00	25.85	2.30	66.50	0.82	1.89	0.00	0.00	30.38	30.91
SAT 000191	SATKAN0002	Kanmantoo	Eucalyptus obliqua	Tree/Palm	Tree	54.7	0.004	0.002	0.017	0.002	0.019	0.002	0.024	0.001	0.003	0.000	0.000	5.99	3.00	22.89	2.45	25.89	2.18	32.70	1.09	3.54	0.00	0.27	29.13	10.11

Supplementary Table S3. Site, location, climate and *n*-alkane data of the soils analysed.

Site ID	Bioregion	Latitude	Longitude	MAP (mm/yr)	MAT (°C)	MI (annual)	MI - lowest quarter mean	Temperature - month hottest max (°C)	Radiation - highest period (MJ/m2/day)	ng/mg C25	ng/mg C26	ng/mg C27	ng/mg C28	ng/mg C29	ng/mg C30	ng/mg C31	ng/mg C32	ng/mg C33	ng/mg C34	ng/mg C35	%C25	%C26	%C27	%C28	%C29	%C30	%C31	%C32	%C33	%C34	%C35	ACL	CPI
NTABRT0004	Burt Plain	-22.2894	133.6164222	341.05	22.74	0.2	0.04	36.18	29	0.001	0.000	0.002	0.000	0.002	0.000	0.005	0.001	0.005	0.001	0.001	3.58	0.00	8.95	2.37	12.69	2.74	29.18	5.46	27.67	3.12	4.26	30.88	6.02
NTADAC0001	Darwin Coastal	-13.1579	130.7779111	1642.88	26.53	0.96	0.02	33.96	24.2	0.062	0.050	0.054	0.040	0.051	0.026	0.025	0.014	0.011	0.006	0.003	18.06	14.63	15.71	11.77	15.00	7.62	7.36	4.03	3.18	1.62	1.02	27.84	1.28
NTAFIN0019	Finke	-24.3577	132.9357472	278.92	21.97	0.17	0.04	36.72	29.4	0.000	0.000	0.000	0.000	0.000	0.000	0.000	0.000	0.000	0.000	0.000	12.25	6.86	10.95	1.80	13.73	2.78	36.60	2.45	12.58	0.00	0.00	29.61	5.76
NTAFIN0022	Finke	-24.6307	133.4521833	251.51	21.85	0.15	0.04	36.49	29.5	0.034	0.035	0.038	0.030	0.026	0.019	0.015	0.010	0.008	0.005	0.003	15.31	15.56	17.18	13.58	11.71	8.36	6.65	4.46	3.77	2.09	1.34	27.94	1.08
NTAGFU0001	Gulf Fall and Uplands	-18.9051	137.0692639	468.81	25.73	0.26	0.01	37.35	27.9	0.000	0.000	0.001	0.000	0.001	0.000	0.001	0.000	0.001	0.000	0.000	8.42	5.98	15.81	4.47	14.04	3.09	19.15	4.01	15.50	2.67	6.85	29.95	3.57
NTAGFU0008	Gulf Fall and Uplands	-18.7856	136.8653389	494.62	25.47	0.28	0.02	37.22	27.8	0.000	0.000	0.000	0.000	0.001	0.000	0.001	0.000	0.000	0.000	0.000	8.12	4.86	9.51	4.03	22.38	4.95	25.37	3.36	10.70	3.06	3.66	29.80	3.64
NTAGFU0010	Gulf Fall and Uplands	-17.8958	137.1006028	673.05	25.92	0.39	0.01	36.82	27.5	0.002	0.001	0.003	0.001	0.007	0.001	0.007	0.001	0.004	0.000	0.001	6.96	2.93	11.02	2.86	25.86	4.14	26.29	1.98	14.06	1.49	2.41	29.85	6.11
NTAGFU0017	Gulf Fall and Uplands	-17.3544	137.1579611	800.91	25.71	0.47	0.02	36.25	27.3	0.006	0.004	0.012	0.003	0.011	0.001	0.004	0.001	0.002	0.001	0.000	13.81	9.00	27.06	6.45	24.22	2.27	9.06	1.71	4.54	1.87	0.00	28.07	3.37
NTAGFU0031	Gulf Fall and Uplands	-14.1254	134.3866778	988.65	27.14	0.57	0.01	37.17	26.2	0.000	0.000	0.000	0.000	0.000	0.000	0.000	0.000	0.000	0.000	0.000	13.75	7.06	14.71	6.00	12.83	5.02	14.36	4.70	9.78	4.93	6.86	29.34	2.24
NTAGFU0040	Gulf Fall and Uplands	-14.6733	133.844775	923.53	27.44	0.52	0.01	38.28	26.1	0.002	0.001	0.004	0.001	0.005	0.001	0.004	0.001	0.002	0.000	0.001	8.79	3.48	19.01	4.22	23.03	3.95	16.99	3.04	10.79	2.17	4.53	29.37	4.54
SAASTP0001	Stony Plains	-26.2777	134.9992	209.25	22.21	0.13	0.05	36.66	29.7	0.029	0.022	0.023	0.014	0.013	0.007	0.009	0.003	0.004	0.001	0.001	23.38	17.54	18.75	10.99	10.54	5.31	6.96	2.27	3.12	0.52	0.63	27.41	1.40
SAASTP0004	Stony Plains	-26.0877	135.4522019	194.65	22.6	0.12	0.04	37.02	29.7	0.000	0.000	0.000	0.000	0.000	0.000	0.000	0.000	0.000	0.000	0.000	13.09	16.58	17.38	13.63	11.69	7.25	10.29	3.73	3.37	1.43	1.58	28.24	1.17
SATFLB0005	Flinders Lofty Block	-31.315	138.5663667	306.95	17.85	0.22	0.07	30.79	28.9	0.028	0.020	0.029	0.015	0.025	0.008	0.023	0.004	0.008	0.001	0.000	17.36	12.69	17.84	9.17	15.73	4.75	14.48	2.30	5.04	0.64	0.00	28.21	2.09
SATFLB0008	Flinders Lofty Block	-32.3205	137.9543899	446.71	15.92	0.35	0.07	29.38	28.9	0.019	0.016	0.016	0.011	0.015	0.006	0.021	0.003	0.005	0.001	0.001	16.48	13.81	14.54	9.30	13.00	5.40	18.54	2.86	4.56	0.61	0.89	28.50	1.85
SATFLB0010	Flinders Lofty Block	-32.8281	138.0326702	402.76	17.59	0.31	0.06	30.52	28.6	0.023	0.018	0.024	0.013	0.024	0.008	0.019	0.004	0.005	0.001	0.001	16.45	12.86	16.88	9.45	17.36	5.75	13.73	2.62	3.54	0.73	0.64	28.21	1.91
SATFLB0012	Flinders Lofty Block	-34.8803	138.7082603	722.62	15.35	0.65	0.11	28.21	27.4	0.000	0.000	0.000	0.000	0.000	0.000	0.000	0.000	0.000	0.000	0.000	16.82	16.82	16.93	9.50	12.36	4.12	18.54	2.17	2.75	0.00	0.00	28.21	1.81
SATFLB0014	Flinders Lofty Block	-34.0047	138.9593701	533.39	14.14	0.46	0.1	27.96	27.7	0.001	0.001	0.001	0.000	0.001	0.000	0.001	0.000	0.000	0.000	0.000	14.97	11.84	13.49	7.24	12.74	4.26	23.26	2.16	8.10	0.72	1.22	28.99	2.50
SATFLB0015	Flinders Lofty Block	-34.933	138.7269537	933.83	14.03	0.87	0.16	25.45	27	0.001	0.000	0.002	0.000	0.002	0.000	0.000	0.000	0.000	0.000	0.000	13.59	8.60	29.21	5.07	35.31	1.50	4.86	0.54	1.33	0.00	0.00	27.84	4.94
SATKAN0001	Kanmantoo	-35.6078	138.261275	753.76	14.55	0.71	0.13	22.65	27.1	0.027	0.015	0.092	0.015	0.117	0.007	0.037	0.007	0.019	0.000	0.003	7.90	4.42	27.17	4.48	34.60	2.06	11.07	1.95	5.53	0.00	0.81	28.58	6.41
SATKAN0002	Kanmantoo	-35.2716	138.690175	823.48	14.44	0.77	0.14	25.01	27.2	0.001	0.001	0.002	0.001	0.002	0.000	0.000	0.000	0.000	0.000	0.000	8.84	8.31	27.37	7.54	33.30	3.70	6.73	1.55	1.59	1.09	0.00	28.10	3.31

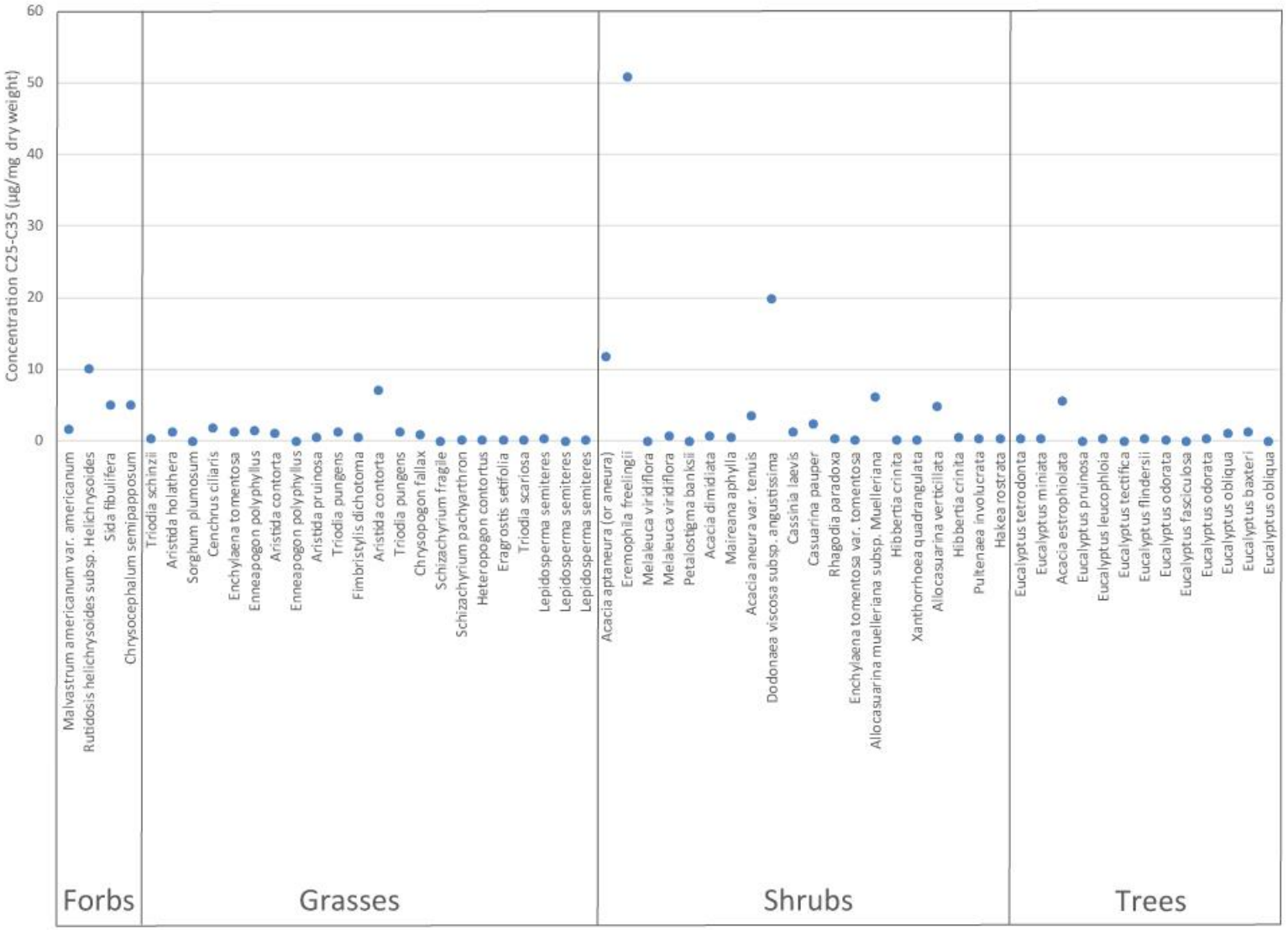

Supplementary Figure S1. Total concentration of *n*-alkanes (C25-C35) for each plant sampled, grouped by growth form.

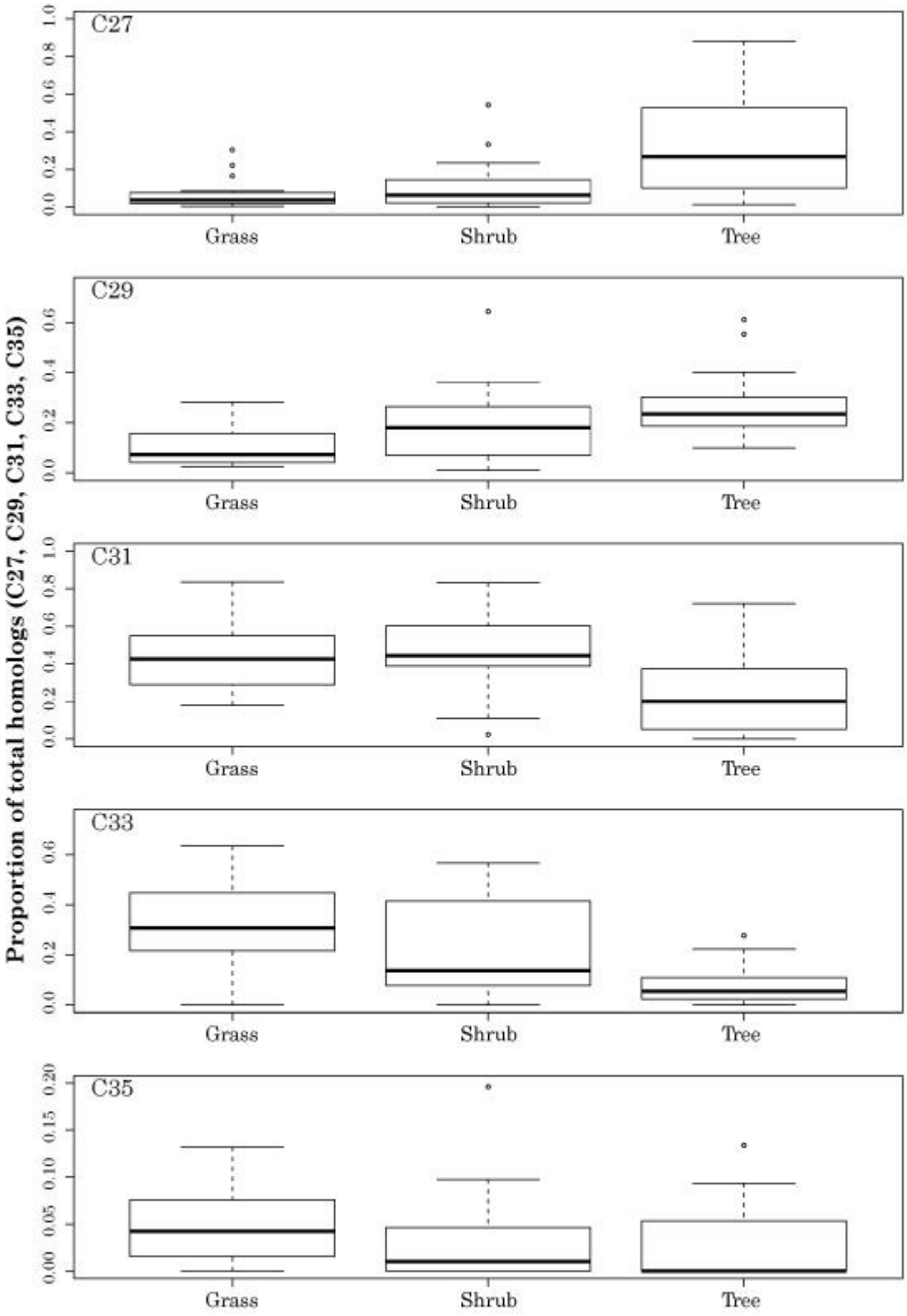

Supplementary Fig S2. Boxplots of the proportion of long odd chain lengths with respect to growth form. C27 and C29 are more dominantly associated with trees, whereas C33 is more dominantly associated with grasses.

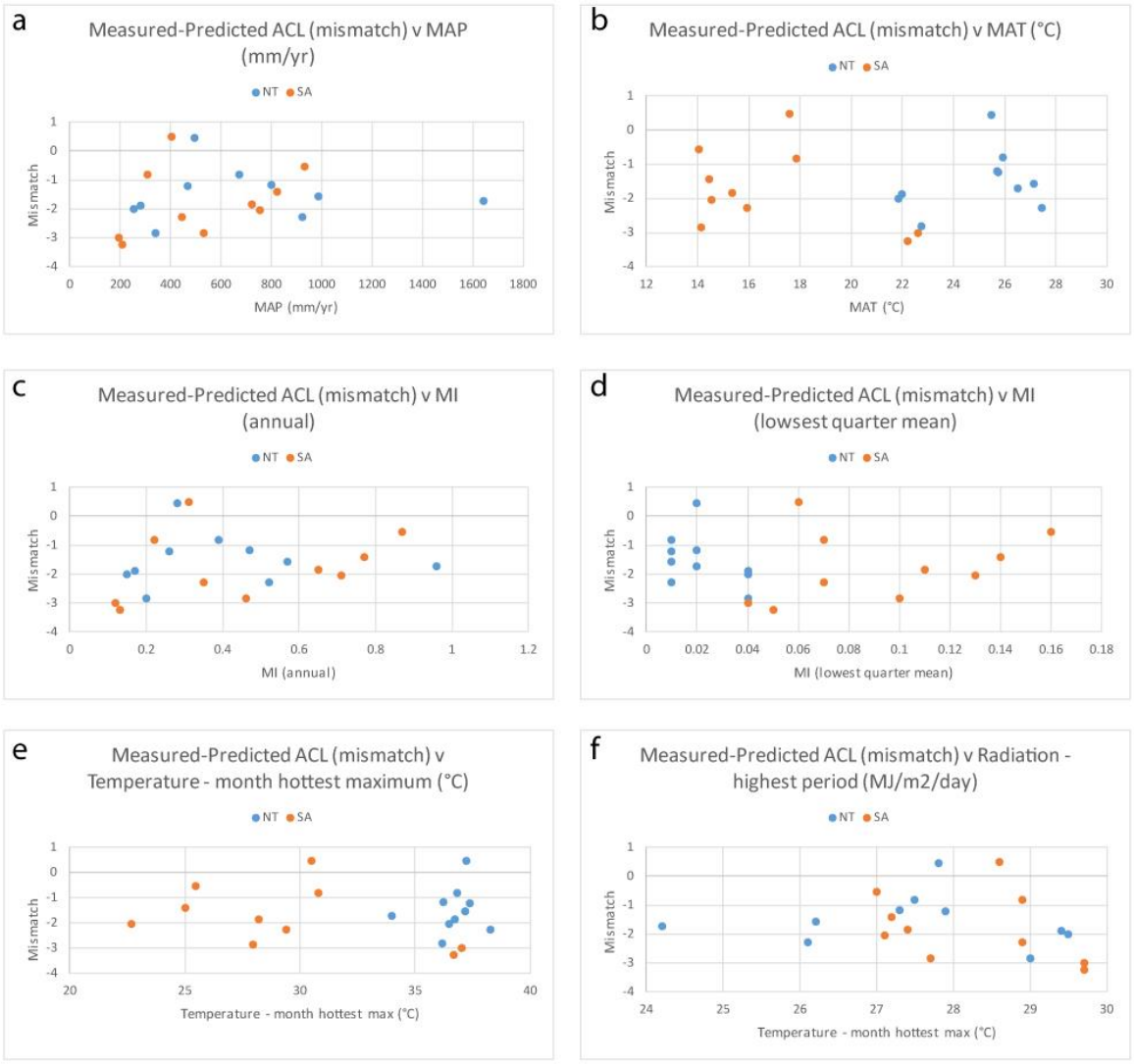

Supplementary Figure S3. Cross plots of ACL mismatch against the different climate variables, a) MAP, b) MAT, c) Annual MI, d) Lowest quarter mean MI, e) Month hottest maximum temperature, and f) Highest period radiation. Blue points are Northern Territory, orange points are South Australia.

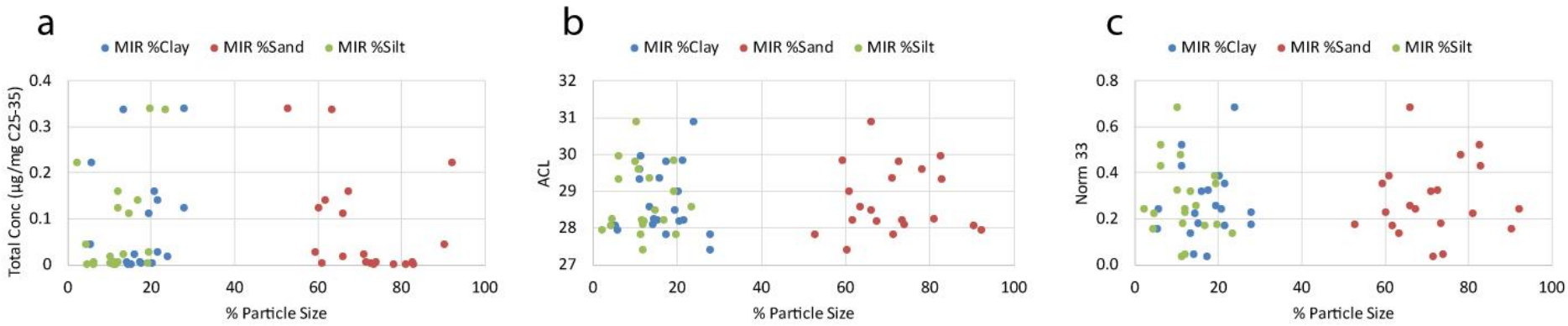

Supplementary Figure S4. Crossplots of a) total soil *n*-alkane concentration (µg/mg dry weight C25-C35) versus percentage particle size, b) soil ACL versus percentage particle size, and c) Norm33 versus percentage particle size

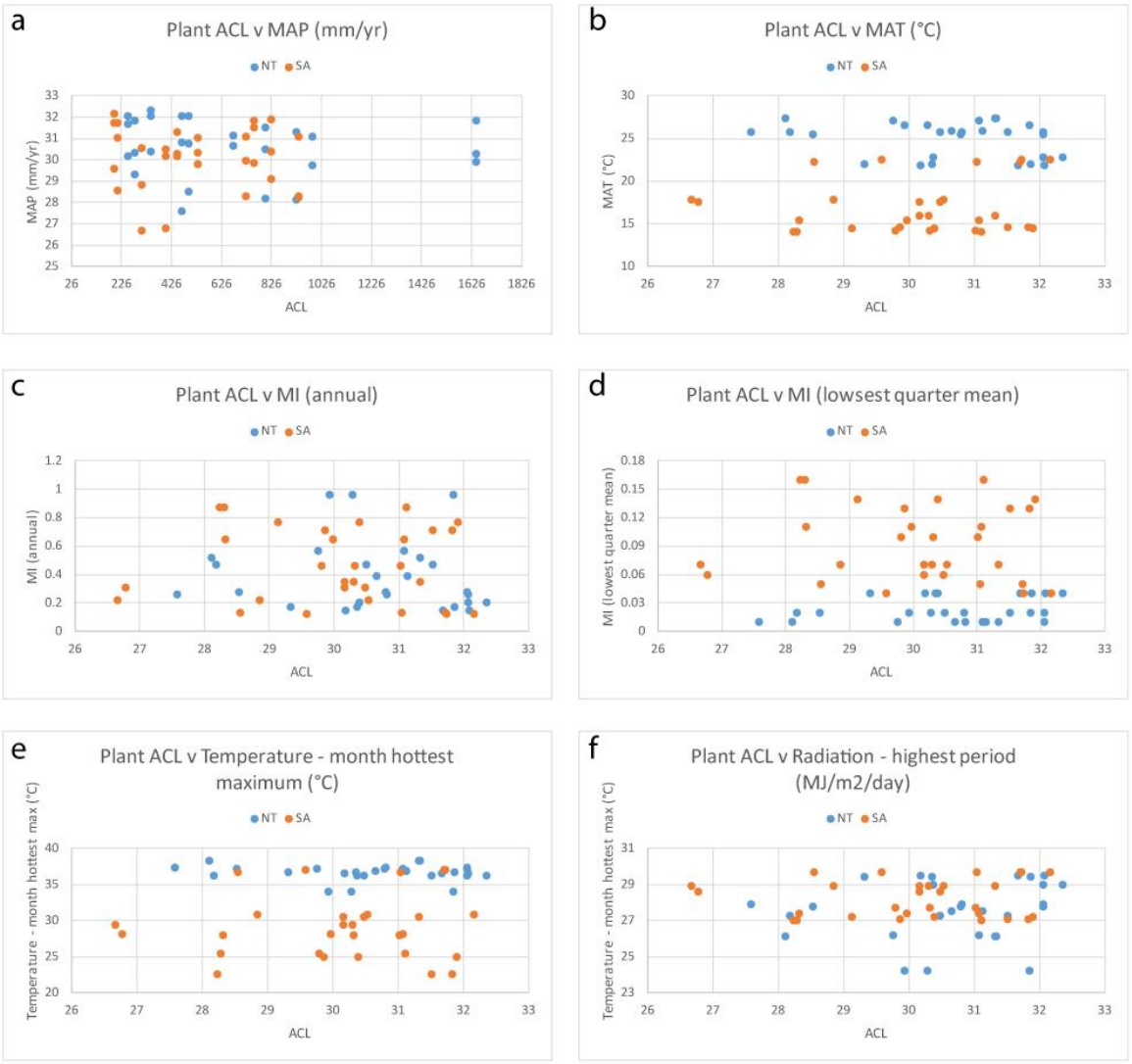

Supplementary Figure S5. Cross plots of Plant ACL against the different climate variables, a) MAP, b) MAT, c) Annual MI, d) Lowest quarter mean MI, e) Month hottest maximum temperature, and f) Highest period radiation. Blue points are Northern Territory, orange points are South Australia.

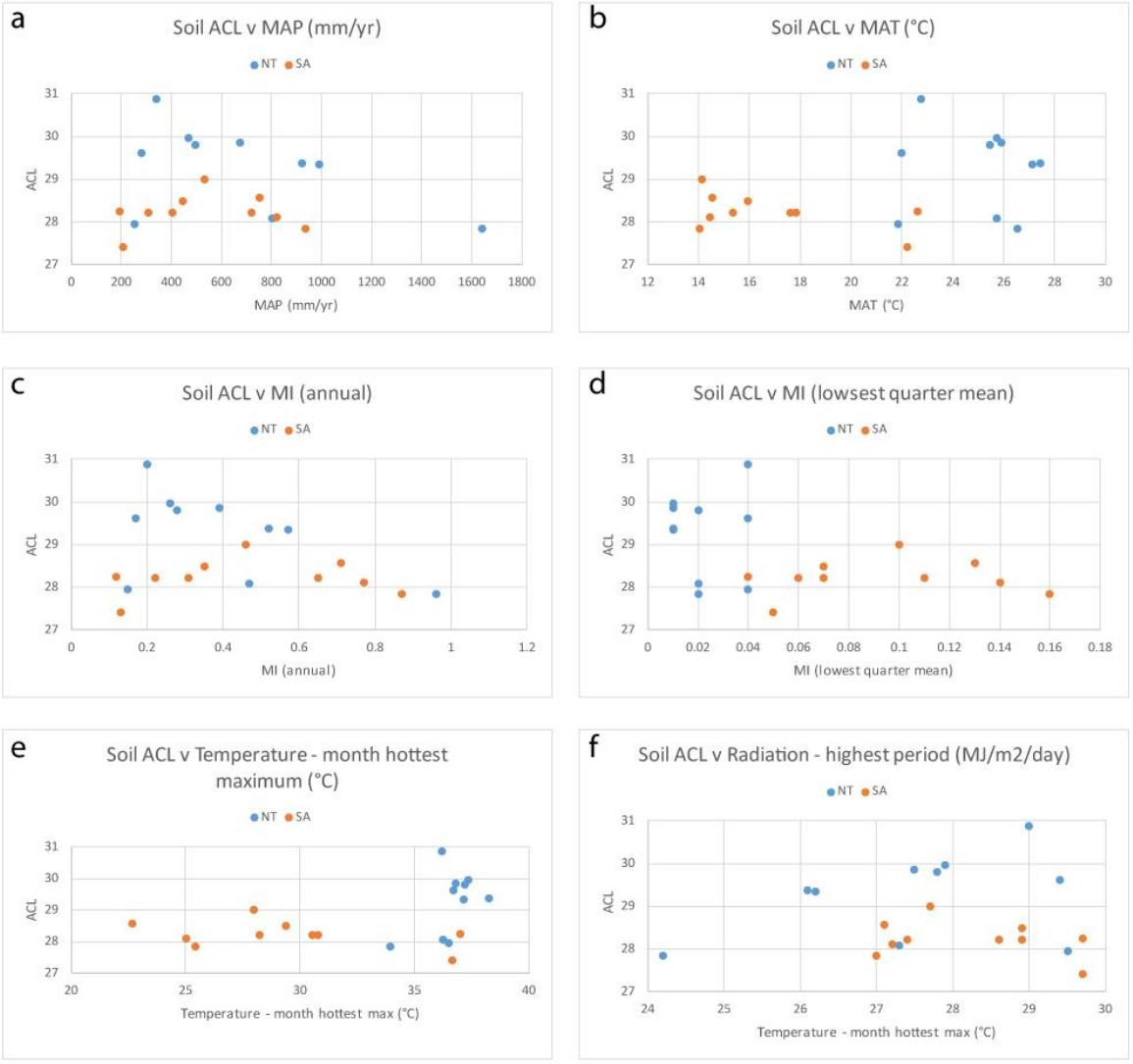

Supplementary Figure S6. Cross plots of Soil ACL against the different climate variables, a) MAP, b) MAT, c) Annual MI, d) Lowest quarter mean MI, e) Month hottest maximum temperature, and f) Highest period radiation. Blue points are Northern Territory, orange points are South Australia.

APPENDIX 2

Post-depositional modification of *n*-alkane signals in incubated soils

Howard, S.[a], McInerney, F.A.[a], Farrell, M.[b] & Hall, P.A.[a]

[a]*School of Physical Sciences, Department of Earth Science, Sprigg Geobiology Centre, University of Adelaide, Australia*

[b]*CSIRO Agriculture & Food, Locked Bag 2, Glen Osmond, SA 5064, Australia*

Supplementary Table

Supplementary Table S1. Soil leaf wax *n*-alkane data, including TOC, alkyl/o-alkyl ratio (A/OA), chain length quantification (µg *n*-alkane/mg soil), ACL and CPI.

					µg n-alkane/mg soil																								
Sample ID	Months Incubated	Sample Weight (mg)	TOC	A/OA	C15	C16	C17	C18	C19	C20	C21	C22	C23	C24	C25	C26	C27	C28	C29	C30	C31	C32	C33	C34	C35	Total (15-35) µg n-alkane/mg soil	ACL	CPI
C001	0	4177	32.01	0.2759	0.067222	1.896093	0.319820	1.768532	0.816872	0.621630	0.179411	0.224264	0.098653	0.072728	0.214972	0.072384	0.636658	0.147062	3.573772	0.218184	6.299241	0.149586	1.255420	0.050015	0.114369	18.797	30.3	18.7
C001	18	4043	22.04		0.013463	0.286145	0.023493	0.349762	0.015442	0.154951	0.014650	0.053586	0.032732	0.043159	0.091466	0.049495	0.248661	0.080775	1.570233	0.107172	2.958194	0.077740	0.450731	0.039464	0.079587	6.741	30.4	15.0
C004	0	5316	31.92	0.3135	0.083727	1.775906	0.285084	1.875143	0.902811	0.606266	0.163268	0.162032	0.094639	0.075560	0.110561	0.059364	0.257220	0.107473	2.069568	0.113375	3.285326	0.079129	0.343899	0.037609	0.068286	12.556	30.2	15.2
C004	18	5836	25.78		0.033408	0.489712	0.059939	0.447007	0.039002	0.183141	0.017233	0.070596	0.035978	0.043763	0.093800	0.051246	0.263639	0.085335	2.067843	0.109069	3.742797	0.085562	0.390470	0.037717	0.055101	8.402	30.3	17.7
C005	0	6080	33.97	1.1937	0.136597	2.431529	0.528776	2.249311	1.186848	0.811218	0.300318	0.281645	0.150137	0.148854	0.325142	0.173191	0.853520	0.286291	6.202742	0.363860	9.851341	0.391870	2.173734	0.155093	0.229077	29.231	30.4	14.1
C005	18	2206	25.90		0.017348	0.419424	0.000000	0.386026	0.001783	0.166992	0.011511	0.072309	0.031615	0.056583	0.085441	0.066472	0.163101	0.069066	0.946177	0.091440	1.381166	0.070201	0.233464	0.058690	0.078794	4.408	30.2	7.9
C008	0	5589	33.02	0.3976	0.109907	2.296609	0.448919	1.889466	1.045602	0.592575	0.191310	0.209133	0.082794	0.106241	0.138095	0.082920	0.367958	0.116038	2.651168	0.145616	4.202128	0.132533	0.653059	0.056502	0.135820	15.654	30.3	15.0
C008	18	2908	25.02		0.061407	0.445020	0.023720	0.395051	0.005659	0.179525	0.015894	0.075374	0.008428	0.057795	0.088980	0.022395	0.224557	0.075976	1.367208	0.100659	2.166100	0.076578	0.272960	0.050450	0.062972	5.777	30.2	12.6
C009	0	5834	33.65	0.1112	0.071237	1.468313	0.345695	2.130514	1.207985	0.744013	0.255506	0.318875	0.136213	0.158126	0.232071	0.151865	0.495699	0.206858	3.175212	0.230801	4.263143	0.177754	0.476070	0.085366	0.094503	16.426	30.0	10.1
C009	1	3632	30.07		0.000022	0.000094	0.000110	0.000176	0.000061	0.000182	0.000047	0.000088	0.000052	0.000063	0.000127	0.000091	0.000308	0.000105	0.002054	0.000113	0.002762	0.000066	0.000253	0.000047	0.000061	0.007	30.0	13.0
C009	3	7129	31.10		0.000008	0.000178	0.000476	0.000171	0.000159	0.000288	0.000128	0.000150	0.000265	0.000130	0.000276	0.000133	0.000487	0.000240	0.002939	0.000267	0.004079	0.000230	0.000554	0.000107	0.000105	0.011	30.1	8.4
C009	6	1675	31.35		0.000030	0.000101	0.000030	0.000101	0.000030	0.000096	0.000036	0.000048	0.000060	0.000060	0.000131	0.000090	0.000322	0.000107	0.002436	0.000131	0.003475	0.000090	0.000322	0.000036	0.000042	0.008	30.1	14.6
C009	12	4014	30.03		0.000017	0.000055	0.000017	0.000057	0.000022	0.000062	0.000030	0.000057	0.000037	0.000047	0.000115	0.000077	0.000296	0.000100	0.002270	0.000130	0.003206	0.000085	0.000316	0.000045	0.000062	0.007	30.1	14.2
C009	18	1170	24.14		0.000146	0.000500	0.000050	0.000826	0.000092	0.000451	0.000047	0.000191	0.000094	0.000153	0.181238	0.173412	0.325816	0.178766	1.609309	0.177943	2.264648	0.154052	0.307692	0.125631	0.156935	5.658	30.1	5.8
C046	0	5393	33.96	1.0581	0.110150	2.399986	0.457063	2.247204	1.374203	0.852299	0.284918	0.290387	0.034708	0.157581	0.180961	0.083701	0.471739	0.131020	3.343407	0.167179	5.156482	0.121143	0.493222	0.042297	0.063836	18.463	30.1	17.6
C046	18	2182	21.80		0.043267	0.121959	0.004314	0.267056	0.002222	0.132155	0.010457	0.052548	0.027581	0.045228	0.064574	0.042352	0.154769	0.065882	0.907309	0.084836	1.345343	0.054771	0.150979	0.041568	0.049019	3.668	30.1	9.0
C047	0	5196	34.50	0.3959	0.031088	1.228366	0.231430	1.526347	0.910236	0.625438	0.277256	0.221701	0.029361	0.079964	0.146515	0.066205	0.310416	0.104604	2.361109	0.114046	3.550731	0.101611	0.488249	0.031548	0.107368	12.544	30.2	16.4
C047	1	3828	31.54		0.000018	0.000071	0.000097	0.000136	0.000039	0.000165	0.000044	0.000086	0.000047	0.000031	0.000086	0.000047	0.000253	0.000063	0.001907	0.000073	0.002618	0.000063	0.000293	0.000052	0.000094	0.006	30.2	17.3
C047	3	8491	31.90		0.000008	0.000240	0.000910	0.000183	0.000221	0.000291	0.000120	0.000148	0.000170	0.000060	0.000143	0.000054	0.000317	0.000104	0.001975	0.000177	0.002774	0.000201	0.000455	0.000062	0.000137	0.009	30.2	9.5
C047	6	2800	30.66		0.000021	0.000082	0.000129	0.000096	0.000032	0.000075	0.000029	0.000043	0.000036	0.000036	0.000079	0.000039	0.000225	0.000064	0.001543	0.000057	0.002268	0.000043	0.000254	0.000057	0.000043	0.005	30.1	16.7
C047	12	3644	30.70		0.000019	0.000093	0.000022	0.000085	0.000022	0.000066	0.000027	0.000049	0.000038	0.000055	0.000121	0.000058	0.000269	0.000085	0.001951	0.000104	0.002763	0.000063	0.000340	0.000066	0.000085	0.006	30.2	14.4
C047	18	1795	16.35		0.000000	0.000566	0.000009	0.000564	0.000016	0.000310	0.000017	0.000106	0.000019	0.000075	0.120121	0.078167	0.276454	0.113055	1.899406	0.153904	3.124679	0.125862	0.424176	0.065801	0.133369	6.517	30.3	10.9
C049	0	7231	32.88	0.5422	0.015214	0.752586	0.171932	1.353139	0.887721	0.516166	0.263742	0.219943	0.094863	0.107971	0.150665	0.071016	0.311595	0.090494	2.427374	0.134766	3.799569	0.092231	0.431989	0.036640	0.079175	12.009	30.2	16.7
C049	18	2517	16.50		0.000000	0.275989	0.000000	0.408422	0.006506	0.211976	0.014691	0.079544	0.045334	0.056877	0.124038	0.074926	0.275779	0.106828	1.752898	0.053099	2.838595	0.091297	0.361829	0.073457	0.104099	6.956	30.2	13.4
C053	0	4953	33.52	0.1203	0.073735	2.515589	0.562821	2.830295	1.738252	1.062548	0.436634	0.349292	0.132952	0.116228	0.180461	0.087494	0.433518	0.112123	3.154882	0.165334	4.868961	0.098516	0.513866	0.041581	0.096692	19.572	30.2	18.0
C053	18	2299	15.79		0.001621	0.635218	0.024018	0.577015	0.043762	0.272447	0.025933	0.102260	0.045973	0.062328	0.125688	0.066159	0.311347	0.116405	2.409879	0.124509	3.659244	0.106680	0.443665	0.063802	0.095776	9.314	30.2	14.5
C054	0	7493	30.85	0.7761	0.059259	1.626578	0.338419	1.727277	0.977701	0.580800	0.188376	0.178736	0.076529	0.065838	0.035044	0.047060	0.260611	0.063736	1.652667	0.092292	2.698490	0.065107	0.293598	0.023987	0.043633	11.096	30.2	16.9
C054	18	2069	25.15		0.031868	0.379997	0.010381	0.567340	0.049974	0.300328	0.027039	0.096086	0.042973	0.078703	0.108640	0.077496	0.231523	0.100190	1.248148	0.103570	1.948511	0.083532	0.232489	0.071702	0.098017	5.889	30.2	8.6
C063	0	5348	33.00	0.1941	0.099429	1.581959	0.278367	1.481503	0.671916	0.495832	0.156678	0.284017	0.236129	0.285844	0.414040	0.430707	0.678765	0.493092	2.083613	0.437385	2.519457	0.325684	0.456391	0.161472	0.129680	13.702	29.7	3.3
C063	18	2360	27.58		0.046017	1.483365	0.039420	1.062777	0.059994	0.331853	0.034238	0.140405	0.108681	0.138992	0.199771	0.215320	0.472101	0.269032	2.272085	0.336093	3.493485	0.310180	0.595702	0.208566	0.230240	12.048	30.2	5.3
Chromosol	0	5640	20.45	0.5702	0.020408	0.000230	0.010588	0.074421	0.012199	0.056161	0.021943	0.007058	0.038591	0.040509	0.137333	0.053399	0.368804	0.091376	3.228700	0.152600	4.578703	0.078103	0.392971	0.029998	0.054856	9.449	30.1	21.4
Chromosol	18	2963	27.86		0.006821	0.682823	0.030693	0.573187	0.052797	0.222555	0.021346	0.079069	0.037008	0.045976	0.084374	0.051407	0.272573	0.083616	1.803935	0.122014	3.154929	0.091447	0.369073	0.046229	0.082858	7.915	30.3	14.4
Chromosol	18	3237	24.20		0.010298	0.355414	0.012063	0.316872	0.028539	0.133280	0.015495	0.064237	0.026774	0.043348	0.065610	0.047859	0.162800	0.066003	1.205702	0.085617	1.892405	0.064041	0.202716	0.034227	0.054626	4.888	30.2	11.8
Chromosol	18	2378	22.22		0.085578	0.333861	0.004766	0.420738	0.011699	0.242867	0.014732	0.089911	0.043330	0.069112	0.101176	0.073878	0.245467	0.096627	1.721733	0.117209	2.798493	0.093377	0.278831	0.066512	0.082544	6.992	30.2	11.5

APPENDIX 3

Vegetation and climate change 70,000 to 17,000 years ago from leaf wax *n*-alkanes preserved in Blanche Cave sediments, Naracoorte, South Australia

Howard, S.[a], McInerney, F.A.[a,] Arnold, L.J.[a], Grice, K.[b], Holman, A.I.[b], Hall, P.A.[a] & Reed, E.H.[a].

[a]*School of Physical Sciences, Department of Earth Science, Sprigg Geobiology Centre, University of Adelaide, Australia*

[b]*Western Australian Organic and Isotope Geochemistry Centre, The Institute for Geoscience Research, School of Earth and Planetary Sciences, Curtin University, Australia*

Supplementary Tables and Figures

Supplementary Table S1. Blanche Cave leaf wax *n*-alkane data, including age data, chain length quantification (n-alk ug/dry sample mg), ACL, $\delta^{13}C$ for C_{29} and C_{31}, isotopic divergence and δD values.

					n-alk ug/dry sample mg																	
Layer Number	Dating Method	Start Age	End Age	MIS	C25	C26	C27	C28	C29	C30	C31	C32	C33	C34	C35	ACL	d13C C29	SD d13C C29	d13C C31	SD d13C C31	Isotopic Divergence (d13C C31 - d13C C29)	dD C31	SD dD C31
18	Radiocarbon	17.235	20.535	MIS2	2.18E-05	1.3E-05	4.31E-05	1.5E-05	0.000141	1.43E-05	0.000315	1.01E-05	0.000141	0	1.19E-05	30.62	-32.03	0.38	-29.84	0.38	2.19	-135.89	2.22
19	Radiocarbon	20.405	24.768	MIS2	3.35E-05	2.27E-05	7.56E-05	2.35E-05	0.000228	2.42E-05	0.000446	1.32E-05	0.000182	0	2.13E-05	30.48	-32.10	0.10	-29.37	0.05	2.74	-132.59	1.88
20	Radiocarbon	23.009	28.838	MIS2	4.05E-05	1.81E-05	9.15E-05	2.73E-05	0.000275	2.77E-05	0.000486	1.64E-05	0.000193	0	2.9E-05	30.41	-31.78	0.04	-28.84	0.21	2.95	-129.13	1.04
21	Radiocarbon	24.249	32.348	MIS2	3.42E-05	2.21E-05	5.87E-05	2.13E-05	0.000159	1.82E-05	0.000306	9.44E-06	0.000141	0	1.94E-05	30.44	-31.96	0.11	-29.34	0.36	2.61	-134.99	1.51
22	Radiocarbon	24.345	32.231	MIS2	2.36E-05	1.69E-05	3.75E-05	1.37E-05	9.72E-05	1.23E-05	0.00024	7.2E-06	0.000132	0	1.57E-05	30.71	-31.90	0.08	-29.78	0.29	2.12	-131.44	0.67
23	Radiocarbon	27.098	31.931	MIS2	9.73E-06	7.75E-06	1.3E-05	5.29E-06	2.85E-05	4.8E-06	7.93E-05	5.11E-06	6.94E-05	0	1.43E-05	31.13	-32.54	0.22	-31.34	0.04	1.20	-134.23	0.63
24	Radiocarbon	31.66	33.656	MIS3	2.61E-05	1.66E-05	4.3E-05	1.36E-05	0.000112	1.44E-05	0.000292	1.58E-05	0.000224	0	2.31E-05	30.98	-32.81	0.19	-32.70	0.21	0.11	-130.02	0.45
25	Radiocarbon	32.402	40.131	MIS3	1.08E-05	7.76E-06	2.15E-05	7.31E-06	5.63E-05	8.34E-06	0.000142	5.37E-06	8.74E-05	0	1.15E-05	30.87	-32.84	0.08	-32.65	0.06	0.19	-136.66	0.72
26	Radiocarbon	35.836	46.473	MIS3	3.32E-05	2.25E-05	7.8E-05	2.36E-05	0.000218	2.5E-05	0.00045	2.33E-05	0.000325	0	3.44E-05	30.86	-34.76	0.61	-34.17	0.42	0.58	-146.32	0.33
27	Radiocarbon	41.7	59.997	MIS3	3.81E-06	3.43E-06	6.1E-06	3.11E-06	1.22E-05	2.29E-06	2.62E-05	0	1.57E-05	0	0	30.37	-32.02	0.25	-32.19	0.05	-0.17	-165.20	0.82
28				MIS3	8.44E-06	5.88E-06	1.59E-05	6.39E-06	4.12E-05	5.95E-06	0.000103	3.64E-06	5.19E-05	0	0	30.58	-32.52	0.20	-31.18	0.14	1.34	-142.68	3.23
29				MIS3	9.46E-06	6.37E-06	1.41E-05	5.8E-06	3.11E-05	4.6E-06	6.82E-05	3.66E-06	3.75E-05	0	0	30.37	-31.93	0.58	-30.40	0.05	1.53	-133.71	1.57
30	OSL	57.6	64.4	MIS4	1.16E-05	7.22E-06	1.85E-05	6.41E-06	4.79E-05	6.16E-06	0.00011	3.99E-06	5.07E-05	0	0	30.42	-31.65	0.18	-30.41	0.18	1.24	-140.16	1.74
31				MIS4	4.37E-06	3.31E-06	5.06E-06	2.5E-06	9.62E-06	2.94E-06	2.47E-05	0	1.3E-05	0	0	30.30			-29.21	0.41		-159.32	0.86
32				MIS4	8.63E-06	5.1E-06	1.36E-05	4.66E-06	3.53E-05	4.78E-06	0.000109	4.53E-06	3.38E-05	0	0	30.46	-31.48	0.13	-29.22	0.20	2.26	-132.73	1.17
33				MIS4	1.15E-05	5.19E-06	2.14E-05	6.56E-06	6.12E-05	7.21E-06	0.00021	7.47E-06	8.23E-05	0	1.12E-05	30.83	-31.66	0.53	-29.24	0.13	2.42	-150.33	2.06
34				MIS4	7.84E-06	4.79E-06	1.31E-05	4.42E-06	3.68E-05	5.48E-06	0.000122	3.11E-06	6.08E-05	0	0	30.79	-31.83	0.38	-30.13	0.11	1.70	-149.96	1.29
35	OSL	63.9	71.5	MIS4	1.53E-05	9.17E-06	2.94E-05	8.85E-06	7.25E-05	8.98E-06	0.000179	5.19E-06	7.02E-05	0	1.71E-05	30.62	-31.75	0.00	-30.65	0.17	1.10	-144.18	1.04
36				MIS4	1.66E-05	8.79E-06	2.97E-05	8.29E-06	7.79E-05	8.66E-06	0.000195	4.92E-06	7.39E-05	0	9.6E-06	30.53	-31.76	0.16	-30.33	0.16	1.43	-136.05	0.18
37				MIS4	1.48E-05	9.14E-06	3.01E-05	1.14E-05	8.36E-05	7.16E-06	0.000192	5.11E-06	7.19E-05	0	1.1E-05	30.53	-32.10	0.05	-30.41	0.18	1.69	-138.90	2.16
38	OSL	61.1	67.5	MIS4	3.8E-06	3.23E-06	5.57E-06	2.72E-06	1.4E-05	2.47E-06	2.89E-05	0	1.31E-05	0	0	30.28						-153.93	3.12
39	OSL	63.4	70.6	MIS4	4.09E-06	2.67E-06	6.69E-06	2.17E-06	1.76E-05	2.91E-06	4.62E-05	0	1.65E-05	0	0	30.41	-31.41	0.06	-28.45	0.23	2.96	-144.61	0.98
40	OSL	63.4	70.6	MIS4	1.76E-05	9.59E-06	4.26E-05	1.23E-05	0.000121	1.22E-05	0.000307	5.87E-06	7.94E-05	0	1.13E-05	30.46	-31.21	0.13	-28.35	0.07	2.85	-133.68	0.79

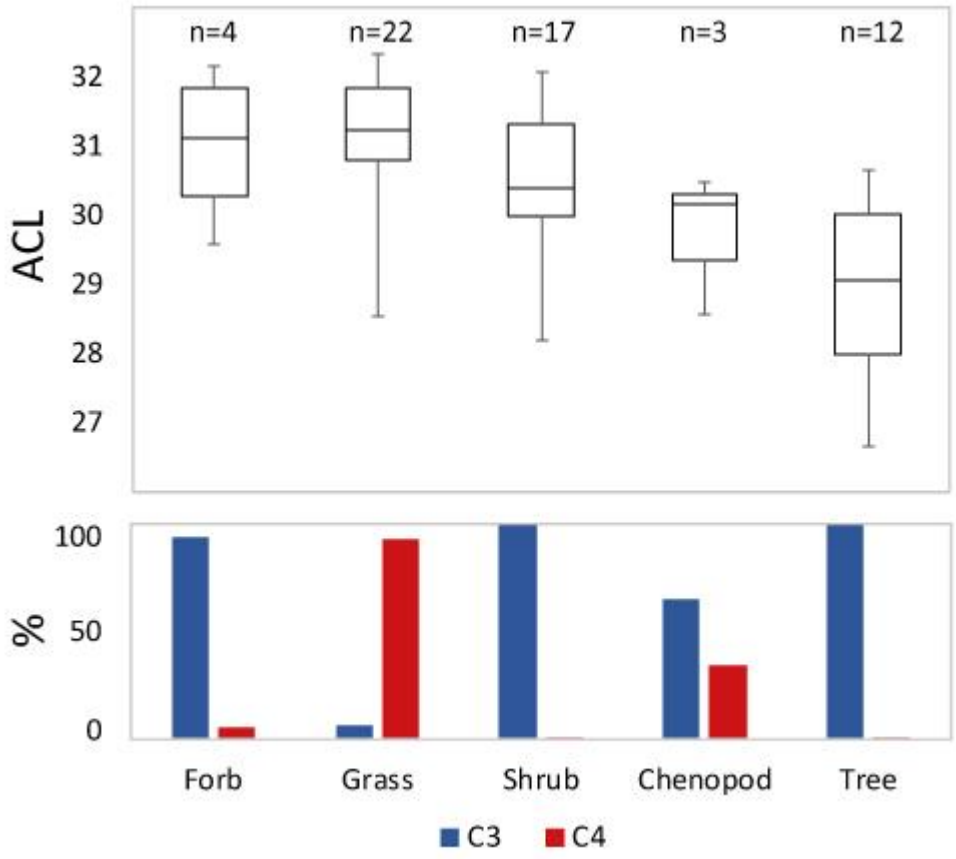

Supplementary Figure S1. (Top) Boxplot showing the average chain length (ACL) of different plant growth forms from *n*-alkane analysis in plants from a latitudinal transect across Australia (Howard et al. 2018) and (Bottom) the percent C3 versus C4 vegetation of different plant growth forms in Australia compiled from the TERN AEKOS data portal (Osborne et al. 2014, The ÆKOS Data Contributors 2014) using the TRY, Sevilleta LTER, TREND, SWATT and NECT transects (Kattge et al. 2011, Prentice et al. 2011, Osborne et al. 2014, Lowrey 2015, Caddy-Retalic 2017).

References

CADDY-RETALIC S. 2017 Quantifying responses of ecological communities to bioclimatic gradients. Faculty of Sciences. University of Adelaide.

HOWARD S., MCINERNEY F. A., CADDY-RETALIC S., HALL P. A. & ANDRAE J. W. 2018. Modelling leaf wax n-alkane inputs to soils along a latitudinal transect across Australia, *Organic Geochemistry*. **121**, 126-137.

KATTGE J., DÍAZ S., LAVOREL S., PRENTICE I. C., LEADLEY P., BÖNISCH G., GARNIER E., WESTOBY M., REICH P. B., WRIGHT I. J., CORNELISSEN J. H. C., VIOLLE C., HARRISON S. P., VAN BODEGOM P. M., REICHSTEIN M., ENQUIST B. J., SOUDZILOVSKAIA N. A., ACKERLY D. D., ANAND M., ATKIN O., BAHN M., BAKER T. R., BALDOCCHI D., BEKKER R., BLANCO C. C., BLONDER B., BOND W. J., BRADSTOCK R., BUNKER D. E., CASANOVES F., CAVENDER-BARES J., CHAMBERS J. Q., CHAPIN III F. S., CHAVE J., COOMES D., CORNWELL W. K., CRAINE J. M., DOBRIN B. H., DUARTE L., DURKA W., ELSER J., ESSER G., ESTIARTE M., FAGAN W. F., FANG J., FERNÁNDEZ-MÉNDEZ F., FIDELIS A., FINEGAN B., FLORES O., FORD H., FRANK D., FRESCHET G. T., FYLLAS N. M., GALLAGHER R. V., GREEN W. A., GUTIERREZ A. G., HICKLER T., HIGGINS S. I., HODGSON J. G., JALILI A., JANSEN S., JOLY C. A., KERKHOFF A. J., KIRKUP D., KITAJIMA K., KLEYER M., KLOTZ S., KNOPS J. M. H., KRAMER K., KÜHN I., KOROKAWA H., LAUGHLIN D., LEE T. D., LEISHMAN M., LENS F., LENZ T., LEWIS S. L., LLOYD J., LLUSIÀ J., LOUAULT F., MA S., MAHECHA M. D., MANNING P., MASSAD T., MEDLYN B. E., MESSIER J., MOLES A. T., MÜLLER S. C., NADROWSKI K., NAEEM S., NIINEMETS Ü., NÖLLERT S., NÜSKE A., OGAYA R., OLEKSYN J., ONIPCHENKO V. G., ONODA Y., ORDOÑEZ J., OVERBECK G., OZINGA W. A., PATIÑO S., PAULA S., PAUSAS J. G., PEÑUELAS J., PHILLIPS O. L., PILLAR V., POORTER H., POORTER L., POSCHLOD P., PRINZING A., PROULX R., RAMMIG A., REINSCH S., REU B., SACK L., SALGADO-NEGRET B., SARDANS J., SHIODERA S., SHIPLEY B., SIEFERT A., SOSINSKI E., SOUSSANA J.-F., SWAINE E., SWENSON N., THOMPSON K., THORNTON P., WALDRAM M., WEIHER E., WHITE M., WHITE S., WRIGHT S. J., YGUEL B., ZAEHLE S., ZANNE A. E. & WIRTH C. 2011. TRY – a global database of plant traits, *Global Change Biology*. **17**, 2905-2935.

LOWREY T. 2015. Master plant species information database for the Sevilleta National Wildlife Refuge, New Mexico (1989-1996) <http://sev.lternet.edu/data/sev-51>. (retrieved.

OSBORNE C. P., SALOMAA A., KLUYVER T. A., VISSER V., KELLOGG E. A., MORRONE O., VORONTSOVA M. S., CLAYTON W. D. & SIMPSON D. A. 2014. A global database of C4 photosynthesis in grasses, *New Phytologist*. **204**, 441-446.

PRENTICE I. C., MENG T., WANG H., HARRISON S. P., NI J. & WANG G. 2011. Evidence of a universal scaling relationship for leaf CO2 drawdown along an aridity gradient, *New Phytologist*. **190**, 169-180.

THE ÆKOS DATA CONTRIBUTORS 2014. A derivative of multiple ecological plot databases for the Advanced Ecological Knowledge and Observation System (ÆKOS) <http://www.portal.aekos.org.au/>. (retrieved 01/02/2017).

APPENDIX 4

AGU100 ADVANCING EARTH AND SPACE SCIENCE

Geophysical Research Letters

RESEARCH LETTER
10.1029/2018GL077833

Key Points:
- Carbon isotope ratios of plant waxes reveal the onset of C_4 expansion during the late Pliocene in Australia, later than other geographic regions
- Palynological analysis reveals increasingly open landscapes in the lead-up to C_4 expansion
- Northern Australian monsoon initiation linked to East Asian winter monsoon intensification is hypothesized as a driver

Supporting Information:
- Supporting Information S1
- Data Set S1
- Data Set S2
- Data Set S3
- Data Set S4
- Data Set S5

Correspondence to:
J. W. Andrae,
jake.andrae@adelaide.edu.au

Citation:
Andrae, J. W., McInerney, F. A., Polissar, P. J., Sniderman, J. M. K., Howard, S., Hall, P. A., & Phelps, S. R. (2018). Initial expansion of C_4 vegetation in Australia during the late Pliocene. *Geophysical Research Letters, 45*, 4831–4840. https://doi.org/10.1029/2018GL077833

Received 7 MAR 2018
Accepted 26 APR 2018
Accepted article online 2 MAY 2018
Published online 17 MAY 2018

Initial Expansion of C_4 Vegetation in Australia During the Late Pliocene

J. W. Andrae[1,2], F. A. McInerney[1,2], P. J. Polissar[3], J. M. K. Sniderman[4], S. Howard[1,2], P. A. Hall[1,2], and S. R. Phelps[3,5]

[1]Department of Earth Sciences, School of Physical Sciences, University of Adelaide, Adelaide, South Australia, Australia, [2]Sprigg Geobiology Centre, University of Adelaide, Adelaide, South Australia, Australia, [3]Biology and Paleo Environment, Lamont-Doherty Earth Observatory, Columbia University, Palisades, NY, USA, [4]School of Earth Sciences, University of Melbourne, Parkville, Victoria, Australia, [5]Department of Earth and Environmental Sciences, Columbia University, New York, NY, USA

Abstract Since the late Miocene, plants using the C_4 photosynthetic pathway have increased to become major components of many tropical and subtropical ecosystems. However, the drivers for this expansion remain under debate, in part because of the varied histories of C_4 vegetation on different continents. Australia hosts the highest dominance of C_4 vegetation of all continents, but little is known about the history of C_4 vegetation there. Carbon isotope ratios of plant waxes from scientific ocean drilling sediments off north-western Australia reveal the onset of Australian C_4 expansion at ~3.5 Ma, later than in many other regions. Pollen analysis from the same sediments reveals increasingly open C_3-dominated biomes preceding the shift to open C_4-dominated biomes by several million years. We hypothesize that the development of a summer monsoon climate beginning in the late Pliocene promoted a highly seasonal precipitation regime favorable to the expansion of C_4 vegetation.

Plain Language Summary This study documents for the first time that C_4 vegetation initially expanded on the Australian continent in the late Pliocene, several million years later than in Asia, Africa, North America, and South America. The expansion of C_4 plants displaced C_3 open habitat vegetation. Understanding the timing and sequence of expansion of C_4-dominated biomes enables us to better constrain the key environmental and evolutionary factors in their development and provides a basis for future conservation of these widespread and important biomes.

1. Introduction

Vegetation utilizing the C_4 photosynthetic pathway is an important component of modern ecosystems globally, comprising ~23% of global gross primary productivity (Still et al., 2003). Biomes dominated by C_4 plants are mainly "open" habitats, that is, with sparse tree canopy density. Australia has the highest proportional area dominated by C_4 vegetation of all continents (Murphy & Bowman, 2007; Still et al., 2003). The majority of the continent is dominated by C_4 rather than C_3 grasses, and the relative abundance of C_4 species within grass communities is closely related to seasonal water availability (Murphy & Bowman, 2007). Survey data on modern Australian vegetation compiled in this study further support a close association between warm-season precipitation and C_4 dominance (Figure 1 and Text S1.1 in the supporting information). Australian biomes with significant C_4 taxa include arid and tropical to subtropical grasslands and savannas, dominating in the north, and chenopod shrublands, dominating in the south (Hattersley, 1983; Leigh, 1994; Murphy & Bowman, 2007).

On many continents, C_4 vegetation began to proliferate by the late Miocene, with this expansion recorded as shifts in carbon isotope ratios of plant-fixed carbon stored within a wide range of terrestrial and marine sediments and paleosols, as well as in fossil tooth enamel (Cerling et al., 1997; Strömberg, 2011; Tipple & Pagani, 2007). C_4 expansion on these continents occurred as the final stage in what has been inferred as a stepwise progression of ecosystem transformation in which C_3 forest transitioned to C_3 open landscapes, and then to C_4 open landscapes (Cerling et al., 1997; Edwards et al., 2010; Strömberg, 2011).

Despite being the most C_4-dominated continent today, little is known about the timing and pattern of C_4 expansion in Australia. Evidence exists for open habitat vegetation increasing in abundance in the late Miocene (e.g., Locker & Martini, 1986; Macphail, 1997; Martin, 2006; Martin & McMinn, 1994; Sniderman et al., 2016). However, it is unknown whether late Miocene Australian grasses and chenopods employed

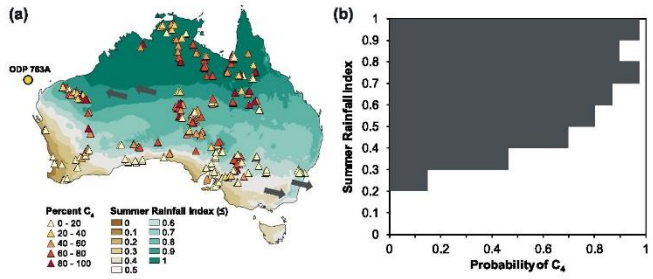

Figure 1. Study site in the context of modern Australian C_4 vegetation and climate. (a) Location of ODP 763A, with mapped Summer Rainfall Index (SRI) and surveyed percent C_4 plant cover (Kattge et al., 2011; Lowrey, 2015; Osborne et al., 2014; White et al., 2012, see Text S1.1 in the supporting information for details). SRI calculated as the proportion of summer rainfall (December, January, and February) out of summed summer (December, January, and February) and winter (June, July, and August) rainfall (Australian Government Bureau of Meteorology, 2016). The arrows indicate modern dust transport pathways (Hesse & McTainsh, 2003). (b) The probability that C_4 vegetation is present for a given range of SRI based on survey data.

the C_3 or C_4 photosynthetic pathway. Reconstructing changes in the dominant photosynthetic pathway has been limited by the spatial and temporal discontinuity of Australian terrestrial geological records (Kershaw et al., 1994; Macphail, 1997). In this paper, we present ~10 Myr records of plant wax *n*-alkane carbon isotopes and pollen abundances from sediments of Ocean Drilling Program (ODP) Hole 763A (hereafter ODP 763A), off north-western Australia, to determine when, how, and why C_4 vegetation expanded on the Australian continent.

2. Materials and Methods

2.1. ODP 763A Sample Preparation

Samples constitute 26 portions of foraminifera to nanno-fossil ooze or foraminifera-bearing nanno-fossil chalk (Haq et al., 1990) from ODP 763A (collected August 1988). To minimize contamination, 0.5 cm of all exposed faces of the samples was removed and all tools and equipment were thoroughly cleaned (washed with dilute Decon 90® decontaminant solution followed by three rinses of reverse osmosis water, and three rinses each of methanol, dichloromethane [DCM], and *n*-hexane). Samples were lyophilized in ashed borosilicate glass containers, prior to homogenization using a mortar and pestle. Total lipids were extracted from 9.5 to 18.9 g of each sample (mean: 13.9 g) using a Thermo Scientific™ Dionex™ ASE™ 350. Samples underwent five cycles of solvent rinse (5-min static rinse with 9:1 DCM:methanol) and purge (2 min) at a temperature of 100 °C and a pressure of ~11,000 kPa. Solvents were evaporated from the total lipid extract under N_2 on a FlexiVap™ heated evaporator. Nonpolar and polar components were separated by solid phase extraction through ~0.5 g of solvent-cleaned activated silica gel of 0.035 to 0.070 mm mesh size using 4 ml of *n*-hexane and 4 ml 1:1 DCM:methanol, respectively. Elemental sulfur was removed using copper shavings activated in hydrochloric acid.

2.2. Biomarker Quantitation and Compound-Specific Carbon Isotope Analysis

n-Alkanes (C_{16} to C_{35}) were characterized and quantified on a Perkin Elmer Clarus 580 gas chromatograph-mass spectrometer (GC-MS) fitted with a PE Elite 5MS capillary column. Samples were dissolved in 100 μl *n*-hexane with 1 μg/ml 1-1′ binaphthyl as internal standard. Quantitation standards were prepared by dilution of a Certified Reference Material (C_7-C_{40} Saturated Alkanes Standard, Supelco 49452-U) with 1-1′ binaphthyl as internal standard for concurrent analysis with the sample batch (see Text S1.2 in the supporting information for full GC-MS instrument setup specifications).

Compound-specific $\delta^{13}C$ measurements were performed for *n*-alkanes (C_{25}-C_{35}) using a Thermo Delta V isotope ratio MS coupled to a Thermo Trace GC Ultra and Isolink through a ConFlo IV interface. Samples were injected into a PTV injector with 2 mm i.d. silicosteel liner packed with glass wool. The inlet was held

splitless at 60 °C during injection and then ramped ballistically to 320 °C where it was held for 1.5 min during the transfer phase. Compounds were separated on an HP-5MS column (30 m length, 0.25 mm i.d., and 0.25 μm phase thickness) with a constant helium flow of 1.0 ml/min. The GC oven was held at 60 °C for 1.5 min, ramped at 15 °C/min to 150 °C and then at 4 °C/min to 320 °C, and held for 10 min. The GC effluent was connected to a custom-made combustion reactor consisting of 1 strand each of 0.1 mm nickel, copper, and platinum wires inside a 0.5 mm i.d. fused alumina tube held at 1000 °C. Continued oxidation and complete combustion of compounds were ensured with the introduction of a trickle of 1% O_2 in helium. Water was removed from the combustion effluent with a custom-built cryotrap consisting of a 20-cm loop of 0.25 mm i.d. deactivated fused silica capillary immersed in an ethanol bath at −85 °C. The trap was periodically thawed and purged to prevent plugging from the buildup of ice. Standard mixtures of *n*-alkanes with known $\delta^{13}C$ values (Mixes B4 and A5 purchased from Arndt Schimmelmann, Indiana University) were interspersed between sample measurements to calibrate the isotopic measurements. Measurement uncertainties (standard error of the mean), including both analytical uncertainty and uncertainty in realizing the Vienna Pee Dee Belemnite reporting scale, were calculated after Polissar and D'Andrea (2014).

2.3. ODP 763A Age Model

Sample ages were calculated using linear interpolations between tie-points in an age-depth model established in Karas et al. (2011), complemented by paleomagnetic reversal event datum tie-points established in Tang (1992) and updated to Hilgen et al. (2012). See Data Set S4 in the supporting information.

2.4. Adjustment for Preindustrial Atmospheric $\delta^{13}C$ and Modeling Percent C_4

The sedimentary *n*-alkane $\delta^{13}C$ values were normalized to preindustrial atmospheric CO_2 $\delta^{13}C$ by applying the offset between $\delta^{13}C$ of atmospheric CO_2 for a given sample age estimated from a 3 Myr moving average benthic foraminifera record and $\delta^{13}C$ of atmospheric CO_2 of −6.5‰ (Tipple et al., 2010; Uno et al., 2016). Fraction of C_4 vegetation was calculated from the carbon isotopic composition of C_{31} in the sediments using a linear two end-member mixing model incorporating the mean carbon isotopic composition of C_{31} in a calibration set of modern C_3 (n = 106) and C_4 (n = 45) plants, also normalized to preindustrial atmospheric CO_2 $\delta^{13}C$ of −6.5‰ (Garcin et al., 2014). The C_{31} alkane was used to minimize plant wax production biases related to plant functional type (Garcin et al., 2014).

2.5. Pollen

Fossil pollen was extracted from 12 sample splits using palynological methods adapted from Moore et al. (1991). Samples were digested in cold HCl, followed by treatment with hot 10% KOH, acetolysis (a 9:1 mixture of acetic anhydride and concentrated sulfuric acid), and overnight immersion in concentrated HF, followed by heavy liquid separation using a Na-polytungstate liquid of specific gravity 2.0 (Munsterman & Kerstholt, 1996). The acid- and alkali-resistant residues were then dehydrated in ethanol and mounted on glass slides in glycerol. Pollen was counted along transects at 300X and 600X magnification on a Zeiss AxioScope A.1 with EC Plan Neofluar objectives, until at least 100 pollen grains were counted. Pollen was identified by comparison with modern reference collections and with images stored in the Australasian Pollen and Spore Atlas (APSA Members, 2007).

3. Results

3.1. Plant Wax *n*-Alkane Distributions and Carbon Isotope Ratios

Sedimentary *n*-alkanes in samples from 8.8 to 1.0 Ma display unimodal homolog distributions, peaking at C_{29}, C_{31}, or C_{33}, with a strong odd-over-even predominance (carbon preference index > 2; Data Set S1 in the supporting information) that is indicative of a higher plant origin (Bush & McInerney, 2013). The oldest sample, at 9.5 Ma, has a bimodal distribution with peaks at C_{26} and C_{29} and a weak odd-over-even predominance (carbon preference index < 2; Data Set S1 in the supporting information), suggestive of petrogenic hydrocarbons from unknown sources that obscure plant-derived $\delta^{13}C$ and chain-length distributions. Thus, we disregard the oldest sample as it is likely not of terrestrial plant origin. The proportional abundance of C_{33} compared to C_{29} *n*-alkanes increases significantly throughout the record (Figure 2 and Data Set S1 in the supporting information).

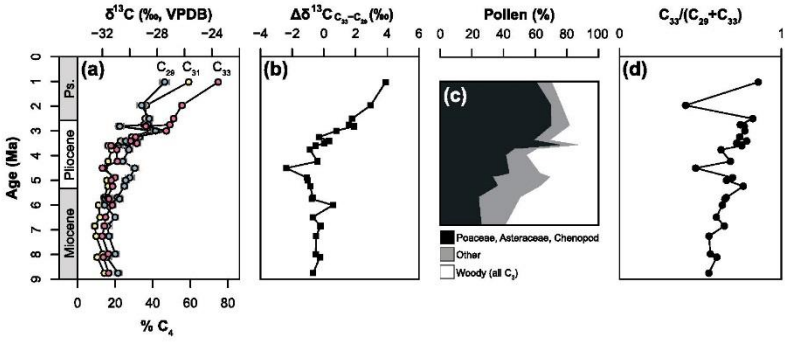

Figure 2. Organic geochemical and palynological data derived from sediments of ODP 763A. (a) Compound specific carbon isotope ratios of *n*-alkane homologs: C_{29} (blue), C_{31} (yellow), and C_{33} (pink), with percent C_4 based on the C_{31} homolog. The error bars represent plus and minus one standard error of the mean. (b) The difference between the carbon isotope ratio of C_{33} and that of C_{29}. (c) Grouped pollen percentages indicating relative proportions of herbaceous, woody, and other taxa. (d) The proportional concentration of C_{33} relative to C_{29} + C_{33}.

From 8.8 to 3.6 Ma, carbon isotope ratios of C_{29}, C_{31}, and C_{33} are stable with values indicative of predominantly C_3 vegetation. Beginning at 3.5 Ma, $\delta^{13}C$ values progressively increase, becoming more enriched in ^{13}C (Figure 2 and Data Set S1 in the supporting information). In addition, at 3.5 Ma, the $\delta^{13}C$ values of C_{29}, C_{31}, and C_{33} *n*-alkanes begin to diverge, causing an increasing difference between $\delta^{13}C$ values of C_{33} and C_{29} after that time (Figure 2 and Data Set S1 in the supporting information). The fraction of the source vegetation that is C_4 plants is estimated from the carbon isotopic composition of the sedimentary C_{31} *n*-alkane (Figures 2 and 3). Estimated C_4 fraction from 8.8 to 3.6 Ma is low, ranging from $9.2^{+27.5}_{-9.2}$ % to $19.2^{+26.5}_{-19.2}$ % (modern plant end-member 1-sigma calculation uncertainty). At ~3.5 Ma, the estimated C_4 fraction begins progressively increasing, save for one sample at 2.8 Ma. Percent C_4 reaches a maximum of 59.2 ± 22.4% at 1.0 Ma (Figures 2 and 3 and Data Set S1 in the supporting information). It must be noted that the uncertainties in calculations of fraction C_4 vegetation are likely overestimated, due to the geographically and climatically broad modern plant calibration set used (Garcin et al., 2014). Variability in the isotopic composition of the C_{31} *n*-alkane in modern C_3 and C_4 plant end-members from any one region is likely to be less than the calibration set.

3.2. Palynological Results

Pollen analysis was undertaken on samples ranging in age from 6.8 to 1.0 Ma, and results are presented as a summary pollen percentage diagram (Figure 2). During the latest Miocene, Gyrostemonaceae, Casuarinaceae, *Acacia*, and *Dodonaea* are important components of the pollen sum. Poaceae, Asteraceae, and *Eucalyptus* pollen are also present in substantial proportions during the latest Miocene. Across the Miocene-Pliocene boundary, values of Gyrostemonaceae, Casuarinaceae, *Acacia*, and *Dodonaea* decline, while those for Restionaceae, indeterminate Myrtaceae pollen, Cyperaceae, and ferns (Polypodiaceae and *Cyathea*) increase steadily until collapsing at ~4.9 Ma. Poaceae, Asteraceae, and chenopods maintain steady or increasing values through the Early Pliocene. Around the early-late Pliocene boundary (3.5–3.6 Ma), the vegetation becomes strongly dominated by Poaceae and Asteraceae, with varying contributions from *Eucalyptus*, Myrtaceae, and chenopods, which persists with little subsequent change for the remainder of the record (note, the full pollen data are presented in Figure S3 and Data Set S2 in the supporting information).

4. Discussion and Conclusions

4.1. Pliocene Expansion of C_4 Vegetation

The carbon isotope ratios of leaf wax *n*-alkanes begin to become enriched in ^{13}C at ~3.5 Ma (Figure 2) implying an expansion of C_4 vegetation in north-western Australia. In addition, beginning at ~3.5 Ma, the $\delta^{13}C$ of

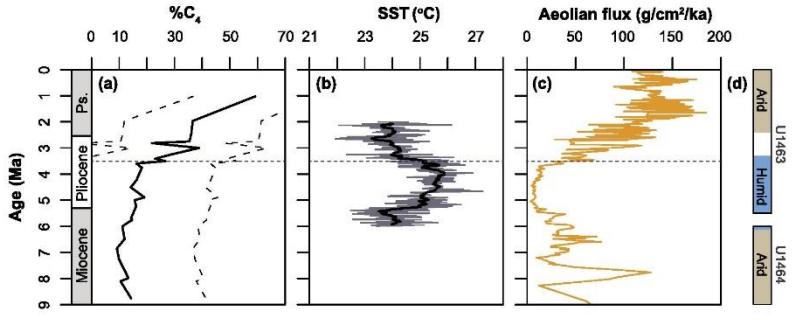

Figure 3. Australian record of C_4 expansion in the context of contemporaneous climate records and interpretations. (a) Percent C_4 reconstructed from the carbon isotope ratio of the C_{31} *n*-alkane homolog, with modern plant end-member 1-sigma calculation uncertainty shown as dashed black lines. (b) Mg/Ca sea surface temperature reconstruction from ODP 763A (the black line is a 15-point simple moving average, calculated using the "TTR" package; Ulrich, 2018, in R; R Core Team, 2016). Data from Karas et al. (2011). (c) Mass accumulation rates from ODP Sites 885/886 in the central North Pacific Ocean (Rea et al., 1993, 1998; Snoeckx et al., 1995), interpreted as increasing a eolian flux into sediments resulting from intensification of the East Asian winter monsoon (Data Set S5 in the supporting information, see Text S1.4 in the supporting information for methods used to calculate mass accumulation rate and to update timescale). (d) Arid (tan) and humid (blue) intervals interpreted from potassium abundance in wireline logs from IODP U1463 and U1464 off north-west Australia (Christensen et al., 2017; Groeneveld et al., 2017). The dashed lines on all panels indicate approximate alignment between a SST change point at 3.44 Ma (Sniderman et al., 2016), the increase observed in percent C_4 at ~3.5 Ma, and increased a eolian dust flux into the central North Pacific Ocean.

the C_{33} *n*-alkane becomes increasingly enriched in ^{13}C compared to the other shorter chain lengths (Figure 2). Modern Australian grasses produce a higher proportion of C_{33} than trees or shrubs (Howard et al., 2018, Figure S2, Table S1, Text S1.3, and Data Set S3 in the supporting information). This pattern is mirrored in North America and Africa, where grasses have higher abundances of longer chain *n*-alkanes (C_{33} and C_{35}) than trees that show higher abundances of shorter chain *n*-alkanes (C_{27} and C_{29}; Bush & McInerney, 2013; Garcin et al., 2014; Rommerskirchen et al., 2006; Vogts et al., 2009). C_{33} is therefore proposed to be more sensitive to the presence of C_4 grasses on the landscape (Uno et al., 2016), while C_{29} is less influenced by grasses. Carbon-13 enrichment and the beginning of isotopic divergence between C_{29} and C_{33} in our sedimentary record at ~3.5 Ma mark the onset of the expansion of C_4 vegetation. Phylogenetic evidence suggests that the moderately diverse C_4 grass tribe Triodiinae, characteristic of central Australian arid vegetation today, radiated in the Australian interior during the late Miocene (Toon et al., 2015). Nonetheless, any late Miocene C_4 vegetation must have been sparse, as it is not detectable in our C_{29} to C_{33} *n*-alkane record. However, ^{13}C enrichment of the C_{35} *n*-alkanes relative to C_{29}, C_{31} and C_{33} (Figure S1 in the supporting information) could be an indication of trace amounts of C_4 vegetation on the landscape prior to 3.5 Ma. The significant expansion in C_4 vegetation beginning at 3.5 Ma indicated by the inflection in our carbon isotope record reflects widespread biologically productive C_4 vegetation like that supported in the Australian monsoon tropics today (Williams et al., 2017). This timing postdates the onset of most C_4 expansions in Asia, Africa, North America, and South America, which occurred across the middle to late Miocene (Cerling et al., 1997; Dupont et al., 2013; Feakins et al., 2013; Fox et al., 2012; Fox & Koch, 2004; Ghosh et al., 2017; Hoetzel et al., 2013; MacFadden et al., 1996; Passey et al., 2002; Passey et al., 2009; Quade & Cerling, 1995; Uno et al., 2016).

4.2. Late Miocene/Early Pliocene Opening of the Landscape

Substantial Poaceae, Asteraceae, and *Eucalyptus* pollen suggest that north-west Australia was dominated by open woodland or shrubland in the latest Miocene. The prominence of Gyrostemonaceae and Casuarinaceae suggests that this vegetation may have had similarities to contemporaneous late Miocene open shrubland recorded on the Nullarbor Plain in the south of the continent, which was dominated palynologically by these two families (Sniderman et al., 2016). Increases in Restionaceae pollen percentages across the late Miocene/early Pliocene transition suggest an increase in effective precipitation, based on the preference of

Restionaceae for seasonally moist wetland habitats (Briggs, 2001). Peaks in representation of Myrtaceae, Cyperaceae, and ferns are consistent with a peak in moisture at ~4.9 Ma, just before these taxa decline abruptly. Rising values of Poaceae, Asteraceae, and chenopod pollen during the early Pliocene imply the increasing dominance of very open vegetation, in which grass and chenopods were more important than previously. Increasing relative abundance of the C_{33} compared to C_{29} *n*-alkane homolog beginning between 7 and 6 Ma also suggests increasing contributions from grasses (Figure 2). Our carbon isotope record indicates that C_4 vegetation did not begin to compose a significant fraction of the increasingly open landscape until ~3.5 Ma. From these data, we interpret an initial late Miocene expansion of C_3 grasses and/or chenopods, followed by a shift to C_4 grasses and/or chenopods near the early/late Pliocene boundary. Fossil marsupial tooth enamel isotope data showing mixed C_3 and C_4 diets from the bio-stratigraphically dated late Pliocene Chinchilla Sands of south-eastern Queensland are consistent with this timing (Montanari et al., 2013). We infer from our record a pattern of ecosystem changes on the Australian continent not dissimilar to other geographic regions (Edwards et al., 2010; Strömberg, 2011), though delayed by several million years.

4.3. Drivers of Late C_4 Expansion on the Australian Continent

Environmental conditions that tend to promote C_4 over C_3 photosynthesis are low atmospheric pCO_2, high temperature, aridity, warm-season precipitation, high irradiance, and fire (Ehleringer, 2005; Keeley & Bond, 2001; Knapp & Medina, 1999; Long, 1999). Decreased pCO_2 has been postulated as a major control on the onset of C_4 expansion globally (Cerling et al., 1993; Cerling et al., 1997; Ehleringer et al., 1991), with new developments in atmospheric pCO_2 reconstruction suggesting a significant decrease through the late Miocene (Bolton et al., 2016; Mejia et al., 2017). However, heterogeneous timing of C_4 expansion across the globe (Figure S4 in the supporting information) indicates that decreased pCO_2 cannot be the only driving factor. This assertion is supported by models showing that while changes in pCO_2 have the potential to transform global vegetation states, the timing of transformation will vary due to regional differences in the timing and rates of change of temperature, rainfall amount and seasonality, and fire severity (Higgins & Scheiter, 2012). We argue that the relative importance of pCO_2 and environmental factors will likely vary by region.

The timing of the expansion of C_4 vegetation documented here coincides closely with evidence for cooling and aridification in north-west Australia. Sea surface temperatures cool significantly in the region at 3.44 Ma (Karas et al., 2011; Sniderman et al., 2016; Figure 3), while at 3.3 Ma, there is evidence for the beginning of a transition from a humid to a more arid and/or more seasonal climate (Christensen et al., 2017; Figure 3). On the Nullarbor Plain, Sniderman et al. (2016) found no pollen in Pliocene speleothems younger than 3.4 Ma, suggesting that increasing aridity slowed speleothem growth after this time. The drivers of Australian aridification are debated; restriction of the Indonesian Throughflow (ITF) has been hypothesized as the driver of changes in precipitation in north-western Australia during the Pliocene (Christensen et al., 2017; Krebs et al., 2011). Krebs et al. (2011) simulated a constricted ITF based on Pliocene ocean bathymetry, finding that this could have caused a precipitation decrease of up to 30% over the eastern Indian Ocean. Conversely, other modeling experiments have indicated that ITF restriction was not associated with a decrease in precipitation over the eastern Indian Ocean, nor was it associated with significant globally pervasive impact on climate (Brierley & Fedorov, 2016; Jochum et al., 2009). Regardless of the driver of late Pliocene aridification, there is also evidence for aridity in north-western Australia during the late Miocene, from ~16 to 6 Ma (Groeneveld et al., 2017), that did not lead to an expansion of C_4 vegetation (Figure 3). This suggests that aridity by itself was not the primary driver of the Australian late Pliocene C_4 expansion, an inference that is substantiated by globally inconsistent relationships between C_4 plant distributions and modern climate (Sage et al., 1999).

Opening of the landscape, increased seasonality of precipitation, and increased incidence of fire are suggested to have played significant roles in promoting the expansion of C_4 vegetation on other continents (Beerling & Osborne, 2006; Edwards et al., 2010; Osborne, 2008; Scheiter et al., 2012; Zhou et al., 2017). Our pollen record suggests that Australian vegetation structure was already open by the late Miocene/early Pliocene. Our record of C_4 expansion also coincides very closely with evidence of increased east Asian dust flux into marine sediments, at ~3.5 Ma (Figure 3; Rea et al., 1993, 1998; Snoeckx et al., 1995), widely interpreted as marking the initial intensification of the East Asian winter monsoon (EAWM) or Siberian High (An et al., 2001; Guo et al., 2004; Rea et al., 1998; Sun et al., 1998; Zheng et al., 2004). Controls governing the Australian monsoon over late Neogene to Quaternary timescales are complex (Z. Liu et al., 2003; Wyrwoll & Valdes, 2003), but are dominated by two opposed influences: within-hemisphere insolation forcing

(Wyrwoll et al., 2007; Wyrwoll & Valdes, 2003), that is comparatively weak because of the relatively small, low relief land surface of northern Australia; and remote forcing driven by cross-equatorial thermal and pressure gradients between Australia and East Asia (An, 2000). The persistence of an east Asian-Australian precipitation teleconnection, in which northern cooling leads to southward migration of the Intertropical Convergence Zone, has been indicated at a range of Quaternary timescales from centennial-millennial (Denniston et al., 2013; Eroglu et al., 2016) to orbital (Y. Liu et al., 2015) and has been observed in sedimentary records from the Holocene (Eroglu et al., 2016), the last deglaciation (Yancheva et al., 2007), and as far back as the mid-Pleistocene (Y. Liu et al., 2015). The sensitivity of the cross-equatorial meridional circulation linking the EAWM and the Australian monsoon to orbital obliquity has been explored using climate model simulations (Shi et al., 2011).

The abrupt increase in the abundance of C_4 plants at ~3.5 Ma is most easily explained as a vegetation response to the onset of the Australian monsoon regime. In this interpretation, the intensification of the EAWM (Figure S4 in the supporting information), itself thought to be related to ongoing late Cenozoic global cooling (Herbert et al., 2016; Ge et al., 2013; Lu et al., 2010; Raymo, 1994), for the first time pushed the Intertropical Convergence Zone far enough southward to develop a substantial summer monsoon in northern Australia, characterized by a strong seasonal precipitation contrast and potentially greater incidence of fire. The relatively late appearance of a distinctly monsoonal moisture regime in northern Australia may help to explain the Plio-Pleistocene evolution of animal clades confined to the Australian monsoon tropics today that are nested within lineages more typical of inland, arid Australia (Laver et al., 2017; Nielsen et al., 2016). The establishment of this new climatic regime would have provided the ecological opportunities necessary for the expansion of C_4 vegetation in Australia beginning at ~3.5 Ma. This supports the hypothesis that the heterogeneous rise of C_4 ecosystems globally reflects variations in the environmental factors providing competitive advantages to C_4 vegetation.

Acknowledgments
The authors declare no conflict of interest. Data can be found in Data Sets S1 though S5 in the supporting information. Supplementary text and figures can be found in the supporting information. This research utilized samples and data provided by the International Ocean Discovery Program (IODP). Funding for this research was provided by an Australian IODP Office Special Post-Cruise Analytical Funding grant awarded to J. W. A and F. A. M., an Australian Research Council Future Fellowship (FT110100100793) awarded to F. A. M., an Australian Government Research Training Program Scholarship and University of Adelaide Faculty of Sciences Divisional Scholarship awarded to J. W. A. and S. H., and an NSF Graduate Research Fellowship to S. R. P (DGE 16-44869). Isotopic analyses were supported by the Climate Center at LDEO. Thank you to David Fox and one anonymous reviewer for their helpful comments. We acknowledge the Terrestrial Ecosystems Research Network for provision of plant survey data and samples. Thank you to Kristine Nielson, Emrys Leitch, Stefan Caddy-Retalic, and Nicole deRoberts for research support.

References

An, Z. (2000). The history and variability of the east Asian paleomonsoon climate. *Quaternary Science Reviews*, *19*(1), 171–187. https://doi.org/10.1016/S0277-3791(99)00060-8

An, Z., Kutzbach, J. E., Prell, W. L., & Porter, S. C. (2001). Evolution of Asian monsoons and phased uplift of the Himalaya–Tibetan plateau since late Miocene times. *Nature*, *411*(6833), 62–66. https://doi.org/10.1038/35075035

APSA Members (2007). The Australasian Pollen and Spore Atlas V1.0. Retrieved from http://apsa.anu.edu.au/

Australian Government Bureau of Meteorology. (2016). Gridded climate datasets. Retrieved from http://www.bom.gov.au/climate/averages/climatology/gridded-data-info/gridded-climate-data.shtml

Beerling, D. J., & Osborne, C. P. (2006). The origin of the savanna biome. *Global Change Biology*, *12*(11), 2023–2031. https://doi.org/10.1111/j.1365-2486.2006.01239.x

Bolton, C. T., Hernandez-Sanchez, M. T., Fuertes, M.-A., Gonzalez-Lemos, S., Abrevaya, L., Mendez-Vicente, A., et al. (2016). Decrease in coccolithophore calcification and CO_2 since the middle Miocene. *Nature Communications*, *7*, 10284. https://doi.org/10.1038/ncomms10284

Brierley, C. M., & Fedorov, A. V. (2016). Comparing the impacts of Miocene–Pliocene changes in inter-ocean gateways on climate: Central American seaway, Bering Strait, and Indonesia. *Earth and Planetary Science Letters*, *444*, 116–130. https://doi.org/10.1016/j.epsl.2016.03.010

Briggs, B. G. (2001). The restiads invade the north: The diaspora of the Restionaceae. In I Metcalfe, et al. (Eds.), *Faunal and Floral Migration and Evolution in SE Asia-Australasia* (pp. 237–241). Boca Raton, FL: CRC Press.

Bush, R., & McInerney, F. A. (2013). Leaf wax *n*-alkane distributions in and across modern plants: Implications for paleoecology and chemotaxonomy. *Geochimica et Cosmochimica Acta*, *117*, 161–179. https://doi.org/10.1016/j.gca.2013.04.016

Cerling, T. E., Harris, J. M., MacFadden, B. J., Leakey, M. G., Quade, J., Eisenmann, V., & Ehleringer, J. R. (1997). Global vegetation change through the Miocene/Pliocene boundary. *Nature*, *389*(6647), 153–158. https://doi.org/10.1038/38229

Cerling, T. E., Wang, Y., & Quade, J. (1993). Expansion of C_4 ecosystems as an indicator of global ecological change in the late Miocene. *Letters to Nature*, *361*(6410), 344–345. https://doi.org/10.1038/361344a0

Christensen, B. A., Renema, W., Henderiks, J., De Vleeschouwer, D., Groeneveld, J., Castañeda, I. S., et al. (2017). Indonesian Throughflow drove Australian climate from humid Pliocene to arid Pleistocene. *Geophysical Research Letters*, *44*, 6914–6925. https://doi.org/10.1002/2017GL072977

Core Team, R. (2016). *R: A language and environment for statistical computing*. Vienna, Austria: R Foundation for Statistical Computing. Retrieved from https://www.r-project.org/

Denniston, R. F., Wyrwoll, K.-H., Asmerom, Y., Polyak, V. J., Humphreys, W. F., Cugley, J., et al. (2013). North Atlantic forcing of millennial-scale indo-Australian monsoon dynamics during the last glacial period. *Quaternary Science Reviews*, *72*, 159–168. https://doi.org/10.1016/j.quascirev.2013.04.012

Dupont, L. M., Rommerskirchen, F., Mollenhauer, G., & Schefuß, E. (2013). Miocene to Pliocene changes in south African hydrology and vegetation in relation to the expansion of C4 plants. *Earth and Planetary Science Letters*, *375*, 408–417. https://doi.org/10.1016/j.epsl.2013.06.005

Edwards, E. J., Osborne, C. P., Stromberg, C. A. E., & Smith, S. A. (2010). The origins of C4 grasslands: Integrating evolutionary and ecosystem science. *Science*, *328*(5978), 587–591. https://doi.org/10.1126/science.1177216

Ehleringer, J. R. (2005). The influence of atmospheric CO_2, temperature, and water on the abundance of C_3/C_4 taxa. In I. T. Baldwin, M. M. Caldwell, G. Heldmaier, R. B. Jackson, O. L. Lange, H. A. Mooney, et al. (Eds.), *A history of atmospheric CO_2 and its effects on plants, animals, and ecosystems*, (pp. 214–231). New York, NY: Springer.

Ehleringer, J. R., Sage, R. F., Flanagan, L. B., & Pearcy, R. W. (1991). Climate change and the evolution of C_4 photosynthesis. *Trends in Ecology & Evolution*, *6*(3), 95–99. https://doi.org/10.1016/0169-5347(91)90183-X

Eroglu, D., McRobie, F. H., Ozken, I., Stemler, T., Wyrwoll, K.-H., Breitenbach, S. F. M., et al. (2016). See–saw relationship of the Holocene East Asian–Australian summer monsoon. *Nature Communications*, *7*, 12929. https://doi.org/10.1038/ncomms12929

Feakins, S. J., Levin, N. E., Liddy, H. M., Sieracki, A., Eglinton, T. I., & Bonnefille, R. (2013). Northeast African vegetation change over 12 m.y. *Geology*, *41*(3), 295–298. https://doi.org/10.1130/G33845.1

Fox, D. L., Honey, J. G., Martin, R. A., & Peláez-Campomanes, P. (2012). Pedogenic carbonate stable isotope record of environmental change during the Neogene in the southern Great Plains, southwest Kansas, USA: Carbon isotopes and the evolution of C_4-dominated grasslands. *GSA Bulletin*, *124*(3–4), 444–462. https://doi.org/10.1130/B30401.1

Fox, D. L., & Koch, P. L. (2004). Carbon and oxygen isotopic variability in Neogene paleosol carbonates: Constraints on the evolution of the C_4-grasslands of the Great Plains, USA. *Palaeogeography, Palaeoclimatology, Palaeoecology*, *207*(3), 305–329. https://doi.org/10.1016/j.palaeo.2003.09.030

Garcin, Y., Schefuß, E., Schwab, V. F., Garreta, V., Gleixner, G., Vincens, A., et al. (2014). Reconstructing C_3 and C_4 vegetation cover using n-alkane carbon isotope ratios in recent lake sediments from Cameroon, Western Central Africa. *Geochimica et Cosmochimica Acta*, *142*, 482–500. https://doi.org/10.1016/j.gca.2014.07.004

Ge, J., Dai, Y., Zhang, Z., Zhao, D., Li, Q., Zhang, Y., et al. (2013). Major changes in east Asian climate in the mid-Pliocene: Triggered by the uplift of the Tibetan plateau or global cooling? *Journal of Asian Earth Sciences*, *69*, 48–59. https://doi.org/10.1016/j.jseaes.2012.10.009

Ghosh, S., Sanyal, P., & Kumar, R. (2017). Evolution of C_4 plants and controlling factors: Insight from *n*-alkane isotopic values of NW Indian Siwalik paleosols. *Organic Geochemistry*, *110*, 110–121. https://doi.org/10.1016/j.orggeochem.2017.04.009

Groeneveld, J., Henderiks, J., Renema, W., McHugh, C. M., De Vleeschouwer, D., Christensen, B. A., et al. (2017). Australian shelf sediments reveal shifts in Miocene Southern Hemisphere westerlies. *Science Advances*, *3*(5), e1602567. https://doi.org/10.1126/sciadv.1602567

Guo, Z., Peng, S., Hao, Q., Biscaye, P. E., An, Z., & Liu, T. (2004). Late Miocene–Pliocene development of Asian aridification as recorded in the red-earth formation in northern China. *Global and Planetary Change*, *41*(3), 135–145. https://doi.org/10.1016/j.gloplacha.2004.01.002

Haq, B. U., von Rad, U., O'Connell, S., Bent, A., Blome, C. D., Borella, P. E., et al. (1990). Proceedings of the ODP Initial Reports, 122.

Hattersley, P. W. (1983). The distribution of C_3 and C_4 grasses in Australia in relation to climate. *Oecologia*, *57*(1-2), 113–128. https://doi.org/10.1007/BF00379569

Herbert, T. D., Lawrence, K. T., Tzanova, A., Peterson, L. C., Caballero-Gill, R., & Kelly, C. S. (2016). Late Miocene global cooling and the rise of modern ecosystems. *Nature Geoscience*, *9*(11), 843–847. https://doi.org/10.1038/ngeo2813

Hesse, P. P., & McTainsh, G. H. (2003). Australian dust deposits: Modern processes and the Quaternary record. *Quaternary Science Reviews*, *22*(18-19), 2007–2035. https://doi.org/10.1016/S0277-3791(03)00164-1

Higgins, S. I., & Scheiter, S. (2012). Atmospheric CO_2 forces abrubt vegetation shifts locally, but not globally. *Nature*, *488*(7410), 209–212. https://doi.org/10.1038/nature11238

Hilgen, F. J., Lourens, L. J., Van Dam, J. A., Beu, A. G., Boyes, A. F., Cooper, R. A., et al. (2012). Chapter 29—The Neogene Period. In *The Geologic Time Scale*, (pp. 923–978). Boston: Elsevier.

Hoetzel, S., Dupont, L., Schefuß, E., Rommerskirchen, F., & Wefer, G. (2013). The role of fire in Miocene to Pliocene C_4 grassland and ecosystem evolution. *Nature Geoscience*, *6*(12), 1027–1030. https://doi.org/10.1038/ngeo1984

Howard, S., McInerney, F. A., Caddy-Retalic, S., Hall, P. A., & Andrae, J. W. (2018). Modelling leaf wax n-alkane inputs to soils along a latitudinal transect across Australia. *Organic Geochemistry*, *121*, 126–137. https://doi.org/10.1016/j.orggeochem.2018.03.013

Jochum, M., Fox-Kemper, B., Molnar, P. H., & Shields, C. (2009). Differences in the Indonesian seaway in a coupled climate model and their relevance to Pliocene climate and El Niño. *Paleoceanography*, *24*, PA1212. https://doi.org/10.1029/2008PA001678

Karas, C., Nürnberg, D., Tiedemann, R., & Garbe-Schönberg, D. (2011). Pliocene Indonesian Throughflow and Leeuwin Current dynamics: Implications for Indian Ocean polar heat flux. *Paleoceanography*, *26*, PA2217. https://doi.org/10.1029/2010PA001949

Kattge, J., Díaz, S., Lavorel, S., Prentice, I. C., Leadley, P., Bönisch, G., et al. (2011). TRY—A global database of plant traits. *Global Change Biology*, *17*(9), 2905–2935. https://doi.org/10.1111/j.1365-2486.2011.02451.x

Keeley, J. E., & Bond, W. J. (2001). On incorporating fire into our thinking about natural ecosystems: A response to Saha and Howe. *The American Naturalist*, *158*(6), 664–670. https://doi.org/10.1086/323594

Kershaw, A. P., Martin, H. A., & McEwen-Mason, J. R. C. (1994). The Neogene: A period of transition. In R. S. Hill (Ed.), *History of the Australian Vegetation: Cretaceous to Recent* (Chapter 13, pp. 299–327). New York: Cambridge University Press.

Knapp, A. K., & Medina, E. (1999). Success of C_4 photosynthesis in the field: Lessons from communities dominated by C_4 plants. In R. F. Sage, & R. K. Monson (Eds.), *C4 Plant Biology* (Chapter 8, pp. 251–283). London: Academic Press. https://doi.org/10.1016/B978-012614440-6/50009-4

Krebs, U., Park, W., & Schneider, B. (2011). Pliocene aridification of Australia caused by tectonically induced weakening of the Indonesian throughflow. *Palaeogeography, Palaeoclimatology, Palaeoecology*, *309*(1), 111–117. https://doi.org/10.1016/j.palaeo.2011.06.002

Laver, R. J., Nielsen, S. V., Rosauer, D. F., & Oliver, P. M. (2017). Trans-biome diversity in Australian grass-specialist lizards (Diplodactylidae: Strophurus). *Molecular Phylogenetics and Evolution*, *115*, 62–70. https://doi.org/10.1016/j.ympev.2017.07.015

Leigh, J. H. (1994). Chenopod shrublands. In R. H. Groves (Ed.), *Australian Vegetation* (Chapter 12, pp. 345–368). Cambridge: Cambridge University Press.

Liu, Y., Lo, L., Shi, Z., Wei, K.-Y., Chou, C.-J., Chen, Y.-C., et al. (2015). Obliquity pacing of the western Pacific Intertropical Convergence Zone over the past 282,000 years. *Nature Communications*, *6*(1). https://doi.org/10.1038/ncomms10018

Liu, Z., Otto-Bliesner, B., Kutzbach, J., Li, L., & Shields, C. (2003). Coupled climate simulation of the evolution of global monsoons in the Holocene. *Journal of Climate*, *16*(15), 2472–2490. https://doi.org/10.1175/1520-0442(2003)016%3C2472:ccsote%3E2.0.co;2

Locker, S., & Martini, E. (1986). Phytoliths from the Southwest Pacific, Site 591. *Initial Reports of the Deep Sea Drilling Project*, *90*, 1079–1084.

Long, S. P. (1999). Environmental responses. In R. F. Sage, & R. K. Monson (Eds.), *C4 Plant Biology* (Chapter 7, pp. 215–249). London: Academic Press. https://doi.org/10.1016/B978-012614440-6/50008-2

Lowrey, T. (2015). Master plant species information database for the Sevilleta National Wildlife Refuge, New Mexico (1989-1996). Retrieved from: http://sev.lternet.edu/data/sev-51

Lu, H., Wang, X., & Li, L. (2010). Aeolian sediment evidence that global cooling has driven late Cenozoic stepwise aridification in central Asia. In P. D. Clift, R. Tada, & H. Zheng (Eds.), *Monsoon Evolution and Tectonics-Climate Linkage in Asia*, (Vol. 342, pp. 29–44). London: Geological Society.

MacFadden, B. J., Cerling, T. E., & Prado, J. (1996). Cenozoic terrestrial ecosystem evolution in Argentina: Evidence from carbon isotopes of fossil mammal teeth. *PALAIOS, 11*(4), 319–327. https://doi.org/10.2307/3515242
Macphail, M. K. (1997). Late Neogene climates in Australia: Fossil pollen- and spore-based estimates in retrospect and Prospect. *Australian Journal of Botany, 45*(3), 425–464. https://doi.org/10.1071/BT96052
Martin, H. A. (2006). Cenozoic climatic change and the development of the arid vegetation in Australia. *Journal of Arid Environments, 66*(3), 533–563. https://doi.org/10.1016/j.jaridenv.2006.01.009
Martin, H. A., & McMinn, A. (1994). Late Cainozoic vegetation history of North-Western Australia, from the palynology of a deep sea core (ODP site 765). *Australian Journal of Botany, 42*(1), 95–102. https://doi.org/10.1071/BT9940095
Mejía, L. M., Méndez-Vicente, A., Abrevaya, L., Lawrence, K. T., Ladlow, C., Bolton, C., et al. (2017). A diatom record of CO_2 decline since the late Miocene. *Earth and Planetary Science Letters, 479*, 18–33. https://doi.org/10.1016/j.epsl.2017.08.034
Montanari, S., Louys, J., & Price, G. J. (2013). Pliocene Paleoenvironments of southeastern Queensland, Australia inferred from stable isotopes of marsupial tooth enamel. *PLoS One, 8*(6), e66221. https://doi.org/10.1371/journal.pone.0066221
Moore, P. D., Webb, J. A., & Collinson, M. E. (1991). *Pollen analysis*, (2nd ed.). London: Blackwell Scientific Publications.
Munsterman, D., & Kerstholt, S. (1996). Sodium polytungstate, a new non-toxic alternative to bromoform in heavy liquid separation. *Review of Palaeobotany and Palynology, 91*(1), 417–422. https://doi.org/10.1016/0034-6667(95)00093-3
Murphy, B. P., & Bowman, D. M. J. S. (2007). Seasonal water availability predicts the relative abundance of C_3 and C_4 grasses in Australia. *Global Ecology and Biogeography, 16*(2), 160–169. https://doi.org/10.1111/j.1466-8238.2006.00285.x
Nielsen, S. V., Oliver, P. M., Laver, R. J., Bauer, A. M., & Noonan, B. P. (2016). Stripes, jewels and spines: Further investigations into the evolution of defensive strategies in a chemically defended gecko radiation (Strophurus, Diplodactylidae). *Zoologica Scripta, 45*(5), 481–493. https://doi.org/10.1111/zsc.12181
Osborne, C. P. (2008). Atmosphere, ecology and evolution: What drove the Miocene expansion of C_4 grasslands? *Journal of Ecology, 96*(1), 35–45. https://doi.org/10.1111/j.1365-2745.2007.01323.x
Osborne, C. P., Salomaa, A., Kluyver, T. A., Visser, V., Kellogg, E. A., Morrone, O., et al. (2014). A global database of C_4 photosynthesis in grasses. *New Phytologist, 204*(3), 441–446. https://doi.org/10.1111/nph.12942
Passey, B. H., Ayliffe, L. K., Kaakinen, A., Zhang, Z., Eronen, J. T., Zhu, Y., et al. (2009). Strengthened East Asian summer monsoons during a period of high-latitude warmth? Isotopic evidence from Mio-Pliocene fossil mammals and soil carbonates from northern China. *Earth and Planetary Science Letters, 277*(3-4), 443–452. https://doi.org/10.1016/j.epsl.2008.11.008
Passey, B. H., Cerling, T. E., Perkins, M. E., Voorhies, M. R., Harris, J. M., & Tucker, S. T. (2002). Environmental change in the Great Plains: An isotopic record from fossil horses. *The Journal of Geology, 110*(2), 123–140. https://doi.org/10.1086/338280
Polissar, P. J., & D'Andrea, W. J. (2014). Uncertainty in paleohydrologic reconstructions from molecular δD values. *Geochimica et Cosmochimica Acta, 129*, 146–156. https://doi.org/10.1016/j.gca.2013.12.021
Quade, J., & Cerling, T. E. (1995). Expansion of C_4 grasses in the late Miocene of northern Pakistan: Evidence from stable isotopes in paleosols. *Palaeogeography, Palaeoclimatology, Palaeoecology, 115*(1-4), 91–116. https://doi.org/10.1016/0031-0182(94)00108-K
Raymo, M. E. (1994). The initiation of northern hemisphere glaciation. *Annual Review of Earth and Planetary Sciences, 22*(1), 353–383. https://doi.org/10.1146/annurev.ea.22.050194.002033
Rea, D. K., Basov, I. A., Janecek, T. R., Arnold, E., Barron, J. A., Beaufort, L., et al. (1993). Sites 885/886. Proceedings of Ocean Drilling Program, Initial Report 145, 303.
Rea, D. K., Snoeckx, H., & Joseph, L. H. (1998). Late Cenozoic Eolian deposition in the North Pacific: Asian drying, Tibetan uplift, and cooling of the northern hemisphere. *Paleoceanography, 13*, 215–224. https://doi.org/10.1029/98PA00123
Rommerskirchen, F., Plader, A., Eglinton, G., Chikaraishi, Y., & Rullkötter, J. (2006). Chemotaxonomic significance of distribution and stable carbon isotopic composition of long-chain alkanes and alkan-1-ols in C_4 grass waxes. *Organic Geochemistry, 37*(10), 1303–1332. https://doi.org/10.1016/j.orggeochem.2005.12.013
Sage, R. F., Wedin, D. A., & Li, M. (1999). The biogeography of C_4 photosynthesis: Patterns and controlling factors. In R. F. Sage, & R. K. Monson (Eds.), *C4 Plant Biology* (Chapter 10, pp. 313–373). London: Academic Press. https://doi.org/10.1016/B978-012614440-6/50011-2
Scheiter, S., Higgins, S. I., Osborne, C. P., Bradshaw, C., Lunt, D. J., Ripley, B. S., et al. (2012). Fire and fire-adapted vegetation promoted C_4 expansion in the late Miocene. *New Phytologist, 195*(3), 653–666. https://doi.org/10.1111/j.1469-8137.2012.04202.x
Shi, Z. G., Liu, X. D., Sun, Y. B., An, Z. S., Liu, Z., & Kutzbach, J. (2011). Distinct responses of East Asian summer and winter monsoons to astronomical forcing. *Climate of the Past, 7*(4), 1363–1370. https://doi.org/10.5194/cp-7-1363-2011
Sniderman, J. M. K., Woodhead, J. D., Hellstrom, J., Jordan, G. J., Drysdale, R. N., Tyler, J. J., & Porch, N. (2016). Pliocene reversal of late Neogene aridification. *Proceedings of the National Academy of Sciences, 113*(8), 1999–2004. https://doi.org/10.1073/pnas.1520188113
Snoeckx, H., Rea, D. K., Jones, C. E., & Ingram, B. L. (1995). Eolian and silica deposition in the Central North Pacific: Results from Sites 885/886. *Proceedings of the Ocean Drilling Program, Scientific Results, 145*.
Still, C. J., Berry, J. A., Collatz, G. J., & DeFries, R. S. (2003). Global distribution of C_3 and C_4 vegetation: Carbon cycle implications. *Global Biogeochemical Cycles, 17*(1), 1006.
Strömberg, C. A. E. (2011). Evolution of grasses and grassland ecosystems. *Annual Review of Earth and Planetary Sciences, 39*(1), 517–544. https://doi.org/10.1146/annurev-earth-040809-152402
Sun, D., Shaw, J., An, Z., Cheng, M., & Yue, L. (1998). Magnetostratigraphy and paleoclimatic interpretation of a continuous 7.2 Ma late Cenozoic Eolian sediments from the Chinese Loess Plateau. *Geophysical Research Letters, 25*, 85–88. https://doi.org/10.1029/97GL03353
Tang, C. (1992). Paleomagnetism of Cenozoic sediments in holes 762B and 763A, central Exmouth Plateau, Northwest Australia. *Proceedings of the ODP, 122*, 717–733.
Tipple, B. J., Meyers, S. R., & Pagani, M. (2010). Carbon isotope ratio of Cenozoic CO_2: A comparative evaluation of available geochemical proxies. *Paleoceanography, 25*, PA3202. https://doi.org/10.1029/2009PA001851
Tipple, B. J., & Pagani, M. (2007). The early origins of terrestrial C_4 photosynthesis. *Annual Review of Earth and Planetary Sciences, 35*(1), 435–461. https://doi.org/10.1146/annurev.earth.35.031306.140150
Toon, A., Crisp, M. D., Gamage, H., Mant, J., Morris, D. C., Schmidt, S., & Cook, L. G. (2015). Key innovation or adaptive change? A test of leaf traits using Triodiinae in Australia. *Scientific Reports, 5*(1). https://doi.org/10.1038/srep12398
Ulrich, J. (2018). TTR: Technical Trading Rules. Retrieved from https://cran.r-project.org/package=TTR
Uno, K. T., Polissar, P. J., Jackson, K. E., & deMenocal, P. B. (2016). Neogene biomarker record of vegetation change in eastern Africa. *Proceedings of the National Academy of Sciences, 113*(23), 6355–6363. https://doi.org/10.1073/pnas.1521267113
Vogts, A., Moossen, H., Rommerskirchen, F., & Rullkötter, J. (2009). Distribution patterns and stable carbon isotopic composition of alkanes and alkan-1-ols from plant waxes of African rain forest and savanna C_3 species. *Organic Geochemistry, 40*(10), 1037–1054. https://doi.org/10.1016/j.orggeochem.2009.07.011

White, A., Sparrow, B., Leitch, E., Foulkes, J., Filitton, R., Lowe, A. J., & Caddy-Retalic, S. (2012). *AusPlots Rangelands Survey Protocol Manual*. Adelaide: Adelaide University Press.

Williams, R. J., Cook, G. D., Liedloff, A. C., & Bond, W. J. (2017). Australia's tropical savannas: Vast, ancient and rich landscapes. In D. A. Keith (Ed.), *Australian Vegetation*, (pp. 368–388). Cambridge: Cambridge University Press.

Wyrwoll, K.-H., Liu, Z., Chen, G., Kutzbach, J. E., & Liu, X. (2007). Sensitivity of the Australian summer monsoon to tilt and precession forcing. *Quaternary Science Reviews*, *26*(25), 3043–3057. https://doi.org/10.1016/j.quascirev.2007.06.026

Wyrwoll, K.-H., & Valdes, P. (2003). Insolation forcing of the Australian monsoon as controls of Pleistocene mega-lake events. *Geophysical Research Letters*, *30*(24), 2279. https://doi.org/10.1029/2003GL018486

Yancheva, G., Nowaczyk, N. R., Mingram, J., Dulski, P., Schettler, G., Negendank, J. F. W., et al. (2007). Influence of the intertropical convergence zone on the East Asian monsoon. *Nature*, *445*(7123), 74–77. https://doi.org/10.1038/nature05431

Zheng, H., Powell, C. M., Rea, D. K., Wang, J., & Wang, P. (2004). Late Miocene and mid-Pliocene enhancement of the East Asian monsoon as viewed from the land and sea. *Global and Planetary Change*, *41*(3), 147–155. https://doi.org/10.1016/j.gloplacha.2004.01.003

Zhou, B., Bird, M., Zheng, H., Zhang, E., Wurster, C. M., Xie, L., & Taylor, D. (2017). New sedimentary evidence reveals a unique history of C_4 biomass in continental East Asia since the early Miocene. *Scientific Reports*, *7*(1), 170–178. https://doi.org/10.1038/s41598-017-00285-7